Twelfth Edition

Photovoltaics International

THE TECHNOLOGY RESOURCE FOR PV PROFESSIONALS

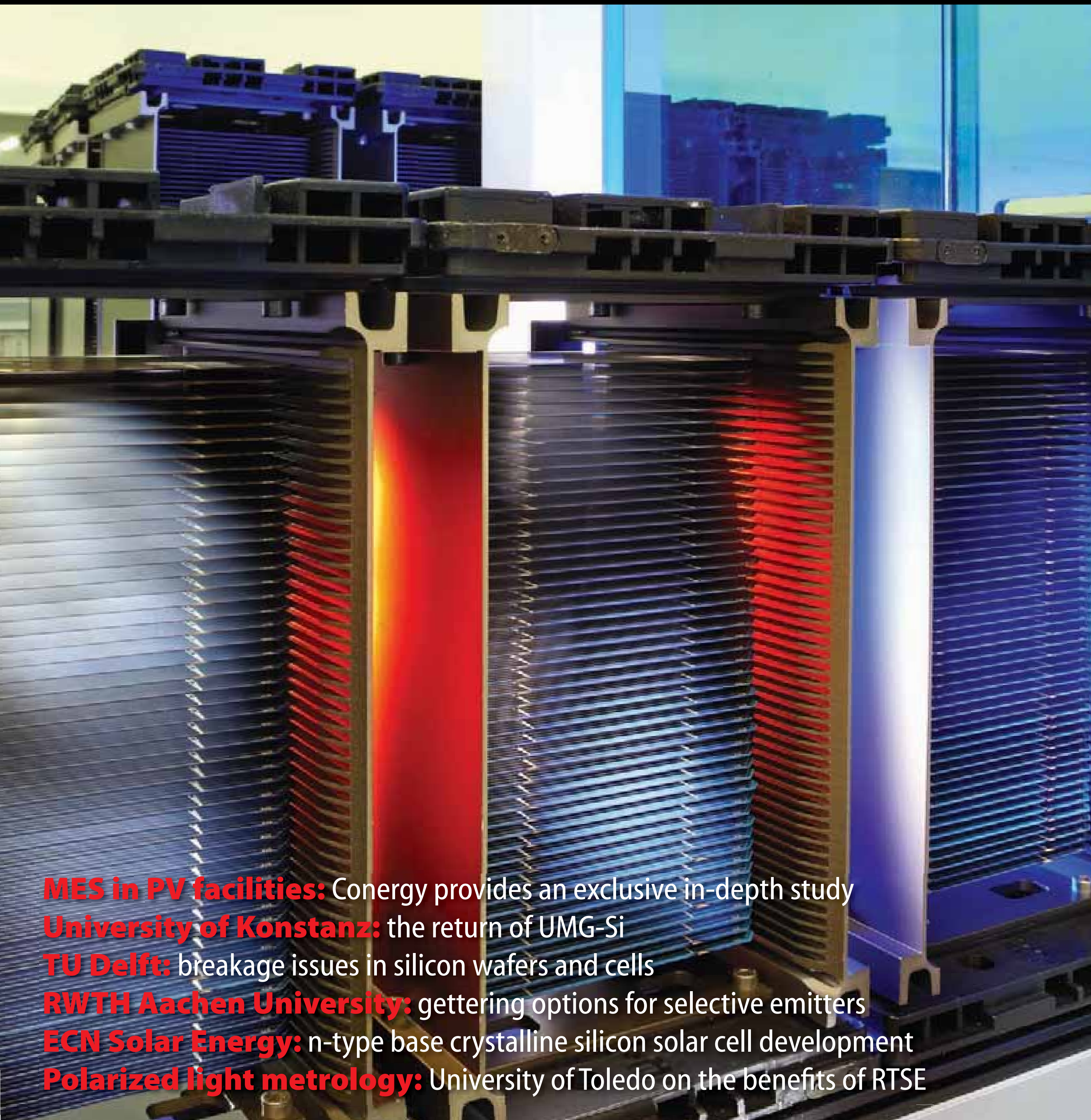

MES in PV facilities: Conergy provides an exclusive in-depth study

University of Konstanz: the return of UMG-Si

TU Delft: breakage issues in silicon wafers and cells

RWTH Aachen University: gettering options for selective emitters

ECN Solar Energy: n-type base crystalline silicon solar cell development

Polarized light metrology: University of Toledo on the benefits of RTSE

Second Quarter, May 2011

www.pv-tech.org

Photovoltaics International

Published by:
Solar Media Ltd.,
Trans-World House, 100 City Road, London
EC1Y 2BP, UK
Tel: +44 (0) 207 871 0123
Fax: +44 (0) 207 871 0101
E-mail: info@pv-tech.org
Web: www.pv-tech.org

Publisher: David Owen
Managing Editor: Síle Mc Mahon
Production Manager: Tina Davidian
Design: Daniel Brown
Senior Editor, North America: Tom Cheyney
Senior News Editor: Mark Osborne
News & Features Editor: Emma Hughes
Junior Editor: Chris Whitmore
Sub-Editor: L.J. Ireton
Commissioning Editor: Adam Morrison
Sales Director: Neill Wightman
Account Managers: Adam Morrison, Graham Davie, Daniel Ryder, Gary Kakoullis, David Evans, Nick Richardson & Ben Irving
Marketing & Operations Director: Joy-Fleur Brettschneider
Marketing & PR Executive: Laura Pleasants

Cover image shows cassettes of crystalline-silicon solar cells in process at Suntech's manufacturing facility in Wuxi, China. Image courtesy of Suntech.

Printed by Quentin Press
Photovoltaics International
Twelfth Edition
Second Quarter 2011
Photovoltaics International is a quarterly journal published in February, May, August and November.

Distributed in the USA by Mail Right International, 1637 Stelton Road B4, Piscataway, NJ 08854.

ISSN: 1757-1197

USPS Information
USPS Periodical Code: 025 313

Periodicals Postage Paid at
New Brunswick, NJ
Postmaster: Send changes to:
Photovoltaics International,
Solar Media Ltd., C/o 1637 Stelton
Road, B-4, Piscataway, NJ 08854, USA

Foreword

Despite a rocky start, this year looks set to bring about an unprecedented turnaround of fortunes. With a slow start in the first quarter – thanks to the FiT-induced slowdown in the major markets of Italy and Germany – leading to between 2 and 3GW of module overcapacity, it seems that the cost margins can only be lowered at source by the wafer and polysilicon producers.

As we go to press with this, the 12th edition of *Photovoltaics International*, news has just emerged that Italy's woes could soon be over. The new Conto Energia IV comes into effect on June 1, and it looks like the country's market could well be back on track by the start of the second half of the year.

The Fukushima nuclear crisis added a new dimension to the markets. March brought about the massive 8.9 magnitude earthquake that led to a devastating tsunami that in turn resulted in the disabling of the reactor cooling systems, nuclear radiation leaks and an overall distrust of all things nuclear. Germany's Angela Merkel ordered the shut-down of seven of the country's nuclear plants for at least three months, and, both for Germany and on a global scale, it looks like what was once considered to be one of the cleanest sources of fuel is now being shunned in favour of renewables – including solar energy.

With this in mind, although the industry is being held back by module oversupply problems, it has been encouraging to see the plethora of cell efficiency records being logged over the past few months. Furthermore, the momentous news of SunPower's takeover by oil industry giant Total created quite a buzz throughout the industry.

We always aim to provide our readers with technical papers that are not only of interest but also practical to real-world manufacturing issues. For this edition of *Photovoltaics International*, we have been successful in securing some of the most detailed studies of potential cost reduction advancements, from the silicon wafer and cell breakage focus by TU Delft (p. 49) to China Sunergy's recommendations for reduction of PV module power loss factors (p. 148). EPIA's PV Observatory project also provides some vital policy recommendations for European markets (p. 194).

Cell efficiencies being the name of the game at the moment, our comprehensive 53-page cell processing section contains contributions from RWTH Aachen University on the gettering options available for selective emitters (p. 65); the University of Newcastle-upon-Tyne proposes the incorporation of TCAD processes in the PV industry (p. 72); while ECN Solar Energy grants us a glimpse at its development thus far on n-type base c-Si solar cells (p. 94).

Events season is already underway, and we're looking forward to the upcoming travels. We have also recently launched www.PhotovoltaicsInternational.com, the new home for everything to do with our publications. This will house all journals, technical papers, Lites, information for advertisers, details on our event attendance, and more.

We look forward to meeting with you at one of this year's exhibitions, and would like to again extend a warm thank-you to all of our contributors, advertisers and advisory board members for their ongoing support.

Síle Mc Mahon
Managing Editor
Photovoltaics International

Photovoltaics International

Photovoltaics International's primary focus is on assessing existing and new technologies for "real-world" supply chain solutions. The aim is to help engineers, managers and investors to understand the potential of equipment, materials, processes and services that can help the PV industry achieve grid parity. The Photovoltaics International advisory board has been selected to help guide the editorial direction of the technical journal so that it remains relevant to manufacturers and utility-grade installers of photovoltaic technology. The advisory board is made up of leading personnel currently working first-hand in the PV industry.

Editorial Advisory Board

Our editorial advisory board is made up of senior engineers from PV manufacturers worldwide. Meet some of our board members below:

Gerhard Rauter, Chief Operating Officer, Q-Cells SE

Since 1979, Gerhard Rauter – a native Austrian – had been working in managerial positions for Siemens AG at different facilities in Germany. In 2005 he became Vice President of Operations & Production with responsibility for the technology transfer between plants at home and abroad. As Vice President and Managing Director at Infineon Technologies Dresden GmbH & CO.OHG he was in charge of the Dresden facilities and their 2,350 employees since 2006. His main responsibilities at the Dresden facility had been in the fields of Development, Production and Quality. In October 2007 Gerhard Rauter was appointed as Chief Operating Officer at Q-Cells SE, being in charge of Production, InterServices, Quality, Safety and Process Technology.

Takashi Tomita, Senior Executive Fellow, Sharp Solar

Takashi Tomita has been working at Sharp for 34 years and is widely recognised as a fore-father of the solar industry in Japan. He was responsible for setting up Sharp's solar cell manufacturing facilities in Nara and silicon production in Toyama. Takashi's passion for solar power has led him to hold numerous posts outside of his roles at Sharp, including: Vice Representative at the Japan Photovoltaic Industry Association; Committee Member of Renewable Energy Portfolio Standard of METI; Adviser Board Member of Advanced Technology of Nara; Visiting Professor of Tohoku University; Adviser of ASUKA DBJ Partners (JAPAN) and Adviser of Global Catalyst Partners (US).

Dr. Kuo En Chang, President of Solar Division, Motech Industries, Inc.

Dr. Kuo En Chang joined Motech in 1999 as Chief Technology Officer and became President of the Solar Division in 2008, with responsibility for all technology and manufacturing. Motech is the sixth largest solar cell producer in the world. Before Dr. Chang joined Motech Solar, he worked on secondary battery research at the Industrial Technology Research Institute (ITRI) for more than three years. Dr. Chang holds a Ph.D. degree in Metallurgical & Materials Engineering from the University of Alabama.

Professor Eicke R. Weber, Director of the Fraunhofer Institute for Solar Energy Systems ISE in Freiburg

Professor Eicke R. Weber is the Director of the Fraunhofer Institute for Solar Energy Systems ISE in Freiburg. Weber has earned an international reputation as a materials researcher for defects in silicon and III-V semiconductors such as gallium arsenide and gallium nitride. He spent 23 years in the U.S. in research roles, most recently as Professor at the University of California in Berkeley. Weber is also the Chair of Applied Physics, Solar Energy, at the University of Freiburg, and during his career has been the recipient of several prestigious awards including the Alexander von Humboldt Prize in 1994, and the German Cross of Merit on ribbon in June 2006.

Dr. Zhengrong Shi, Chief Executive Officer, Suntech

Dr. Zhengrong Shi is founder, CEO and Chairman of the board of directors of Suntech. Prior to founding Suntech in 2001, he was a Research Director and Executive Director of Pacific Solar Pty., Ltd., the next-generation thin-film technology company, before which he was a Senior Research Scientist and leader of the Thin Film Solar Cells Research Group in the Centre of Excellence for Photovoltaic Engineering at the University of New South Wales in Australia. Dr. Shi holds 11 patents in PV technologies and is a much-published author in the industry. His work has earned him such accolades as "Hero of the Environment" (TIME magazine 2007) and "Corporate Citizen of the Year" at the China Business Leaders Awards 2007. A member of the NYSE advisory board, Dr. Shi has a Bachelor's degree in optical science, a Master's degree in laser physics and a Ph.D. in electrical engineering.

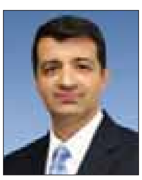

Dr. John Iannelli, Chief Technology Officer, Emcore Corp

Dr. John Iannelli joined Emcore in January 2003 through the acquisition of Ortel. Prior to his current role as Chief Technology Officer, Dr. Iannelli was Senior Director of Engineering of Emcore's Broadband division. Currently, Dr. Iannelli oversees scientific and technical issues, as well as the ongoing research to further Emcore's technology. He has made seminal inventions, has numerous publications and has been issued several U.S. patents. Dr. Iannelli holds a Ph.D. and M.S. degree in applied physics from the California Institute of Technology, a B.S. degree in physics from Rensselaer Polytechnic Institute, and a Master's degree in Business Administration from the University of Southern California.

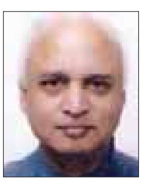

Dr. G. Rajeswaran, President and CTO of Moser Baer Photovoltaic Ltd

Raj served as President and CTO of Moser Baer Photovoltaic Ltd. from July 2007 until October 2008, since which time he has been Group CTO for all the Moser Baer business units and holder of the CEO function for launching new businesses. He spent 22 years with Eastman Kodak Company as the Vice President of Advanced Development & Strategic Initiatives, where he managed Kodak's Japan display operations including technology & business development in Japan, Taiwan, Korea and China. He has also served as Vice President and on the board of SK Display Corporation, and worked in technology development with Brookhaven National Laboratory. Raj has a Ph.D., an M.Tech. and a B.E. in electrical engineering. A much-published author, speaker and patent holder, Raj is a member of the Society for Information Display (SID) and has chaired several international conferences in the field of OLEDs.

Contents

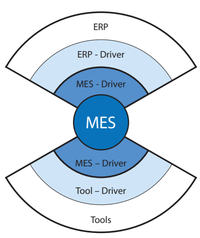

15

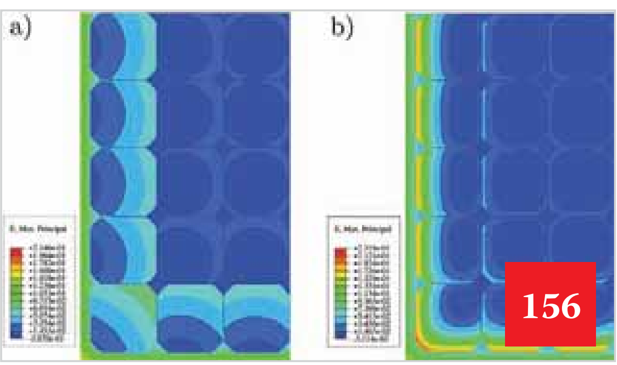
a)
b)
156

THERE IS A NEW PATHWAY

CRYSTALLINE SILICON
High-grade silicon ensures superior quality

INGOT AND WAFER PROCESSING
Controlled environment for consistency and reliability

CELL MANUFACTURING
Integrated manufacturing enhances performance and efficiency

MODULE ASSEMBLY
Market leading products for utility, commercial, and residential applications

Fab & Facilities

News

GE to build 400MW CdTe thin-film module plant; NREL verifies 12.8% aperture area efficiency

PrimeStar Solar module array.

With the acquisition of US-based CdTe thin-film start-up PrimeStar now behind GE, the conglomerate is planning to expand its investments in PV with the building of a 400MW manufacturing plant, potentially bringing its total investment in the sector to over US$600 million. GE also announced that NREL had verified that CdTe thin-film modules from PrimeStar's 30MW manufacturing line in Arvada, Colorado have achieved 12.8% aperture area efficiency. NREL had transitioned the technology to PrimeStar through a cooperative research and development agreement signed in 2007.

GE noted that the new plant will be built in the US, but did not provide any further details regarding the site selection timelines. The company also said that it has entered into more than 100MW of new commercial supply agreements for modules, inverters and total solar power plants.

The company highlighted agreements signed with Invenergy for the supply of thin-film solar panels and GE Brilliance inverters to the tune of 20MW. GE's largest solar agreement to date is with NextEra Energy for 60MW of thin-film solar modules.

Capacity News Focus

Hyundai-Avancis starts work on 100MW South Korean module facility

Hyundai-Avancis has started building work on South Korea's largest CIGS thin-film solar module plant in Chungcheongbuk-do. Over KRW220 billion (US$200 million) has already been invested in the project, which has a scheduled completion date of January 2012. Funding has come from Saint-Gobain and Hyundai Heavy.

This first phase of building work will take the facility's capacity to 100MW CIGS, although Hyundai-Avancis has already announced plans to expand this to 400MW by 2015. The company hopes the plant can propel it into the world's top five CIGS solar module manufacturers by 2015.

Solaria opens new manufacturing plant and solar array at Fremont headquarters

Solaria has officially unveiled its new manufacturing plant and solar array at the company headquarters in Fremont, California. The opening ceremony was attended by Lieutenant Governor of

Photo: Solaria

Solaria's frameless modules are tested according to UL and IEC flat plate standards.

California Gavin Newsom, EPA Regional Administrator Jared Blumenfeld and several other state dignitaries. Solaria's latest development has increased its global capacity to 50MW, and plans are already afoot to build on this expansion next year.

"California has been instrumental in implementing incentives that help foster the growth of solar and other green technologies," Governor Newsom said. "Solaria is an exemplar of clean tech job growth in California – the kind of growth that can be furthered through effective public-private partnerships. Developing and attracting new manufacturing facilities and jobs to our state is my top priority as we work to reinvigorate job growth and retention."

OCI to invest US$1.7 billion in new 24,000MT polysilicon plant

Significant long-term polysilicon supply contracts signed by OCI are fuelling its rapid polysilicon capacity expansion plans. The Korean-based producer has said it will start construction in the second half of this year on its P5 polysilicon plant, which will have an annual production capacity of 24,000MT. It is being built at a cost of US$1.7 billion in Saemangeum Industrial Complex, North Jeolla, South Korea.

The new P5 plant will be OCI's largest, having completed a 10,000MT plant in 2010. Further investments in debottlenecking will take annual capacity to 42,000MT by the end of 2011. However, OCI is planning to begin operations at its P4 plant with a capacity of 20,000MT late next year, taking capacity to 62,000MT.

The new P5 plant is expected to operational at the end of 2013, taking total annual capacity to 86,000MT, though this figure could still rise significantly if debottlenecking can occur at both the P4 and P5 facilities.

SunPower receives conditional loan guarantee from DOE as it dedicates 75MW plant in Milpitas

Prior to the announcement of oil giant Total's takeover of the company, SunPower celebrated the opening of its Milpitas module manufacturing plant while also announcing that the US Department of Energy (DOE) offered the company a conditional loan guarantee for up to US$1.187 billion for its California Valley Solar Ranch (CVSR) power plant. US Energy Secretary Steven Chu and California Governor Edmund "Jerry" Brown joined company officials in April as it dedicated its 75MW solar panel manufacturing facility in Milpitas, California.

Built in cooperation with Flextronics, which is credited with bringing the plant into full production less than four months after the first panel was produced, the

Photo: SunPower

Illustrative potential layout of SunPower's 250MW California Solar Valley Ranch (CVSR) in San Luis Obispo County (as of March 2011).

75MW Milpitas manufacturing plant will supply solar panels for SunPower's 250MW California Solar Valley Ranch in San Luis Obispo County. Construction on the project is anticipated to begin this summer once permitting and financing have been settled. Operations at the plant should begin by the end of this year with the balance coming on line in 2012 and 2013.

Although SunPower will design, build and initially operate and maintain the CVSR project, NRG Solar, a subsidiary of NRG Energy, will adopt all ownership and financing responsibilities, subject to certain conditions. Pacific Gas and Electric Company will plans to purchase all of the output energy from the project.

LDK Solar expands Chinese operations with new US$40 million sapphire wafer manufacturing plant and US$35 million silane gas production facility

LDK Solar is expanding its production base by building a new sapphire wafer plant in Nanchang, and a new silane gas production facility in Jiangxi Province, China. The vertically-integrated PV firm will spend US$40 million on the new sapphire wafer facility, which will have the capacity to supply two million two-inch equivalent pieces of sapphire wafers per year. The new silane gas production facility, located on the site of LDK's Mahong Plant in Xinyu City, Jiangxi Province, China, will supply up to 2,000MT of silane gas to help meet the growing demand from several industries.

Building work on the new silane facility

LDK Solar's trichlorosilane production plant (night view).

is expected to begin in Q3 and finish in Q1 2012, with commercial production likely to start in Q2. The company also recently announced plans to open a cell manufacturing facility in Hefei.

Hanwha spends US$955 million on polysilicon plant in South Korea

Hanwha Chemical is planning to spend KRW1.04 trillion (US$955 million) on a new polysilicon plant to help double sales over the next five years. When construction is completed in July 2013, the Yeosu plant will have the capacity to produce 10,000 metric tonnes of polysilicon a year, and will generate in excess of KRW500 billion (US$4.6 million) in sales in 2014.

"By advancing to the business of producing polysilicon, Hanwha Group could achieve a complete, vertical integration of solar-related businesses, from polysilicon to ingots, wafer, solar cells and modules. This will allow the group to attain strong global competitiveness in the field," a Hanwha spokesperson said.

3M plans to break ground on its ninth manufacturing plant in China

3M is continuing its solar material expansion initiative with plans to construct a manufacturing plant for PV solar materials and renewable energy products in China's Hefei High-Tech Park. The new site, known as 3M Materials Technologies, will focus on the production of the company's Scotchshield Film. The company aims to break ground on the new plant during 2011's second quarter with a two-phased construction period. This is 3M's ninth manufacturing facility in China.

centrotherm, Kinetics Germany to build Africa's largest module production facility

centrotherm photovoltaics and Kinetics Germany have signed an agreement with Société Nationale de l'Electricité et du Gaz (Sonelgaz) to build an integrated solar module manufacturing facility in Rouiba, Algeria. When completed, the 43,000m2 site, located 30km east of Algiers, will be home to Africa's largest solar module factory and have an annual production capacity of around 116MW. Module production will begin in 2014 and help meet the consortium's combined order volume of €290 million.

With the exception of silicon production, the site will cater for the entire solar manufacturing chain, ranging from ingot firing through to solar module end-products. Turnkey systems for the factory, such as ingot furnaces and module production technology, will be provided

by centrotherm, which has also offered its support to Sonelgaz throughout the system commissioning process. Engineering services, construction management, the turnkey production of the building and the technical fittings for the building will be handled by Kinetics.

Solutia ahead of schedule in starting EVA encapsulants production in China

In line with its announcement to produce EVA encapsulants in China in time for June 2011, Solutia has said that its new manufacturing facility in Suzhou is ready to supply commercial-grade Vistasolar EVA encapsulant. This is Solutia's first new EVA production facility to be developed after the acquisition of Etimex Solar GmbH of Germany.

First Philec Nexolon to build 400MW solar wafer-slicing facility

First Philippine Electric, the electronics arm of the Lopez Group, is building a 400MW solar wafer-slicing facility alongside Korean firm Nexolon. The 3.5-hectare factory will be located in the Philippine province of Batangas.

The joint venture, named First Philec Nexolon, is planning to invest around US$100 million in the wafer-slicing facility, which will have the capacity to manufacture 240 million wafers annually. The Lopez Group holds a controlling 80% share in the facility, with SunPower holding the remaining 20%.

Wacker Chemie starts construction of polysilicon plant in US

Wacker Chemie's long-planned construction of a 15,000MT per annum polysilicon plant in Cleveland, Tennessee has officially broken ground. The project is said to cost around US$1.5 billion and will create some 650 new jobs when the plant becomes operational in late 2013. With other planned capacity expansions in Germany, Wacker reiterated that it expects to reach an annual polysilicon capacity of 67,000MT in 2014.

Rudolf Staudigl, Wacker Chemie AG's CEO noted that almost the entire output of the Tennessee plant has already been contractually secured for 2014, and the project is the single largest investment ever made by the company. Interestingly, Wacker had previously stated that the plant would cost about US$1.1 billion.

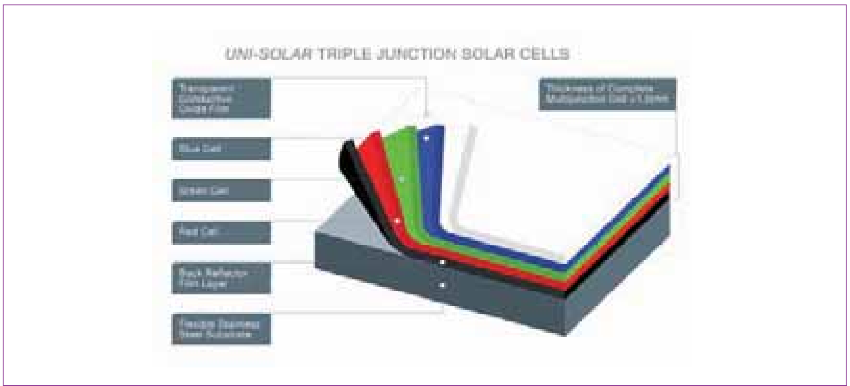

Photo: United Solar

United Solar's triple-junction thin-film cell composition.

ECD's United Solar to set up thin-film PV laminates manufacturing facility in Ontario

Energy Conversion Devices' (ECD) subsidiary, United Solar, revealed its plans for a 75,347 square foot manufacturing facility in Ontario, Canada. Anticipated to be operational by August, the facility will create up to 80 jobs for the production of the company's thin-film solar laminates, which will be sold specifically in the Ontario solar market. United Solar plans to modernize the building and organize capital equipment, with an expected total first-year project capital of US$4 million.

Basing its manufacturing facility in LaSalle, Ontario, United Solar fulfils the domestic content requirement of the Ontario Power Authority's FiT program. An initial annual capacity of 15MW is scheduled, with a designed ramp-up ability to 30MW once market demand is established.

Daqo to build solar module plant in Ontario, Canada

Daqo New Energy has added to its plans to become an integrated PV producer with the news that it is planning to tap the Ontario market by building a majority-owned module assembly plant in the province. In collaboration with JNE Consulting, the polysilicon producer will invest an initial CAD$5 million (85% Daqo/15% JNE) in a 25MW (first phase) capacity plant, which is expected to be operational in the fourth quarter of 2011.

DC Electronics expands San Jose manufacturing facility

DC Electronics, a PV cable manufacturing firm, is adding 12,500 square feet to its production facility in San Jose, California. The expanded site will span 42,500 square feet and be used to create a new, state-of-the-art ESD (Electro Static Discharge) and testing area. It will also be used to ramp up capacity by adding an additional four manufacturing cells.

The expansion follows on from the successful introduction of high-level systems at the facility. All production lines are now ISO 9100:2008, AS9100B certified and have obtained UL/CSA safety approval. DC has also installed advanced IT and data management systems to ensure real-time quality and on-time delivery tracking.

Photo: Wacker Polysilicon

Wacker's granular polysilicon.

Other News

Hilco Industrial to act as agent in sale of Evergreen Solar's Devens, Massachusetts, facility

Hilco Industrial will be overseeing the sale of Evergreen Solar's PV solar panel facility in Devens, Massachusetts. The

Aerial view of Evergreen Solar's Devens, MA manufacturing plant.

manufacturing facility produces wafers, solar cells and solar panels with a rated output of 160MW per year and an actual output of over 180MW per year. The site's original cost in 2009 was over US$425 million. Although Evergreen's Devens facility is still in operation, it began a scheduled phased shut down in March this year.

Eyelit posts record-breaking 2010 revenue figures

The photovoltaic manufacturing management software provider, Eyelit, has posted record-breaking Q4 and annual revenue figures for 2010. The figures were driven by significant increases in revenues for both products and support services and helped Eyelit to experience its seventh consecutive quarter-on-quarter rise.

Dan Estrada, Eyelit's vice president of sales, has attributed the popularity of Eyelit's MES system as a cornerstone of the company's ongoing success, "We are also seeing increased interest from wafer fabs running Promis MES, which are looking to migrate to a new platform such as the Eyelit MES. We expect a record turnout of customers and stakeholders at our User Conference in August, where a former Promis MES customer will present how they were able to complete the migration to the Eyelit MES in just 60 days."

Hanwha Solar America unit to establish advanced PV R&D centre; names Chris Eberspacher president

Hanwha Holdings (USA) has established Hanwha Solar America LLC as a US subsidiary, which will set up an advanced photovoltaic technology research and development centre in Silicon Valley. Industry veteran Chris Eberspacher has been named president of HSA and will also serve as global CTO of Hanwha's various solar businesses.

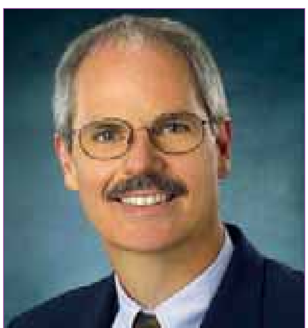

Chris Eberspacher has been appointed president of Hanwha Solar America LLC and global CTO of Hanwha's various solar businesses.

Eberspacher will provide technical leadership for all of Hanwha's solar businesses, including Hanwha's global solar R&D and manufacturing networks. He has more than 25 years' experience in the PV industry in a variety of technology and management roles, most recently at Applied Materials, where he served as CTO of the company's solar division.

No additional details about the specific location, construction/operational timeline, or capabilities of the R&D centre were disclosed.

Product Review

Schiller Automation

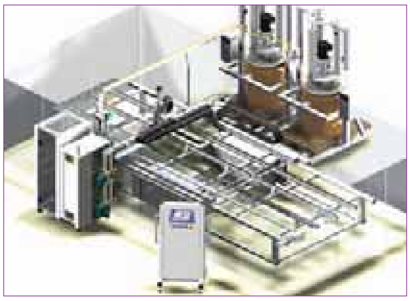

Schiller automates junction box assembly for higher reliability and lower cost

Product Outline: Schiller Automation has developed a module production concept known as the Sunriser, which facilitates the realization of production line designs, engineering concepts and factory plans that have a consistent cost-of-ownership per watt ratio. One of the first aspects of the application to be released is the JBO Junction Box 250–300, which automates and improves the reliable terminal box assembly for both crystalline and thin-film photovoltaic modules.

Problem: Rising cost pressures are leading to increased demand for automated concepts in the PV industry. The right automation strategies can also improve product assembly reliability and quality consistency, especially in difficult assembly processes such junction boxes.

Solution: The JBO Junction Box 250–300 is a fully automatic process solution for safe and reliable terminal box assembly. The system links the module and junction box to each other in one processing step, almost 'on the fly.' Designed for when time-consuming, costly and error-prone manual labour is not available, the SunRiser is claimed to keeps up with the rising degree of automation and higher capacity rates, delivering a high degree of connection quality and functionality over the entire product lifecycle.

Applications: Fully-automated junction box assembly of both crystalline and thin-film photovoltaic modules.

Platform: The system is claimed to have >97% availability and > 99.9% operating yield. Module dimensions of up to 1.1 × 1.7m; scalable machining cycle of between 20 and 90 seconds per module. Floor space requirement is 30m^2, which allows the bonding of up to 300MW of modules.

Availability: Currently available.

Oerlikon Leybold Vacuum

Oerlikon Leybold Vacuum's magnetically levitated turbo molecular pumps offer full system integration

Product Outline: Oerlikon Leybold Vacuum has launched a new magnetically levitated turbo molecular pump series that offers full system integration of all components. Resistant to process particles and deposits, the Magintegra pumps save costs and space for manufacturing processes within coating and industrial applications in the rough, medium, high and ultra-high vacuum regime.

Problem: Today, full system integration of all components without any superfluous cabling is one of the most important requirements for the design and operation of a vacuum system in industry, R&D and analytical business fields.

Solution: Turbovac Macintegra removes the need for space dedicated to a separate frequency converter, and provides a compact, flexible design, excellent vacuum performance and a standardized program of accessories, offering maintenance-free operations in most industrial processes. The pumps are resistant to process particles and deposits, while process-induced shock venting is tolerated to a high degree. Assembly is possible in any position and angle, and the rotationally symmetrical housing is combined with a frequency converter that can also be mounted flexibly.

Applications: Coating and industrial applications in R&D and pilot production.

Platform: The use of five-axis magnetically levitated bearings means the pump requires little maintenance, displays a high degree of safety against hydrocarbons, operates at extremely low vibration levels, and is offered with communication interfaces and an intelligent monitoring of pump parameters.

Availability: Currently available.

MV Products

MV Products' vacuum foreline traps improve pump lifetimes

Product Outline: MV Products is introducing a line of vacuum foreline traps for manufacturing processes that create large volumes of solid byproducts, such as those used in producing solar cells, HB-LEDs and Li-ion batteries.

Problem: Vacuum pump lifetimes can be impacted by byproducts used for deposition processing. This can lead to increased manufacturing costs and, in the case of forced downtime for repair or replacement, disruption of the flow of production.

Solution: Featuring user-selectable filter elements, MV Products' Vacuum Inlet Traps include the MV Multi-Trap, which has a knock-down stage plus two stages of filter elements. It is capable of up to 2,500 cubic inches of solids accumulation; for applications up to 50 CFM (cubic feet per metre), the Posi-Trap is most suited. Both are offered in several sizes and feature stainless steel, copper gauze, molecular sieve, activated charcoal, pleated polypropylene (in 2, 5 and 20µm pore sizes) and Sodasorb filters.

Applications: Suited for MOCVD, HVPE, PECVD or LPCVD processes used in manufacturing solar cells, HB-LEDs, and Li-ion batteries which can generate high volumes of particulates.

Platform: Offered in several models to accommodate different manufacturing process applications and volume requirements, the range can incorporate a wide range of filters for trapping solids, organic solvents, and other contaminants and protecting vacuum pump systems from oil back-streaming.

Availability: Currently available.

The Manufacturing Execution System (MES) at Conergy

Maiko Kenner, Conergy AG, Frankfurt, Germany

ABSTRACT
In 2006, Conergy AG started construction on one of the most advanced solar factories in the world in Frankfurt (Oder). On 35,000 square metres, a fully integrated and fully-automated wafer, cell and module production facility was created – all under one roof. Since 2008, production has been running at full speed and every day more than 3,000 premium modules roll out of the factory. This paper outlines the Manufacturing Execution System (MES) process put in place by Conergy during the planning phase of the factory, to monitor and control the complex and merging production processes.

Three good reasons for an MES

Interaction of production areas

In the manufacture of solar modules, each area of production has its own optimum. Wafer production, for example, is based on the key performance indications of wafer quantity per kilogram of silicon and throughput per hour which, from a wafer manufacturer's point of view, should be as high as possible. However, what is good in wafer production may be counter-productive for the subsequent cell production. Thinner wafers or wafers that were sawn at high speed can break more easily or have surface damage and therefore could potentially cause problems in subsequent production steps. A perfect interaction of the production areas is therefore of enormous importance. The advantage experienced by Conergy is that all production steps from sawing the wafer to the finished module, take place under one roof in Frankfurt. A process-spanning control system brings all the production areas to an optimum level, thereby supporting the production of good wafers, cells, and durable solar modules.

Process control and traceability

Additional reasons for setting up an MES are the necessary traceability and process control, especially in the area of sensitive chemical processes in solar cell production. Conergy grants a 25-year performance and a five-year product warranty for its PowerPlus modules – a complete and accurate data collection of the history of origins is therefore essential. This was modelled on the experiences of related industries. In the production of control units for airbags, for example, the continuous monitoring and logging of production steps and materials used is required by law. Although there are no rules to this respect in the solar industry, Conergy is still committed to a similar process control.

The control of sensitive processes

Highly automated production steps enable a high degree of repeatable quality with very low fluctuations. This approach to manufacturing allows for fewer interruptions and tighter process limits. The result is a more sensitive process that must be closely controlled. Based on these fundamental ideas, the individual functional groups within the required MES were compiled and prioritised in the early planning phases of the factory. The system should be primarily used for production monitoring. The final decision and control processes, however, should remain in the hands of process managers.

The focus of attention in setting up the MES was the master data and data collections such as production data acquisition (PDA) and machine data acquisition (MDA), which provide the basis for machine monitoring, reporting, analysis, metrics, process visualization and traceability. The system was developed to MES-level according to the original IPO principle (input, processing, output). This initially required the creation of a database through input layers like data interfaces and input terminals. This was followed by the processing of data and ultimately the presentation of the data from different perspectives and levels of abstraction in the output layer. The long-term goal for setting up the MES is the optimization and monitoring of the process windows, production orders, machine utilization and the machine throughput.

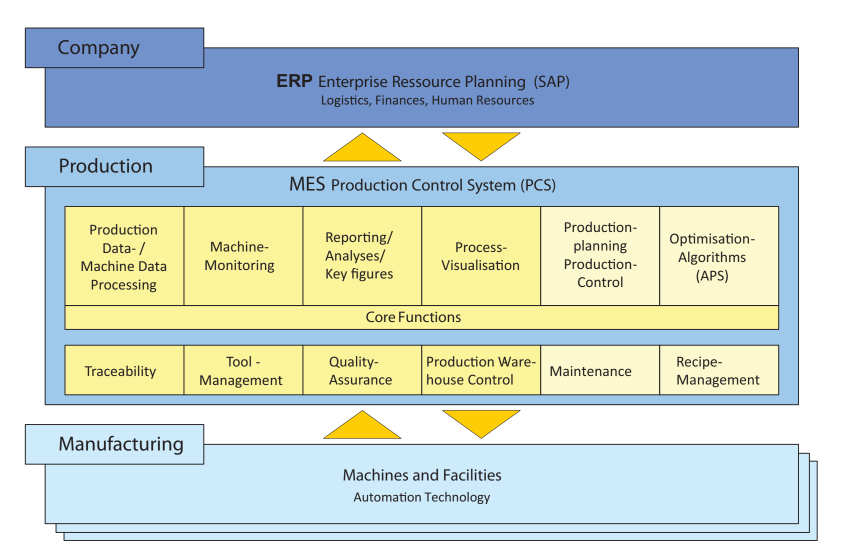

Figure 1. Core functions of an MES.

Creating the foundations

The goal of building a new MES was an exciting challenge for our IT professionals. The primary reasons for this lay in the still-fledgling PV industry. Standard processes and solutions were or still are a rarity. Production processes, fresh from the lab, were converted into mass production processes in the factory in Frankfurt for the first time.

The production tools were, for the most part, prototypes, which were initially custom manufactured in small numbers. There was no long-term experience with those processes under industrial conditions and standardization was still in its infancy. Data interfaces were not usually available and if so, only in rudimentary ways, quite contrary to the standardized interfaces considered a

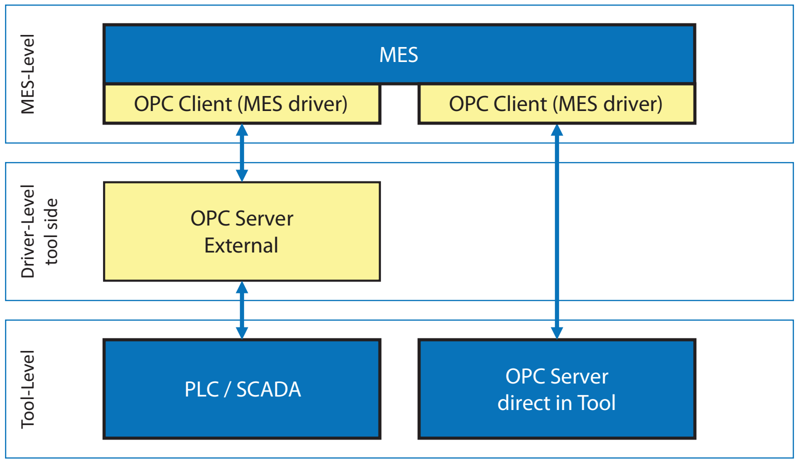

OPC is a standardised interface for data exchange between different systems, primarily used in automation technology. It is based on the data transmission with standard data types, events and methods. OPC utilises a server-client architecture.

The most common specifications within the OPC:
OPC DA: Process data transfer
OPC A/E: Event and alarm handling

Figure 2. Diagram showing OPC data exchange.

'must-have', such as "SEMI Equipment Communication Standard (SECS)" and "Generic Model for Communications and Control of Manufacturing Equipment" (GEM) (see: http://www.semi.org) in the semiconductor environment.

The technical interface

The primary data source of an MES is the automated data communication with its process tools. The interfaces extend from digital signals on an electrical level and proprietary text files, up to direct access to data blocks PLCs (Programmable Logic Controllers). During the building of the Conergy solar factory, however, the interfaces were for the most part not included in the machine manufacturers' standard package. Interfaces such as PV2 (Communication Equipment Interface Standard for PV production systems, including PVECI) (see SEMI: http://www.semi.org/en/Press/CTR_030751) were not approved until mid-2009 as the industry standard and are only gradually being included in machine technology. The Swiss manufacturer Meyer Burger, whose wafer saws Conergy uses in its factory, was among the first machine suppliers to retrofit the existing tools with the new standards.

OPC: the language of automation technology

At Conergy, tools that only give digital signals are usually connected to the MES via PLC. Here, the PLC act merely as data converters of the electrical signals. The communication channels mainly the integrated transport systems that have internal PLC systems, and are connected through them. Conergy was able to retrieve most of the handling steps and simplest plant components via this standardized interface. For communication between these systems and the MES, finished software packages are used to route the data from the controllers via the OPC server to the MES (see Fig. 2). Here, the OPC servers are used as an interface converter between the controllers and the MES. Through the use of standard software packages, the connection of machines can be carried out quickly and easily. The connection between PLC – if they are a common type – and the OPC server, installed for this purpose, usually takes 30 minutes to an hour. The access, created between the OPC server and the PLC in this case, is directly to the data blocks existing in the PLC. Through the use of OPC as a data transport protocol, only "transfer logic" is required. Conergy accommodated this in a MES-oriented driver layer – in so-called MES-drivers who take on these functions centrally (see Fig. 3).

MES drivers: pre-processing and compression of data

The dependencies between the data and the understanding of the data are located within the MES drivers. The benefits for Conergy are, on the one hand, a significant relief to the MES and a clear division of responsibilities, and on the other, the company can limit the amount of data that has to be processed by the MES-core to what is necessary, forwarding the payload directly into the defined internal MES modules. One example is the data gathered regarding wafers and cells at Conergy's Frankfurt (Oder) facility. Within a minute, approximately 120–130 wafers or cells can be processed in a single step. For each process step, the resulting data is transferred to the MES driver, which checks the consistency of the data received with the expected data structure and the allowed value limits.

Upon successful input, verification of the data will be converted into the internal communication structures and transferred to the assigned MES internal modules for processing, such as the online statistical process control (SPC) module. The internal MES modules can process the data directly, without having to check for errors in the structure or values outside the measuring ranges. If the MES drivers recognize incorrect data or data that needs to be filtered out, no load is created inside the MES core.

As described in the OPC sample, the MES driver determines the time of data retrieval, the conversion and classification of data and indicates which MES module within the core must receive which data from the data packet.

Extensible mark-up language (XML): the universal interface

Another interface option in the Conergy solar factory is the data communication via XML files or XML streams (see Fig. 4). This is mainly a way to provide data from measuring systems. The advantage of XML files is the platform-independent data interpretation. In addition, the data processing within the MES drivers takes place asynchronously and thus independently of time; after a successful measurement, the measuring system

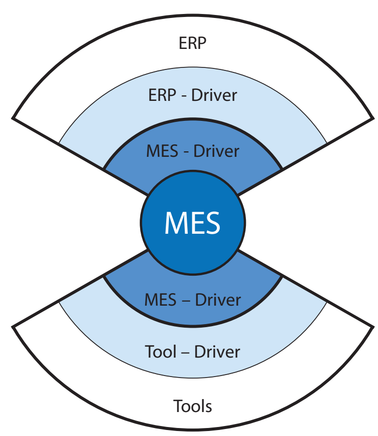

Figure 3. MES data transfer layers.

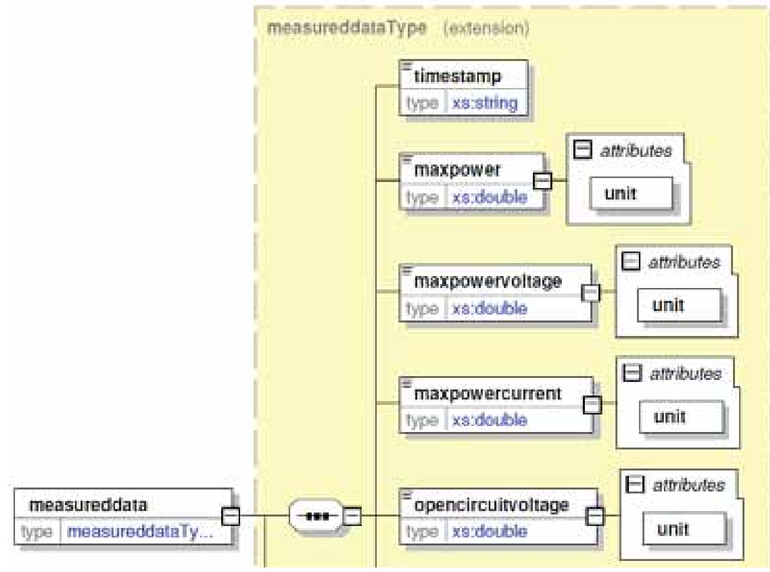

XML is a structure definition for character-based data files. It is used to exchange structured data, is platform- and implementation-independent, but remains readable for employees. XML was specified by the World Wide Web Consortium (W3C) in the first version in 1998.

By means of XSD files (XML scheme definition), the contents of an XML file can be automatically validated in relation to its structure and data. XML data can be transferred platform-independently as a file or as a stream (e.g. TCP/IP), which makes them flexible.

Figure 4. Schematic showing XML structure breakdown.

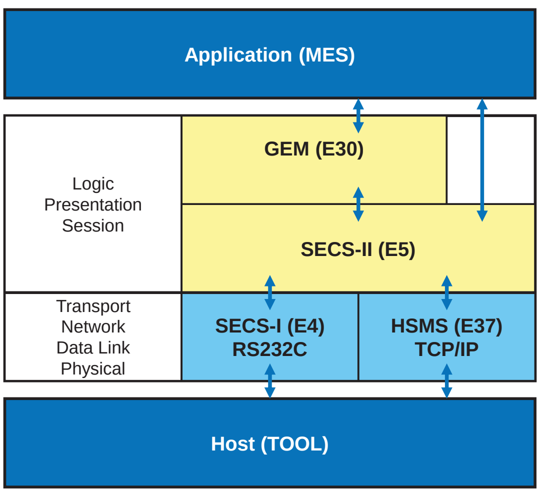

SECS / GEM an interface protocol standardized by the SEMI Association (Semiconductor Equipment and Materials International). It unifies and simplifies the communication and the exchange of data between production tools and parent control and monitoring systems. The protocol includes both the cyclic and event-driven process data and status retrieval as well as transmission of control commands and configuration parameters.

Within SECS/GEM Standards SECS-I, SECS-II and HSMS are used as communication protocols.

SECS-I:	SEMI-E4	Protocol for the communication via the serial interface RS232C
HSMS:	SEMI-E37	Protocol for the communication via TCP/IP
SECS-II:	SEMI-E5	Definition of message types and of message structure
GEM:	SEMI-E30	A generic model for defining the behaviour of a tool, its conditions, the business logic and the combined use of the available message types

Figure 5. The SECS/GEM interface protocol.

creates an XML file and stores it in a defined transfer point. The MES driver is now able to retrieve the files at a later date and process them. These XML files also have the advantage that they can be exchanged on different channels, such as FTP, email or other forms of file transfers between different systems, cyclically or event driven. This allows data to be easily inserted at a later point. Conergy uses the data import of information provided by external testing laboratories or materials suppliers; this means that the XML files are easily readable by employees and can be validated by XSD files (XML scheme definition). This strongly supports the fast integration of new data into the MES and a facilitation for the successful exchange of data.

SECS / GEM and PV2: the sophisticated interfaces

In a process that requires real-time monitoring as well as collections of data and information on the condition, XML files are only partially suitable. For data communication close to the process, specialized interfaces such as SECS / GEM or PV2 can be used (see Fig. 5). They are considerably more sophisticated and more standardized. However, due to their complexity, it requires an increased effort to integrate them into the MES. PV2, for the most part, is based on SECS/GEM. Their advantage becomes apparent during the integration of these interfaces. For example, the abstract machine model, standardized through the GEM (SEMI E30), controls the interpretation of the machine condition according to SEMI E10. In terms of material tracking and process data processing, a SECS/GEM interface also offers standardized functions. One major advantage is that events can be stored for so-called message structures. The buffering of events and their associated message packets in terms of data collection is an essential advantage. This way, very short pending messages are not overlooked.

Derived from the SEMI SECS / GEM norm 2009, the interface standard PV2 was adopted for the photovoltaic industry. PV2 comprises the TCP / IP transport layer (SEMI E37 (HSMS)), the data presentation layer SEMI E5 (SECS-II), the abstract machine model SEMI E30 (GEM), the machine condition definition according to SEMI E10 as well as the time synchronization according to SEMI E148 that integrates the known network standard Network Time Protocol (NTP).

SEMI E10 and E79: machine conditions and efficiencies

For Conergy, the SEMI norms E10 and E79 are a great support in the analysis of machine time and productivity, making

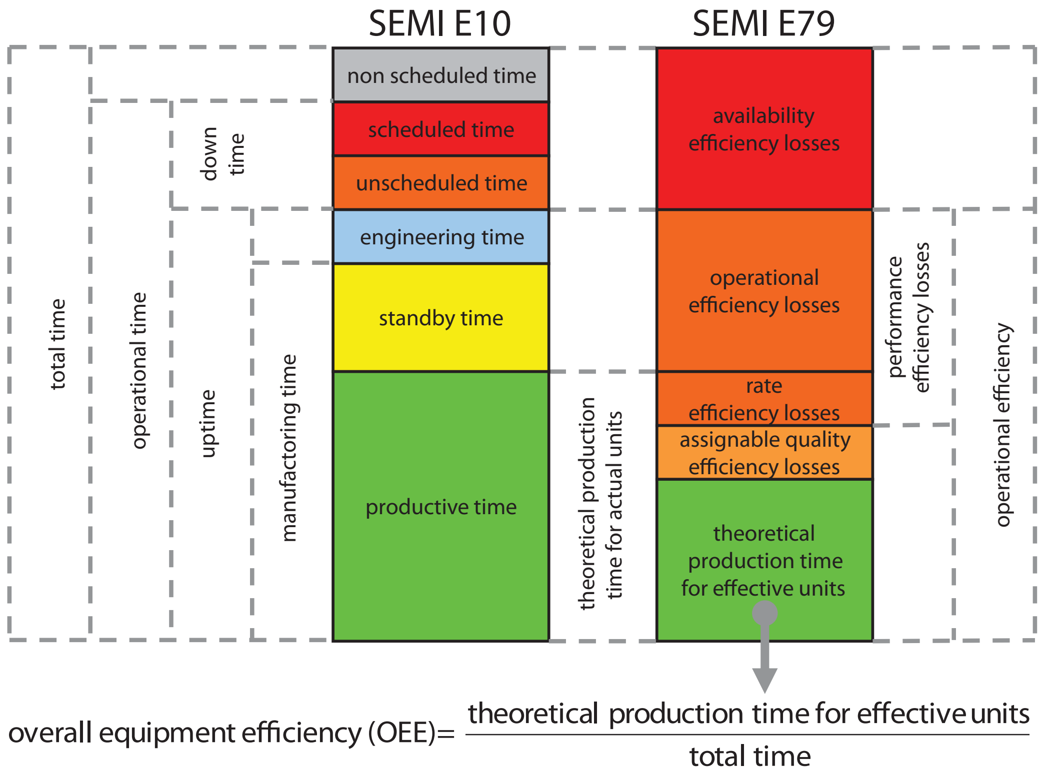

Figure 6. Condition analysis.

the processes and tools comparable to each other and measurable. SEMI E10 defines the machine reliability, availability and serviceability. In contrast, SEMI E79 looks at the productivity and quality yield. Through the norm, the overall machine efficiency was defined as an abstract level for the first overall efficiency equipment (OEE). According to the SEMI E10 norm, six main

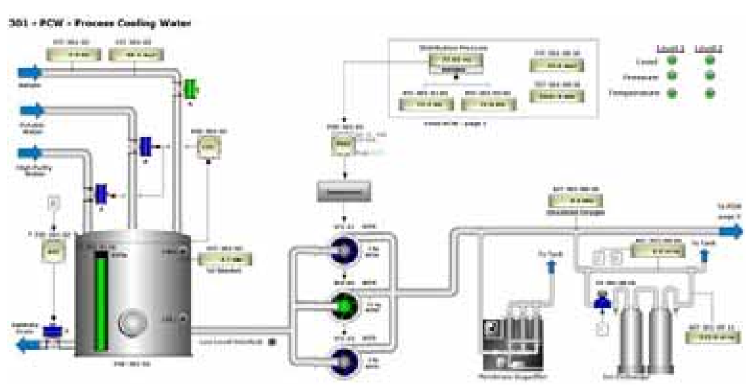

conditions are permitted. The SEMI E79 norm uses these and combines them from the perspective of efficiency (see Fig. 6).

In the course of continuous improvement processes, necessary in every business, an essential increase in time productivity is derivable from the SEMI E10. The SEMI E79 implies less process delays and an increase in quality. The OEE values describe whether or not a production tool is used optimally. Based on the condition classification and efficiency definitions, standardized through the SEMI norms E10 and E79, key figures needed from a production perspective are easy to calculate. Among these key figures are, for example: mean time between failures, mean time to repair, mean time between assist and mean time between interrupts.

Core function 1: reporting, analyses and key figures

Through the central data collection at Conergy, the automated data interfaces and the user terminals create an internal database, which the core functions of the MES builds on. When the construction of the Conergy solar factory began, the online data analysis, through the use of SPCs, was quickly created, based on the acquired process data. Because of these, raw measurement values can be concentrated, set in correlation and provided with threshold values and control limits.

An example of this is the monitoring of the measured cell efficiencies of the individual production lines. A machine-induced change in the cell efficiencies can be monitored per line – in case of deviations, the MES automatically send notification. This direct online monitoring provides a prompt statement about the current situation of the production for a variety of data measurements and process steps. A central reporting system, which is a type of intranet for production data, allows a view into the development of process values. Through this tool, any authorized employee, from any workstation within the production, can access all historical and current data of the production and have it presented in various graphical and tabular reports with selectable filters and groupings. Shortly after the introduction of this central access to the data analysis, it became one of the most widely used systems in the solar factory and an integral part of the everyday working life.

Core function 2: machine monitoring

Machine monitoring is one of the most common methods for monitoring a factory. The usual standards in the semiconductor industry, according to the norms SEMI E10 and E79, also allow a comprehensive and comparative analysis of machine conditions in the related solar manufacturing industry.

Conergy has more than 300 production machines. Analyzing them is part of daily business for the employees and individual reporting of the base systems is possible through only a few clicks of the mouse. For example, the operational time in use of individual tools within one line can be compared with each other but also with tools of several lines. This allows Conergy the rapid ability to identifiy critical tools, which would reduce the throughput per line for an extended period of time.

To obtain a finer breakdown and representation of the individual condition details, next to the abstract machine conditions according to SEMI E10, the main conditions are broken up further. The analysis of the machine conditions allows production managers a permanent view of the capacity utilization of the tools, one can also keep an eye on any failure vulnerabilities or maintenance efforts.

Core function 3: quality assurance

Quality assurance is one of the most important criteria in a facility. Because the MES is primarily installed in many parts of the production, it accompanies all work processes of employees. MES supports quality assurance as early as from the receipt of goods. Through an integrated assurance system, all bought-in goods must pass a quality verification. A material subject to an audit requirement will be actively suspended from the MES until the final outcome of the investigation and not available for use within the production. All data collected during the quality inspection will be logged. Based on defined limits, the system will decide independently whether or not the relevant batch or pallet can be released for production. These MES functions exist throughout the factory, from the value-adding steps, to the final quality verification of finished products.

The semi-finished wafers and cells are monitored meticulously. This is mainly done through automated processes. They detect the slightest deviation from the desired parameters, monitor them and incorporate them into the quality grading. This ensures that only efficient and visually flawless cells are installed in the Conergy PowerPlus module. In the final inspection of the photovoltaic modules, the optical inspection is also carried out by specially trained employees who report even the smallest abnormality of a module to the MES. Based on the collected data from visual inspections, product master data and electrical measuring data, the MES determines the class of quality assigned to the product and which sales order number it will receive.

Core function 4: tracking

To meet stringent quality requirements, all process data, process steps and detailed classifications are recorded for each individual and centrally provided on the reporting system. Using the example of module production, each working step up to the customer delivery can be tracked. Conergy maintains this traceability through permanent monitoring and continuous identification of each individual for each step of the process flow.

Conclusion

The development of an MES is extrremely complex. Therefore, Conergy decided in the very beginning to establish the MES in such a manner that each step of the process – from the silicon block to the finished module – can be recorded in detail. The basic considerations of which functions the MES should have were already of crucial importance during the planning phase of the factory. Thus, the individual core modules within the system were selected in such a way that despite the wide range of functions, clear distribution of tasks and responsibilities were created, yet the system still offered enough flexibility for changes and additions. These benefits can be seen in everyday business operations; Conergy is able to analyze its production data from several years in seconds and run comparisons. This is based on the extensive data structure that over time formed a comprehensive database.

An advantage for process technologists at the site is that within a short time, they can examine historical mass data for potential improvements, test new ideas and provide effective process developments with fast successes. In addition, Conergy can comprehend the history of origins for each individual module and thus, even with a module that is already installed on a roof, can trace its history, up to the respective silicon block.

About the Author

Maiko Kenner has been Head of IT in Frankfurt (Oder) since 2006. The graduate IT business engineer has been responsible for the development of the MES since construction began. Prior to joining Conergy, Kenner worked as an independent IT consultant for several companies.

Enquiries

Conergy SolarModule GmbH & Co. KG
Conergy-Strasse 8
15236 Frankfurt (Oder)
Germany
Tel: + 49 335 521130
Email: m.kenner@conergy.de

Performing experiments in photovoltaic manufacturing using knowledge management technologies

Michael Hoffmeister & **Matthias Zapp**, Fraunhofer Institute of Manufacturing Engineering and Automation (IPA), Stuttgart, Germany

ABSTRACT

Supporting a smooth application of new wafer materials and handling equipment into photovoltaic mass production requires extensive testing of new wafers and equipments under a range of potential operating conditions. The management of such experiments, both in laboratory and production environments, demands the integration and management of a multitude of differing information. This includes static data-like equipment, specifications and experiment settings, online machine data regarding process signal and events – but also unstructured human knowledge, which is available in manual and test reports. To efficiently deal with these kind of complex environments, knowledge management techniques have proven to be a promising approach in various industrial applications.

This paper depicts, by means of a photovoltaic wafer-testing platform at Fraunhofer IPA, how the application of automation systems and knowledge management techniques leads to more effective experiment management. More precisely, the gathered knowledge from the wider range of information included in the analysis of experiments can be re-used during future experiments and the manual effort is significantly reduced.

Introduction

Effective and accountable experiment management is essential for a smooth transition of new wafer materials and handling equipment in mass production environments. As a prerequisite for the start of production, new wafer materials and equipment need to be carefully assessed under a variety of future production conditions. Therefore, simulation tools – and more importantly physical testing environments – need to be applied.

In such testing environments, the gathering, analysis and re-use of the wide range of available information like parameters, machine data and human experience during experiments, have proven to be a major challenge. The complexity of a formal approach for experiment management is based on the fact that the relevant information is represented in very different ways: documents, databases, spreadsheet tables, machine-data and data available on the internet. Transforming human knowledge into a machine-understandable format and interconnecting it to other data is especially challenging when using only traditional data management technologies.

In general, managing knowledge inside companies and making it re-usable is a challenge for any organization. According to Fraunhofer IAO [1], companies estimate that more than 50% of their added value is a direct result of knowledge. However, 50% of these companies state that they only use 20–40% of this information. Knowledge management systems are widely expected to leverage efficiencies in a multitude of application fields.

This paper depicts a concept for a knowledge management system (KMS) to support experiments in the photovoltaic industry. The concept will be based on semantic technologies and interconnects static data, online machine data and human knowledge. Any information gained during an experiment will be systematically stored and will be available for re-use in future analysis.

In the following, the concept will be described using the photovoltaic testing and demonstration platform at Fraunhofer IPA which serves to evaluate different wafer types and automation equipments like grippers, actuators and sensors.

In the first section, the underlying business cases for performing experiments and for applying experiment management systems in both laboratory and production environments are investigated. The photovoltaic testing platform at Fraunhofer IPA and the data items occurring during experiment management are then described in more detail. In addition, the requirements for an ICT system to automatically execute and track experiments as well as for a complementary knowledge management system are defined.

Furthermore, existing knowledge management technologies and tools are looked at with respect to their suitability for the described business cases. In particular, the potential of semantic technologies for the integration of information from different sources and domains is highlighted. Finally, the formal concept for a knowledge management system to manage experiments in photovoltaic manufacturing is described, which is currently in development at Fraunhofer IPA.

Motivation and business cases

Experiment management in photovoltaic manufacturing

Today, the photovoltaic industry is strongly characterized by short innovation cycles. Products, production processes, and equipment is continuously adapted to improve the process quality and to cut down the overall production cost. The reduction of photovoltaic wafer thickness and the optimization of the throughput of production lines are just two such major leverage factors.

At the same time, wafer breakage needs to be prevented in order to ensure stable production processes. Therefore, the optimization of production parameters and automation solutions needs to work alongside careful investigation of their effect on quality and scrap rates [2]. A systematic testing of new wafer materials and handling equipment needs to be conducted to ensure a smooth transition to mass production environments. Besides the use of material and process simulation models, the execution of experiments in physical testing systems under a variety of test conditions can play a key role.

Knowledge management for experiments

During such experiments, a variety of static data-like equipment, material and product specifications, experiment settings like machine parameters, online machine data like process signal and events are available as well as a large amount of unstructured information from engineers such as observations about incidents during an experiment. Traditionally, only a subset of this data is structured and used for the experiment analysis.

Unstructured human knowledge about materials, equipment and events is highly important information for the analysis of experiments and for the re-use of the analysis results in the future; however, it is challenging to efficiently include it in an experiment management system. The engineer needs to be able to easily insert his knowledge into the experiment management system to make it re-usable during later experiments. In practice, simple spreadsheet and word processing tools are mostly applied. As a consequence, the re-use of experiment results and relevant information mainly depends on personal experience.

In order to strive for more substantial analysis, a wider range of information needs to be incorporated. At the same time, the complexity and the manual effort for the engineer need to remain limited. In synthesis, the objective needs to be the conduction of more experiments with profound analysis in less time. As a consequence, the use of sophisticated knowledge management tools should be envisaged.

The application: PV testing platform at Fraunhofer IPA

The testing and demonstration platform for wafer handling experiments at Fraunhofer IPA (see Fig. 1) is applied to evaluate and optimize handling equipments like grippers as well as their configurations in the context of industrial and research projects. In addition, the platform is used to test innovative wafer types, e.g. thin wafers, under a variety of production conditions. Investigating the influence and interference of single production and handling steps on the wafer is the focus of this investigation [3], which results in complex experiment processing and data analysis requirements.

A large amount of different data items and experience knowledge is available at this laboratory environment (see Fig. 2). All these data items are relevant to plan experiments and for analyzing their results.

As is the case in other production environments, a high number of static information is available regarding the testing platform. Equipment and components have specifications, manuals and operational guidelines, which exist in one form of written documents or are available on web pages. Other static information may include the specifications of tested wafers, which are available in the form of Excel tables.

In addition, experiment settings such as the number of runs and machine recipes are available through the line control system. Online machine data such as sensor data and event notifications can be gathered from the equipment and can be used for analysis of the experiment results (see Fig. 3).

Figure 1. Automated test and demonstration platform for wafer handling experiments.

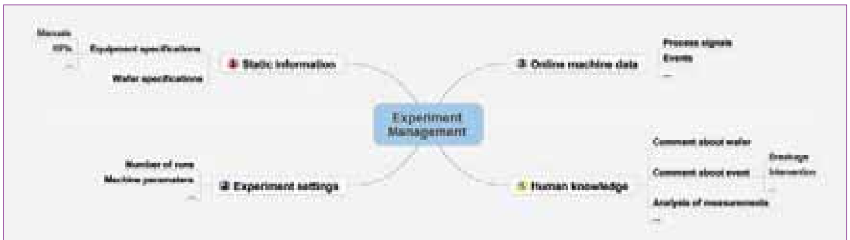

Figure 2. Data items of the PV test platform.

The most important – but often not stored and analyzed – information is available from human personnel. This could include a simple comment on the wafer properties or a more detailed description of an event occurring during an experiment run as well as information about potential root causes for test results.

In addition, test reports of former experiments contain highly valuable information. In practice, this information is kept only as the personal experience of the engineer and not often systematically re-used.

Requirements towards system-based knowledge management

In order to perform knowledge management for photovoltaic testing and demonstration platforms or for similar manufacturing environments, requirements can be defined both towards the automation of the experiments as well as towards the knowledge management system working over it. The user requirements towards the automation of the PV test platform are:

UR1 The automation system shall be able to track the execution of an experiment ('run') and which experiment parameters have been used.

UR2 The automation system shall be able to track process and measurement signals and shall link these to individual experiment runs.

UR3 The automation system shall be able to track recipe parameters given to the individual laboratory equipments for each individual experiment run.

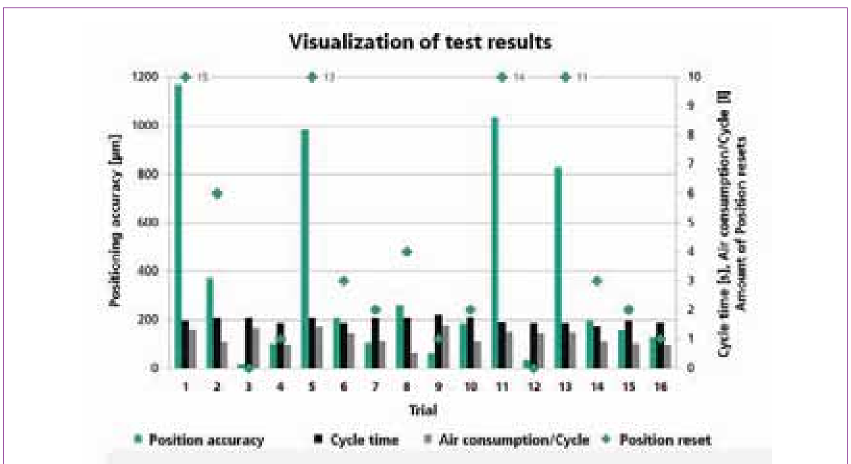

Figure 3. Visualizations of test results for wafer testing.

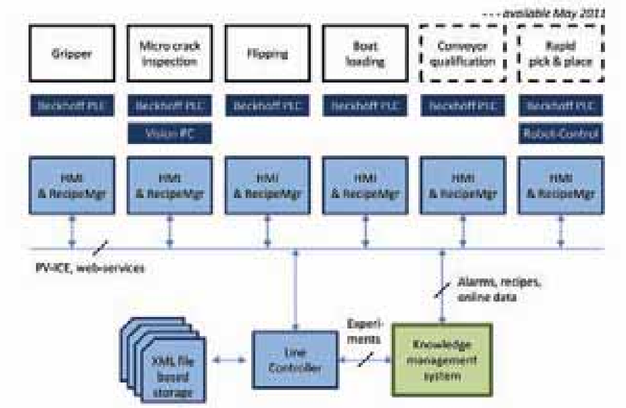

Figure 4. ICT landscape for PV testing line.

UR4 The automation system shall be able to track important alarms and events arising while performing individual experiment runs and shall allow the use of consistent time stamps throughout all equipments.

UR5 Ideally, requirements UR1-4 should be achieved without the need of costly, customized software or demanding further human input.

The user requirements for the knowledge management system working on top of the automation system are:

UR100 The knowledge management system (KMS) shall conceptualize experiments and individual runs and shall describe experiment parameters in detail.

UR101 The KMS shall be able to incorporate and track user comments at any time and shall relate them to experiment runs and/or laboratory equipments.

UR102 The KMS shall provide a structured way to acquire human observations as well as the settings of important manually controlled parameters for individual experiment runs.

UR103 The KMS shall maintain all equipment and product (wafer) specifications and shall make single specification information available to analyses and reporting.

UR104 The KMS shall allow integrating existing factory data bases (e.g. SQL data bases) and expose their data contents towards correlation, integrative analyses and reports.

UR105 The KMS shall allow dealings with human readable documents (PDF, Word and Excel documents) and expose their contents towards full-text search, analyses and reports.

UR106 The KMS shall allow browsing the contained knowledge and specifications at each equipment's HMI (human machine interface).

UR107 The KMS shall be scalable and shall avoid costly customizations when being introduced at a company.

ICT landscape of the PV testing line

In order to fulfill the above requirements and to support the processing of a high number of experiment runs with different recipes, a dedicated ICT landscape has been developed at Fraunhofer IPA (see Fig. 4).

Equipment level

A key element of the ICT landscape is the 'HMI & RecipeMgr', which replaces conventional human machine interface (HMI) solutions with an extensible, plug-in based adaptor framework. This .NET based framework runs directly on the Beckhoff PLCs and interacts deeply with the executed PLC programs. A HMI plug-in imports the Beckhoff HMI project definition and allows executing the Beckhoff HMI panels within the integrated solution, while maintaining common look-and-feel and benefitting from advanced .NET screen rendering (e.g. for high-speed trend graphs).

At the same time, the RecipeMgr plug-in reads and interprets the variable definitions inside the Beckhoff PLC and makes them available for recipe upload and report download. Using a point-and-click approach, the plug-in defines different recipe and report templates, which allows reporting different aspects of the process execution in great detail, while keeping message sizes small. By identifying only eight control variables, the plug-in permits the remote control execution of the equipment including automatic capturing of reports. The plug-in allows reading XML recipes and writing XML reports directly at the equipment; it enables standalone execution of laboratory equipment. Further on, the plug-ins enable online connection to supervisory systems by realizing standard SEMI PV-2 [4] and easy-to-use web-service interfaces.

Further plug-ins are interfacing with cameras, industrial vision software and robot controls, which capture screen recordings and browse the internet –all integrating into a common look-and-feel user-interface, which can be adopted to different company designs and styles.

By reading existing HMI definitions and by accessing PLC variable declarations, the HMI & RecipeMgr realizes the user-requirement UR5, as no costly proprietary implementation effort is needed. The RecipeMgr plug-in realizes the user requirements UR1-UR4 and makes the information, which is needed for later knowledge management, available to various host systems.

Supervisory level

The second cornerstone in the ICT landscape is the 'line controller', which implements supervisory control functions for the PV testing line and small manufacturing lines without the need for costly customization. The line controller interfaces via SEMI PV-2 or web services with the RecipeMgr plug-ins of each piece of equipment and takes advantage of the herein defined recipe and report templates. For maintaining recipe settings and for storing reports, the line controller relies on the storage of individual XML and CSV (Excel) files, which seems a very basic

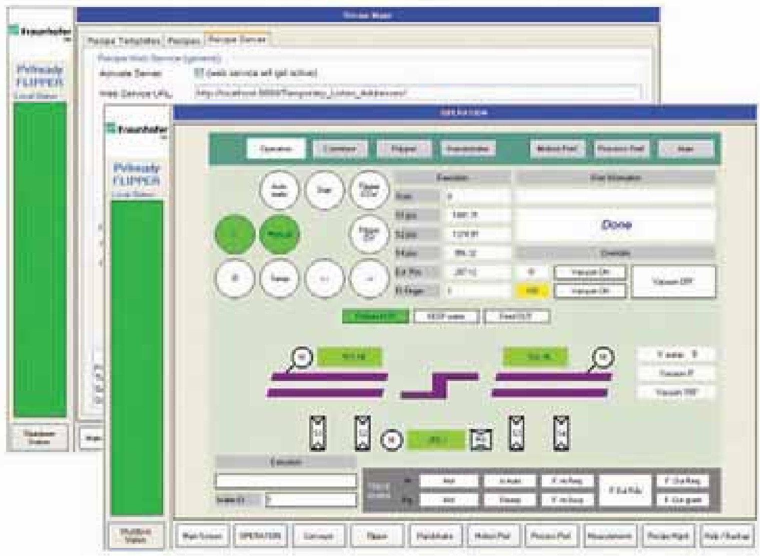

Figure 5. Equipment-level HMI and recipe management.

approach but avoids costly customization and allows the re-use of the files within a large multiplicity of computer programs. Hence, this approach is optimally suited for the application within the rapidly changing laboratory environment. All recipe and report functions are available through drag-and-drop operations, which implement an easy-to-learn, but efficient user interface. By providing a two-dimensional grid of recipe settings, the line controller allows the execution of multi-step experiment sequences. This feature enables performance of complex experiments without introducing variances brought in by human operators into the experiment result data. The automatic capture of report files ensures that a maximum of experiment result data is always available for later analysis.

Conclusion and suggestions for further development

The set of RecipeMgr plug-ins within individual equipment and the line controller supervisory control allows for orchestrated line behaviour and the conductance of even complex experiment scenarios; in this sense, it exposes the same functionalities as equipment controls and manufacturing execution systems in conventional production shop floors. Despite these proven capabilities of the system, there are still important links missing for an effective knowledge management for the management of experiments. More

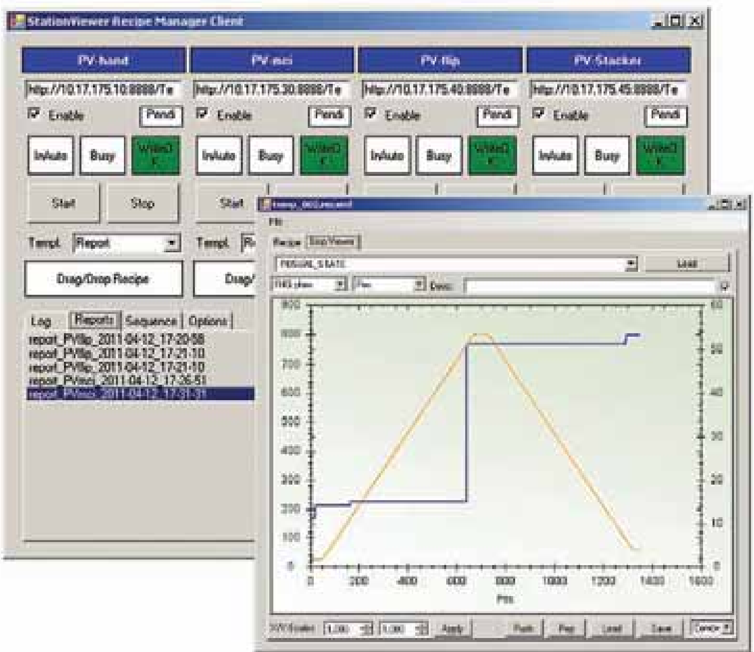

Figure 6. Supervisory-level line controller and recipe management.

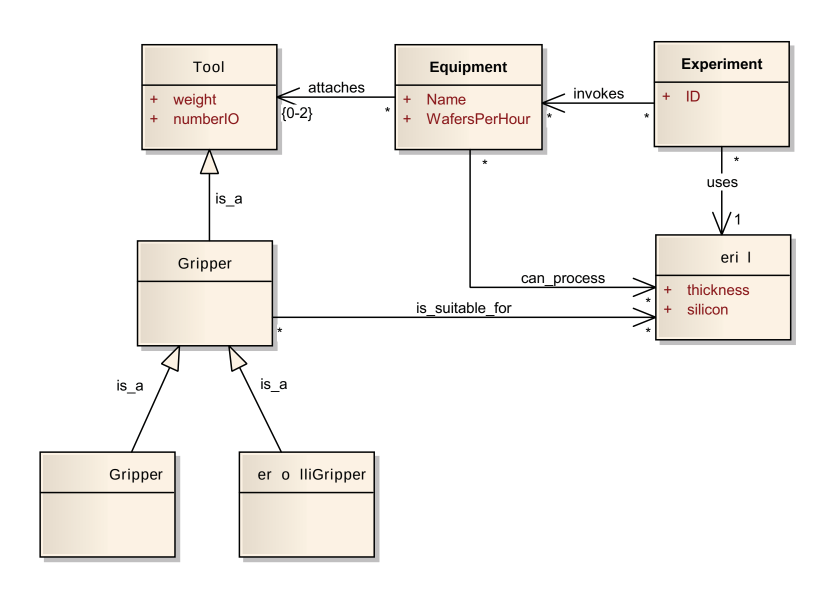

Figure 7. Exemplary ontology for the PV testing line.

precisely, it is not known to the system which exact equipment and material combinations were used when conducting the experiments, what the intention of the planning engineers was (design of experiments) and what observations were made by human personnel.

This gap shall be filled by introducing a knowledge management system, which is online coupled with the manufacturing system of the photovoltaic testing line.

Semantic technologies and knowledge management systems

Knowledge management can be accomplished by a large variety of approaches; in the last year, it has been widely acknowledged that ontology-based knowledge management systems can be used effectively, when the context of the KMS can be kept constrained and well-defined. Based on this philosophy, later used extensively by linguistics, ontology is now becoming an ICT approach for organizing data.

Ontology as a method of structuring information

According to Gruber [5], an ontology is a "formal, explicit specification of a shared conceptualization". Conceptualization is performed in order to decompose the knowledge about a specific domain (the context) in well-defined and non-overlapping terms. It is formal in order to be used by technical systems, it is explicit in order to avoid inconsistencies and it is shared commonly among a group of people in order to be used by all of them.

Aside from this theoretical definition, ontology can be seen as a carefully chosen dictionary of 'concepts' on a specific domain, which describes not only the concepts but also their meaning, and uses different relations in order to interlink them. This can attach knowledge items to the different concepts and perform analysis and reasoning along the different relations. An exemplary ontology is depicted in Fig. 7.

The widely known unified modelling language (UML) syntax is used to graphically describe this ontology. Concepts of the ontology are expressed as classes; the relations between concepts are expressed as associations. Concept definitions may have attribute declarations, which are inherited to sub-concepts.

In this small ontology, 'experiments' are defined, which are restricted to use one wafer type: 'material'. The experiments are indentified by an attribute 'ID'. For performing experiments, 'equipments' are invoked by the experiment, which are described by the attributes 'name' and 'WafersPerHour'. Every equipment declares to 'can_process' a range of materials. The materials are described by 'thickness' and 'silicon type'.

Ontologies are perfectly suited for classifications. In this small ontology, a classification is done towards the ranges of tools for the PV testing line. A 'gripper' is a certain 'tool', which means that every gripper can be treated as a tool, sharing the same attributes. 'VacuumGripper' and 'BernoulliGripper' are both specializations of the concept gripper. When reasoning, the ontology will conclude that when a certain material 'is_suitable_for' the concept gripper, it will be automatically suitable for all VacuumGrippers and BernoulliGrippers.

Rules can be stated towards ontologies; they can be used to create 'virtual' relations and attributes by concluding on knowledge, which is already contained in the ontology. For instance, the weight of a wafer can be approximated by its thickness and side lengths, using some specific mass density. A gripper can describe that it can handle wafers up to a certain weight and maximum dimensions.

During analysis, these 'virtual' relations and attributes will be treated exactly the same as the direct ones. This means a 'query' can be stated, detailing which grippers were already used for a certain experiment and which grippers will be additionally suitable for performing this experiment.

Ontology-based knowledge management systems

Referring back to knowledge management systems, which are now supposed to be ontology-based, only very fundamental concepts will be expressed by UML or further specification languages. The users of a KMS will require an adequate tool for expressing knowledge in human readable form but, at the same time, should be able to express relations to other concepts and set attributes as above. One way of achieving this is through ontology-based Wikis (so called semantic Wikis). Regarding content management

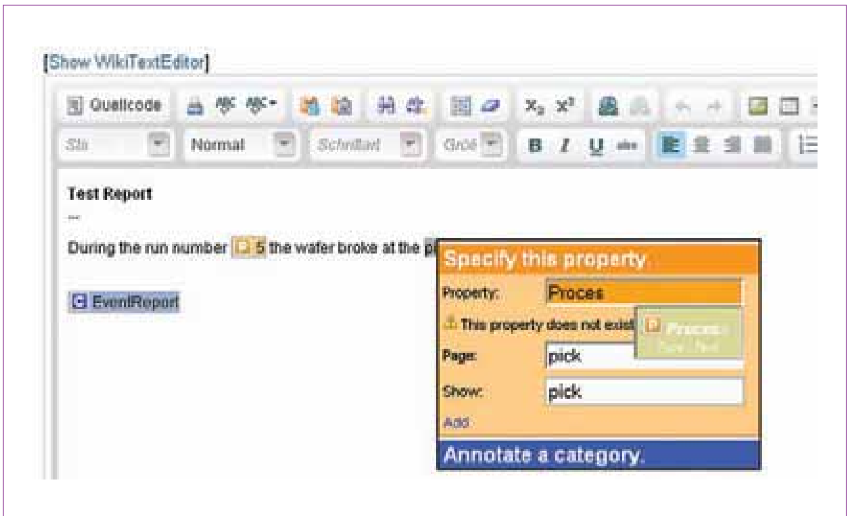

Figure 8. Exemplary annotation of rich text in Semantic Media Wiki+[6].


FESTO
Maximise output!
The new complete wafer handling solution from Festo – the High Speed H-Portal
Maximised use of space with extremely high speed and dynamics.
For more information about the exiting H-portal contact us at solar@de.festo.com

Figure 9. Unique features of the realized knowledge management system.

systems, these Wikis are becoming very user-friendly ways of expressing contents by editing text pages and using special annotations to link to graphics, make lists or captions. In this manner, Wiki pages are already a form of knowledge inside a KMS, as pages have captions and its subsections also have captions. Linking between different pages is already supported.

Moving on to ontology-based Wikis, these Wikis attempt to gather semantic knowledge (relations and attributes) from the users. This can be achieved in two ways:

- A 'standard form' section is displayed whenever the user creates a new Wiki page based on an ontology concept. By filling out this standard form, the user can quickly elaborate important relations and attributes for this sub-concept. After filling it out, the user can proceed to the 'free format' section of the Wiki page and can add descriptions, specification, experiences as with any other Wiki system.
- A 'semantic annotation palette' is provided to mark some special semantic attributes, while writing free format Wiki text. This is as easy as marking text with the mouse cursor, going to the 'semantic annotation palette' and selecting, so that this marking sets a specific semantic attribute for the edited page (see Fig. 8).

In either approach, additional knowledge might be added to the Wiki page by adding files and documents in proprietary format (such as PDF documents, Excel tables or Word documents).

Proposition towards a system-based knowledge management system

Fraunhofer IPA is currently integrating a state-of-the-art semantic Wiki system

Intranet-based environment	The semantic Wiki system will run on an internal web-server within the protected intranet of a company and can be used through web-browsers. This will make it possible for any personnel (engineers and students) to use and contribute to the system, even directly on the equipment HMI (see UR106).
Standard forms feature	The system allows providing standard forms to be filled out for every Wiki page. This feature will drastically increase experiment quality. The content of the standard forms will be directly available for analyses, interactive querying and reporting (see UR102).
Free format user comments	A 'semantic annotation palette' will allow easy addition of user comments in free format. This will enable users to freely describe observations. Photos, drawings, tables and sound files can be used to contribute to these observations (see UR101).
Document management	The system will allow attaching any kind of documents and specifications to each Wiki page. Therefore, the system can act as single source of information (see UR103).
Full-text search capabilities	Some semantic middlewares are integrating text-mining tools into the environment, such as [7]. This allows doing a full-text search on documents indexed by the systems. Important terms can be provided by using auto-completion features. Classification of documents can be automated (see UR105).
Connection to data bases	Due to their import capabilities, nearly every semantic middleware can import data from conventional SQL data bases. Furthermore, some middleware allow the online-integration of data base entries [8,9]. Using that feature, during querying and analysis, the middleware will not only search the own data bases but also the online integrated databases for applicable knowledge. This unique feature allows integrating and unifying an landscape of data bases, which evolved over time such as in manufacturing environments (see UR104).
Online connection to PV equipment	As described, data from experiment runs will end up automatically within the system as applicable knowledge and can be directly used for analyses and interactive querying (see UR100, UR102).
Interactive querying	The system supports the generation of analyses and queries by means of a point-and-click feature. Queries can be created using lists of already available concepts, relations and attributes of the stored knowledge. These queries can be stored afterwards and made available as regular Wiki pages using this mechanism, every user can utilize a set of highly specialized analyses.
Plug-ins for analysis	The semantic Wiki systems provide the possibility to create ones own plug-ins for displaying content within the system. This will ultimately lead to the capability to apply statistical functions (e.g. from SPC) directly within the analysis workflow of the system.
Scalability and cost-effectiveness	The chosen commercial product is relatively low-cost; the deployment on web-servers allows for scalability (see UR107).

Table 1. Unique features to be integrated into proposed knowledge management system.

within the existing ICT landscape of the PV testing line. The objective is to create and demonstrate an easy-to-apply knowledge management system for manufacturing environments in laboratory or even on an industrial scale. The novelty will lie on the capability of the system to integrate data online from shopfloor automation level, recipe data and report data together with conventional sources of knowledge like wiki pages, various documentations and feedback from human personnel.

The ICT landscape of the PV testing line is already realizing the user requirements of UR1-4, as described above. Together with the unique approach of RecipeMgr and line controller, it will collect all sensible data, such as tracking of experiment parameters, recipe settings and sensor measurements, for almost no additional effort in customization and costs. User requirement UR5 is therefore fulfilled.

The chosen approach allows integrating a set of unique features, as seen in Table 1.

Summary

During the course of this paper an approach for a semantic-based knowledge management concept was presented by using a photovoltaic wafer testing and demonstration platform. The main objective is to improve the quality and efficiency of automatic execution and analysis of experiments. Using this automation and knowledge management system, the range of data considered for the experiment management is expanded and the complexity of the operation as well as the required manual effort is reduced. Based on the defined ontology, the gathered knowledge can be more easily interconnected and re-used.

As a consequence, an automation and knowledge management system with integration of online machine data was outlined, which was built onto the existing ICT landscape of the PV test platform with minimal effort. Various unstructured documents, operator feedback and expert knowledge are now recognized, stored and linked in a more efficient manner than before. The presented concepts are not only suitable and beneficial for test and staging environments, but can in future also be applied in small manufacturing lines.

References

[1] Lectures from Fraunhofer IAO's 'WIKI course' [available online at http://wiki.iao.fraunhofer.de].

[2] Reddig, K. 2009, "Overview of automation in the photovoltaic industry", *Photovoltaics International*, Vol. 4, pp. 18–29.

[3] Fischmann, C. et al. 2010 "Automated handling and transport of crystalline photovoltaic wafers" *Proc. 25th EU PVSEC*, pp. 1677–1681.

[4] Boettinger, F. et al. 2010, "Methodology and benefit for the equipment integration with standardized PV equipment communication Interface", *Proc. 25th EU PVSEC*, Valencia, Spain.

[5] Gruber, T. R. 1993, "A translation approach to portable ontology specifications", *Knowledge Acquisition* Vol. 5, No. 2, pp. 199–220.

[6] Semantic Enterprise Wikit [available online at http://smwforum.ontoprise.com/smwforum/index.php/Semantic_MediaWiki_Plus].

[7] Semantic Miner [available online at http://www.ontoprise.de].

[8] Jena semantic framework and Oracle database: [available online at http://download.oracle.com/docs/cd/E18283_01/appdev.112/e11828/sem_jena.htm].

[9] Onto Studio product [available online at http://www.ontoprise.de/en/products/ontobroker/].

About the Authors

Michael Hoffmeister is a researcher and project manager at Fraunhofer IPA. His research interests are intelligent production modules, semantic and knowledge-based technologies and advanced statistical process automation. In addition to providing consultancy for large international IT projects (requirement engineering, system architecture), he looks after European projects in the domains of ramping-up assembly systems, knowledge management in the machine tool industry, micro part joining technologies and multi-staged manufacturing automation systems (ERP, MES and shopfloor).

Matthias Zapp is a project manager at Fraunhofer IPA. Prior to joining Fraunhofer he studied business informatics at the University of Cologne and worked for an international IT consultancy in the area of logistics and product costing. His fields of expertise within the photovoltaic industry are modelling and simulation of logistic processes, knowledge management in production, semantic technologies and production IT.

Enquiries

Fraunhofer Institute of Manufacturing Engineering and Automation (IPA)
Nobelstrasse 12
70569 Stuttgart
Germany
Tel: +49 711 970 1604
Email: zapp@ipa.fraunhofer.de

The Q-Cells research line: a development tool for new silicon solar cell technologies

Markus Fischer, **Peter Engelhart**, **Helmut Hinneburg**, **Christian Klenke**, **Andreas Mohr**, **Jörg Müller**, **Sven Schmidt**, **Kevin Wachsmuth** & **Peter Wawer**, Q-Cells SE, Thalheim, Germany

ABSTRACT
This paper presents the Q-Cells research line (RL) as a core of the Reiner Lemoine Research Centre, including the technical set-up, the organization of the operation and current results of cell concepts processed in the RL on a regular basis. Trends of cell parameters for those processes are shown, and a focus is presented regarding the results of our high-efficiency cell concepts for multi- and monocyrstalline material processed in the RL with stabilized record efficiencies of 18.4% and 19.2%, respectively. In addition, we discuss the process flow and the results of a monitoring procedure that is used to check the rear-side passivation quality of the company's equipment. Results of our current passivation stack show a surface recombination velocity of below $S_{rear} < 10$cm/s, well suited to fabricating p-type Si solar cells with efficiencies above 20%.

Introduction

The production capacity of the photovoltaic industry has grown tremendously during the last few years with annual growth rates of around 30% [1]. New capacity can be built either from state-of-the-art technology or from new technologies with an increased ramp-up risk. A trade-off between speed and risk minimization is needed to keep pace with the tremendous developments encountered during the race for higher cell efficiencies, higher throughput, and lower costs per cell and per Wp respectively. The PV roadmap for c-Si gives an idea of the challenges to be expected in the years to come [2]. Thus, a tool is needed to close the gap between development at laboratory level for evolutionary and revolutionary new technologies and their fast implementation in the mass production environment.

Q-Cells has been producing solar cells for more then 10 years and has been ranked in the Top 10 Si solar cell producers for several years. Since 2010, the company has also been processing these solar cells into modules under its own brand name. These modules are consequently installed in solar systems, at utility scale as well as in rooftop installations of residential and commercial scale. Thus, Q-Cells is widening its scope from a cell producer to a provider of PV solutions. Much experience in mass production and automation, a high quality level during production and testing, as well as the availability of leading-edge technologies have been and will continue to be the basis for satisfying the demands of customers. In response to this, in 2007 Q-Cells built a research centre that was intended to fit current and future needs of Si solar cell development, characterization, module and cell reliability as well as equipment evaluation. The Reiner Lemoine Research Centre (RC) officially opened in summer 2008. It took about 12 months from the initial idea in summer 2006, to first equipment move-in onto the shop floor and a further six months to the start of processing in December 2007. The RL has been in regular operation since January 2008.

Conception of the Q-Cells research line

The RL is installed in an at-grade industrial building with a factory work floor of about 3000m^2 at the Q-Cells "Solar Valley" Campus in Bitterfeld-Wolfen, Germany as shown in Fig. 1.

The chemistry supply and disposal area is situated on one side of the building. Supply of H_2, N_2, SiH_4, O_2, KOH, DI-water, compressed air and cooling water, as well as the disposal of rinsing water and used chemicals, is connected to the Q-Cells bulk supply system. Supply and disposal of special chemicals is provided in Intermediate Bulk Containers (IBCs). A separated room for gases enables a centralized connection of special gases to the RL equipment. The piping to the point of use is fixed at the ceiling. This set-up enabled a fast and cost optimized building, installation and hook-up phase, and gives flexibility for future installations. This flexibility is vital to enable quick reaction to new machine trends. Fixed lanes for

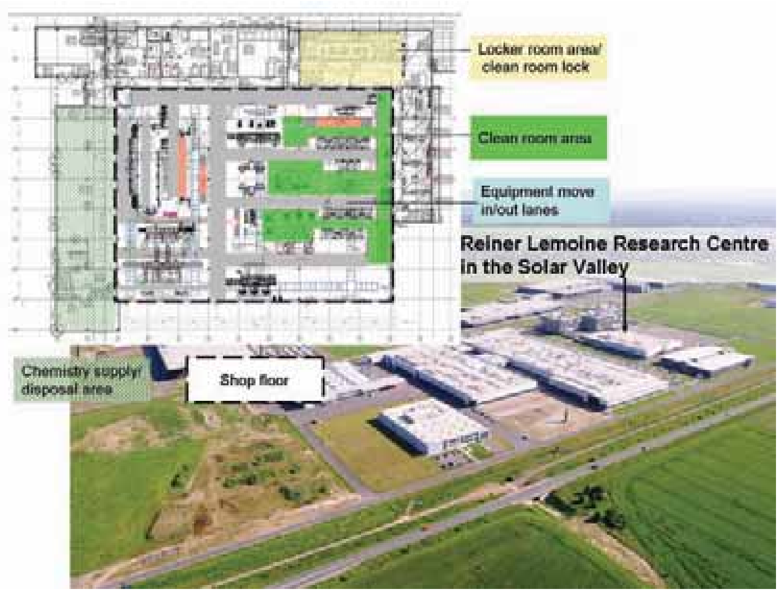

Figure 1. Layout of the Q-Cells RL with indicated main functional areas and view of the Q-Cells location in the Solar Valley area.

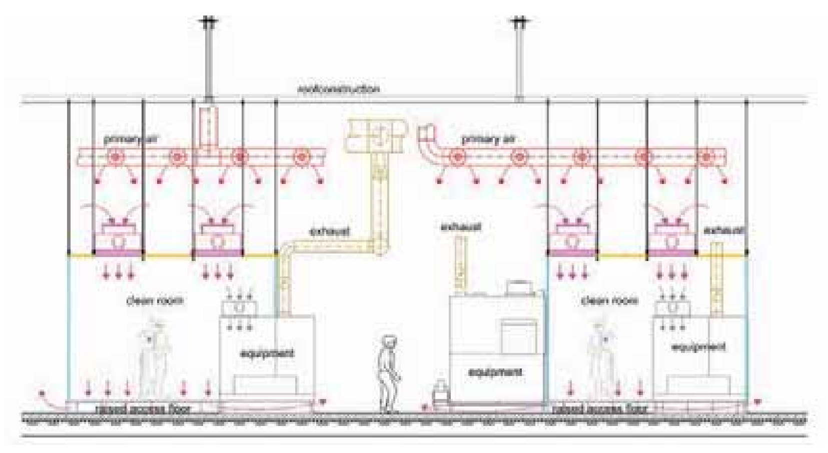

Figure 2. Schematic of the construction of the 'room-in-room' cleanroom concept applied in the Q-Cells research line [2].

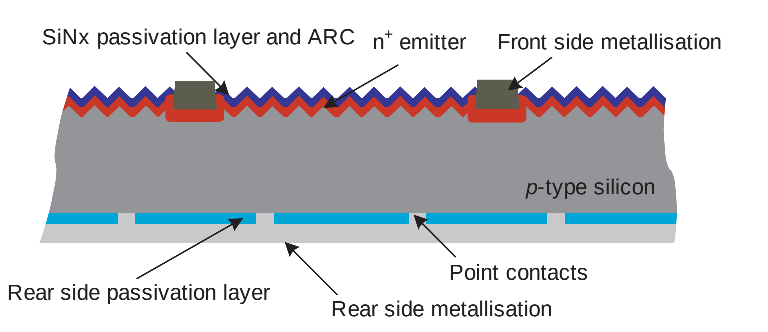

Figure 3. Schematic cross-section of the solar cell design with passivated front and rear (not to scale).

equipment move-in and move-out were defined to fulfil this requirement, as shown in Fig. 1. The RL can be used for the pre-production evaluation of new machine concepts and equipment types.

Throughput equipment was selected to enable experiments as well as production of standard multi- and monocrystalline Al-BSF-cells, back contact cell concepts as well as cell concepts with new front- and back-side passivation technologies [3–5]. A trade-off between processing small sized wafer batches and batches of up to several thousand wafers was realized by installing in-line and batch processing equipment having either automated standard wafer carrier interfaces to enable compatibility with the Q-Cells fab environment or manual loading/unloading interfaces. The equipment consists of more then 20 different production like proto-type machines, partially automated for wet chemical processing, diffusion, oxidation, and annealing, PECVD, PVD, laser processing, screen printing and patterning.

A cleanroom area of 600m^2 (see Fig. 1) was integrated into the shop floor using a 'room-in-room' concept. Fig. 2 shows a schematic cross-section of the cleanroom. It is designed to maintain class M6 down to M3.5 at 0.5µm according to the process requirements. Using this concept, the whole shop floor can be held at a cleanroom level of M6.5 without the need for additional filter equipment.

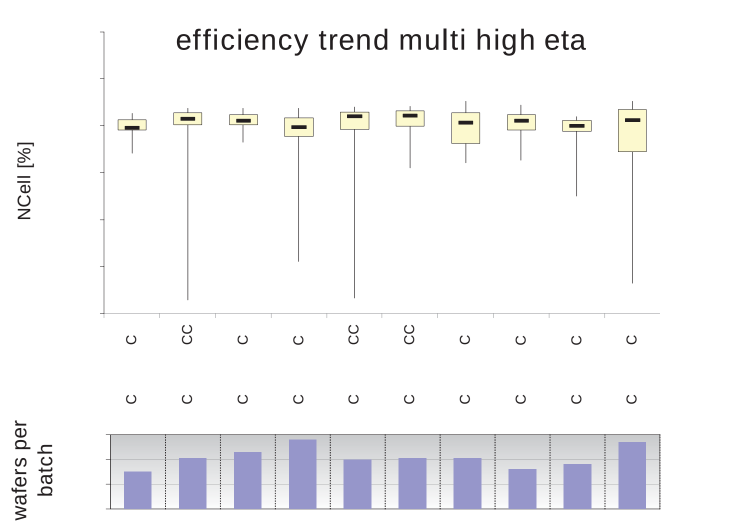

Figure 4. Trend of the high efficiency multi batches processed in the RL during week 43 in 2010 and week 9 in 2011. Each batch contains between 30 and 60 wafers.

Organizational set up within Q-Cells

Organizing a strong operation RL was a key success factor. The strong mass production manufacturing competence of Q-Cells was capitalized using synergies and by gaining experienced production line staff to join the RL organization. These employees and a core team of engineers and technicians have been the backbone of the RL organization together with newly hired skilled workers. The responsibilities in processing and engineering respectively are shared between the front end of line (FEOL – processing until ARC) and back end of line (BEOL – metallization process + test). Experiments, base line monitoring processes, pre-production, and production orders have been processed since spring 2008 on a regular two-shift work base from Monday to Friday. Round-the-clock shift work was tested during a six month period and can be introduced on demand after clearance with the local Q-Cells workers council. This enables high flexibility during the introduction of new products with reduced impact on the standard production lines.

Maintenance and facility management support as well as IT and logistics services are delivered from the Q-Cells production organization and were not built up within the organization of the RL. Besides the cost savings, the experience and know-how, equipment, service contracts, cleaning services and other synergies can be implemented as a 24/7 support, ensuring a lean RL organization that is focused on research and development activities.

Results

Processing different pilot and monitoring processes as well as experiments in parallel, standard procedure in semiconductor manufacturing is a new way of working in the PV industry. A tight planning procedure, clearly documented recipes, well-defined supply notes for the process of record and standard operating procedures enable this high flexibility, which is carried out by RL's operational team.

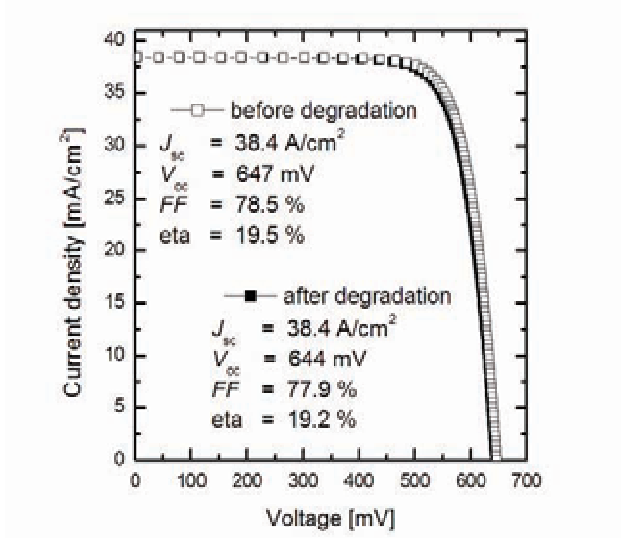

Figure 5. ***I-V*** **characteristic (total area measurement) of a 6" monocrystalline Si solar cell before and after light-induced degradation. The data are independently confirmed by Fraunhofer ISE CalLab.**

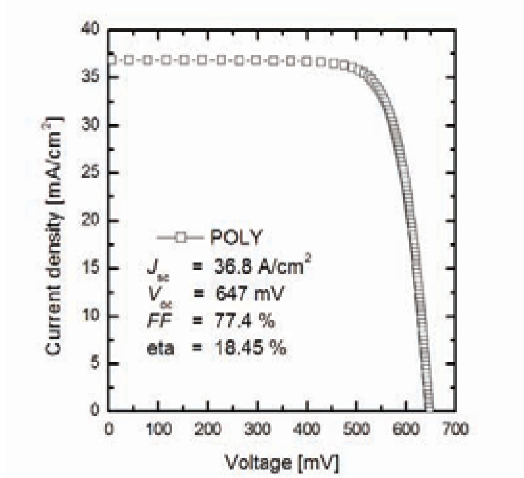

Figure 6. ***I-V*** **characteristic (total area measurement) of 6" multicrystalline Si solar cells using poly Si feed stock material (after light-induced degradation). The data are independently confirmed by Fraunhofer ISE CalLab.**

A pilot series fabrication of high-efficiency *p*-type Si solar cells on a regular basis both on 156 × 156mm^2 sized mono- and multicrystalline Si wafers is one of the processes maintained in the RL. The pilot series is based on technological features like low-temperature surface passivation on both sides with local contacts on the rear and fine line-printed grid metallization in combination with plating at the front (see in Fig. 3).

A typical trend of high-efficiency multi batches processed during a period of several weeks is shown in Fig. 4. The box plot indicates the median values of the efficiencies of the batches together with minimum, maximum, upper and lower quartiles. It is important to note that the processed wafers in each batch represent the distribution of whole Si bricks. Thus, the spread also includes the defect rich material from the bottom and top of the brick. The batch sizes vary between 30 and 60 wafers as indicated beneath the diagram. The different batches comprise Si wafers based on different feedstocks (without additional light-induced degradation).

Figs. 5 and 6 show the *I-V* characteristic (total area measurement) of high-efficiency mono- and multicrystalline Si solar cells processed in our RL. The data of the mono and multi cells are independently confirmed by Fraunhofer ISE CalLab. The cell area of the monocrystalline cell is 239.0cm^2 and the multi cell 243.4cm^2, respectively.

High current densities of 38.4mA/cm^2 (mono) and 36.8mA/cm^2 (multi) are reached due to the optimized front side metallization, improved infra-red light trapping and efficient current collection due to the passivating dielectric layer on the rear side and the lowly-doped emitter as shown in Fig. 3. The combination of the emitter and the passivated rear side enables open circuit voltages of 644mV on monocrystalline Si (after light-induced degradation). The corresponding efficiency reaches 19.5% before and 19.2% after degradation respectively as indicated in Fig. 5 [6].

Similar combinations of emitter and passivation stack features result in open circuit voltages of 647mV on multicrystalline poly-Si wafers as shown in Fig. 6. A more detailed analysis of these results compared to a standard BSF cell design can be found in [7].

We link the cell development in our RL close to our module technology by finishing the processed cells into large area modules. This enables an efficient technological development for maximum output power at module level. With an independently confirmed module efficiency of 17.84% on an aperture area of 1.5m^2, we reported on a new multicrystalline module world record [8]. We realized a 60-cell module with a power output of 268Wp at STC using multicrystalline cells with rear-side passivation.

Monitoring processes are necessary in a research line environment to ensure a high level of quality and to guarantee a fast failure analysis in case of deviations. Such monitoring runs in parallel to the cell production in the RL to check the performance of single processing steps or sequences. In particular, for the cell design described in Fig. 3, we monitor the rear-side passivation scheme by lifetime samples and the surface passivation quality during the processing sequence of the solar cell. Fig. 7 describes the process flow of this lifetime monitoring using Boron-doped (resistivity ~ 10Ωcm) monocrystalline Cz Si wafers. We measure the lifetime by QSSPC method to detect the lifetime at different injection levels and by photoluminescence to evaluate the homogeneity of the passivation quality as shown in Fig. 8. We detect handling issues on the passivation quality especially after firing, such as tweezers or scratches; however, our optimized passivation stacks results in a surface recombination velocity of below S_{rear} < 10cm/s, which is well suited to fabricate *p*-type Si solar cells with efficiencies above 20%.

The discussed pilot process for multi material demonstrates typical average efficiencies about 1%$_{abs}$ above our standard

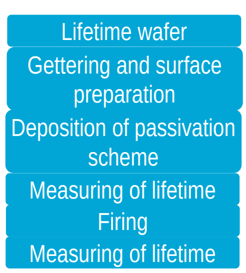

Figure 7. Process sequence to monitor the passivation quality of Q-Cells' rear side passivation scheme before and after a firing step.

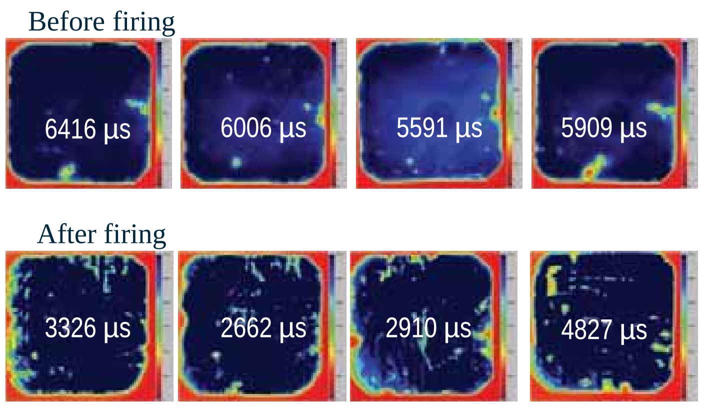

Figure 8. Photoluminescence images of lifetime monitoring wafers having our rear side passivation scheme on both wafer sides before and after a firing step. The effective lifetime is additionally quantified by QSSPC measurement at an injection level of $\Delta n = 5\times10^{14}cm^{-3}$.

BSF multi cell product. Some process features are therefore transferred into the production using this knowledge. The resulting mass production of ready cell concepts will ensure future technology leadership.

Summary

In this paper we presented the RL of the Q-Cells Reiner Lemoine Research centre as a development tool for Si-based high-efficiency solar cell concepts. The flexible design is well suited for current and future development requirements in order to satisfy the needs for fast transfer of new concepts into high volume production. High flexibility of the RL ensures fast reactions to current and future technology trends. Results of our high-efficiency cell concepts for multi and for mono material with record efficiencies of 18.4% and 19.2% respectively, as well as process flows and results of a monitoring procedure were discussed. Results of our current passivation stack show a surface recombination velocity of below $S_{rear} < 10cm/s$, which is well suited to fabricate p-type Si solar cells with efficiencies above 20%. Following our strategy to optimize our technology for maximum module output we reported on a new world record of multicrystalline large area module efficiency. The RL establishes itself as a powerful tool for fast process transfers into production and ensures in this way the sustainability of Q-Cells as a leading supplier of c-Si solar cells, PV modules and PV solutions.

References

[1] European Commission, 2010, "PV status report 2010", EUR 24344, p.21.

[2] CTM Group, 2011, "International Technology Roadmap for Photovoltaics (ITRPV.net) Results 2010", [http://www.itrpv.net/doc/roadmap_itrpv_2011_brochure_web.pdf].

[3] SME Smart Micro Engineering GmbH, 2007 "Research Centre Q-Cells AG", Project documentation Gilching, Germany.

[4] Huljic, D. et al. 2006, "Development of 21% back-contact monocrystalline silicon solar cell for large scale production", *Proc. 21st EU PVSEC*, Dresden, Germany.

[5] Peters, C. et al. 2008, "Development of 18 % Multicrystalline Si EWT Solar Cells for Industrial Fabrication at Q-Cells", *Proc. 23rd EU PVSEC*, Valencia, Spain.

[6] Mohr, A. et al. 2011 (to be published), "Large Area PERC Solar Cells with Efficiency Exceeding 19% in Pilot Series Designed for Conventional Module Assembling", *1st International Conference on Silicon Photovoltaics*, Freiburg, Germany.

[7] P. Engelhart et al. 2011 (to be published), "17.84% module record efficiency enabled by pilot production of multi-crystalline Si solar cells exceeding 18 %", *1st International Conference on Silicon Photovoltaics*, Freiburg, Germany.

[8] Q-Cells SE, 2011, "Q-Cells SE develops world-record-breaking polycrystalline solar module", [Press release, see: www.q-cells.com], Bitterfeld-Wolfen, Germany.

About the Authors

Markus Fischer received his Ph.D. in electrical engineering in 1997 from the University of Stuttgart. After working in the semiconductor industry for Siemens, Philips and NXP in different engineering and management functions he joined Q-Cells SE in 2007. The Q-Cells research line is part of his responsibility as director of R&D Processes.

Peter Engelhart did his Ph.D. research in the field of back-contacted Si solar cells at the Institute for Solar Energy Research Hamelin (ISFH) in 2007. He joined Q-Cells SE in 2007 and as senior staff expert he has responsibility for R&D of high-efficiency Si solar cells.

Helmut Hinneburg received his diploma degree in technical physics from Lübeck University of Applied Sciences. Having held various leading management positions, he has worked in the semiconductor industry for more than 30 years. In 2007, he joined Q-cells as chief technology consultant.

Christian Klenke joined Q-Cells in 2008 and holds responsibility for phase-in and process optimization of different monitoring processes in the Q-Cells research line. From 2006–2008 he worked as a designing engineer for a leading manufacturer of large-area PVD coaters for thin-film photovoltaic production.

Andreas Mohr did his Ph.D. research in the field of high-efficiency silicon solar cells for concentrator systems at Fraunhofer ISE Freiburg in 2005. He joined Q-Cells SE in 2006 and has responsibility in the field of optimization, research and development of solar cells.

Jörg Müller received his Ph.D. degree from Hannover University in 2005. He joined Q-Cells SE in 2004 working in several positions in the technology division. Since 2007 he has lead crystalline silicon cell development at Q-Cells.

Sven Schmidt joined Q-Cells in 2007. He is currently head of the research line and module test line. Before Q-Cells he was a project leader for several years in a leading German synthetic quartz manufacturer.

Kevin Wachsmuth joined Q-Cells as a trainee in 2005. He received his diploma degree in business informatics from the University of Leipzig in 2006. Since 2008, he has had responsibility for line controlling in the research line.

Peter Wawer received his Ph.D. about his work on thin crystalline silicon solar cells. In 1997 he started his career as a development engineer at Siemens Semiconductors in Dresden. In 2004 he moved to the headquarters of Infineon AG in Munich. Since November 2008, Peter Wawer has been responsible for the overall development activities in the core business of Q-Cells SE.

Enquiries

Q-Cells SE,
Sonnenallee 15-17,
D-06766 Bitterfeld Wolfen OT Thalheim,
Germany
Tel: +49 3494 6699 51177
Email: markus.fischer@q-cells.com

Materials

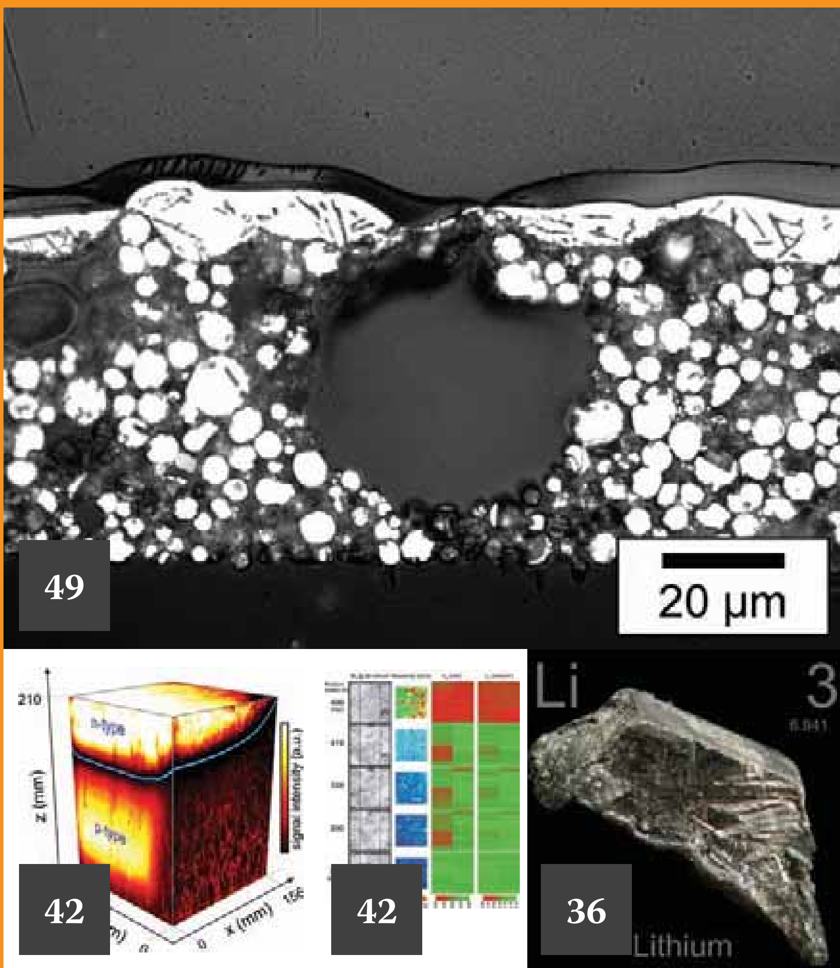

Meyer Burger acquires shares in Roth & Rau

Meyer Burger has acquired 17.7% of Roth & Rau's shares in a friendly two-stage takeover. Meyer Burger acquired a total of 11.3% of the share capital of Roth & Rau AG from the founders and key shareholders at the start of April 2011 for an approximate cost of €356.6 million. Roughly two weeks later, the company then proceeded to acquire a further 6.34% of the share capital of Roth & Rau through a share purchase and exchange contract. These new shares, purchased from the previous major shareholder, OTB Group, at a price of €22 per non-par value bearer share, took Meyer Burger's stake in Roth & Rau to 17.7%.

The acquisition fills in significant gaps in Meyer Burger's c-Si cell processing capabilities, as the company has already made several strategic acquisitions in recent years to bolster its equipment product offerings downstream into module manufacturing and certain other manufacturing equipment areas.

Roth & Rau's operations will likely form the core of a new 'Cells' technology and competence centre within the Meyer Burger Group.

Polysilicon News Focus

Wacker almost sold out of polysilicon through 2015

Despite continued polysilicon capacity expansion plans at Wacker and at its competitors, the company has reported that it is virtually completely sold out of polysilicon to the PV industry through 2015. Significantly, Wacker noted that it had received prepayments of over €230 million in the first quarter of 2011 and a total net prepayment balance of €1.2 billion, almost equivalent to the cost of building its new polysilicon plant in the US.

Furthermore, the sold-out situation suggests a continued flight to guarantee high-purity polysilicon supply from major PV manufacturers as the quality aspects impact c-Si cell efficiencies. The company noted that customers continued to show a strong interest in new multi-year contracts that involved advance payments.

Solarvalue claims cost advantage with solar-grade silicon production process

Solarvalue has advised that its process of developing solar-grade silicon has yielded production costs of US$18 per kilogram after ramp-up. The company maintains that this is a cost advantage compared to mainstream production processes, citing Solarvalue's production capital expenditure of only 30% as evidence of the claim.

Solarvalue's polysilicon products.

Image: Solarvalue

In light of its findings, the company has built a pilot production facility for the unidirectional solidification of silicon, which will qualify the output material produced using their proprietary process. The bricks produced at the facility have an approximate weight of 60kg and will be cut into ingots for delivery to potential customers and investors.

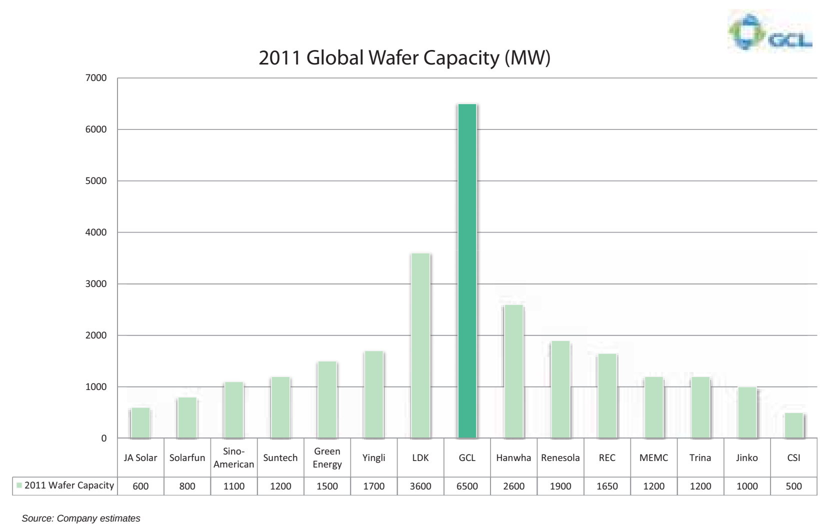

	JA Solar	Solarfun	Sino-American	Suntech	Green Energy	Yingli	LDK	GCL	Hanwha	Renesola	REC	MEMC	Trina	Jinko	CSI
2011 Wafer Capacity	600	800	1100	1200	1500	1700	3600	6500	2600	1900	1650	1200	1200	1000	500

Planned global wafer production capacity of major suppliers for 2011.

Image: GCL-Poly Energy Holdings Ltd.

GCL-Poly claims polysilicon cost down to US$22.5 per kilogram; wafer capacity to hit 6.5GW

Having ramped its polysilicon production capacity from 18,000MT at the end of 2009 to 21,000MT at the end of 2010, GCL-Poly claims its polysilicon production costs are down to US$22.5 per kilogram, making it one of the lowest-cost producers of the product. GCL's average production cost for wafers in 2010 was reported to be US$0.57/W.

Annual solar wafer production capacity reached 3.5GW at the end of 2010, while production reached 1.4GW. On a nominal capacity basis, GCL is one of the largest in the industry, just a year after entering production and expanding capacity via its acquisition of Konca Solar in December 2009.

GCL reported polysilicon shipments for 2010 of 10,507MT, while wafer sales reached 1,451MW in volume. Revenue was reported at HK$14,043.3 million for the year. The average selling prices of polysilicon and wafers were approximately HK$408.6 (US$52.1) per kilogram and HK$6.32 (US$0.82) per watt, respectively. The yield rate for wafer production was said to have reached 95%.

LDK Solar appoints Goran Bye to president and CEO of its polysilicon operations

Multicrystalline wafer manufacturer LDK Solar has added two new members to its management team. Goran Bye will take on the role of president and CEO of LDK's polysilicon arm, while Jiazhen

Zheng has been appointed senior vice president of integration of cell and module operations.

For the last two years, Bye has been the director of the industry unit and a member of the investment committee at Abu Dhabi Future Energy Company (Masdar). Prior to this, he was at REC Silicon for seven years, first as vice president and CFO, before moving into the position of president and CEO. Zheng has also been involved at senior management level in the solar industry, as president and chief operation officer of Best Solar, vice president and chief operation officer at Hua Hong-NEC Electronics and R&D director at Chartered Semiconductor.

M. Setek's Japan-based polysilicon plant looks to resume operation this June

M. Setek, the Japan-based polysilicon plant of AU Optronics, is looking to bring its 7,000-tonne per annum production facility back online in June 2011. Located in Soma Fukushima, the plant was shut down after the March 11 earthquake. Company sources confirmed that the plant sustained some damage and will be undergoing repairs.

Georgia Tech study finds 18.8% average cell efficiencies with GT Solar's monocast silicon technology

Researchers at Georgia Institute of Technology have found average cell efficiencies of 18.8% on monocast silicon material grown in GT Solar International's ingot casting furnace. Georgia Tech researchers also noted that some of the highest efficiencies reached in their tested exceeded 19% using GT Solar's technology.

Image: GT Solar

GT Solar's DSS650 multicrystalline ingot growth system has a furnace output > 9MW per year.

"The results of our recent cell efficiency tests using monocast material provided by GT are well above the best large-area, screen-printed monocast material reported by anyone to date. It is a new record," said Dr. Ajeet Rohatgi, Regents' Professor and director of Georgia Institute of Technology's Center of Excellence for Photovoltaic Research and Education."

GT Solar states that once their monocast crystalline growth technology reaches full commercialization it should assist PV manufactures in reducing costs while making solar technology more cost competitive with other energy forms.

R&D News Focus

Ferro opens R&D laboratory in Taiwan

Ferro has opened a new photovoltaic research and development laboratory in Taipei, Taiwan. The Ferro Taiwan Technology Center, situated within the Neihu Technology Park, will help Ferro provide technical support for its Taiwanese customers and also to improve cell performance and lower manufacturing costs.

Materials Order Focus

GT Solar nabs US$93.9M deal with Powertec Energy for polysilicon tools and technology

GT Solar International has signed a new deal with Powertec Energy worth US$93.9 million that will see GT Solar deliver a complete collection of its polysilicon production equipment and technology, including its SDR 400 reactors, hydrochlorination, filament and product processing equipment to the Taiwan polysilicon producer. A delivery date for the equipment was not released.

Installation of GT Solar's tool and technology suite will take place at Powertec's new polysilicon facility, which is anticipated to launch production in 2012. GT Solar will include this order in its backlog for its current first quarter fiscal year 2012, which ends on July 2nd, 2011.

Meyer Burger receives CHF100 million in follow-on orders

An existing customer based in Asia has placed a follow-on order worth CHF70 million with Meyer Burger for wafer slicing equipment and wafer inspection tools. Delivery of the complete order is expected during 2011. MB Wafertec, the company's subsidiary, is to supply the wire saws, while another subsidiary, Hennecke Systems, is to supply the solar wafer inspection systems.

This is the second such announcement in just over a month from the company, following MB Wafertec's March announcement that it won a wire-saw order worth over CHF30 million with an existing Asian customer. The slurry-based solar wafering tools will be delivered over the course of 2011.

TechPrecision receives orders of US$2 million for wafer equipment

TechPrecision, a manufacturer of metal components and systems for the renewable energy industry, has received new orders totalling US$2 million for its wafer production equipment. The equipment, manufactured by TechPrecision's US and Chinese subsidiaries, Ranor and Wuxi Critical Mechanical Components, respectively, is expected to be shipped before the end of Q3 2011.

Solutia wins heat transfer fluid contract for the US$2 billion Solana project

Solutia has been awarded a contract to supply its Therminol VP-1 synthetic heat transfer fluid for the US$2 billion Solana solar power plant project, which is being developed by Abengoa. Once completed, the Arizona-based plant is expected to be the largest parabolic trough concentrating solar plant in the world, and the first large-scale solar plant in the US capable of storing energy for continued power generation during periods of low light.

Solutia's Therminol heat transfer fluid will play a key role in the concentrating solar power (CSP) capabilities at Solana, which is expected to generate 250MW. Full production at the solar power plant is scheduled for 2013.

MB Wafertec snags $33 million order for wire saws from Asian customer

Meyer Burger's MB Wafertec unit has won a wire-saw order worth over CHF30 million (US$33 million) with an existing Asian customer. The company said the slurry-based solar wafering tools will be delivered over the course of 2011. With the new order, MB Wafertec has announced more than CHF235 million (US$260 million) in bookings since the beginning of the year.

Danen signs US$161 million contract with OCI in the midst of wafer production expansion

As Danen works on its second phase of construction for its wafer plant II in Guanyin Shiang, Taoyuan County, Taiwan, the company has also signed a US$161 million contract with OCI, whereby Danen will buy polysilicon from the company for seven years.

Danen's wafer plant II expansion plans will extend the total wafer capacity of Danen to 520MW. The US$91.4 million investment will add a 200MW capacity to the facility and is expected to bring the company record-breaking revenue in 2011.

Tests relating to the deposition of metallization pastes on solar cells will be carried out on site, enabling Ferro to analyse cell printing and firing, electrical performance, wafer property, solderability and adhesion. Ferro customers will also be able to supply wafers to evaluate conductive pastes when their own test facilities are unavailable, thus speeding up the paste qualification process.

BioSolar reduces UL certification period through volume sampling program

BioSolar hopes to reduce the preparation time for PV panel manufacturers prior to submitting their PV panels for Underwriters Laboratories (UL) certification or recertification under UL1703 through its new volume sampling program.

The company's BioBacksheet product has officially obtained UL material certification, and is currently undergoing a long-term test by UL to determine the relative thermal index (RTI) of the material. Once this is complete, PV manufacturers can submit the full BioBacksheet solar panel for further certification.

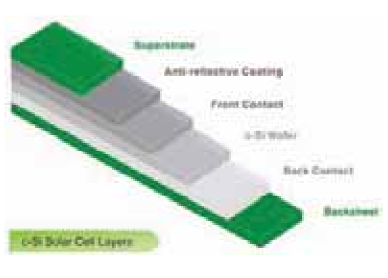

Image: BioSolar

BioSolar's backsheet composition.

Kuraray commercializes methacrylic resin-based CPV lens; begins supply contract with Amonix

Kuraray has simultaneously announced its commercialization plans for its concentrating PV lens and its intended supply of its technology to Amonix.

Kuraray has been working on expanding its business divisions over the past two years and in the energy sector has been working on developing a concentrating lens by producing methacrylic resin.

Image: Kuraray

Kuraray's CPV lenses are manufactured using methacrylic resin molding technology.

37th IEEE Photovoltaic Specialists Conference

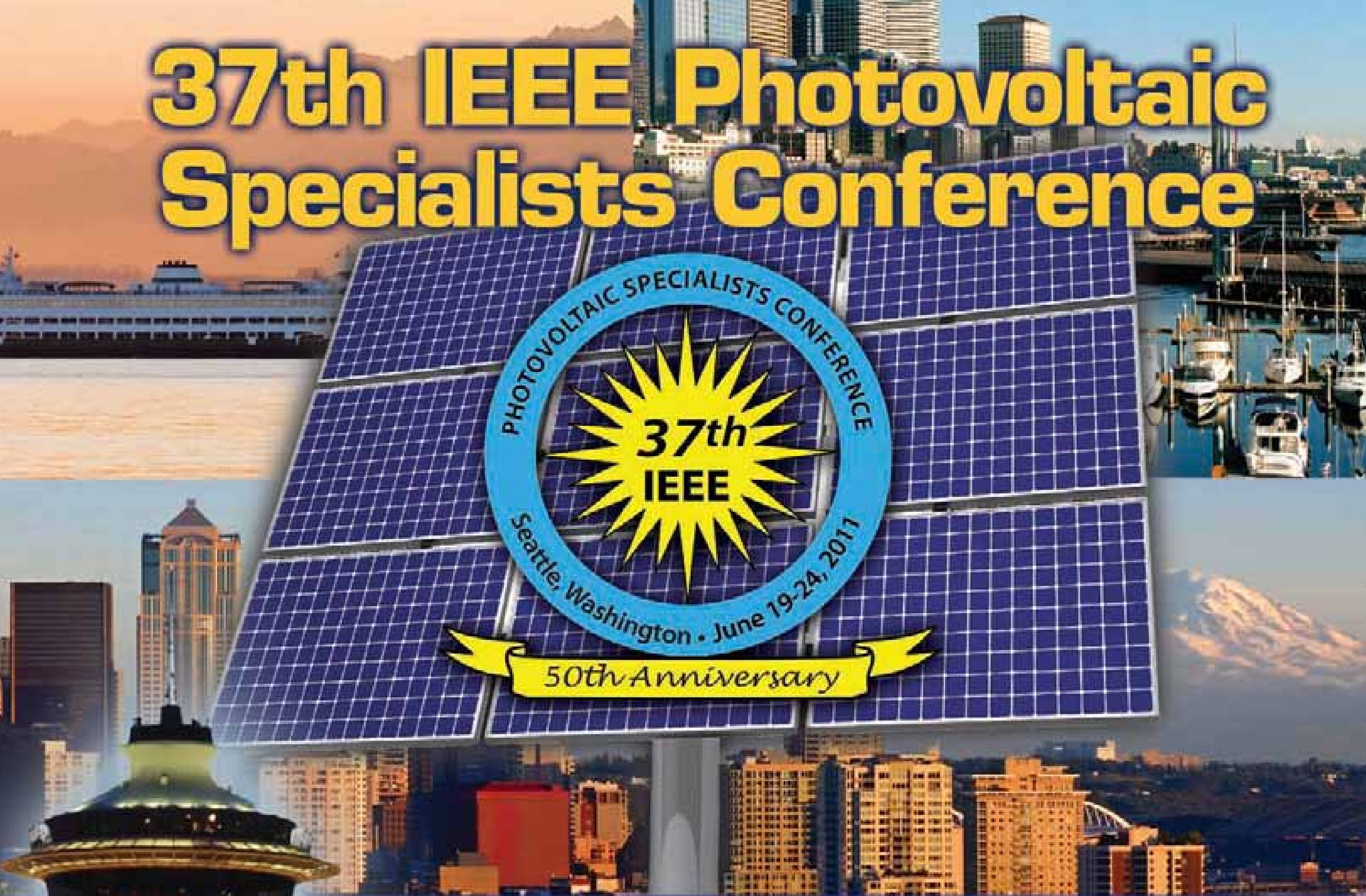

June 19-24, 2011

Washington State Convention Center | Seattle, Washington

Important Dates:

May 16, 2011 • Early Registration Deadline

Save the date for the **37th IEEE Photovoltaic Specialists Conference** to be held at the Washington State Convention Center in lively Seattle, Washington. Come celebrate the 50th anniversary of the first PV Specialists Conference and join the world's top PV scientists and engineers for the preeminent photovoltaic technical conference in the world, **June 19-24, 2011**.

IEEE PV Specialists Conference Technical Program Areas:

Area 1: Fundamentals and New Concepts for Future Technologies
Area 2: Chalcogenide Thin Film Solar Cells and Related Materials
Area 3: III-V and Concentrator Technologies
Area 4: Crystalline Silicon Technologies
Area 5: Amorphous, Nano, and Film Si Technologies
Area 6: Organic Photovoltaics
Area 7: Space Technologies
Area 8: Advances in Characterization of Photovoltaics
Area 9: PV Modules and Terrestrial Systems
Area 10: PV Velocity Forum: Accelerating the PV Economy

Sponsored by:
IEEE
Electron Devices Society
IEEE photonics Society
IEEE PES Power & Energy Society

Contacts: *IEEE Technical Program:* ProgramChair@ieee-pvsc.org • *General Chair:* ConferenceChair@ieee-pvsc.org
Exhibition and Sponsorship: Exhibits@ieee-pvsc.org • *Media:* Kimberly Setliff 415.977.1942
or kimberly@antennagroup.com

News

The company maintains that its improved methacrylic resin molding technology allows the lens to achieve advanced light and water resistance. Additionally, by using innovative transcription properties that are based on precision molding technology, Kuraray states that the CPV lens is able to reach high degrees of precision and light-concentrating efficiency.

Other News

ReneSola's revenue and shipments take a hit in Q1; company opts for cautious approach on Q2 outlook

ReneSola has released its unaudited financial results for its first quarter 2011, which ended on March 31. Overall, the company saw its solar shipments – module shipments in particular – and its net revenues take a downturn during the first quarter. Q1 revenues were reported at US$328.2 million, a 15.1% decrease from the US$386.4 million posted in the fourth quarter of 2010.

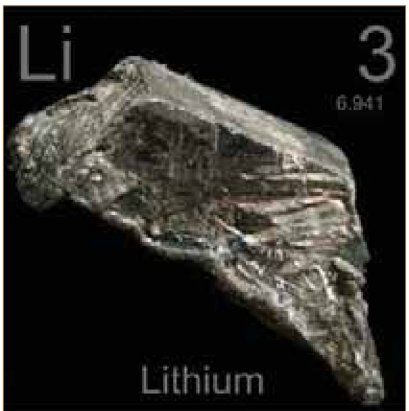

Lithium deposits are said to be plentiful in the Saxony region of Germany.

ReneSola attributes its dip in revenues from Q4 2010 to Q1 2011 to a drop in the average selling price of solar wafers and modules to US$0.87 and US$1.72, respectively. Furthermore, the company saw its module shipments decline, which also affected its revenues for the quarter. Solar product shipments in Q1 reached 330.4MW. Although this surpassed company guidance, solar product shipments were still down 5.4% from the 349.4MW in Q4 2010.

Module shipments took the largest hit in the solar shipment division. The first quarter saw ReneSola ship 86.9MW, compared to 2010's fourth quarter shipment of 126.8MW. The ASPs for solar module shipments during Q1 were US$1.72 per watt. Wafer shipments, however, saw a 9.4% improvement from Q4 to Q1, posting a finalized shipment total of 243.5MW in Q1, compared to 222.6MW from Q4.

SolarWorld goes from modules to mining

SolarWorld may be looking to enter the solar battery power industry as it recently announced plans to start prospecting for lithium on its doorstep in Saxony, Germany. SolarWorld said it had received official approval from the Saxon State Minister for Economic Affairs to start prospecting in the Eastern part of the Erzgebirge Mountains.

In cooperation with the Freiberg University of Mining and Technology (TUBAF), SolarWorld intends to investigate the deposits found within the next few months as the university also performs research into new technologies for lithium-ion batteries.

The Saxony-located lithium deposits are claimed to be among the 10 largest lithium deposits in the world. The alkali metal lithium is used as an anode in the rechargeable lithium-ion batteries that are needed for electric cars, laptops and solar batteries.

Innovalight targets Japan for silicon ink sales

Interest in Innovalight's silicon inks from Japanese solar cell and module producers has led to the materials supplier partnering with local firm Marubeni to sell and support potentially new customers in the country. Marubeni Corporation is one of Japan's largest general trading companies.

Sign of the times: LDK Solar lowers first-quarter outlook

Although not the first PV manufacturer to lower financial forecasts, LDK Solar is the first of the major producers reacting to weaker-than-expected market demand by sharply revising downward its first-quarter 2011 financial forecast. However, LDK expects the first-quarter market softness to be short-lived, as the integrated PV producer reiterated guidance previously given for the full year.

For the first quarter, LDK Solar expects to report revenue in the range of US$745 million to US$755 million, down approximately US$100 million compared to previous guidance of revenue between US$800 million and US$850 million. However, guidance of gross margin between 30.0% and 31.0% is higher than the previous guidance of between 27.0% and 29.0%.

The company also revised its production levels for the first quarter. In-house polysilicon production was revised upwards to between 2,450MT and 2,470MT, compared to the previously guided range of 2,300MT and 2,400MT, which could explain


Image: LDK Solar
Polysilicon reactors at LDK Solar's Ma Hong polysilicon plant.

the higher gross margin as polysilicon spot prices continue to provide excellent returns on tight supply conditions.

Wafer shipments were revised to around 625–635MW, compared to previous wafer shipment guidance of 610–660MW. Wafers have been in short supply, despite the increased capacity. Module shipments were guided to be in the range of 109–114MW in the first quarter, down from the previous guidance range of between 120 and 140MW.

The lower-than-expected wafer and module shipments supports views of several market research firms that module inventories in the supply chain are currently estimated to be in the 2–3GW range.

Scientex, Mitsui Chemicals Tohcello sign joint venture deal to manufacture solar EVA material

Malaysian conglomerate Scientex and Japanese materials supplier Mitsui Chemicals Tohcello (MCTI) have signed a joint-venture agreement to manufacture and distribute ethylene-vinyl acetate (EVA) encapsulating materials for PV modules and other applications. A new company will be formed, MCTI Scientex Solar, in which each party holds a 50% equity interest.

The venture will build an EVA manufacturing plant in Malacca, Malaysia, which is scheduled to start production in the third quarter of 2012. The factory is expected to have a 10,000MT capacity during the first phase of expansion.

Under the terms of the agreement, MCTI Scientex shall be granted the nonexclusive right to manufacture the product, using the technological know-how of the Japanese company. The new firm will also be granted the nonexclusive right to use the trademark and sell and distribute the product to companies owned by MCTI and other companies designated by MCTI as the buyer of the product.

GET signs supply deals with Motech Industries and Taiwan Polysilicon

Taiwan-based Green Energy Technology (GET) has formed a supply partnership with local firms, Motech Industries and

Green Energy Technology's c-Si solar modules.

Image: Green Energy Technology.

Taiwan Polysilicon. A statement from GET, issued to the Taiwan Stock Exchange (TSE), said that a JV would be established between the companies to form a multicrystalline wafer company vertically integrating with polysilicon, solar wafer and solar cell manufacturing.

Initial registered capital of the JV would be approximately NT$1 billion (US$33.8 million), with shares of 40% assigned to GET of 40%, 30% to Motech and 30% to Taiwan Polysilicon.

GET recently signed a seven-year polysilicon supply contract with OCI, worth US$507 million. GET had ramped ingot and wafer capacity to 1GW in 2010, and has planned capacity expansions to reach 1.5GW in the second quarter of 2011.

Targray expands solar silicon division with new Japanese office and additional team members

Following a year of respectable growth for Targray Technology International's solar silicon division, the company has expanded the division by venturing into new markets, including Japan. To help foster this expansion, Targray has added new personnel including Soichiro Yonetsu as the regional manager for its new Fukuoka, Japan location. Additionally, Steve Ghaleb and Jessica Lifshitz join the company at its Montreal, Canada headquarters as global sales manager and junior product manager, respectively.

"Extending our market presence and building up our internal silicon team is vital to ensuring our continued support of an expanding global customer base and increasing demand for Silicon materials," said Howard Alter, director of the silicon division at Targray. "We're therefore delighted by the addition of Yonetsu-san in Japan, a market where it's imperative to have local presence and support in order to drive expansion. On the home front, Steve's extensive and highly relevant distribution experience will play a key role in helping us increase our sales management capacity and execute our strategic plan."

Ghaleb and Yonetsu bring a combined 25 years of experience in the electronic components distribution sphere and the silicon recycling and trading field. Ghaleb was most recently a branch manager for Eastern Canada at Electro Sonic while Yonetsu-san served as president of Silfine Japan.

Targray's head office in Kirkland, Canada.

Return of UMG-Si: a new hope

Dietmar Kohler, **Sven Seren** & **Bernd Raabe**, University of Konstanz, Konstanz, Germany

ABSTRACT

Upgraded metallurgical-grade silicon (UMG-Si), once looked on as a cost-effective and energy-efficient alternative to Si produced via the Siemens route, has experienced a severe regression of late. This has been caused both by the market conditions and by specific physical properties of these materials. Meanwhile, the qualities and the rated influence of negative physical effects have changed partially. Hopes are again rising that these materials, which have to be compensated to meet the desired net doping specifications, might achieve an economical breakthrough instead of long-dreaded low breakdown voltages. In the following paper, we summarize a few of our results on multicrystalline UMG silicon as well as results published by other research groups in the last few years.

Introduction

In May 2011, for the first time in history, a member of the German Green Party was elected to the head of government of a German federal state. Together with the national Renewable Energy Law which defines guaranteed feed-in tariffs, and the gradual political change in thinking, this could mean that the energy turnaround from fossil to renewable energy sources will speed up significantly. Photovoltaics is also included as an important element, especially in combination with wind energy, even in spite of the solar irradiation which is low in comparison to southern European countries [1].

If the feed-in tariffs for solar power are transformed as intended, grid parity will be achieved by 2012 in agreement with last year's forecast by Breyer [2]. The planned increase of renewable energies means increased development of the European electricity networks as well as energy accumulators, and significant cost reductions for photovoltaic systems. Meanwhile, there are about 100 relevant enterprises that deal with the production of silicon for solar cells. One option for new silicon factories for solar cell requirements is compensated UMG-Si, although Bernreuter forecasts less than 1% of market share for UMG-Si in 2012 [3]. Depending on material and manufacturing processes, the terms solar-grade silicon (SoG-Si) and UMG-Si are also used in this context with varying meanings.

'Solar-grade silicon'

Just a few years ago, UMG-Si was discussed as a promising approach to the solar industry to cover the immensely growing demand for solar silicon. As a result of setting up many new solar silicon factories, the high price for highly purified silicon collapsed in 2009 and thus brought UMG-Si production to the edge of profitability. In the same year, Calisolar and PV Crystalox Solar started their new line productions, while other solar cell producers like Canadian Solar and Q-Cells SE reduced their UMG solar cell production. Silicon manufacturers like Timminco or Dow Corning nearly stopped their production of UMG-Si altogether. In addition, UMG-Si was becoming more and more associated with the danger of hot spots due to low breakdown voltages. This trend remained unchanged despite the proposed treatment of symptoms with, for example, bypass diodes [4]. This could be one reason why most companies switched to different titles for their materials instead of the term 'UMG-Si.' More importantly, the quality of their materials has now changed greatly. In general, UMG-Si means that metallurgical silicon is cleaned by metallurgical methods instead of the chemical cleaning via the Siemens process.

> "SoG-Si means that the material's purity is sufficient for use in solar cells, regardless of metallurgical or chemical cleaning."

SoG-Si, on the other hand, means that the material's purity is sufficient for use in solar cells, regardless of metallurgical or chemical cleaning [5]. Ten years ago, UMG-Si typically featured a purity of about 99.99% which is nearly achievable for a pure metallurgical feedstock [6]. UMG-Si wafers were tested as substrates for thin-film LPE solar cells [7]. For use as solar silicon, UMG-Si with such a low purity is only a preliminary stage to SoG-Si. Photosil used the term UMG-Si in this way in an article in the ninth issue of *Photovoltaics International* [8]. However, these processes were often improved to such an extent that some sorts of UMG-Si could be used directly as SoG-Si without further treatment. Therefore the term 'solar-grade silicon' better reflects the changed material properties. For example, the SoG-Si from 6N Silicon – which is currently merging with Calisolar – claims to reach a purity of up to 99.9999% via a sequence of aluminium glazes with a subsequent acid bath [9, 10]. Therefore, the material quality might be well suited to solar cells – at least if the content of aluminium is mastered. The first promising results of solar cells with efficiencies of well above 16% have been presented [10], illustrating that it is difficult to compare the results from UMG-Si materials today and in the past. To do so, the concentrations of impurities and dopants would have to be considered, which are not always revealed by manufacturers. This has to be kept in mind considering the following results.

The use of pure metallurgical feedstock is essential. The above mentioned cleaning refers not only to the concentration of metals, but also to the dopant concentration. In contrast to the silicon which was produced via the Siemens process, UMG-Si feedstock contains generally high fractions of both boron and phosphorus. The total impurity contents remain unchanged without chemical cleaning during crystallization. Metals tend to stay mainly in the melt during crystallization and move with the crystallization front to be enriched in the upper part of the ingot.

On the contrary, the dopants boron and phosphorus are strongly incorporated into the crystal due to their higher segregation coefficients. Their concentrations increase with the height in the ingot for slow crystallization according to the Scheil equation. Since phosphorus segregates stronger than boron, it accumulates in the remaining melt while boron is more easily incorporated in the crystal yielding a p-type net doping of the crystal. At a certain height of the crystallized ingot, the phosphorus concentration exceeds the boron concentration in the melt to such an extent that the same amount of phosphorus and boron is incorporated in the crystal. With a net doping concentration of zero, the bulk resistivity is at its maximum here. Above this point, the local surplus of phosphorus leads to an inversion of the polarity type yielding n-doped material with a high impurity concentration, due to the upwards segregated metals. This explains why the n-type part is typically cut off and not used for the production of solar cells. The wafer

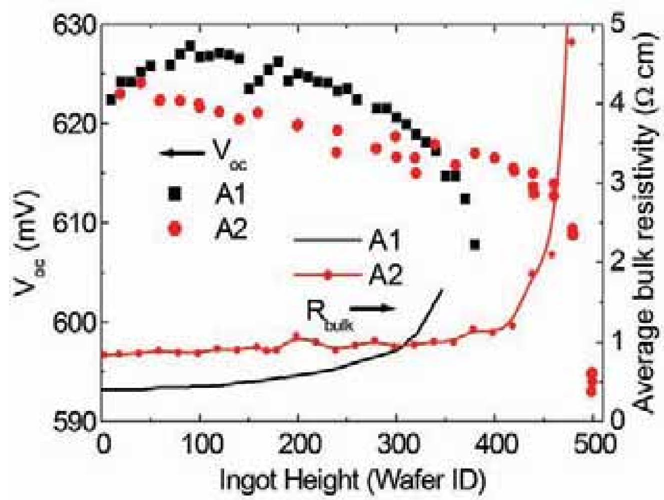

Figure 1. Comparison of open circuit voltage and average bulk resistivity for materials A1 and A2 [13].

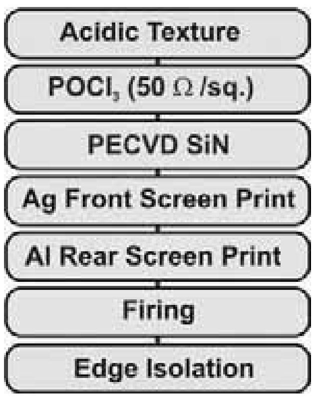

Figure 2. Process flow for the presented multicrystalline UMG-Si solar cells.

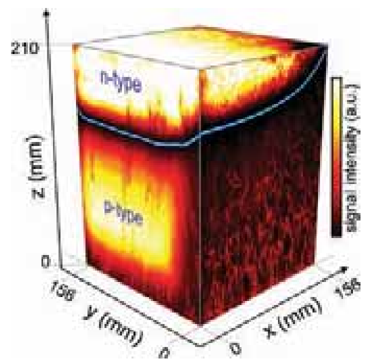

Figure 3. Composition of PL images from the side faces of a UMG mc-Si brick including a type inversion [11].

Courtesy of J. Haunschild, Fraunhofer ISE

yield of an ingot is mainly defined by the concentrations of boron and phosphorus. In order to reach acceptable resistivities, boron must usually be added and the resulting material is called compensated silicon.

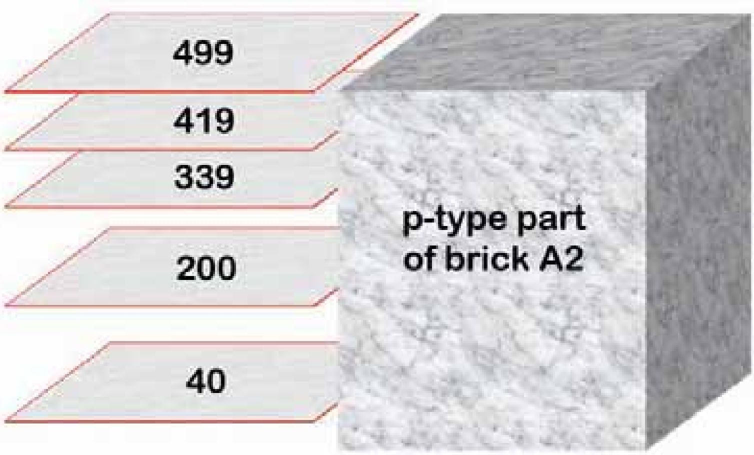

Figure 4. Scheme of the wafer positions of the processed wafers which are shown in Fig. 5 [13].

Net doping

The resistivity which is induced by net doping B-P has a strong influence on open circuit voltage (as can be seen in Fig. 1) of materials A1 and A2. Both materials are p-type wafers from the edges of two different multicrystalline 100% UMG-Si ingots from the same supplier. All wafers shown were processed to screen-printed 12.5 × 12.5cm^2 solar cells according to a typical industrial solar cell process (Fig. 2).

Higher ingot positions mean a lower net doping and therefore higher resistivities. This in turn leads to a smaller splitting of the quasi-fermi levels which means a decrease of the open circuit voltage V_{oc}. This is also the reason why V_{oc} starts at a lower level for material A2 compared to material A1, although other factors may also decrease the V_{oc}. These materials cannot be compared to the Photosil materials because the impurity concentrations are unknown to us.

Besides the variation in height, the resistivity also changes for wafers from the same ingot height. This is a consequence of the crystallization process. Horizontally inhomogenous cooling down leads to a non-planar crystallization front, the efficiency of which depends on the heating mechanism and the possibilities for varying the local temperatures of the crucible furnace. The crystallization of silicon that is in contact with the crucible can be controlled easily, but it is difficult to induce a homogeneous horizontal crystallization. As a result, this varies resistivities for wafers from the same height but different horizontal positions may occur.

An example of such an inhomogenous crystallization can be seen in Fig. 3. These photoluminescence images of the surfaces of a brick from a small ingot were measured and assembled for a 3D impression by Haunschild at Fraunhofer ISE and illustrate the variations of resistivity and lifetime for a small ingot. The blue line indicates the location of the type inversion. Wafers from the upper part of this ingot will consist of both p- and n-type parts, a material which is ineligible for cell production [11]. This spatial inhomogeneity could be reduced substantially by a better control of the crystallization in the meantime. For larger ingots, a lower spatial resistivity variation is possible, as can be seen in a comparison of material from a centre and an edge brick of the same ingot [12]. For further investigation, it is necessary to measure the resistivities of the wafers with a spatial resolution instead of the average values shown in Fig. 1. The selection of the measured wafers and solar cells from different heights is illustrated in Fig. 4. The resulting measurements, e.g. the resistivity maps, are shown in Fig. 5 [13].

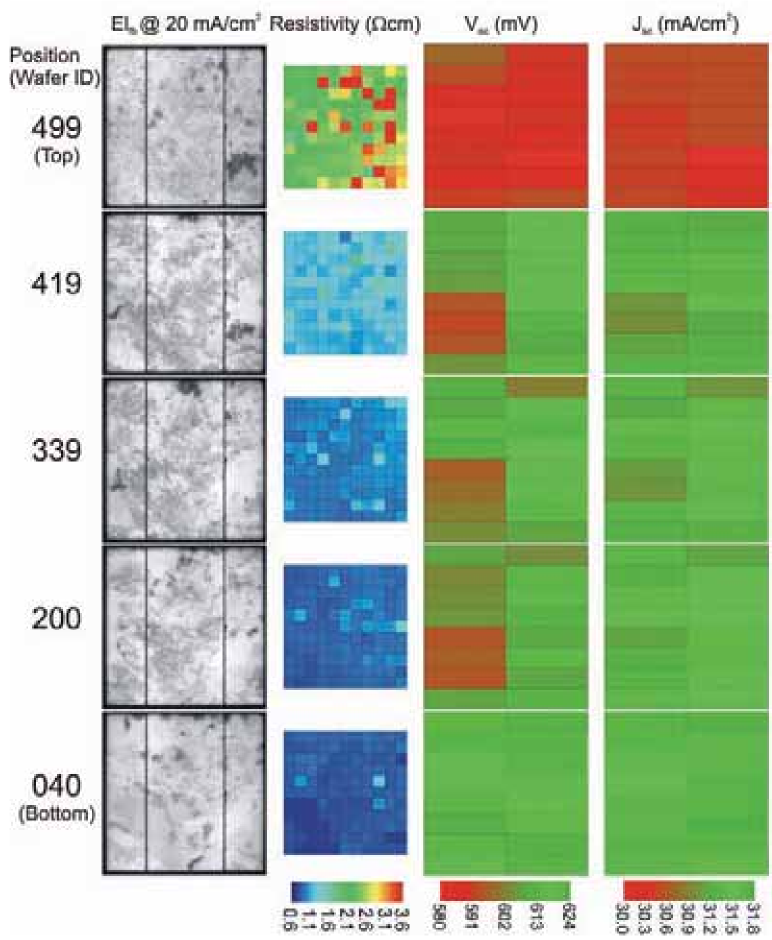

Figure 5. Survey of the measurements on sawn sample solar cells from material A2 in relation to the ingot height position [13].

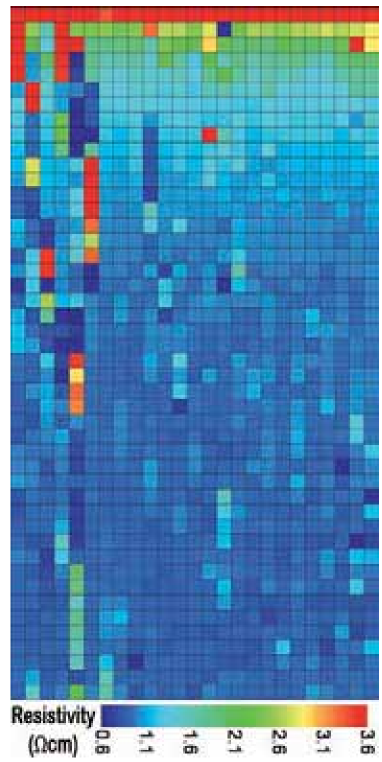

Figure 6. Resistivity map of a vertical cut from brick A2.

The edges of the wafers are not included to avoid systematic errors for the resistivity. The lower sides of the images correspond to the former ingot edge where the measured resistivity is only slightly lower. Large spatial variations are only observed for wafer 499 from the highest position of the p-type part. Here, the measured bulk resistivities also differ from the measured value in Fig. 1, and to a much greater extent than for the other wafers, where the resistivity is about 0.6 to 1.6Ωcm. The comparison with the resistivity map of a vertical cut (shown in Fig. 6) from the edge of the same brick verifies these measurements and also indicates possible homogeneity problems during the crystallization at the edge.

Although it is unknown to us how much of the ingot's top part was cut off, the deviation for the highest part is probably due to the increased impurity concentrations, as measurements using the Seebeck effect proved that this material is still below the type inversion. High impurity concentrations mean that the inversion point is placed higher than for A1. This is then combined with a higher wafer yield, not or not only caused by an increased ingot height. This is in agreement with the behaviour of the short circuit current density J_{sc} in Fig. 7 which is in contrast to the following results.

While the J_{sc} of A2 is stable also in the upper part, for the first UMG-Si material from the same supplier, A1, we found an increase of J_{sc} towards the inversion level. The materials B1 and B2 were cast as small test ingots as shown in Fig. 8 for the German SolarFocus project [14] and showed the same behaviour for the bulk resistivites. This is in agreement with the

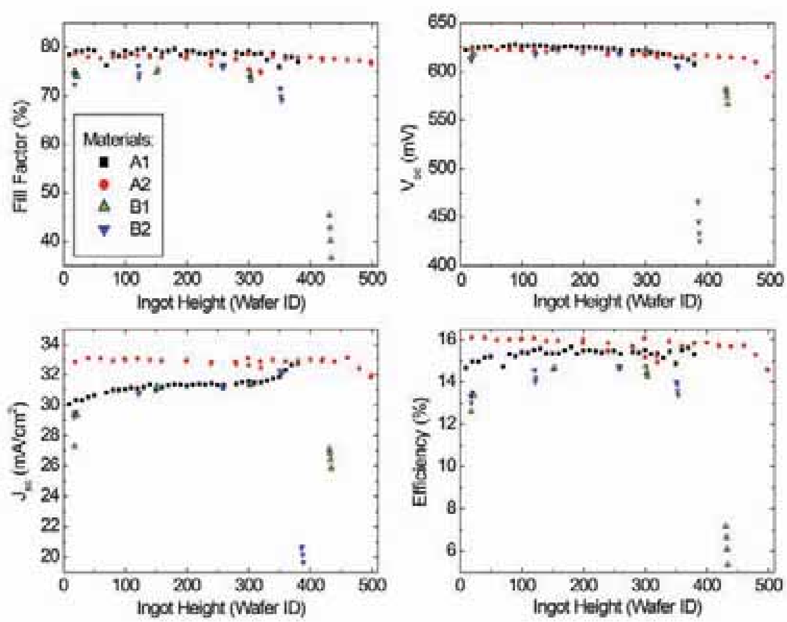

Figure 7. IV parameters for the solar cells processed with materials from two ingot suppliers A, B relative to the vertical position in the ingot [13].

Figure 8. Example of a small ingot casted by SolarWorld AG for the SolarFocus project in 2008, similar to the ingots of the materials B1 and B2 in Fig. 7.

well-known increase of internal quantum efficiencies for long wavelengths (as shown in Fig. 9) [12, 13].

For compensated material, J_{sc} seems to depend on the net doping concentration. One possible explanation is the formation of B-P pairs, which have been suggested by several authors [15–18]. As mentioned, we assume for A2 that the inversion level was shifted further to the top part of the ingot. This probably increased the wafer yield so far that the solar cells from this part are close to the top of the ingot and already have a relevant impurity concentration. While J_{sc} and V_{oc} in Fig. 7 are rather stable, the electroluminescence (EL) images under a forward bias of 20mA/cm^2 (Fig. 5) show more dislocations and the spatially inhomogenous formation of recombination active clusters of crystal defects are shifted towards the centre of the original ingot with increasing height. EL reverse bias images at -10V as well as dark lock-in thermography (dLIT) measurements revealed that these clusters were also areas of increased shunting [13].

To understand these contradicting properties of the A2 solar cells, several of them were cut into smaller cells. For the resulting J_{sc} and V_{oc} maps (Fig. 5), the total J_{sc} is about 2mA/cm^2 lower than for the entire cells mainly due to the lack of a suitable IV calibration for these small cells (because of size and reflection) resulting in a too-low illumination intensity. Both the V_{oc} and especially the J_{sc} map indicate worse values for the small solar cells, which showed a growing defect cluster as well as an increased dislocation density in the left part of the images. In contrast, the cluster on the right side does not influence the IV parameters significantly. This might be explained by the simultaneously improving influence of the dislocation free area right next to this cluster. At least for these solar cells, the results might be even better for a lower dislocation density, which is a matter of improved ingot casting. As a result, the remaining variation of efficiencies for this material is caused by the decrease of the open circuit voltage, mainly due to the increased bulk resistivity [13]. This is probably the main obstacle for height-independent efficiencies and also for a further increase of the wafer yield. Both might be solved by the systematic addition of boron to the melt during crystallization, although this is difficult to control. However, there are further properties that differ for compensated silicon compared to electronic-grade silicon.

Bulk lifetime and mobility

Reductions in the bulk lifetimes and mobilities are reported in compensated silicon in comparison to electronic-grade silicon with the same net doping concentration, due to compensation and the related increased scattering of charge carriers by the dopants. The increasing resistivities towards the type inversion can cause higher bulk lifetimes because the lifetimes are connected to the net doping concentration [18–20]. High contents of metal should also reduce the minority carrier lifetime significantly.

Hot spots and breakdown voltages under reverse bias

According to the results of Kwapil et al. and Breitenstein et al., at least three different

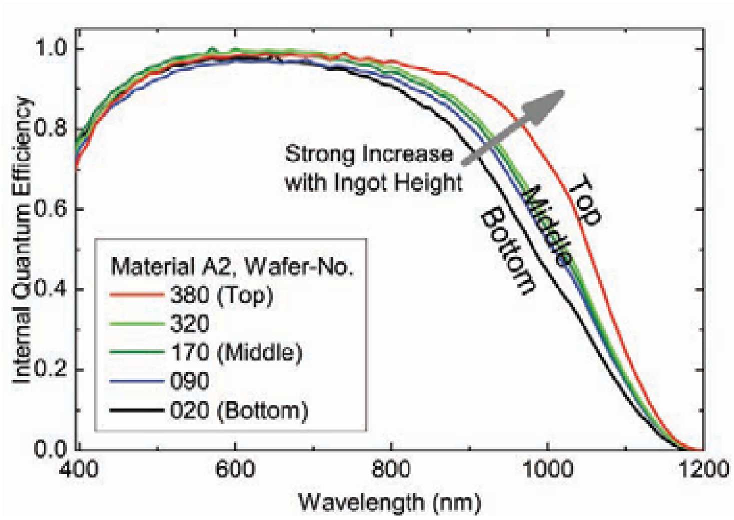

Figure 9. Internal quantum efficiency (IQE) for the material A1 versus the wavelength clearly shows the relation to the J_{sc} due to the increasing bulk resistivity [12].

breakdown types under reverse bias can be distinguished in multicrystalline silicon solar cells, not only for UMG-Si.

The 'early' breakdown type occurs in the range between -5 to -7V at 'singular spots' which seem to be process-induced and do not lead to high leakage currents. The 'soft' breakdown right above this voltage level is related to the crystal defect structure and appears mainly at recombination-active dislocations or grain-boundaries. As these recombination-active regions are caused by impurity decorations in general, this breakdown type dominates in areas of higher metal contaminations in the material [21]. Breitenstein distinguishes for these soft breakdown sites between weakly and strongly contaminated crystal defects. For UMG-Si it can be concluded that whether or not soft breakdown is of importance depends greatly on the impurity content. For typical impurity concentrations and realistic voltages under reverse bias, the reverse current is low. A further observation is that the reverse breakdown voltage, at which the soft breakdown occurs, is lower for rougher (e.g. acidic-etched) surfaces compared to rather flat surfaces. This is relevant for multicrystalline solar cells in general [22].

At a reverse bias exceeding -13V, an avalanche-dominated breakdown is also observed for acidic textured materials at etch pits located around dislocations. Due to strongly increasing currents under reverse bias, this 'hard' breakdown type turns out to be the most dangerous, but can probably be reduced by improved texturization. For UMG-Si solar cells, the influence of the bulk resistivity seems to predominate for reverse biases [23]. Metal contents and crystal defects in contrast only seem to be detrimental at high impurity concentrations [24]. Thus it may be concluded that the breakdown under reverse bias is again strongly affected by the feedstock and cleaning process.

Degradation effects

Light-induced degradation (LID) refers to the decrease of the efficiency under illumination. The best known form of LID is due to the formation of boron-oxygen complexes which act as efficient recombination centres and therefore reduce the lifetime in the bulk. According to Bothe's empirical equation, the upper limit of the lifetime decreases approximately with the increase of [B] and $[O_i]^2$ [25]. The formation of these recombination centres require both of the elements, so that the LID at a fixed concentration of boron can be assumed to follow the oxygen concentration quadratically. Although standard multicrystalline silicon contains less oxygen than Czochralski-grown silicon (Cz-Si), the concentrations of both elements can be higher in UMG-Si. This makes LID an issue that has to be considered at least in qualitatively high material. Due to its high segregation coefficient, oxygen is preferentially incorporated in the crystal and is therefore primarily present in high concentrations in the lower part of the ingot while the boron and phosphorus concentrations increase towards the top. In fact degradation can be serious if the oxygen concentration exceeds a certain value. The degradation can only be improved by an adjusted crystallization.

Degradation is reported to be in the range of $1\%_{rel}$ or even lower [10, 26, 27]. This can be explained first by further cleaning steps for the feedstock material that reduce the content of impurities, and second by the formation of boron-phosphorus pairs (mentioned above). According to this proposed model, many of the boron atoms pair with phosphorus atoms which means that they are not available for the formation of B-O recombination centres during illumination [15, 17, 18]. For compensated Cz-Si, another defect model can explain the dependence on the net doping concentration instead of the electrically active boron concentration by focussing on the concentration of interstitial instead of substitutional boron in B_iO_{2i}. Metals (except alkali metals) do not present an obstacle for the use of UMG-Si due to their effective segregation to the very top part of the ingot. For lower metal and oxygen concentrations, the LID does not differ widely from the results for multicrystalline solar cells made from electronic grade silicon. Any potentially remaining degradation could vary for different ingots and even for solar cells made from different ingot heights. One way to deal with this is an 'electrically-induced pre-degradation' that proceeds much faster than light-induced degradation [29].

Efficiencies

Finally, as the wafer yield, LID and the low breakdown voltages seem to be manageable, solar cell efficiency affects profitability strongly. Good results have been obtained by several groups in recent years, but the best reported efficiencies for industrial-sized solar cells were still limited to a range of 16.1 to 16.4% – still below the typical reference efficiencies [10, 12, 27, 29, 30]. Efficiencies up to 18.5% could be reached only with specialized high efficiency cell processes on lab-type 2 × 2cm² solar cells [31, 32]. Now, in April 2011, Engelhart has reported for Q-Cells the successful production of large-scale solar cells in the same efficiency range, with the best efficiency being 18.35% for a 6" UMG solar cell and a median of about 18% for wafers from the whole p-type part [33]. So it seems that UMG-Si is back on the road to success. Time will tell if it will also be an economical success for the different UMG-Si solar cell producers and feedstock suppliers.

References

[1] German Advisory Council on the Environment (SRU) 2011, "100% renewable electricity supply by 2050", Report: [http://www.erneuerbare-energien.de/inhalt/46959/4590/].

[2] Breyer, Ch. & Gerlach, A. 2010, "Global overview on grid-parity event dynamics", *Proc. 25th EU PVSEC*, pp. 5283–5304.

[3] Bernreuter, J. & Haugwitz, F. 2010, "The Who's Who of Solar Silicon Production", Bernreuter Research Report, Germany.

[4] Day4 Energy Inc. Press Release: Aug 7, 2008, [http://www.day4energy.com].

[5] Braga, A.F.B. et al. 2008, "New processes for the production of solar-grade polycrystalline silicon: A review", *Solar Energy Materials & Solar Cells*, Vol. 92, pp. 418–424.

[6] Pires, J.C.S., Braga, A.F.B. & Mei, P.R. 2003, "Profile of impurities in polycrystalline silicon samples purified in an electron beam melting furnace", *Solar Energy Materials & Solar Cells*, Vol. 79, pp. 347–355.

[7] Peter, K. et al. 2002, "Thin film silicon solar cells on upgraded metallurgical silicon substrates prepared by liquid phase epitaxy", *Solar Energy Materials & Solar Cells*, Vol. 74, pp. 219–223.

[8] Einhaus, R. et al. 2010, "Purifying UMG silicon at the French PHOTOSIL project", *Photovoltaics International*, Vol. 9, pp. 58–65.

[9] Sollmann, D. 2009, "Pure and Simple", *Photon International*, May 2009, pp. 110–113.

[10] Halm, A. et al. 2010, "Large area industrial solar cells on low cost 100% mc SoG si substrates: efficiencies exceeding 16%", *Proc. 35th IEEE PVSC*, pp. 2–6.

[11] Haunschild, J. et al. 2010, "Quality control using luminescence imaging in production of mc-silicon solar cells from UMG feedstock", *Proc. 35th IEEE PVSC*.

[12] Kohler, D. et al. 2009, "Upgraded metallurgical grade silicon solar cells: A detailed material analysis", *Proc. 24th EU PVSEC*, pp. 1758–1761.

[13] Kohler, D. et al. 2010, "Comparison of UMG materials: Are ingot height independent solar cell efficiencies possible?", *Proc. 25th EU PVSEC*, pp. 2542–2547.

[14] Riepe, S., Reis, I. E. & Koch, W. 2008, "Solar silicon material research network SolarFocus (Solarsilizium Forschungscluster)", *Proc. 23rd EU PVSEC*, pp. 1410–1413.

[15] Pizzini, S. & Calligarich, C. 1984, "On the effect of impurities on the photovoltaic behavior of solar-grade silicon", *J. Electrochem. Soc.*, Vol. 131, No. 9, pp. 2128–2132.

[16] Kruehler, W. et al. 1988, "Effect of phosphorous-compensation on the electronic properties of solar-grade silicon", *Proc. 8th EU PVSEC*, p. 1181.

[17] Kopecek, R. et al. 2008, "Crystalline Si solar cells from compensated material: Behaviour of light induced degradation", *Proc. 23th EU PVSEC*, pp. 1855–1858.

[18] Macdonald, D. et al. 2009, "Light-induced boron-oxygen defect generation in compensated p-type Czochralski silicon", *J. Appl. Phys.*, Vol. 105, p. 93704.

[19] Peter, K. et al. 2008, "Future potential for SoG-Si feedstock from the metallurgical process route", *Proc. 23rd EU PVSEC*, pp. 947–950.

[20] Herzog, B., Hahn, G. & Wambach, K. 2009, "Studies of compensation behaviour in p-type mc-silicon", *Proc. 24th EU PVSEC*, pp. 1015–1019.

[21] Kwapil, W. et al. 2010, "High net doping concentration responsible for critical diode break down behavior of upgraded metallurgical grade multicrystalline silicon solar cells", *J. Appl. Phys.*, Vol. 108, p. 23708.

[22] Breitenstein, O. et al. 2010, "Defect-induced breakdown in multicrystalline silicon solar cells", *IEEE Transactions on electron devices*, Vol. 57, No. 9, pp. 2227–2234.

[23] Wagner, M. et al. 2009, "Shunts, diode breakdown and high reverse currents in multicrystalline silicon solar cells", *Proc. 24th EU PVSEC*, pp. 2028–2031.

[24] Kwapil, W. et al. 2010, "Cause of increate currents under reverse-bias conditions of upgraded metallurgical grade multicrystalline silicon solar cells", *Proc. 35th IEEE PVSC*.

[25] Bothe, K., Sinton, R. & Schmidt, J. 2005, "Fundamental boron-oxygen-related carrier lifetime Limit in mono- and multicrystalline Silicon", *Prog. Photovolt: Res. Appl.*, Vol. 13, pp. 287–296.

[26] Friestad, K. et al. 2004, "Solar grade silicon from metallurgical route", *Proc. 19th EU PVSEC*, pp. 568–571.

[27] Margaria, T. et al. 2010, "Status of the Photosil project for the production of solar grade silicon from metallurgical silicon", *Proc. 25th EU PVSEC*, pp. 1506–1509.

[28] Voronkov, V. V. & Falster, R. 2010, "Latent complexes of interstitial boron and oxygen dimmers as a reason for degradation of silicon-based solar cells", *J. Appl. Phys.*, Vol. 107, p. 53509.

[29] Petter, K. et al. 2010, "Latest result on production of solar cells from UMG-Si feedstock", *Silicon for the Chemical and Solar Industry*, Norway.

[30] Braun, S. et al. 2009, "Comparison of buried contact- and screen printed 100% UMG solar cells resulting in 16.2 % efficiency", *Proc. 24th EU PVSEC*, pp. 1736–1739.

[31] Kaes, M. et al. 2006, "Over 18% efficient mc-Si solar cells from 100% solar grade silicon feedstock from a metallurgical process route", *Proc. 4th IEEE World Conference on Photovoltaic Energy*, pp. 873–878.

[32] Junge, J. et al. 2010, "Evaluating the efficiency limits of low cost mc Si materials using advanced solar cell processes", *Proc. 25th EU PVSEC*, pp. 1722–1726.

[33] Engelhart, P. et al. 2011, "R&D pilot line production of multi-crystalline Si solar cells exceeding cell efficiencies of 18%", *Proc. 1st Silicon PVEC*.

About the Authors

Dietmar Kohler studied physics at the University of Karlsruhe (KIT), Germany, and received a Diploma in 2007 for research on the morphology of polymer solar cells. He is currently working towards his Ph.D. at the University of Konstanz, Germany, on the material properties of upgraded metallurgical-grade silicon solar cells.

Sven Seren studied at the University of Konstanz, Germany where he earned his Ph.D. in 2007 for research on low-cost solar cells from fast-grown silicon ribbon materials. Since then, he has been heading the 'new materials' group at the University of Konstanz. The emphasis of the research is on characterization and processing of multicrystalline silicon ribbon materials.

Bernd Raabe received his Diploma in physics from the University of Stuttgart. He joined the photovoltaic division at the University of Konstanz in 2003, where he became the group leader of 'novel silicon solar cell concepts' in the middle of 2007.

Enquiries

University of Konstanz
Department of Physics
Jacob-Burckhardt-Str. 27
D-78464 Konstanz, Germany

Tel: +49 7531 883174
Email: dietmar.kohler@uni-konstanz.de
Web: http://www.uni-konstanz.de/pv

Breakage issues in silicon solar wafers and cells

V.A. Popovich[1], **M. Janssen**[1], **I. J. Bennett**[2] & **I.M.Richardson**[1]
[1]Delft University of Technology, Delft; [2]Energy Research Centre of the Netherlands (ECN), Petten, The Netherlands

ABSTRACT
Reduction of silicon wafer thickness without increasing the wafer's strength can lead to a high fracture rate during subsequent handling and processing steps. The cracking of solar cells has become one of the major sources of solar module failure and rejection. Hence, it is important to evaluate the mechanical strength of silicon solar wafers and influencing factors. The purpose of this work is to understand the fracture behaviour of multicrystalline silicon wafers and to obtain information regarding the fracture of solar wafers and solar cells. The effects on silicon wafer strength of saw damage and of grain size, boundaries and triple junctions are investigated, while the effects of surface roughness and the damage layer removal process are also considered. Significant changes in fracture strength are found as a result of different silicon wafer crystallinity and surface roughness. Results indicate that fracture strength of a processed silicon wafer is mainly affected by the following factors: the saw-damage layer thickness, surface roughness, cracks/defects at the edges and the number of grain boundaries – which all serve as possible crack initiation points. The effects of metallization paste type and firing conditions on the strength of solar cells are also considered, with findings indicating that the aluminium paste type and firing conditions influence the strength of solar cells.

Introduction

An increase in silicon wafer size, combined with wafer thickness reduction without strengthening the wafer, leads to a high breakage rate during subsequent handling and processing, and results in high costs [1, 2]. It is well known that silicon is a brittle material that breaks easily during in-line processing due to stresses induced on the wafer surface and edges [3]. The cracking of silicon solar cells has become one of the major sources of solar module failure and rejection. Therefore, while it is important to investigate the electrical properties of silicon solar wafers and cells, the mechanical properties – especially the strength – also need to be carefully analyzed.

"Cracking of silicon solar cells has become one of the major sources of solar module failure and rejection."

The purpose of this research is to determine the nature and source of defects (flaws) controlling the strength of multicrystalline silicon solar cells and to provide information regarding the strength of cells. In this paper several aspects regarding silicon wafer crystal structure, saw-damage removal, surface roughness parameters and metallization processing conditions are described in relation to mechanical strength. This strength is measured by a four-point bending method and results are statistically evaluated by a Weibull analysis, which provides information on the flaw distribution in the sample. The resulting data can be used to enhance production yields, improve cell reliability and establish mechanical criteria that ultimately lead to a reduction in cell costs.

Experimental conditions

Material preparation

Strength measurements were performed on rectangular multicrystalline (mc) silicon wafers and cells of 10 × 30mm^2 with a thickness of 200µm. Specific types of silicon crystallinity were chosen in order to investigate the effect of crystallinity features on the mechanical strength of the silicon wafer. All specimens were laser cut from a single cast block. In order to statistically evaluate the results, 15 neighboring specimens (thus featuring the same crystallinity features) were prepared.

The wafer specimens were divided into six groups according to crystallinity type (see Fig. 1), namely: one big grain, a triple junction, many small grains, a twin boundary, several grains and a grain boundary perpendicular to the loading direction. All the solar cell specimens were prepared using a standard industrial process.

In order to investigate the effect of saw-damage removal, specimens without a metal layer were etched for 30s in a HF(10%) + HNO_3(30%) + CH_3COOH(60%) solution. To investigate the effect of maximum firing temperature of the Al back-contact, six neighbouring wafers were processed under identical conditions, but with different peak temperatures; i.e., 750°C, 800°C, 850°C, 900°C and 950°C. Two different drying temperatures (250°C and 350°C) were also chosen in order to examine the influence on mechanical strength. In all these cases the same commercially available Al paste was used, a type which causes only a limited amount of cell bowing after firing. In addition, the influence of the aluminium paste composition on the strength of the cells was investigated for three different commercially available pastes (designated as paste A, B and C). Measurements of the amount of bowing that results from metallization were made by an optical method, using a Quick Vision Mitutoyo system over the full length of the solar cell (156mm).

The surface of the damaged layer in as-cut neighbouring samples was analyzed by Raman spectroscopy. This stress measurement technique was carried out at room temperature in the backscattering configuration using a Renishaw Raman spectrometer equipped with a He-Ne laser with an excitation wavelength of 633nm and a 100× objective. This resulted in a focused spot with a diameter of ~1µm and a penetration depth of a few µm.

Three types of specimens were prepared in order to analyze the effect of surface roughness. The surface conditions of these specimens included: the as-cut state (with saw-damage layer), a textured surface (an in-line process, used to remove the damaged layer and

Figure 1. Four of the groups of specimens showing different crystallinity features.

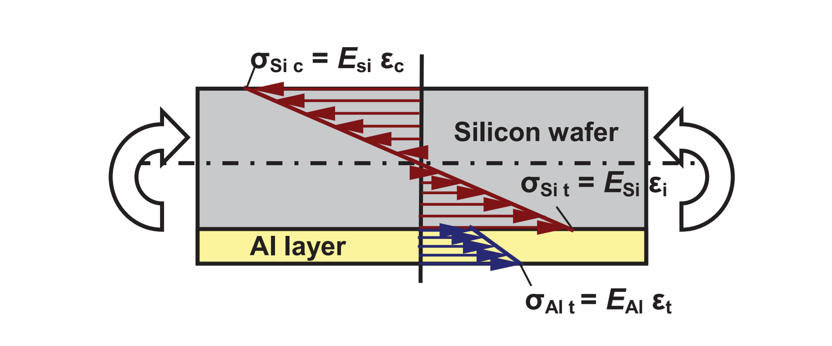

Figure 2. Stress distribution along the thickness of a silicon beam with an aluminium layer loaded in bending.

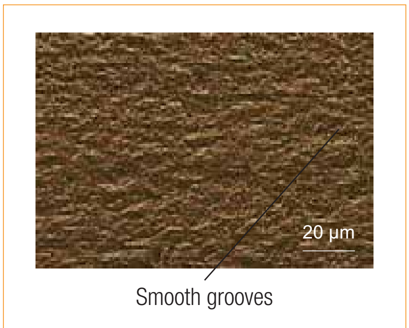

Figure 3. SEM micrograph of a typical surface of an as-sawn multicrystalline silicon wafer.

to create a highly textured silicon surface for trapping the light) and a chemically polished surface (15µm removal from both wafer surfaces).

It should be noted that the edges of all specimens were polished down to a 1µm finish and carefully examined with optical microscopy.

Strength measurement

The four-point bending test was chosen in this research because it results in a uniform bending moment across the specimen between the inner loading pins.

The test configuration, based on ASTM standard C 1161-02c [4], was used to measure the ultimate strength at ambient temperature [4]. The bending tests were performed using a 100kN Instron 5500R tensile machine equipped with a 10N load cell. The test fixture, designed especially for thin specimens, had a loading span equal to half the support span (i.e., a four-point – ¼ point configuration) and was semi-articulating. The crosshead speed was set such that the strain rate in the specimen was of the order of $10^{-4}\,s^{-1}$. From loading until fracture, the load and the deflection were monitored.

The stress, σ, and strain, ε, in the outer fiber of a specimen with a rectangular cross section loaded in four-point bending can be calculated as follows [5]:

$$\sigma = \frac{3PL}{4bd^2}, \quad \varepsilon = 4\;3\;\frac{Dd}{L^2}, \qquad (1)$$

where P is the applied force, L the outer support span, b the specimen width, d the specimen thickness, D the deflection at the specimen centre. However, for solar cell specimens these standard formulae are not directly applicable. Specimens with an Al back-contact layer should be represented as a composite beam, consisting of two materials with different stiffnesses [6]. A linear strain distribution is assumed across the composite beam thickness. The stresses are then obtained by multiplying the strains by the modulus of elasticity for silicon (E_{Si}) and the aluminium metal layer (E_{Al}), respectively, leading to the stress distribution shown in Fig. 2.

The stress distribution is largely affected by the difference in elastic modulus of silicon and of the aluminium layer. In this work, the elastic modulus of the silicon was obtained from the wafer-bending tests and amounted to E_{Si} = 170GPa, averaged over the different crystallinity types. In our previous research [7], it was possible to calculate the overall elastic modulus of the Al contact layer using experimentally obtained bowing results and a bimetallic strip model. This amounted to an elastic modulus of around 43GPa, which is an average for the three different aluminium pastes investigated.

Results and discussion

Effect of saw-damage removal and silicon wafer surface roughness on mechanical strength

Silicon is a hard and brittle material and in order to cut Si ingots into thin wafers, a multi-wire sawing process is used, which can creates a highly stressed and damaged layer.

Fig. 3 shows an SEM micrograph of a typical surface of an as-sawn multicrystalline silicon wafer. As silicon is a brittle material, the smooth grooves on the surface cannot be explained by a melting and quenching of the surface leading to the formation of a thick silicon oxide layer. Therefore the samples were analyzed with a Raman spectrometer in order to check for phase transformations in the damaged layer.

The Raman spectrum, shown in Fig. 4, clearly indicates the presence of amorphous Si (a-Si) beside polycrystalline Si on the as-sawn surface. Measurements were made at many different positions of the wafer and in many locations an a-Si peak was visible, either big or small.

It is known that when indented or scratched at low load, silicon shows a phase transformation, rendering it ductile [8]. This results in a layer of amorphous silicon or – if the scratch is slow enough – a mixture of amorphous and metastable phases, which is similar to the phase transformation occurring during nanoindentation [9]. When the indenting (or scratching) tip is pressed on the silicon, it induces a high local pressure, transforming the brittle silicon into a ductile phase. On unloading, this ductile phase is not stable and transforms into a mixture of amorphous and metastable silicon phases [10]. In our study, amorphous silicon was

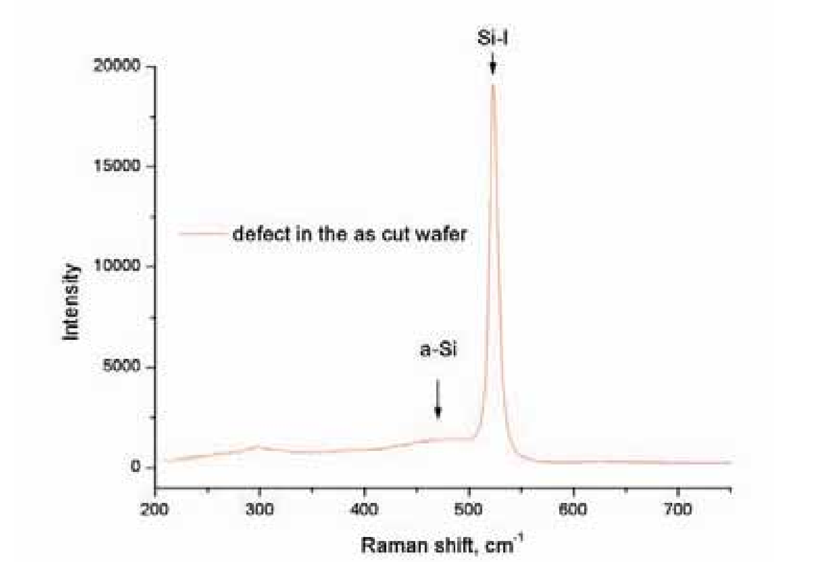

Figure 4. Representative Raman shift for the as-cut wafer, showing a local indentation-induced transformation of Si into a-Si.

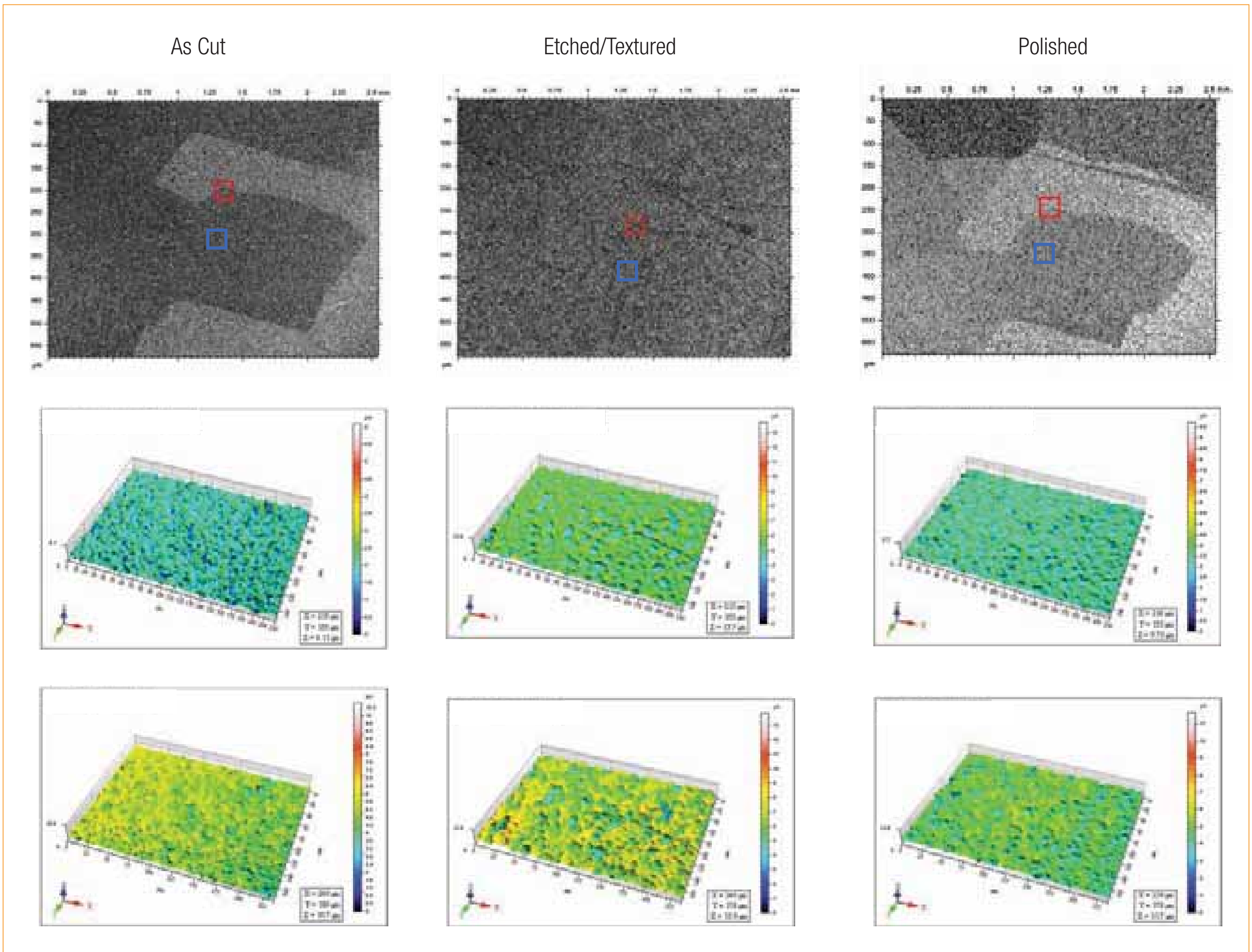

Figure 5. Representative surface roughness profiles for as-cut, textured and polished neighbouring wafers. Areas including the grain boundary are marked in red; areas in the grain are marked as blue.

found only in the smooth grooves (Fig. 3). The rough parts of as-sawn silicon wafers, where material is chipped off, mainly consist of stable crystalline silicon.

In order to view the influence of saw-damage etching (damage removal process) on the stress state and the mechanical strength of silicon wafers, two types of specimens were chosen: as-cut specimens and specimens etched by an acidic solution ($HF + HNO_3 + CH_3COOH$) for 30s.

In mc-silicon wafers, flaws and crack-like defects induced during processing cannot be avoided and it is known that wafer strength is directly related to the density, size and distribution of such microcracks. As can be seen in Table 1, the specimens without additional etching have a lower Weibull characteristic strength, σ_o, which is due to the presence of microcracks and a transformed amorphous silicon phase at the surface.

Etching conditions	σ_0 (MPa)	*m*(-)
No etching	155	9.4
With etching	234	8.3

Table 1. Effect of damage-layer removal on Weibull characteristic strength (σ_o) and modulus (*m*).

As a result of the etching process, the depth of surface microcracks is reduced; some cracks disappear completely; some crack tips become more blunted and the layer of transformed a-Si is removed. All of these effects reduce the risk of macrocrack initiation, making the material less susceptible to failure.

In this study, the wafer thicknesses are the same and the wafer edges are polished down to 1µm. Therefore these aspects will not affect the wafer strength and the surface roughness will determine the fracture strength of the multicrystalline silicon wafer. Fig. 5 shows representative confocal microscopy surface roughness profiles for sample with different surface conditions, i.e. as-cut, textured and polished down to 15µm, taken in the same areas of neighboring wafers.

As can be seen in Fig. 5, samples with a textured surface show a significant increase in surface roughness compared to the as-cut state. The roughness parameters *Sz* and *Sdr*, presented in Table 2, also indicate this; this most likely indicates the formation of etch pits.

It should be also noted that etching/texturing at the grain boundaries creates a much rougher surface, probably due to the preferential etching at the grain boundaries (see etched sample in Fig. 6a). The low value of the Weibull modulus (*m* < 8.5) (Table 2) shows that there is a large variation in the size of the largest defects, present at the tensile surface of tested textured silicon specimens.

Furthermore, despite the increase of surface roughness, there is still an improvement in mechanical strength of textured samples, probably due to the removal of the damaged layer.

"Further polishing of silicon wafers revealed a characteristic reduction in surface roughness."

In this research, the strength of the mc-silicon wafer increased by about 50% as a result of the etching/texturing (damaged layer removal) process. Thus, it can be suggested that the density of micro-cracks in the damaged layer is a more significant factor affecting mechanical strength of silicon wafers than surface roughness. Further polishing of silicon wafers revealed a characteristic reduction in surface roughness, as well as a significant increase in fracture strength (Table 2). A larger Weibull modulus, as

European Photovoltaic Technology Platform

6th General Assembly

Benefits of Photovoltaics for Europe's Energy & Economy

30 June 2011 - European Parliament, Brussels, Belgium

PhotoVoltaic TECHNOLOGY PLATFORM

Coordinator of the Platform Secretariat

EPIA European Photovoltaic Industry Association

Platform Partners

WIP

JRC EUROPEAN COMMISSION

EUREC AGENCY European Renewable Energy Research Centres Agency

More information: www.eupvplatform.org

Credit: Conergy AG

Silicon surface treatment	In the grain Sz, μm	Sdr, %	Grain boundary Sz, μm	Sdr, %	four-P bending strength, MPa	σ_0 (MPa)	m (-)
As-cut	5.70	14.6	6.11	12.2	78.0	160	9.4
Textured	12.7	28.2	13.7	45.8	90.0	240	8.3
Polished	9.73	10.8	10.6	10.0	117.5	285	10.1

Table 2. Effect of surface roughness on bending strength and Weibull characteristic strength, σ_0, and modulus, *m*, of multicrystalline silicon wafers. Here, *Sz* is the average difference between the five highest peaks and five lowest valleys; *Sdr* – the developed Interfacial area ratio, is expressed as the percentage of additional surface area contributed by the texture as compared to an ideal plane the size of the measurement region [11].

compared to the as-cut and textured state, indicates that polishing gives a much smoother silicon surface and a narrower defect distribution.

It can be concluded that in the absence of a damaged layer the fracture strength is inversely proportional to the surface roughness, i.e. $\sigma_0 \sim 1/R_a$, where σ_0 is the fracture strength and R_a is the surface roughness. It can also be concluded that as soon as the saw-damage layer is removed, the surface roughness profile is the second most detrimental factor affecting mechanical strength of silicon wafers.

Effect of mc-silicon wafer crystallinity on mechanical strength

Specific types of silicon wafer crystallinity were chosen for this research in order to investigate the effect on mechanical strength. All specimens were etched and polished in order to remove the damage induced by the sawing process. The four-point bending strength was analyzed using Equation 1. The results are given in Table 3, which lists the Weibull characteristic strength (σ_0) and the Weibull modulus (m) of 15 tests.

As can be seen from Table 3, it is possible to define three main characteristic groups based on the strength results. The specimens with one big grain in the middle have a much higher strength than those with many small grains in the middle. The four other crystallinity types, all having several grains in the middle, have an intermediate strength.

As for most brittle materials, the fracture strength of mc-silicon depends on both material-intrinsic properties, such as grain size, grain boundaries and crystal orientation, and on extrinsic variables such as flaws and microcracks [12]. The strength reduction due to the presence of many small grains might be related to the number of grain boundaries, which is proportional to the number of grains. Alternatively, the surface roughness might be different for varying crystallinity types, due to preferential etching of the grain boundaries; however, this effect can be excluded from this work, since polished samples were used. Furthermore, fracture patterns of the polished silicon samples subjected to four-point bending revealed a preferential propagation of the cracks near the grain boundaries.

Based on these results, it can be concluded that for polished mc-silicon wafers, crystallinity is the most significant factor affecting the strength, probably due to weak grain boundaries leading to intergranular fracture. Conversely, there is a mixed mode fracture for as-cut and for textured silicon wafers, where surface roughness and damaged layer are the most detrimental factors.

Crystallinity type	σ_0 (MPa)	m (-)
One big grain	293	8.5
Twin boundary	274	8.9
Triple junction	268	6.7
GB parallel to the loading direction	266	9.1
Several grains	260	7.4
Many grains	251	6.9

Table 3. Effect of crystallinity type of polished wafers on mechanical strength.

Effect of metallization paste type on mechanical strength of silicon solar cells

Three types of aluminium metal pastes were investigated in order to find the influence of the resulting metal layer microstructure on the mechanical strength of silicon solar cells. These specimens were treated as composite beams, consisting of two layers, i.e., a bulk mc-silicon wafer and an aluminium layer. The bending strength of the specimens was corrected using the appropriate flexural formulae [6]. Using these formulae, it was possible to determine the maximum tensile stress in each layer at the moment of specimen fracture. Unfortunately, the strength of the silicon wafer and the Al layer (i.e., the composite beam) cannot be determined individually in this research due to uncertainty concerning the layer from which the fracture originates.

As can be seen from Table 4, the type of aluminium metallization paste used has a significant effect on the strength when the specimens are loaded with the Al layer in tension. In this loading position, both of the specimen layers, i.e. the silicon wafer and the Al layer, are loaded in tension. Furthermore, due to its higher stiffness, the silicon wafer experiences the highest tensile stresses; unsurprisingly, for the reverse loading position the effect of paste type on the mechanical strength is not so significant.

The maximum tensile stress in a silicon solar cell loaded with the Al layer under tension will be located at the interface between the silicon wafer and the aluminium layer. In order to understand the effects on the solar cell's strength, it is important to consider the microstructure of the layers present locally.

From previous investigations [7], it was found that the Al layer consists of a eutectic layer with a porous layer on top. The eutectic layer is a uniform Al-Si bulk alloy, being in full contact with the BSF layer, and as a result with the silicon wafer. The porous layer has a composite-like microstructure consisting of three main components: 1) spherical hypereutectic Al-Si particles, 2) bismuth-silicon glass and 3) porosity. It was shown that the porous layer is not uniform and does not fully cover the eutectic layer.

All specimens with an Al layer show an increase in bending strength (as compared to the reference etched silicon wafer specimens), probably due to the formation of the eutectic layer (~12% Si). Since silicon is a very brittle material that only exhibits elastic behaviour, the presence of a second ductile phase (i.e., the eutectic layer) could induce some plasticity at the outer fiber, thus altering the stress distribution and affecting possible crack initiation. This ductile phase (eutectic layer) can serve as a bridge for possible critical microcracks, thereby improving the strength of mc-silicon solar cells.

The different effects of Al pastes on the mechanical strength of mc-silicon solar cells can be explained by the differences in layer microstructure. There are a number of features that might affect the mechanical strength, such as the eutectic layer and its thickness, the total Al layer thickness (which results from the Al particle size and its distribution) and the amount of porosity and the bismuth glass fraction.

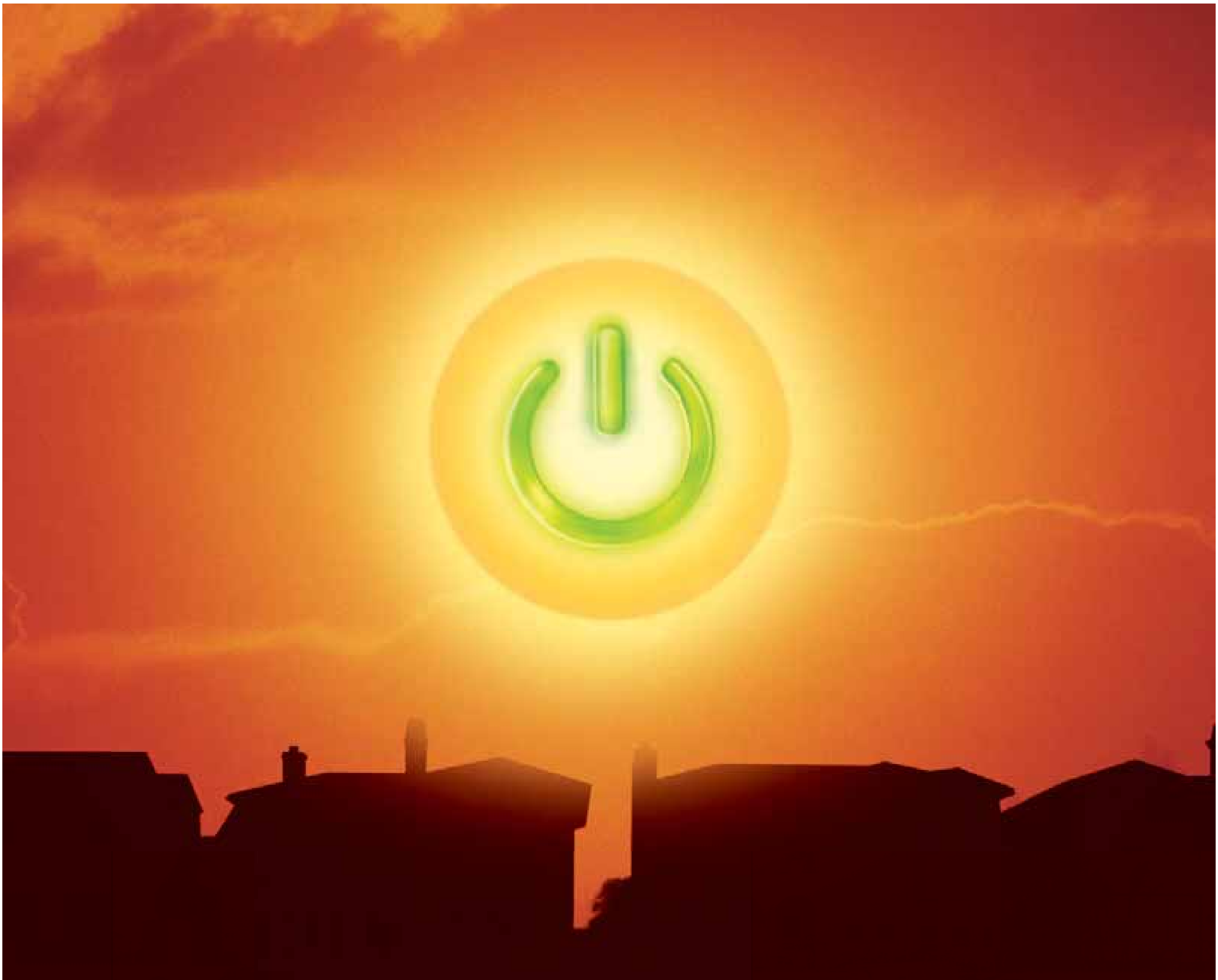

Al paste type	Al suface in tension			Si surface in tension		
	Stress at fracture in Al (MPa)	Stress at fracture in Si (MPa)	Weibull modulus, *m* (-)	Stress at fracture in Al (MPa)	Stress at fracture in Si (MPa)	Weibull modulus, *m* (-)
A	110	266	6.3	71	206	7.8
B	94	237	6.5	68	195	8.5
C	82	217	4.8	67	193	9.6

Table 4. Effect of aluminium paste type on the characteristic stress at fracture in silicon solar cells.

Drying temperature (°C)	Characteristic stress at fracture (Al under tension)		Weibull modulus m (-)
	σ_{Si} (MPa)	σ_{Al} (MPa)	
250	266	110	6.3
350	220	90	6.8

Table 5. Effect of aluminium paste drying temperature on the characteristic stresses at fracture in silicon solar cells.

Firing temperature (°C)	Characteristic stresses at fracture (Al under tension)		Bowing of a complete cell (mm)
	σ_{Si} (MPa)	σ_{A1} (MPa)	
750	149	59	0.48
800	171	68	1.16
850	187	73	1.40
900	193	77	1.43
950	203	80	1.80

Table 6. Effect of maximum firing temperature on the characteristic stresses at fracture and amount of bowing of silicon solar cells.

Effect of aluminium paste drying and firing temperatures on mechanical strength of silicon solar cells

Two different Al paste drying temperatures (250°C and 350°C) were chosen in order to investigate the influence on mechanical strength. As can be seen from Table 5, the paste drying temperature has an effect on the bending tensile stresses in mc-silicon solar cells at fracture. Specimens dried at low temperature (250°C) show higher characteristic stresses at fracture than specimens dried at high temperature (350°C).

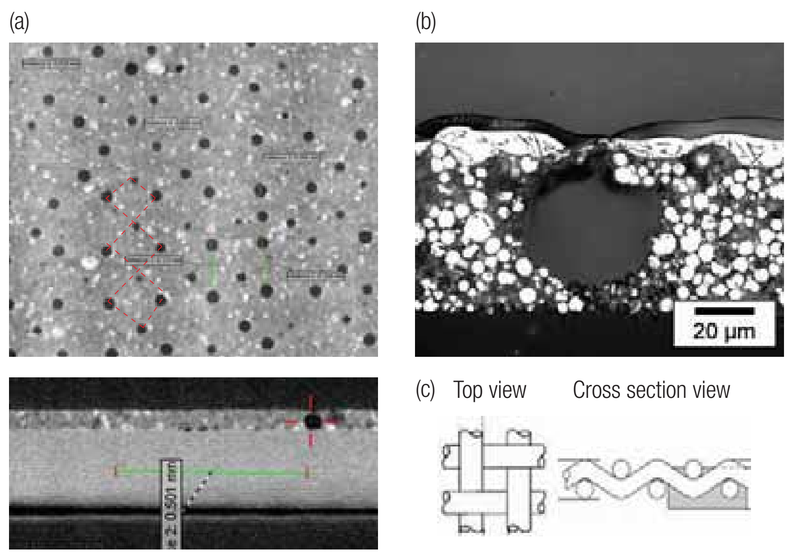

Figure 6. a) Volumetric representation (top image) of a solar cell cross-section and a 2D X-ray (bottom image) of the Al layer, showing defects induced by the screen-printing process (black part: voids; white: bismuth; grey: Al and Si). The dashed red line represents a reconstructed screen-printing mesh. b) Optical image of the solar cell cross-section showing a process-induced cavity. c) Schematic of an industrial screen-printing mesh, used for the application of metallic pastes.

In previous investigations [13], a computed tomography (CT) study of the Al back-contact layer revealed the presence of spherical voids inside the porous Al layer. It was shown that these voids have a homogenous and systematic distribution across the entire Al layer, and were caused by the screen-printing process (Fig. 6). It was found that there is a significant change in the defect concentration between the samples processed at different drying temperatures; i.e., drying at 350°C creates relatively large holes (10 to 20µm^2) in a well-defined pattern, resulting in a more porous layer.

Drying at 250°C gives smaller holes and a denser Al layer structure. The presence of voids in the aluminium layer, produced by the screen printing process, creates a non-uniform stress field at the interfaces, thus affecting the strength. Hence, drying aluminium paste at lower temperature (250ºC) can be advised as the most optimal condition from a mechanical stability point of view.

The other effect that has been investigated in the course of this study is the relationship between the maximum firing temperature of the aluminium layer and the fracture strength of the silicon solar cell. For this purpose, six neighbouring wafers were processed with the same conditions, but with different peak temperatures; i.e., 750–950°C (Table 6).

Table 6 shows the effect of the maximum firing temperature on the characteristic stresses at fracture in the Al and Si layers. As can be seen, there is a strong correlation between the maximum firing temperature and the stresses at fracture; the higher the firing temperature, the higher the characteristic stresses. Furthermore, it should be noted that increasing the firing temperature increases the amount of bowing of the complete cell, as shown in Table 6.

These effects can be explained by the increased eutectic layer thickness with peak firing temperature. As can be understood from the Al-Si phase diagram [14], increasing the firing temperature leads to an increased amount of Si dissolution and an increased amount of liquid phase, resulting in a thicker eutectic layer.

Thus, both the thickness of the eutectic layer as well as uniformity (fewer defects) of the aluminium back-contact layer can be considered as important parameters controlling mechanical stability of silicon solar cells.

Conclusions

Breakage issues and mechanical strength of mc-silicon wafers and solar cells were investigated using a combination of four point bending test, bowing measurements, confocal microscopy, Raman spectroscopy and X-ray computed tomography. The study yields the following information:

- Multicrystalline silicon wafer crystallinity has a significant effect on the mechanical strength.
- Surface and edge defects, such as microcracks, grain boundaries and surface roughness, are the most probable sources of mechanical strength degradation. Reduction of potential microcracks leads to an increase of the fracture strength of an mc-silicon wafer.
- There is a relationship between aluminium paste composition, mechanical strength of a cell and amount of cell bowing.
- When loaded in tension, the aluminium layer improves the strength of a solar cell. The eutectic layer within this structure probably shows some plasticity and can also serve as a bridge for possible critical microcracks at the silicon wafer surface.
- Drying aluminium paste at low temperature (250°C) yields a better mechanical strength of mc-silicon solar cells than drying at a higher temperature (350°C).
- There is a strong correlation between maximum firing temperature, bowing and fracture strength of solar cells; the higher the firing temperature the higher the fracture strength and the greater the bowing.
- Thickness of the eutectic layer as well as uniformity (fewer defects) of the aluminium back-contact layer can be considered as important parameters controlling mechanical stability of silicon solar cells.

References

[1] Brun, X.F & Melkote, S.N. 2009, "Analysis of stresses and breakage of crystalline silicon wafers during handling and transport", *Sol. Energy Mater. Sol. Cells,* Vol. 93, pp. 1238–1247.

[2] Wang, P.A. 2006, "Industrial challenges for thin wafer manufacturing" in *Proc. 4th WC PVEC*, Waikoloa, Hawaii, USA, pp. 1179–1182.

[3] Lawn, B.R. 1993, *Fracture of Brittle Solids*, Cambrige University Press, Cambrige, UK.

[4] ASTM Standard C 1161-02c, 2008, *Standard Test Method for Flexural Strength of Advanced Ceramics at Ambient Temperature*, ASTM International, West Conshohocken, Pennsylvania, USA.

[5] ASTM Standard C 1341-06, 2006, *Standard Test Method for Flexural Properties of Continuous Fiber-reinforced Advanced Ceramic Composites*, ASTM International, West Conshohocken, Pennsylvania, USA.

[6] Gere, J.M. & Goodno, B.J. 2009, *Mechanics of Materials,* Seventh ed., Cengange Learning, USA.

[7] Popovich, V.A. et al. 2010, "Microstructure and mechanical properties of aluminium back-contact layers", *Sol. Energy Mater. Sol. Cells,* Vol 95, No 1.

[8] Gassilloud, R. et al. 2005, *Phys. Stat. Sol.* (a) Vol. 202, No. 15, pp. 2858–2869.

[9] Kailer, A. et al. 1997, *Appl. Phys,* Vol. 81, No. 7, pp. 3057–3063.

[10] Jang, J. et al. 2005, *Acta Materialia,* Vol. 53, pp.1759 – 1770.

[11] Roughness Parameters [available online at http://www.imagemet.com/WebHelp/spip.htm#roughness_parameters.htm].

[12] Cook, R.F. 2006, "Strength and sharp contact fracture of silicon", *J. Mater. Sci.*, Vol. 41.

[13] Popovich, V.A. et al. 2010, "Application of x-ray computed tomography in silicon solar cells", *Proc. 35th PVSC*, Honolulu, Hawaii, USA.

[14] a/u MATTER [available online at http://aluminium.matter.org.uk].

About the Author

V.A. Popovich is a Ph.D. researcher at Delft University of Technology, Department of Materials Science and Engineering, The Netherlands. Her project is focussed on materials behavior of multicrystalline silicon solar cells. This project is carried out at TU Delft and supported by ECN and ADEM (Advanced Dutch Energy Materials Innovation Lab). The results of this project have already provided valuable knowledge to the industry and have been used in consultancy projects with industrial partners including cell manufacturers and metallization paste suppliers.

Enquiries

V.A. Popovich
Delft University of Technology, Department of Materials Science and Engineering,
Delft, The Netherlands
Tel: +31 (0) 15 27 895 68
Email: v.popovich@tudelft.nl

Cell Processing

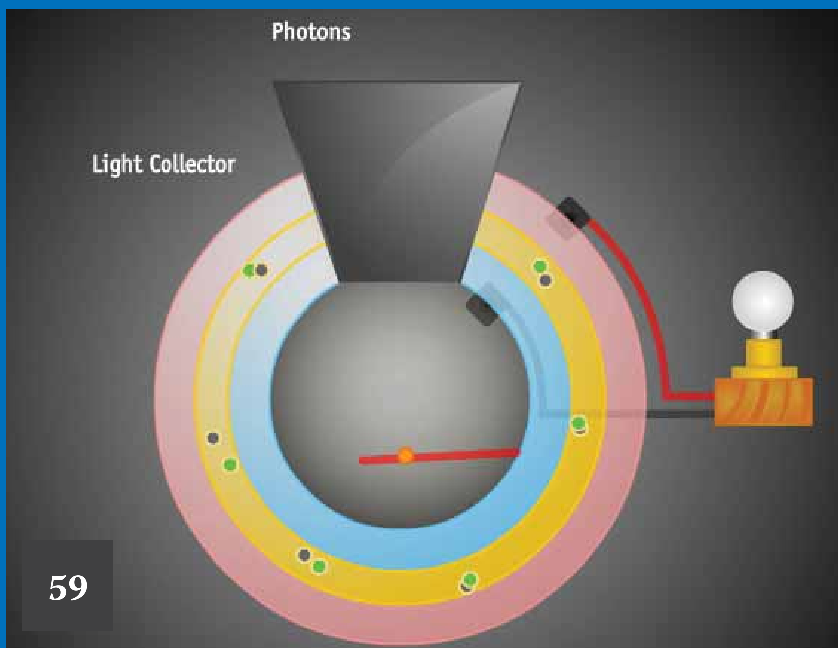

News

The last of the 'old guard' leaves Q-Cells

Instrumental to Q-Cells' manufacturing rejuvenation, Gerhard Rauter, Chief Operation Officer (COO) at Q-Cells, has resigned his position at the company, effective May 4th, 2011. As is the norm in such situations, Q-Cells did not give any reasons for his resignation, simply wishing him well for the future.

Regarded as part of the 'old guard' executive team that for one brief year became the leading PV manufacturer, Rauter is the last senior executive from that era to leave the company.

A replacement has yet to be appointed but Q-Cells said that his responsibilities would be assumed by CEO Nedim Cen, supported by Jirko Lohse and Peter Wawer for the time being.

Q-Cells is now in a unique position within the PV industry, having no executive with any previous PV or semiconductor background prior to joining the company.

Rauter (53) had held the position of COO at Q-Cells since October 2007 and was most recently responsible for production and technology. He was also instrumental in establishing Q-Cells' low-cost manufacturing operations in Malaysia and bringing its thin-film operations at Solibro to fruition.

Rauter has been a member of the editorial advisory board for *Photovoltaics International* since its inception.


Image: Q-Cells.

Gerhard Rauter, former COO at Q-Cells, has resigned his position at the company.

Cell Efficiency News Focus

Schmid's selective emitter technology supports Sunrise Global Solar's record 19.2% cell efficiencies

Another day, another cell efficiency record as selective emitter technology from Schmid has been used to support a claimed new cell efficiency record by customer, Sunrise Global Solar, of 19.2%. The cells were verified by the University of Konstanz and the Fraunhofer Institute for Solar Energy Systems (ISE).

Interestingly, the cells were produced on standard volume production equipment, based on industrial grade 6" monocrystalline wafer material with conventional screen-printed aluminium backside.

"In Schmid's combined printing and etching process, the high phosphorous doping layer on the cell is selectively etched and only remains in those places where contacts are subsequently printed - for this purpose a wax mask is applied by an inkjet-type printer," noted Dr. Christian Buchner, Vice President of Schmid's Cell Business Unit. "The utilization concept of the selective emitter increases the efficiency of the solar cell by up to 0.6% absolute... The digital inkjet printing technology and the optical characterization techniques utilized create an outstanding level of precision and process stability."


Image: Schmid Group

Digital printing of etch masks on Schmid solar cells.

The use of selective-emitter technology, primarily developed by a number of PV process equipment suppliers, has been a key enabler of recent cell efficiency gains using conventional production equipment with minimum investment in new technologies.

Sunrise expects to have fully ramped its first high-efficiency cell fab of 330MW within the next two months.

Bosch Solar Energy's PERC cell achieves record-breaking efficiency

Bosch Solar Energy's new large-scale PERC solar cells have achieved record-breaking efficiencies of 19.6% during testing at the Fraunhofer Institute for Solar Energy Systems (ISE). The monocrystalline cells managed to record a peak output of 4.73W.

The rear side of Bosch's PERC (Passivated Emitter and Rear Cell) cells are coated with a dielectric and a metal layer and equipped with point contacts, which improves incident light reflection on the cell's rear side and enables the emitter to convert more light into electricity. Consequently, modules with these cells yield proportionately more output under weak light incidence and increased ambient temperatures.

"This is a great success for the engineering team, especially since we've exclusively used industrial production steps to manufacture those record-breaking cells," said Bosch's chief technology officer, Volker Nadenau.

Bosch's PERC cell was unveiled at last September's 25th EUPVSEC in Valencia and it signals the first stage of the expansion of Bosch's solar division; a new research and development centre in Arnstadt, scheduled to be opened this summer, is being built as part of the capacity expansion.

Trina Solar to develop n-type silicon solar cells with Australian National University

In an effort to boost conventional solar cells to conversion efficiencies of 20% for mass production, Trina Solar has signed a three-year research agreement with the Australian National University (ANU). Some of the AUD$3 million funding for the project is expected to come from the Australian Solar Institute, which is part of the Australian Government's Clean Energy Initiative.

The new collaboration will focus on improving cell efficiencies of Trina Solar's standard p-type multicrystalline silicon

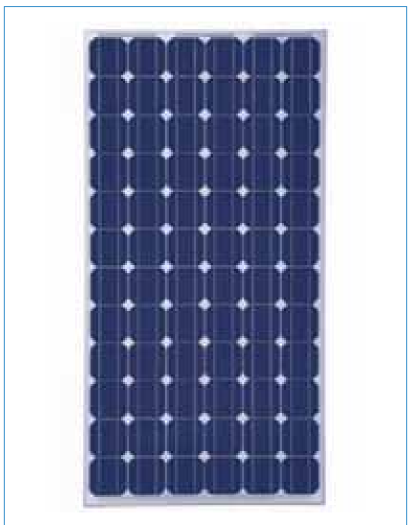
Image: Trina Solar

Trina Solar's monocrystalline solar modules.

solar cells to approximately 19%. However, the key focus will be on the development of high-efficiency n-type silicon solar cells with conversion efficiencies of 20% for mass production using conventional processes and equipment.

R&D News Focus

Solar3D finishes light collector design; 3D prototype cell planned for later this year

Solar3D's three-dimensional solar cell technology has reached a new milestone in the form of completion of the design for its light collector element. This achievement should allow the research and development team to take the first steps toward calculating the 3D solar cell's efficiency.

"Our innovative solar cell design has two main sections: a light collector section coupled with a micro-photovoltaic section. The completion of the light collector design is the key to expediting the entire project," commented Jim Nelson, president and CEO of Solar3D. "The structure of every other element of the cell is dictated by the light collector and flows from its design. While the design element is complete now, we expect minor modifications to further fabricate a prototype."

Solar3D's technology uses a three-dimensional design that is said to trap sunlight inside micro-photovoltaic structures where photons bounce around until they are transformed into electrons. The company was motivated to create 3D solar cell technology after studying the use of light management in fiber optic devices.

"The light collector was the first giant step. We will now be able to know how much of the light will come through to the absorbing structure," continued Nelson. "With that understanding, we will soon know what the increase in efficiency will be with our new cell relative to current technology."

With this new advancement, Solar3D expects to complete a working prototype by the end of the year.

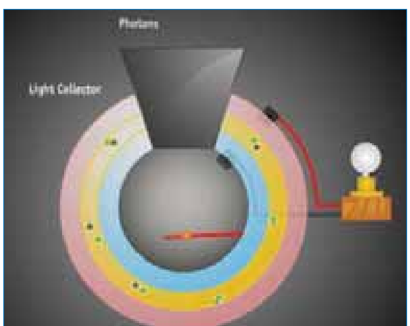

Image: Solar3D

Schematic showing cell design similar to that of Solar3D's '3D Micro-Cell' prototype (exact design not supplied for confidentiality reasons).

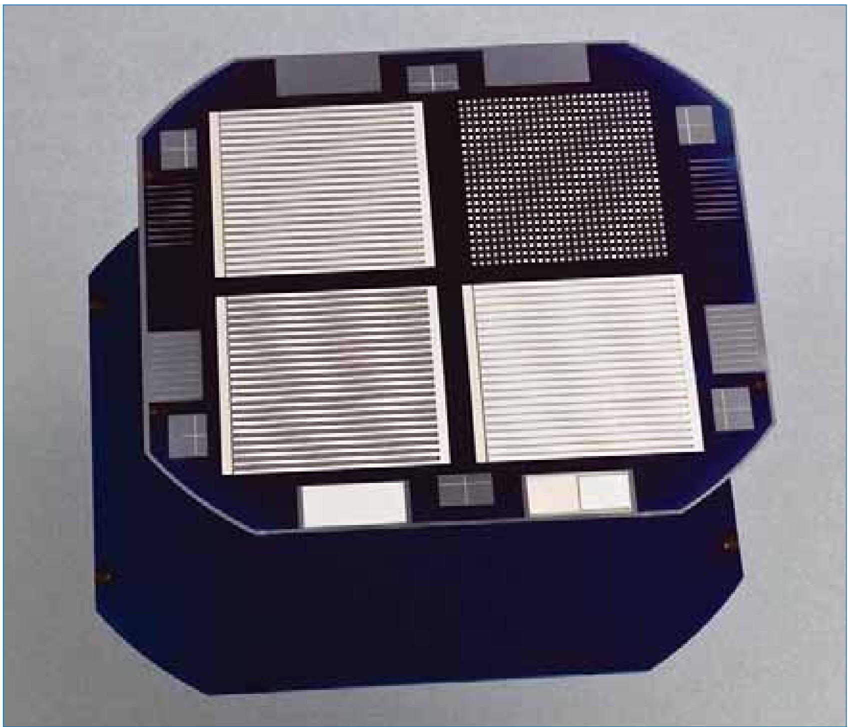

Image: Fraunhofer ISE

Structure of Fraunhofer ISE's 20%+ efficiency n-type silicon wafer. The four BC-BJ solar cells feature screen-printed contacts and Al-alloyed emitters.

Fraunhofer ISE achieves efficiencies over 20% using screen-printing technology

At the Photovoltaic Technology Evaluation Center (PV-TEC) of the Fraunhofer Institute for Solar Energy Systems (ISE) in Freiburg, researchers have reached efficiencies of up to 20.2% for back-contact silicon solar cells. For the so-called MWT-PERC solar cells, two different approaches for increasing efficiency were applied, including the screen-printed aluminium back-contact being connected to the p-type silicon material using local laser alloying.

The PV-TEC team also achieved efficiencies of 20.0% for Back-Contact Back-Junction (BC-BJ) solar cells based on n-type monocrystalline float-zone silicon material. For this solar cell concept, both the metallization with Al-alloyed emitter as well as the structuring steps are carried out exclusively with screen-printing technology.

Natcore begins production of its 'intelligent' AR coating station

Natcore Technology has set up shop at MicroTech Systems' Fremont, California facility in order to begin work on its first production model of its intelligent liquid phase deposition (LPD) processing station. The LPD process grows an antireflective (AR) coating in a warm chemical bath, which is said to eliminate the need for silane, diminish energy needs and reduce silicon use.

MicroTech's intelligent process control will be used in the LPD technology, which is to be built as an enclosed system utilizing a pre-clean subsystem for wafer cleaning before wafers are brought into the LPD process. Additionally, the system will feature Natcore's sizing and process control input with MicroTech's drying module for low metallic contamination.

The device will be used to monitor the coating process by means of MicroTech's spectrometer-based technology, which will measure the thickness of the AR coating on the wafer while it is in the chemical bath. This allows for the composition and duration of the bath to be changed so that cells can be more easily generated.

The device will be produced in two phases. The first phase will be conducted over eight to 10 weeks concluding in a manual development system that will measure 8 × 6 × 6ft. In its final composition the production system will measure 20 × 6 × 8ft, and will serve as a self-contained modular system capable of recycling its waste and generating 3,000 AR-coated wafers per hour.

Other News

Schmid produces 1,000th wet processing system

Less than eight years after opening its Shenzhen manufacturing facility in China, Schmid has produced its 1,000th wet processing system. Since production began at the factory, located close to Hong Kong, in August 2003, output has risen steadily to meet ever-increasing demand for its wet processors; in 2004, 50 systems were shipped and today Schmid delivers over 100 a year to a worldwide client base.


Image: Schmid Group

Schmid's plant in Zhuhai, opened in April 2008.

Schmid's Chinese subsidiary has grown to include a new plant in nearby Zhuhai that was opened in April 2008. The company also plans to double capacity in the near future, a move that will take its workforce past 600.

Cell manufacturers ramp up production to meet ambitious 2011 shipment forecasts

Solar cell manufacturers are undertaking aggressive expansion plans in an attempt to meet ambitious 2011 shipment forecasts, according to Solarbuzz's latest quarterly report. This ramping-up of production has the potential to create US$15.2 billion in revenue for manufacturing firms – a year-on-year rise of 41%.

Contributing to this rise will be a 31% year-on-year increase in c-Si equipment spending and a massive 71% jump in thin-film demand. Underpinning this thin-film growth is a resurgence of investments in a-Si and CIGS technologies, which account for 78% of planned thin-film capacity expansions.

Tier 1 production expansions remain dominated by aggressive schedules announced by publicly-listed Chinese c-Si producers, followed by cell producers in Taiwan and thin-film market leader First Solar. Among the companies issuing revised year-end nameplate capacities are JA Solar (3GW), Trina Solar (1.9GW), Neo Solar Power (1.8GW) and Jinko Solar (1.5GW).

"Fab investments during 2011 are providing opportunities for the PV equipment supply-chain, reflected in tool backlogs at the US$1 billion level reported during Q1 2011 by equipment leaders Applied Materials, Centrotherm, GT Solar and Meyer Burger," said Solarbuzz's senior analyst Finlay Colville. "While suppliers of choice to tier-1 manufacturers have been forced to increase monthly tool shipments, tier-2 c-Si and thin-film investments are offering significant revenue upside for emerging equipment suppliers."

Despite this capacity expansion, market demand is projected to increase by just 12% this year, as the market reacts to feed-in tariff cuts in several major European nations. This imbalance will have a profound impact on the equipment supply chain, starting with a reset of capacity growth plans during the second half of 2011.

JA Solar, Jabil Circuit sign manufacturing partnership deal

JA Solar Holdings has signed a two-year strategic partnership with electronics

BTU International wins multiple hydrogen annealing furnaces order

A major Asian solar cell manufacturer has placed an order for multiple hydrogen annealing furnaces from BTU International after the customer experienced a significant increase in absolute cell efficiency using the technology especially on Class B cells during an evaluation period.

BTU has more than 125 hydrogen furnaces in operation in the semiconductor, nuclear and other industries.

CVD Equipment brings in orders worth US$15.5 million

CVD Equipment received new orders totalling US$15.5 million for its production and research equipment in the opening months of 2011. The orders came from clients in the solar, aerospace, LED and nanotechnology industries.

Last year, CVD posted final sales figures of US$25 million – a year-on-year rise of 152% – and experienced four consecutive quarter-on-quarter rises, taking US$8 million in Q4.

Despatch sees large demand for VOC Thermal Oxidizer upgrade

Despatch Industries' patent-pending VOC Thermal Oxidizers have been making an impact on the market. Despatch reports that in the past six months it has collected orders to upgrade over 1.2GW of its installed base of CF series firing and drying services with its VOC technology.

Manz selects Rehm for advanced PV metallization line offerings

After an extensive evaluation process, Manz Automation has selected Rehm Thermal Systems' RFS-D 500 Fast-Firing System for advanced PV metallization line as part of its turnkey packages. The system will be placed directly after Manz's printer technology, which is responsible for the application of front-side fingerprint with silver sintering paste. The evaluation and selection was carried out by Manz's Solar cSi division, based in Reutlingen, Germany.

Rehm's RFS-D 500, a dual-lane fast-firing system with integrated Rehm RDS HT high temperature dryer, is now offered as an integrated system in the Manz 60MV peak c-Si line.

Image: JA Solar

JA Solar's Maple 6" multicrystalline solar cell.

solutions company Jabil Circuit. The agreement will see JA Solar supply up to 400MW of cells over the duration of the contract, as well as the certified module designs to enable Jabil to manufacture up to 200MW of modules annually.

The OEM modules will be produced at Jabil's facilities in Mexico, Poland and China, with work beginning in Q3. The companies will also join forces on marketing and selling the modules to customers, focusing particularly on their US clients.

centrotherm photovoltaics opens Indian subsidiary

Adding to its presence in Asia with subsidiaries in China, Korea, Singapore and Taiwan, centrotherm photovoltaics has opened its newest subsidiary located in Bangalore, India. The company looks to this new office to magnify its sales and service endeavours in the growing Indian PV market.

centrotherm's expansion into the Indian solar market will help put the company in a good position to take advantage the "National Solar Mission", which aims to create 20GW of solar electricity by 2022. The government program further dictates that, starting next year, crystalline solar cells for their domestic market must be manufactured in India.

Chinese firm breaks into VLSI Research's Top 10 PV equipment supplier rankings for 2010

The emergence of major PV manufacturers from China has resulted in half of global module production now emanating from the country. However, China-based PV equipment suppliers have been slow to break into the major league, which has been dominated by Europe- and US-based companies. However, VLSI Research's Top 10 PV equipment supplier rankings for 2010 tells a different story.

The 48th Research Institute of CETC, based in Changsha, the capital city of Hunan province, placed ninth in the VLSI Research rankings for 2010, with revenue of US$295 million. CETC claims a domestic market share of 80%, buoyed previously by being a key supplier of process equipment such as diffusion furnaces and etching systems to Suntech, the largest c-Si module manufacturer in 2010.

Another new entrant to the equipment rankings was Rena Sondermaschinen, noted for its wet processing technology and complete integrated system approach. Rena had revenue of US$300 million in 2010, driven by the significant capacity expansion plans of ingot/wafer producers and companies expanding their integrated manufacturing operations.

According to VLSI Research, the overall trend of capital spending shift away from amorphous silicon towards crystalline silicon cell technology supported both new entrants making the Top 10 rankings.

Despite the shift away from amorphous silicon, Applied Materials was the clear market leader overall. Revenue from both its thin-film and crystalline silicon segments reached nearly US$1.5 billion in 2010. Having strong market exposure in both wafer and cell segments meant Applied capitalized on rapid capacity expansions in wafer sawing and screen printers in particular.

Ranked second for another year was centrotherm photovoltaics with revenue of US$825 million. According to the market research firm, centrotherm was the top supplier of cell and module equipment for the crystalline silicon market in 2010.

Another firm that continues to benefit from the growth in ingot/wafer markets was ranked third in 2010: GT Solar. The company gained from revenue of US$775

p uppliers f anufacturing uipment		
Company	Ran	Reven es
Applied aterials		
centrot erm p otovoltaics A		
Solar ncorporated		
eyer r er		
e r Sc mid m +Co		
lvac nc		
Rot Ra A		
R NA Sondermasc inen m	-	
t Researc nstit te o C C	-	
erli on Solar		

VLSI Research's PV equipment supplier rankings for 2010.

million, representing 168% growth over the previous year, enabling the DSS furnace market leader to move one position higher than it reached in 2009.

Meyer Burger jumped two places to be ranked sixth on the back of sales reaching US$570 million. The company benefitted from the global polysilicon demand crisis, but also from acquisitions that have broadened its product offerings into downstream markets.

Ulvac, the top Japanese equipment supplier to the PV industry also gained one position, moving from seventh to sixth with sales of US$380 million. Germany-based Roth & Rau also moved up behind Ulvac to seventh on the back of sales of US$325 million.

With several new entrants and others moving up the rankings, several firms lost out in 2010. One of those was Gebr. Schmid, which dropped two positions with sales of US$570 million, now ranked number five.

The biggest loser would seem to be silicon thin-film turnkey supplier, Oerlikon. The company was ranked fifth in 2009 but scraped into the 2010 rankings at tenth.

According to VLSI Research, 2010 was a record-breaking year, with sales of PV manufacturing equipment crossing the US$10 billion mark (US$10.4 billion) for the first time.

Product Reviews

Denso

Denso launches speedy six-axis articulated robot series

Product Outline: Denso has launched its VS-Series six-axis articulated robots, claimed to offer the world's highest speed and precision for robots of their class, with cycle times from 0.37 to 0.33 sec. and repeatability from ±0.03 to ±0.02mm. Reaches are from 500 to 900mm and payload capacities from 4 to 7kg.

Problem: Increasing use of automation throughout the PV manufacturing supply chain has resulted in the need for high flexibility but also high productivity from robotics. Smaller units save valuable floor space and offer higher levels of robotics integration.

Solution: The new Denso VS-Series six-axis articulated robots are claimed to offer the world's highest speed and precision for their class. Their design is more compact than previous models, featuring ultra-slim arms to facilitate integration and an optional bottom-side cable connection that saves on floor space. The robots can be mounted on the floor, ceiling or wall with no special hardware needed. An extremely high maximum allowable moment of inertia enables more flexible end-effector designs and a wider range of applications than conventional robots. In addition, a new internal wiring option allows users to easily connect Gigabit Ethernet devices and servo grippers directly to the flange, preventing tangling of cables.

Applications: The robots can be used for a wide variety of applications such as assembly, dispensing, inspection, machining, machine tending, material handling, material removal, packaging, pick and place, surface finishing and test handling.

Platform: In addition to their standard IP40 protection level, a new IP67 dust- and splashproof protection option allows the robots to resist cutting chips and high-pressure washing, extending their application range.

Availability: Currently available.

Heraeus

Heraeus develops back-side tabbing conductors with lower paste laydown

Product Outline: Heraeus, developer of advanced front- and back-side silver paste for crystalline solar cells, has introduced the SOL200 Series for back-side tabbing conductors for mono- and multicrystalline silicon solar cell wafers. SOL200 has been claimed to demonstrate lower paste laydown while maintaining high adhesion and high electrical performance as well as excellent solderability with both leaded and lead-free solders.

Problem: Silver metallization pastes have become one of the highest material cost parameters in c-Si solar cell fabrication due to the dependence on the core market price of silver (Ag). The need for both high-performance silver-based pastes for improved cell performance and cost-effective conducting materials is a critical requirement for PV manufacturers.

Solution: Heraeus's new SOL200 Series for back-side tabbing conductors has been shown to demonstrate lower paste laydown while maintaining good solderability, high adhesion and high electrical performance. The increase in adhesion also demonstrates a better quality solder joint. The affect of humidity or contaminants on the integrity of the solder joint is minimized, delivering reliable thermal cycling and improved lifetime testing results, according to the company. Increased paste coverage with improved results can provide savings via improved performance as well as lower paste consumption. Coverage with SOL200 is claimed to be significantly better than competitive materials.

Applications: Back-side tabbing conductors for mono- and multicrystalline silicon solar cell wafers.

Platform: The new SOL200 Series is available in SOL220 and SOL210. The SOL210 solver paste is said to use 10% less silver than the SOL230.

Availability: Currently available.

Konica Minolta

Konica Minolta's AK Series photovoltaic reference cells provide consistent cell measurements

Product Outline: Konica Minolta Sensing Americas has introduced the AK Series of new PV reference cells to the US market to be used as a standard point of calibration to ensure consistent measurements of newly-developed PV cells. Created with the cooperation of The National Institute of Advanced Industrial Science and Technology (AIST), Konica Minolta used its advanced optical filter technology to provide high-accuracy measurement for adjusting the intensity of solar simulators used for evaluation of solar cells including tandem cells.

Problem: As cell manufacturers strive to improve the performance and characteristics of solar cells, it is necessary to perform evaluation of each product under standard test conditions. For accurate measurements, it is necessary to utilize a reference PV cell with a calibrated short-circuit current to adjust the intensity of the solar simulator to be used for measurements.

Solution: Initial offerings in the AK Series will include the AK-100 (for amorphous silicon cells), the AK-110 (for microcrystalline silicon cells), and the AK-200 (for crystalline silicon cells). Reflection characteristics for the AK-100 highlight that errors found in the short-circuit current (I_{sc}) due to multiple reflection are greatly reduced. Improvements in the optical structure suppress multiple reflections and claim to reduce the 1.3% error of conventional products to 0.0%.

Applications: Amorphous, microcrystalline and crystalline silicon cells.

Platform: The reference cells are comprised of a stable, single-crystal silicon solar cell combined with newly designed glass filters and covered with a glass plate in a specially-manufactured frame.

Availability: Currently available.

Applicability of screen-printable dopant pastes: gettering and selective emitters

T. M. Pletzer, **H. Windgassen** & **H. Kurz**, RWTH Aachen University, Institute of Semiconductor Electronics, Aachen, Germany

ABSTRACT

Phosphorus dopant pastes are an attractive alternative to the conventional phosphorus oxychloride ($POCl_3$) dopant source for emitter processing in solar cells, as they allow the fabrication of selective emitters on an industrial scale. In this paper it is demonstrated that single-sided uniform screen-printed emitters, processed with phosphorus dopant pastes, can getter multicrystalline silicon (mc-Si) wafers more effectively than conventional double-sided uniform $POCl_3$ emitters. This result is confirmed by minority carrier lifetime measurements with the quasi-stead-state photoconductance (QSSPC) method. Solar cells with selective emitters were processed using phosphorus dopant pastes on mc-Si wafers and were subsequently characterized. The current-voltage (*I-V*) results are improved compared to uniform $POCl_3$ emitter solar cells and an increased internal quantum efficiency (IQE) for selective emitter solar cells is demonstrated.

Introduction

The development of new industrial solar cell concepts is being accelerated by selective emitter technology [1]. Such emitters feature high doping (~30Ω/sq.) beneath the front contact grid and moderate doping elsewhere (~100Ω/sq.). Thereby selective emitters can increase the efficiency of solar cells by improving the IQE in the ultraviolet (UV) wavelength range due to reduced Auger recombination in the emitter [2,3]. Furthermore, selective emitters permit lower contact resistance values at the front-side metallization resulting in a lower series resistance compared to conventional solar cells [3].

Producing selective emitters by screen-printing of phosphorus dopant pastes [4–6] in combination [3,7] with conventional $POCl_3$ diffusion is an attractive fabrication method and is employed in this work. This article presents a summary of current and previous work to show the applicability of screen-printable dopant pastes in regard to gettering and selective emitter structures, which have been investigated in more detail by Pletzer et al. [7,8]. In order to successfully apply these selective emitter structures, it is crucial to investigate gettering [8–10] and emitter doping profiles [11,12]. During emitter formation, efficient gettering of impurities such as metal, is essential to improving the wafer quality, as these impurities lead to unwanted Shockley-Read-Hall (SRH) recombination.

Gettering of impurities occurs when phosphorus diffuses into the wafer from a phosphorus source such as a $POCl_3$ gas or a phosphorus dopant paste. Driven by the concentration gradient of phosphorus, the impurities diffuse towards the emitter surface during emitter formation at high temperatures. At the surface the impurities have a high solubility. Subsequently, the formed phosphorus impurity complexes are strongly bound in the emitter by Coulomb forces. This binding is strong enough to prevent recontamination by, for example, metal silicide precipitation at grain boundaries [13]. Afterwards, these bound impurities have only negligible influence on the characteristics of the fabricated solar cells.

Conventional double-sided $POCl_3$ emitters allow the fabrication of uniform emitters and provide an effective double-sided gettering [9]. In contrast, screen-printed emitters, as presented in this study, provide only single-sided gettering. Thus, the formation of a parasitic p-n junction at the back side of the cell is suppressed [14], giving way to new cell designs, such as rear-side passivated cells [15].

This work focuses on the gettering efficacy in mc-Si wafers using uniform screen-printed emitters [7,8], the measurement of selective emitter profiles and the investigation of solar cells with selective emitters.

For the second section, the gettering efficacy of uniform screen-printed emitters was obtained by minority carrier lifetime measurements using the QSSPC method [16] and has been compared with results of conventional uniform $POCl_3$ emitters, which were used as references in this work.

The best phosphorus dopant paste was used to process selective emitters on mc-Si wafers. These emitters were characterized to determine phosphorus doping profiles, compared to conventional uniform $POCl_3$ emitters.

Finally, entire solar cells with screen printed selective emitters were processed and characterized to explore their potential for industrial production.

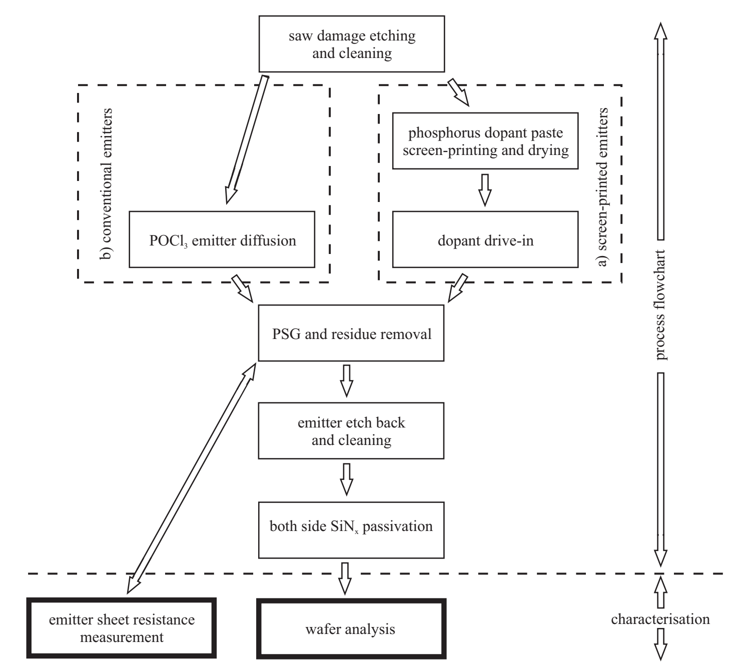

Figure 1. Process flowchart of the gettering investigation.

Process technology for gettering

Eleven dopant pastes with different phosphorus concentrations were compared in the fabrication process of single-sided emitters. All samples were processed on neighbouring mc-Si wafers from the same brick with boron doping (p-type). The process sequence and analysis steps are outlined in Fig. 1. An alkaline saw damage etch and a subsequent cleaning were followed by the emitter formation in two different ways: (i) screen-printing of different phosphorus dopant pastes on one side of the wafer, followed by diffusion (samples one to 11) and (ii) conventional batch $POCl_3$ diffusion on both sides of the wafer as reference (sample 12).

Control samples without emitter diffusion were included in the study to monitor the as-received material quality (sample 13).

The diffusion process was carried out in the same quartz tube furnace at a temperature of about 820°C with constant gas flow and time [5,11]. Later, the phosphorus silicate glass (PSG), formed as a by product of the diffusion process, was removed along with any residues by a dip in diluted hydrofluoric acid.

Emitter sheet resistance (R_{sh}) measurements (Fig. 1) were carried out using a four-point-probe technique. In Table 1, single-sided uniform screen-printed emitters with different phosphorus pastes, their respective R_{sh} and standard deviation (σ) are listed. An emitter is regarded as sufficiently uniform if $\sigma \leq 10\%$, so that local differences in the contact formation do not significantly influence the whole solar cell. The emitter R_{sh} of the samples one to three and the $POCl_3$ reference sample are in a typical range of emitters used in industrial solar cell production (approx. 50–60Ω/sq.). Samples four to eight show emitter R_{sh}, which is typical for weakly-doped emitters with low phosphorus concentration. Samples eight, 10 and 11 have $\sigma > 10\%$, apparently caused by very low phosphorus concentration in the pastes. It is mainly observed that an increase in R_{sh} is correlated to the value of σ. The significantly high value of σ from samples six and nine was presumably caused by visible dopant paste residues that remained even after PSG removal.

Afterwards these emitters were removed through a wet etch on both sides of all samples and a subsequent cleaning (Fig. 1). The silicon nitride (a-SiN_x:H) anti-reflection coating (ARC) was deposited on both sides of the wafers [15], followed by a thermal treatment as a co-firing step, which is necessary to allow hydrogen diffusion to defect passivation.

The surface passivation layers were processed identically with high passivation quality [15] to achieve low surface recombination velocities. Therefore, the measured effective minority carrier lifetime [16] (wafer analysis in Fig. 1) can be related directly to the bulk lifetime ($\tau_{eff\ bulk}$), listed in Table 1.

Sample/source	R_{sh} [Ω/sq.]	σ [%]	$\tau_{eff\ bulk}$ [µs]
1/p-paste	51	9	12.6
2/p-paste	52	6	9.6
3/p-paste	54	5	11.6
4/p-paste	68	5	11.2
5/p-paste	74	5	11.9
6/p-paste	79	22	7.5
7/p-paste	95	7	8.5
8/p-paste	104	20	6.3
9/p-paste	119	36	6.9
10/p-paste	145	26	10.0
11/p-paste	711	19	3.2
12/$POCl_3$ reference	59	5	8.5
13/Material control	—	—	1.9

Table 1. Comparison of sheet resistances (R_{sh}) and standard deviation (σ) in R_{sh} of screen-printed emitters and a $POCl_3$ reference emitter on mc-Si wafers as well as their effective lifetime ($\tau_{eff\ bulk}$) at 5×10^{15}cm^{-3} averaged over a sample area of ≈13cm². Repeated measurements differ by < 10%.

Compared to the material control sample 13 having a $\tau_{eff\ bulk}$ of 1.9µs in agreement with the material specification of $\tau_{eff\ bulk} \geq 2$µs, all other test samples – including reference samples – showed an increase in the effective bulk lifetimes, mainly because of gettering. The $\tau_{eff\ bulk}$ of samples one to five, and seven and 10 exhibit even more effective gettering and achieve $\tau_{eff\ bulk}$ equal to or higher than the reference samples. However, samples six, eight, nine and 11 getter less effectively than the reference, due to a lower phosphorus concentration used during diffusion, as determined by R_{sh}. In general, the results in Table 1 demonstrate that screen-printed emitters can getter even more effectively than conventional $POCl_3$ emitters.

The gettering efficacy is displayed in Fig. 2, where the relative difference between $\tau_{eff\ bulk}$ of the non-gettered and gettered sample is plotted against the R_{sh} values.

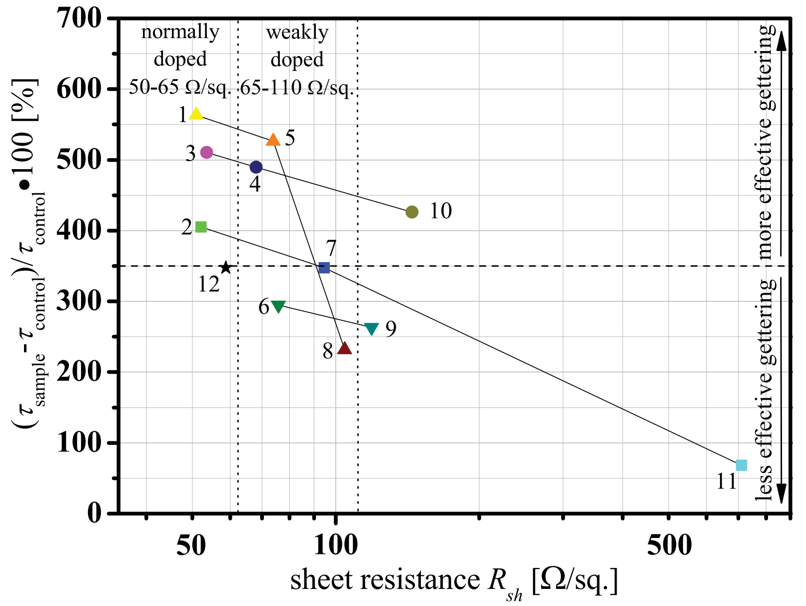

Figure 2. Gettering efficacy based on material control sample versus sheet resistance R_{sh}. A low R_{sh} allows a more effective gettering. Samples processed with dopant pastes from the same manufacturer are connected by a line as a guide to the eye.

A low R_{sh} associated with a high phosphorus concentration [11] yields higher gettering efficacy and vice versa. A similar correlation between gettering efficacy and the phosphorus concentration in $POCl_3$ emitters was found by Bätzner et al. [17]. High phosphorus concentration leads to better gettering by binding a higher number of impurities and enabling higher impurity solubilities, which decreases SRH recombination significantly [13].

> **"High phosphorus concentration leads to better gettering by binding a higher number of impurities and enabling higher impurity solubilities."**

Comparing a screen-printed and a $POCl_3$ emitter of similar R_{sh}, a higher peak and surface electrically active phosphorus concentration (CP) is found for the $POCl_3$ emitter (Fig. 3). Whereas the overall phosphorus concentration is slightly higher (~10%), it is significantly higher if both sides of the $POCl_3$ emitter are accounted for. Yet the gettering efficacy of the dopant paste process is still better, as evidenced by the bulk lifetime measurements (Table 1). It is apparent that another process parameter changed, thus influencing the gettering process more than the phosphorus concentration.

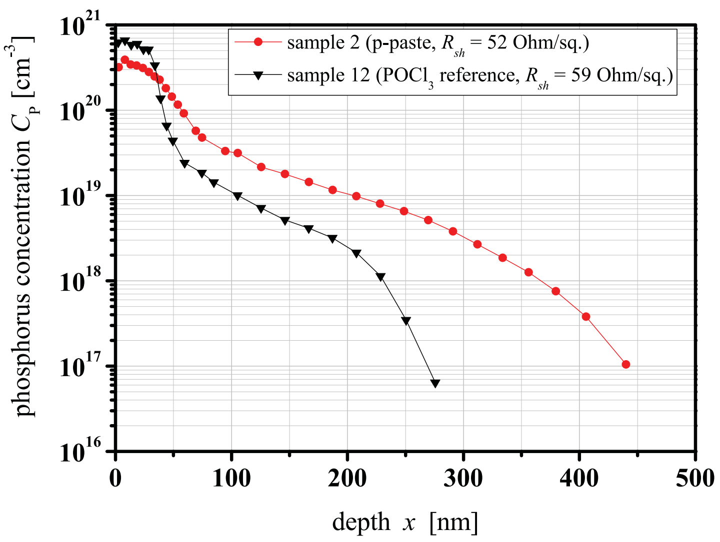

Figure 3. Typical electrically active phosphorus concentration C_P measured by the electrochemical capacitance voltage (ECV) method versus depth (x) in the silicon wafer. Included are a $POCl_3$ reference emitter (sample 12) and a screen-printed emitter (sample 2) with comparable R_{sh}. The $POCl_3$ emitter shows a higher phosphorus surface concentration than the screen-printed emitter, but otherwise the screen-printed emitter features a deeper phosphorus profile. R_{sh} values calculated from these profiles are identical to the values extracted from four-point-probe measurements (Table 1).

The most likely candidate is the effective gettering time, which had been kept constant in the previous studies, where the correlation between gettering and phosphorus concentration has been investigated [17]. Here, however, the emitters are processed in fundamentally different ways. In the case of the screen-printed emitters a dopant paste layer of several μm in thickness is deposited

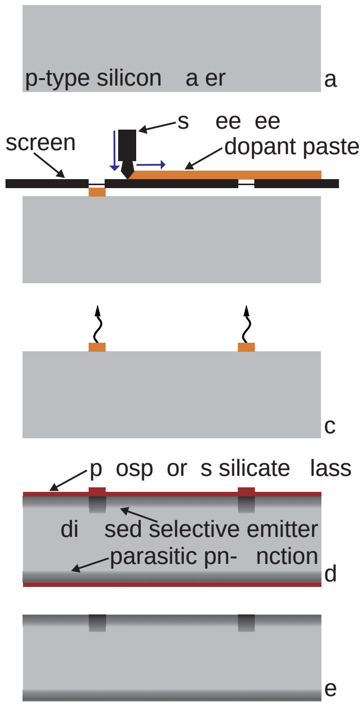

Figure 4. Process sequence for the selective emitter fabrication: a) wet chemical texturing and cleaning; b) screen-printing of phosphorus dopant paste; c) dopant paste drying; d) single-step diffusion of highly-and lowly-doped areas of the selective emitter; e) PSG removal.

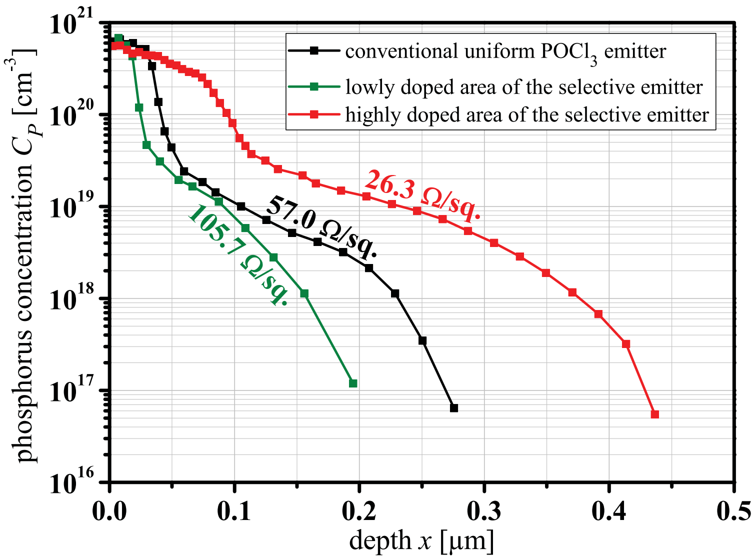

Figure 5. Electrically active phosphorus concentration C_P versus emitter depth (x). C_P was determined by ECV measurements. The selective emitter shows highly- and lowly-doped areas in contrast to the conventional uniform POCl$_3$ emitter.

onto the wafers. This represents a finite doping source, which is available during the entire high temperature process, including furnace stabilization time. Diffusion and gettering start immediately upon reaching the necessary temperature. In the case of POCl$_3$ emitters, a PSG layer of a typical thickness of 10nm has to form after the high temperature is stabilized and the POCl$_3$ gas flow has been activated. Phosphorus diffusion into the silicon, and hence gettering, cannot start without a PSG layer. During diffusion the phosphorus supply in the PSG is refilled from the gas phase, creating an infinite doping source and leading to a higher surface and peak phosphorus concentration (Fig. 3).

Consequently, the overall time during which gettering was possible, i.e. the effective gettering time, was about 42 minutes for the POCl$_3$ process, minus the time for PSG layer formation. For the screen-printed emitters, the effective gettering time, including temperature stabilization, was about 61 minutes – almost 50% longer. This difference in gettering and diffusion times is responsible for the increased gettering efficacy (Table 1) and deeper emitter profiles of the screen-printed emitters (Fig. 3). It should be noted that this increased effective gettering time does not change the overall process duration, but is rather a consequence of the earlier availability of phosphorus.

Analysis of selective emitters

The samples for selective emitter characterization and subsequent solar cell analysis were processed on similar material as before, but with a thickness of 190µm after texturing. The samples for the selective emitter analysis were prepared by a wet chemical acid texturing and a subsequent cleaning (Fig. 4a), which were followed by the emitter formation steps: screen-printing of a phosphorus dopant paste for the highly-doped area of the selective emitter on the wafer front side (Fig. 4b), drying of the dopant paste (Fig. 4c) followed by a uniform POCl$_3$ diffusion to form the lowly-doped area of the selective emitter and to drive the phosphorus from the paste into the wafer (Fig. 4d). Additional reference emitters were processed with only the conventional batch POCl$_3$ diffusion on both wafer sides. After emitter diffusion, the PSG was removed (Fig. 4e) and the emitter was characterized by four-point-probe measurements to determine R_{sh}.

ECV measurements [18] were conducted to determine the spatially resolved phosphorus doping profiles of the selective emitters. In addition, R_{sh} values were also calculated using the corresponding doping profiles and results were compared with the values from the four-point-probe measurements.

The analysis of selective emitter structures revealed two well distinguished areas with respect to different doping, which was observed by four-point-probe and ECV measurements. The ECV measurements of C_P (Fig. 5) and the extracted values of R_{sh} certify the uniform POCl$_3$ reference emitter with a typical R_{sh} of 57.0Ω/sq. For

Emitter type	V_{oc} [mV]	J_{sc} [mA/cm^2]	FF	η [%]
Selective	615.6±1.2	34.0±0.1	0.73±0.01	15.3±0.2
POCl$_3$	613.7±1.5	33.3±0.0	0.75±0.01	15.1±0.1

Table 2. Parameters of the *I-V* measurements on mc-Si solar cells with screen-printed selective emitters and uniform POCl$_3$ emitters as reference. Values listed are averaged over five cells and errors given are σ.

Emitter type	J_{01} [pA/cm^2]	J_{02} [nA/cm^2]	R_s [Ωcm^2]	R_p [kΩcm^2]
Selective	0.7±0.0	87.6±8.2	0.53±0.08	1.4±0.1
POCl$_3$	0.9±0.0	78.2±6.8	0.56±0.10	1.1±0.3

Table 3. Parameters of the *I-V* data fit by the two-diode-model of mc-Si solar cells with screen-printed selective emitters and uniform POCl$_3$ emitters as reference. Values listed are averaged over five cells and errors given are σ.


bundle of energy loves regeneration
Innovative solutions from BASF ensure that solar panels remain full of energy even if the sun doesn't shine for brief periods. Our solutions and expertise cover the entire solar cell production process from wafer cutting to module framing. Sunlight can be efficiently turned into energy. At BASF, we create chemistry.
solar-cells@basf.com
BASF
The Chemical Company

the selective emitter R_{sh} the highly-doped area is around 26.3Ω/sq. and for the lowly-doped area around 105.7Ω/sq. These measurements demonstrate the existence of the selective emitter structure, which is also visible in the different C_p profiles (Fig. 5). This claim is further supported by the four-point measurements of R_{sh}, where very similar values were measured.

Performance of selective emitter solar cells

All solar cells presented in this work were processed in a conventional industrial process line with wet chemical acid texturing, emitter formation, an SiN_x:H deposition for the ARC [15] and metallization by screen-printing, which also creates an aluminium back-surface field (BSF). Solar cells with selective emitters were processed with the combination of screen-printing and $POCl_3$ diffusion as described earlier (Fig. 4). The reference solar cells were processed with uniform emitters using the conventional $POCl_3$ diffusion. Consequently, the solar cells were characterized by *I-V*, suns V_{oc} [19], spectral response (SR) and reflection measurements. The *I-V* data were fitted by the two-diode-model and the IQE was calculated from the SR and reflection data [20].

The *I-V* measurements (Table 2) certify the selective emitter solar cells with the highest average solar cell efficiencies (η), with values of up to 15.3%. The η gain of up to 0.2% absolute is realized with lower fill factors (FF) than the reference solar cells with uniform $POCl_3$ emitters. The slightly lower FF of the selective emitter solar cells are presumably caused by the solar cell process, which was not optimized for this emitter type. Nevertheless, values of the open circuit voltage (V_{oc}) and short circuit current density (J_{sc}) are also increased and show the highest values for the selective emitter solar cells.

In the following section the differences in the *I-V* curves are discussed using the two-diode-model parameters [21] (Table 3) and further solar cell characterization. From the *I-V* data, the parameters' diffusion current density (J_{01}), recombination current density (J_{02}), series resistance (R_s) and parallel resistance (R_p) are derived according to the two-diode-model and listed in Table 3. The R_P of all solar cells is sufficiently high to exclude shunting loses, which would result in a low FF. The solar cells with selective emitters have slightly lower R_s values due to the lower contact resistance using selective emitter structures as well as differences in individual co-firing parameters.

J_{02} is traditionally considered a measure for recombination in the space charge region and can be related to the density of recombination centres in solar cells. A more effective gettering should reduce the SRH recombination, yielding to a low J_{02}. The lowest J_{02} values of 78.2nA/cm² are observed by the reference solar cells due to stronger gettering caused by the higher doping of the reference $POCl_3$ emitter with R_{sh} of around 59Ω/sq., compared to the selective emitters with R_{sh} of around 103Ω/sq. for ~ 92% of the emitter area.

J_{01} mainly provides information about the recombination in the emitter and at the surface. The lower doping in the illuminated area of the selective emitter structure results in lower J_{01} values of 0.7pA/cm² for these solar cells compared to the reference solar cells with J_{01} values of 0.9pA/cm². The difference in J_{01} is directly responsible for the difference in V_{oc}, as confirmed by a simulation using the two-diode-model.

The differences in J_{01} are also monitored in the IQE curves (Fig. 6). The selective emitter solar cells feature a higher IQE than the uniform $POCl_3$ reference solar cells in the wavelength range from 300 to 600nm. This IQE gain is caused by reduced recombination in the selective emitter structure due to the lower emitter doping. Furthermore, the demonstrated IQE gain of the selective emitter solar cells increases the J_{sc} of these cells (Table 2). The IQE spectra of both solar cell types are nearly identical above 600nm.

Finally, the processed solar cells were characterized by Suns V_{oc} measurements [19] to evaluate the potential of the developed selective emitter cells. These measurements neglect the influence of R_s in the solar cells and allow the calculation of a pseudo FF and pseudo η. The values determined are listed in Table 4. The pseudo FF of selective emitter solar cells shows a gain of 0.01% absolute over the reference solar cells. Considering the higher real FF (Table 2) of the reference solar cells, it is obvious that selective emitter solar cells can benefit greatly from further optimizations. The pseudo η of selective emitter solar cells show a gain of 0.5% absolute over the reference solar cells. Taking into account that R_s is neglected in this measurement, the largest optimization potential is in the geometrical design of the selective emitter grid lines and in the individually adjusted metallization using modified silver pastes.

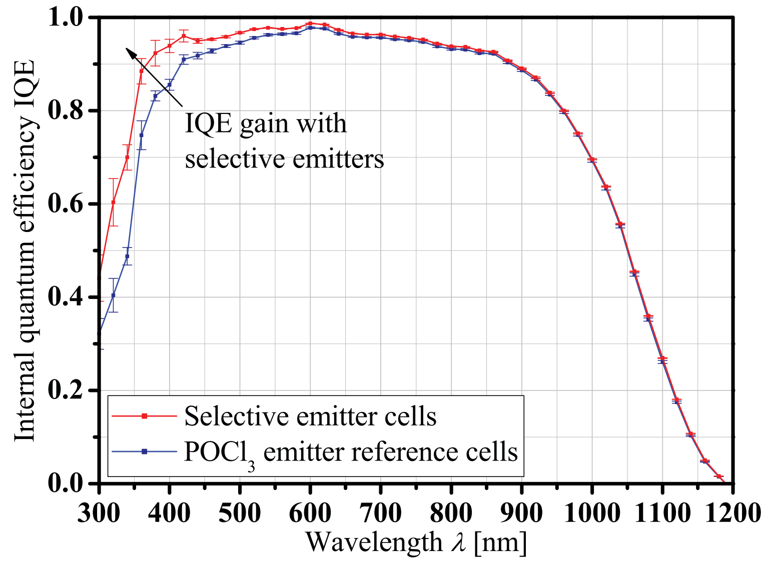

Figure 6. Internal quantum efficiencies (IQE) versus wavelength λ for selective emitter solar cells (red curve) and reference cells with uniform $POCl_3$ emitters (blue curve). All IQE data are averaged over five solar cells, error bars indicate σ.

Emitter type	Pseudo FF	Pseudo η [%]
Selective	0.80±0.01	16.3±0.2
$POCl_3$	0.79±0.01	15.8±0.2

Table 4. Parameters of the Suns V_{oc} measurements of mc-Si solar cells with screen-printed selective emitters and uniform $POCl_3$ emitters as reference. Values listed are averaged over five cells and errors given are σ.

Conclusion

The developed selective emitter concept allows an η gain of 0.2% absolute in processed mc-Si solar cells on an industrial scale and shows a possible η gain of 0.5% absolute. The gain originates from the front surface, as evidenced by the IQE gain in the UV region. J_{sc} and V_{oc} are also seen to increase.

ECV and four-point-probe measurements

prove the existence of selective emitter structures consisting of highly- and lowly-doped areas, which were processed in a single diffusion step by combining screen-printing of phosphorus dopant pastes and $POCl_3$ diffusion.

Most of the employed phosphorus dopant pastes are suitable for emitter formation and allow a high gettering efficacy. This is shown with single-sided uniform screen-printed emitters, which can getter mc-Si wafers more effectively than the reference double-sided uniform $POCl_3$ emitter.

Acknowledgements

The authors would like to thank E. F. R. Stegemann (Q Cells SE) and D. L. Bätzner (Roth & Rau Switzerland AG) for their helpful work during their time at the Institute of Semiconductor Electronics, RWTH Aachen University. We would also like to thank R. Bleidiessel from Solland Solar Cells B.V. in the Netherlands for his cooperative involvement. Further, the authors are also thankful to K. Wolter and S. Suckow from the Institute of Semiconductor Electronics, RWTH Aachen University for careful reading of the manuscript and B. Mayer for his assistance with sample preparation and measurements. This work is part of the project "Admitter – Innovative Emitterstrukturen für Solarzellen", which is in cooperation with AMO GmbH (Germany), Solland Solar Cells B.V. (The Netherlands) and has been supported by the Ministry of Economic Affairs and Energy of the State of North Rhine-Westphalia in Germany and the European Commission.

References

[1] Chunduri, S.K. 2009, "Be selective!", *Photon International*, Vol. 11, pp. 108–116.

[2] Horzel, J. et al. 2000, "High efficiency industrial screen printed selective emitter solar cells", *Proc. 16th EU PVSEC*, Glasgow, pp. 1112–1115.

[3] Pletzer, T.M. 2010, *Die multikristalline Silizium-Solarzelle: Die Entwicklung zum selektiven Emitter*, Ph.D. Thesis, RWTH Aachen University, Aachen, Germany.

[4] Salami, J. et al. 2004, "Characterization of screen printed phosphorous diffusion paste for silicon solar cells", *Proc. 14th International Photovoltaic Science and Engineering Conference*, Bangkok, Thailand, pp. 263–264.

[5] Edwards, M. et al. 2008, "Screen-print selective diffusions for high efficiency industrial silicon solar cells", *Progress in Photovaltaics*, Vol. 16, No. 1, pp. 31–45.

[6] Pletzer, T.M. et al. 2009, "Extensive investigation and characterisation of solar cells with screen-printed emitters using phosphorus dopant pastes", *Proc. 24th EU PVSEC*, Hamburg, Germany, pp. 2080–2083.

[7] Pletzer, T.M. et al. 2010, "Gettering efficacy of screen-printed emitters in multicrystalline silicon for solar cells with selective emitters", *Proc. 5th WCPEC*, Valencia, Spain, pp. 2039–2042.

[8] Pletzer, T.M. et al. 2011, "Gettering in multicrystalline silicon wafers with screen-printed emitters", *Progress in Photovoltaics*, John Wiley & Sons Ltd.

[9] Janßen, L. et al. 2004, "Phosphor diffusion gettering and emitter optimization of multi-crystalline silicon solar cells", *Proc. 19th EU PVSEC*, Paris, France, pp. 628–631.

[10] Bätzner, D.L. et al. 2005, "Dependence of phosphorous gettering of multicrystalline silicon on diffusion sheet resistance and ingot position", *Proc. 20th EU PVSEC*, Barcelona, Spain, pp. 655–658.

[11] Tsai, J.J.C. 1969, "Shallow phosphorus diffusion profiles in silicon". *Proc. IEEE*, Vol. 57, No. 9, pp. 1499–1506.

[12] Brammer, T. et al. 2001, "Analysis of phosphorus doped emitter profiles of multicrystalline Si solar cells", *Proc. 17th EU PVSEC*, Munich, Germany, pp. 1842–1845.

[13] Meyers, S.M. et al. 2000, "Mechanisms of transition-metal gettering in silicon", *Journal of Applied Physics*, Vol. 88, No. 7, pp. 3795–3819.

[14] Pletzer, T.M. et al. 2006, "Screen-printed phosphorous emitter for industrial thin multi crystalline silicon solar cells", *Proc. 21st EU PVSEC*, Dresden, Germany, pp. 838–841.

[15] Janßen, L. et al. 2007, "Passivating thin bifacial silicon solar cells for industrial production", *Progress in Photovoltaics*, Vol.15, No. 6, pp. 469–475.

[16] Sinton, R. et al. 1996, "Contactless determination of current-voltage characteristics and minority-carrier lifetimes in semiconductors from quasi-steady-state photoconductance data", *Applied Physics Letters*, Vol. 69, No. 17, pp. 2510–2512.

[17] Bätzner, D.L. et al. 2005, "Dependence of phosphorous gettering of multicrystalline silicon on diffusion sheet resistance and ingot position", *Proc. 20th EU PVSEC*, Barcelona, Spain, pp. 655–658.

[18] Bock, R. et al. 2008, "Accurate extraction of doping profiles from electrochemical capacitance measurements", *Proc. 23rd EU PVSEC*, Valencia, Spain, pp. 1540–1543.

[19] Sinton, R.A. et al. 2000, "A quasi-steady-state open-circuit voltage method for solar cell characterization", *Proc. 16th EU PVSEC*, Glasgow, Scotland, pp. 1152–1155.

[20] Yang, W.J. et al. 2008, "Internal quantum efficiency for solar cells", *Solar Energy*, Vol. 82, No. 2, pp. 106–110.

[21] Wolf, A. et al. 1977, "Investigation of the double exponential in the current-voltage characteristics of silicon solar cells", *IEEE Transactions on Electron Devices*, Vol. 24, No. 4, pp. 419–428.

About the Author

Tobias Markus Pletzer is a postdoctoral research fellow and project manager in the photovoltaic group of the Institute of Semiconductor Electronics at RWTH Aachen University, Germany. He received his Ph.D. in 2010 in the Faculty of Electrical Engineering and Information Technology at the RWTH Aachen University and completed his study in computer engineering successfully with a diploma degree as a graduate engineer in 2004 at the University of Siegen, Germany. In his scientific work, he focuses on solar cell technologies, especially on new concepts and characterization techniques.

Enquiries

RWTH Aachen University
Sommerfeldstraße 24, D 52074 Aachen, Germany
Tel: +49 241 80 27892
Email: pletzer@iht.rwth-aachen.de

TCAD in the semiconductor industry and its advantages for solar cell manufacturing

Nick E.B. Cowern & **Chihak Ahn**, School of Electrical, Electronic and Computer Engineering, University of Newcastle-upon-Tyne, UK

ABSTRACT

Technology computer-aided design (TCAD) is pervasive throughout research, development and manufacturing in the semiconductor industry. It allows very low-cost evaluation of process options and competing technologies, guides process development and transfer to production and supports more efficient process improvement with minimal down time in the factory environment. This paper reviews the use of TCAD in the semiconductor industry and shows, with some illustrative examples, its important enabling role for the PV industry.

Introduction

Technology computer-aided design (TCAD) is a computer-based procedure used to predict the structure and performance of fabricated semiconductor devices. Within TCAD, 'process simulation' tools are used to predict the device structures formed as a result of a specific chain of processing steps, and 'device simulation' tools compute the electrical response of devices to boundary conditions, such as contact potentials/currents and compute energy inputs/outputs such as light and heat. TCAD simulation tools typically solve continuum equations for atomic or electronic transport. At nanometre length scales, techniques such as kinetic Monte Carlo are used to increase accuracy and gain insight into statistical variations, while at the atomic scale, first principle quantum calculations are used to determine fundamental parameters of materials and TCAD models. Structures computed by process simulation can be used in device simulation tools to explore the impact of process variations on device performance.

TCAD is widely used in the microelectronics industry to reduce process development time and costs, and to ensure optimal performance of fabricated devices. It is a key component of the International Technology Roadmap for Semiconductors (ITRS) and of every semiconductor IC manufacturer's research, development and production program. In recent years, TCAD models, especially those used to compute the effects of processing steps, have matured considerably as a result of widespread research in universities, institutes and companies over recent years [1,2]. Process models now require relatively little 'calibration' to specific Si-based technology processes.

At the same time, industry-standard device models have been extended to include opto-electronic interactions, thus enabling application to light-emitting devices and PV [3].

These advances have created a capability ripe for application in the PV industry, where the use of TCAD is rapidly increasing but is not yet well established. As in the microelectronics industry two to three decades ago, the focus has mainly been on device modelling [4,5]. Little work is currently done (as of early 2011) to use integrated process and device TCAD to explore the impact of process changes on solar cell efficiency. Such investigations are often done using in-line processing experiments and expert intuition, despite difficulties in picking out true optima because of the many trade-offs between process parameters, and experimental fluctuations arising from processing variability and drift.

"Little work is currently done to use integrated process and device TCAD to explore the impact of process changes on solar cell efficiency."

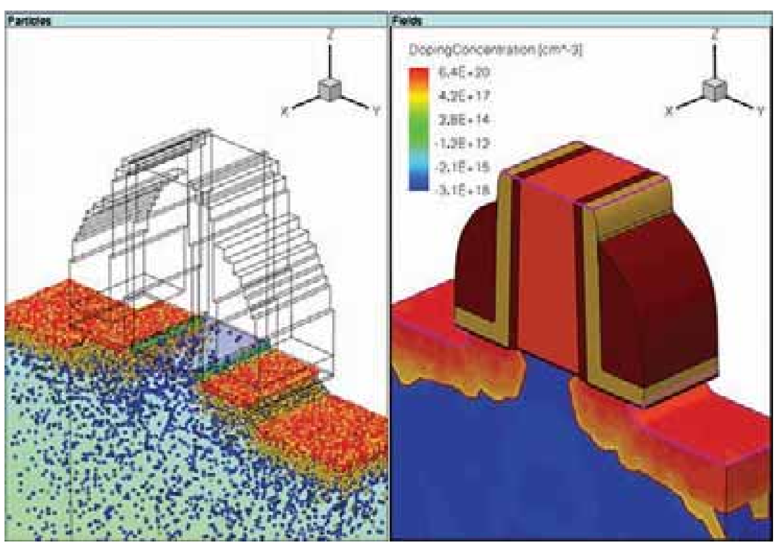

Figure 1. Atomistic 'Kinetic Monte Carlo' simulation of dopant atoms (left) and corresponding doping distribution (right) in a deep-submicron planar silicon MOS transistor.

Image courtesy of N. Zographos, Synopsys.

In this paper we look at the ways in which TCAD can accelerate enhancements in cell efficiency, often at very little or even negative cost – impacting strongly on industrial competitiveness, just as occurred historically in the semiconductor industry. This is illustrated using four examples: integrated process and device TCAD optimization of doping in an LGBC c-Si cell process; study of 3D current crowding effects in a cell with passivated rear side and local contacts; 3D simulations of emitter wrap-through (EWT) and metal wrap-through (MWT) cells; and a brief look at modelling light absorption in a textured thin-film solar cell.

Application of integrated TCAD to an established c-Si cell technology

This section explores the potential of integrated process and device modelling to optimize the processing of front-contacted solar cells with respect to

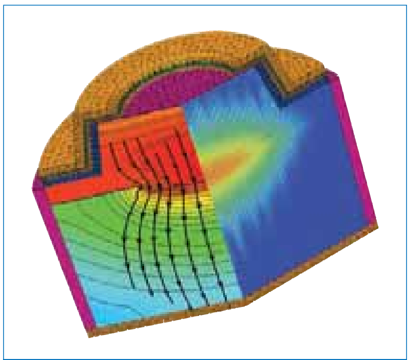

Image courtesy of Stefan Odermatt, Synopsys.

Figure 2. Internal device physics of a vertical cavity surface emitting laser, as used in a computer mouse. Left side: lattice temperature with stream traces of the electronic current. Right side: optical emission intensity.

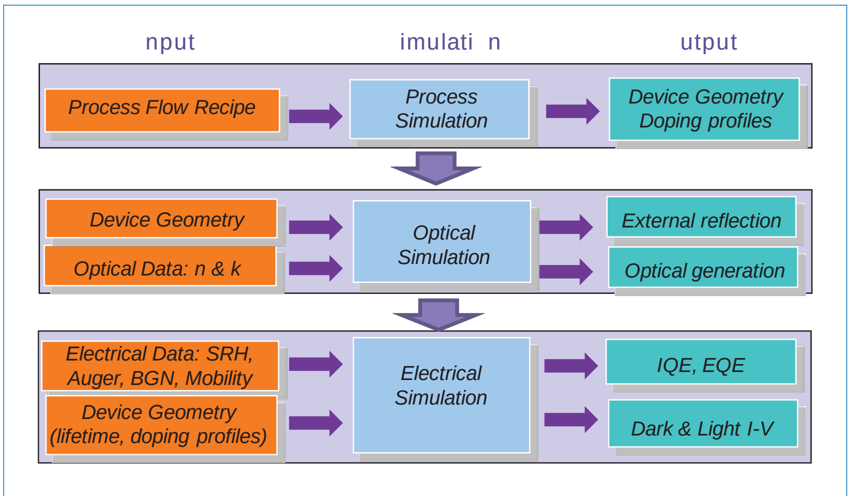

Figure courtesy of Synopsys.

Figure 3. Schematic flow of integrated process and device simulation.

efficiency. The example illustrated is a well established, well characterized technology: the laser-grooved buried contact (LGBC) solar cell manufactured by the UK National Renewable Energy Centre (Narec). Process simulations are compared to short-loop process experiments; integrated process and device simulation is then used to develop conclusions on trade-offs and potential further process optimization of the LGBC process [6]. Overall efficiency enhancements of ~1% appear possible, even before improvements such as local rear-side contacts are added.

The procedure used is similar to what is needed to explore a novel technology. We first discuss the modelling of the fabrication process and then use the resultant simulated structures as input information for device simulation of the operation of the fabricated solar cells.

Process modelling

The structure of the LGBC cell is reproduced in Fig. 4. It includes a shallow emitter, passivation/antireflection coating, laser-cut grooves, groove diffusion and Al back-surface field and contacts.

The evolution of the wafer structure during processing is modelled in 2D using the 1–3D simulation tool Sentaurus process [3]. Some of the advanced process models implemented in this tool have originated from collaboration with our group. The tool also provides an interface for specifying custom physical models, by coding them mathematically in a TCL-based language. We use this feature to model the $POCl_3$ deposition process and the back-surface field (BSF).

The range of length scales in a PV cell presents a challenge for process simulation. A manufactured cell usually has an area of

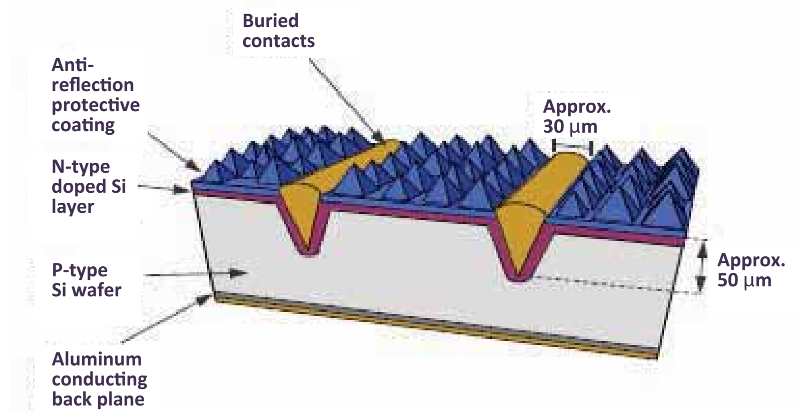

Figure 4. Schematic diagram of the LGBC solar cell structure.

Figure courtesy of Narec.

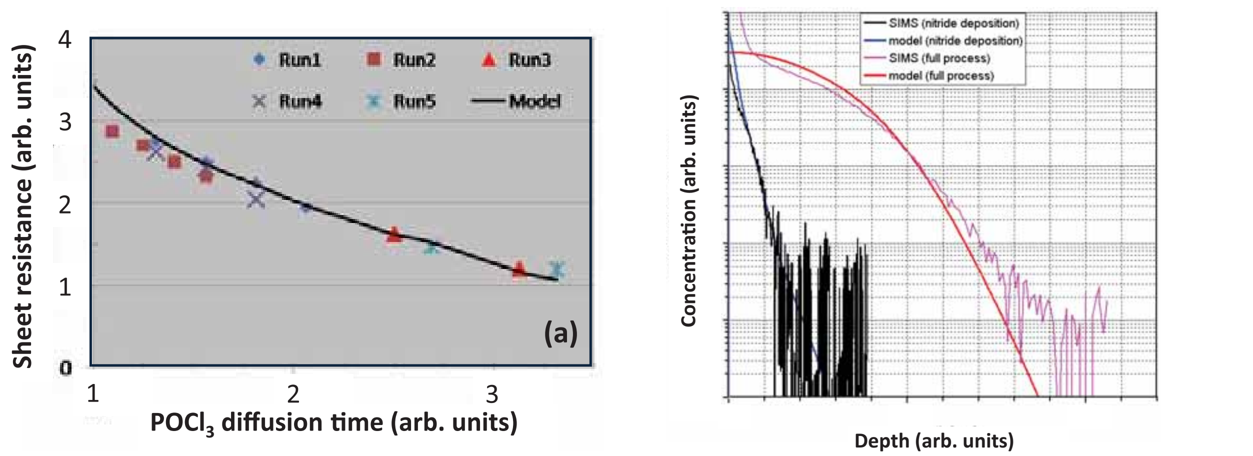

Figure 5. a) Emitter sheet resistance values after a thermal budget equivalent to the full LGBC process. Symbols show experimental data; the curve shows the simulation result. Indicated values are in arbitrary units. b) SIMS profiles and model simulations for the phosphorus emitter profile after nitride deposition, and after full thermal process.

$100cm^2$ or more, while diffusion features can be less than 100nm deep. We take advantage of the repeating finger structure to model an 'elementary' cross-section through the cell, extending laterally between the mid-points of two adjacent pairs of fingers and vertically right through the wafer. To save further computation time, process simulation is restricted to areas where the dopant concentration varies. The results are then translated or merged into the full simulation area for device simulation. Regions simulated are the shallow emitter, corner regions of the groove structure, and the BSF doping. Surface texturing used in manufactured cells is not explicitly modelled here, which influences some aspects of device simulation results. Modelling texture effects on light distribution is discussed in the last section of this paper.

The first step in the LGBC process is P deposition using a $POCl_3/O_2$ gas mixture. PSG is simulated as an oxide layer containing a high level of P, with calibrated interface states and P diffusivity. Fig. 4a shows the resultant trend in emitter sheet resistance versus deposition time. Measured values for planar non-textured wafers are well described by the model simulations, and SIMS measurements of P emitter profiles (Fig. 4b) are also in reasonable agreement. The resulting calibrated model is used to study the effects of different thermal cycles for the emitter diffusion.

The next few simulation steps see the nitride being deposited, the laser-cut groove structure is modelled, and a high temperature $POCl_3/O_2$ diffusion selectively dopes the groove region with a high P concentration. This completes the doping steps for the front side of the wafer; however, a further thermal budget arises from the subsequent BSF anneal. As a result the emitter and groove diffusion profiles broaden further. Fig. 6 shows the groove diffusion profiles obtained under the same annealing conditions as for the emitter diffusion in Fig. 5b. The calibration established for the emitter diffusion works equally well for the groove diffusion profiles, without any need for adjustments.

The following steps are used to model formation of the BSF and Al alloy back contact. Al is deposited and Al diffusion

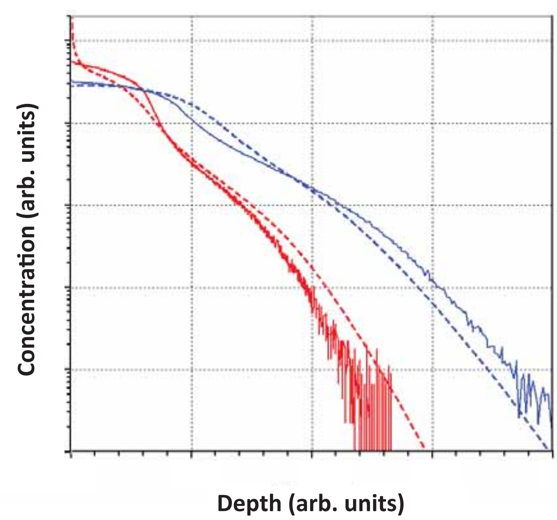

Figure 6. Experimental and simulated groove diffusion profiles after nitride deposition (red); at end of process (blue).

into the wafer is modelled by assuming that an Al-Si alloy has formed and the Al concentration on the silicon side of the alloy/silicon interface is equal to the solid solubility limit for Al in silicon at the diffusion temperature. During cool-down from the peak set temperature, diffusion is neglected and the Al doping profile is controlled by epitaxial regrowth of Al-doped silicon following the thermodynamic model derived and experimentally confirmed by Lölgen [7]. The p-type doping profile resulting from this thermal cycle is shown in Fig 7. This curve is an uncalibrated simulation and does not necessarily correspond to the true doping profile in the existing Al BSF process.

The proposal by Lölgen to incorporate B with Al for a higher concentration BSF [7] is modelled as an alternative process option. The model assumes that the thermodynamic properties of the liquid alloy are unaffected by the presence of B at the level of a few percent, and that, with such B concentrations in the alloy, B is incorporated during regrowth at its solid solubility limit in silicon, an order of magnitude higher than for Al [8].

Device simulation

The geometry used for device simulations of the LGBC cell, including the simulation grid, is shown in Fig. 8. The structure is contacted along the back side (base contact) and along the groove surface (emitter contact). Simulations using the Sentaurus device tool are performed as follows. Reflection and transmission of light at material interfaces and light absorption in Si are calculated using the transfer matrix method (TMM). Electronic transport is simulated largely using default device models at 300K. Doping-dependent recombination (SRH and Auger), carrier mobilities and bandgap narrowing are taken into account. The contact resistance of the groove finger is determined from room temperature measurements on fabricated cells with a range of dimensions. The front surface recombination velocity is set to 7500cm/s. The simulation assumes AM1.5 solar radiation incident normal to the cell surface.

Results for the total current in the cell are shown in Fig. 9. Most electrons flow upwards into the emitter and along into the groove region. Here, as Fig. 10 shows, they flow down around the groove, sinking into the contact at a rate limited by contact resistance. Before the current reaches the groove bottom, most electrons have entered the metal. Thus, contact resistance does not significantly bottleneck the emitter current at the groove dimensions used.

In addition to electron current arriving from the emitter, a small proportion of electron current (about one to three percent dependent on groove width and

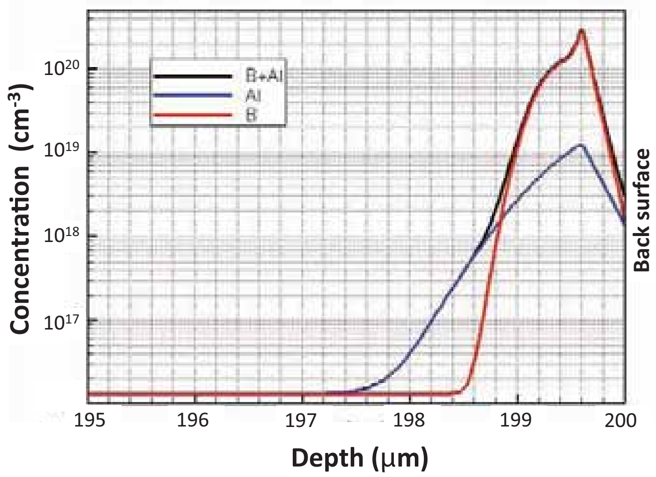

Figure 7. Simulated BSF doping profiles deposited using Al (existing process, blue curve), or Al:B alloy (black). The red curve shows the B concentration profile in the Al:B case.

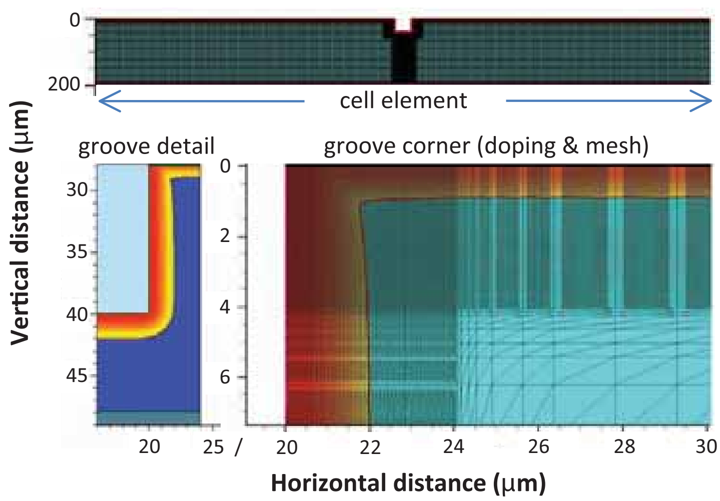

Figure 8. Geometry of simulated cell element (top) and details (bottom) showing the doping and mesh close to the groove. The emitter junction is marked by a solid line. The area below the groove (top) appears black due to the locally high density of mesh lines.

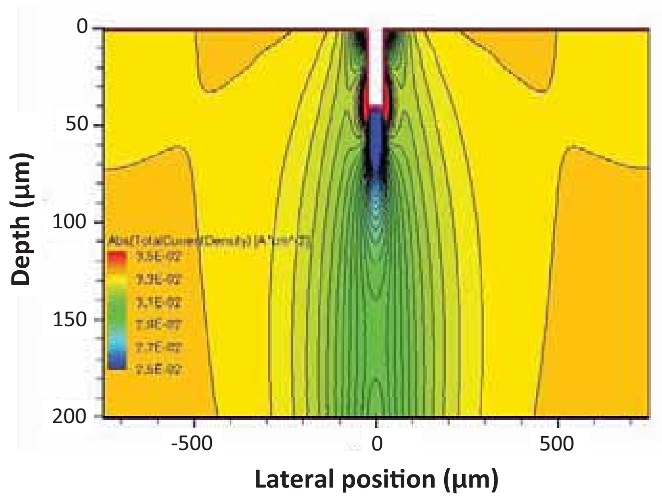

Figure 9. Simulation results for total absolute current in the full simulation unit cell (for a 200μm-thick wafer).

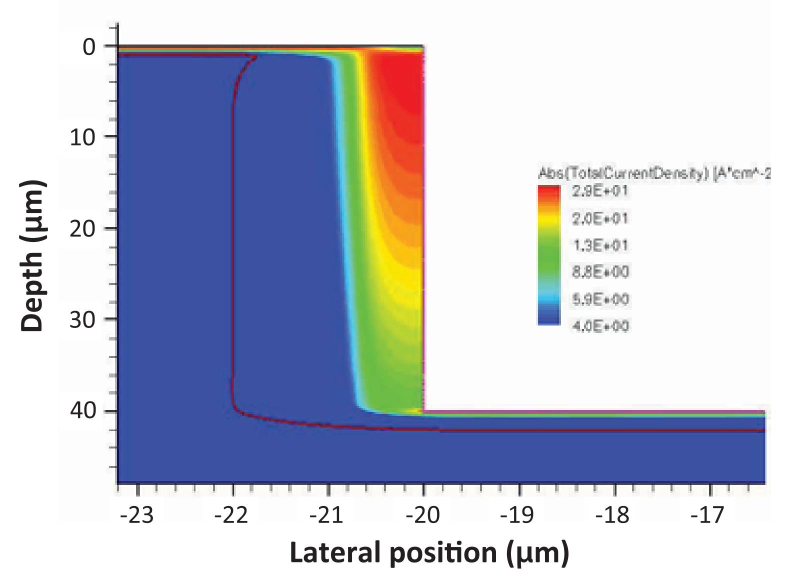

Figure 10. Current flow into the groove. Contact resistance causes the current to enter the contact over an extended area. The horizontal scale is expanded to 10× the vertical scale.

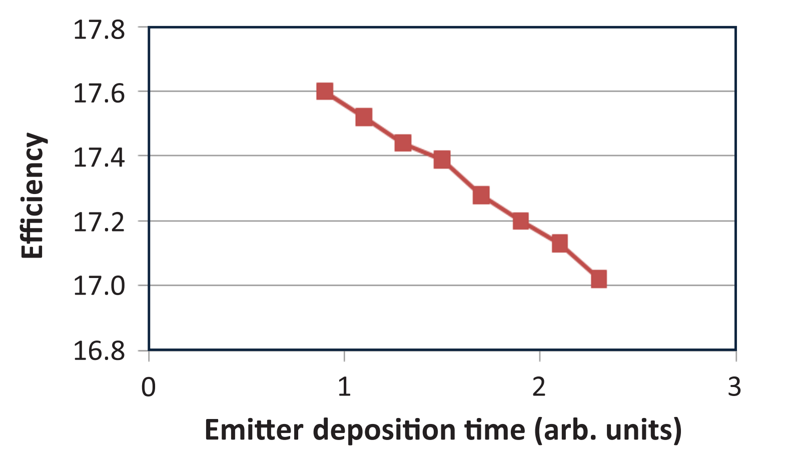

Figure 11. Simulated efficiency of the final fabricated cell, plotted versus the duration of the emitter deposition anneal.

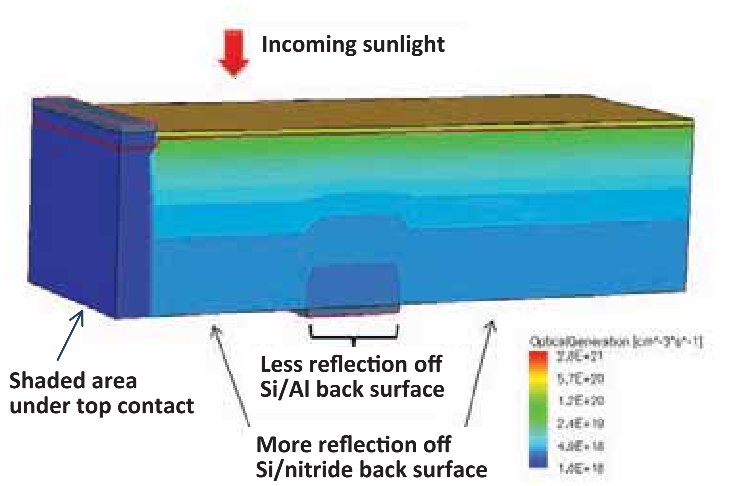

Figure 12. Optical intensity in the cell element as a result of front-side finger shadowing and different reflectivities at the back contact and back-side passivating Si/nitride interface.

Image courtesy of V. Moroz, Synopsys.

spacing) enters the groove directly from the base region. The impact of this current on the overall operation of the cell is quite small, and so the current flow in the base can be viewed as quasi-1D, while that in the emitter/groove region is inherently 2D.

Integrated simulations of the impact of processing on cell parameters

By sequentially running process and device simulations, the impact of a given series of process steps on cell parameters such as V_{oc}, I_{sc}, *FF* and efficiency can be evaluated. By varying input process parameters – diffusion temperatures, deposition thicknesses, groove width and spacing, etc. – an accurate picture of the process sensitivities of the cell technology can be obtained. This clarifies the potential optimum efficiency of the process, how closely this has been approached in current manufacturing processes, and what steps may be taken to improve efficiency further.

> "TCAD, often used together with experiments, can help push the envelope of cell efficiency."

In general, this approach can be used to evaluate both the impact of cell geometry and the impact of altering processing steps on cell performance. Here we focus on the impact of changes in processing steps. The effects of modifications to the emitter and BSF doping processes have been evaluated in some detail. Efficiency at AM1.5 illumination is shown in Fig. 11 as a function of P (n-type) emitter deposition time. This shows the benefit of a lightly doped, shallow emitter, if surface recombination is well controlled.

Finally, as illustrated in Fig. 7, adding B to the BSF enables a peak p-type doping concentration > $10^{20}cm^{-3}$, an order of magnitude higher than with Al alone. Device simulations show that the resulting decrease in back surface recombination enhances the cell efficiency from a nominal 17.5 to 18.1% (an increase of 0.6%).

These results illustrate the cost-effective way in which TCAD, often used together with experiments, can help push the envelope of cell efficiency. This is true even for a process that is well established and appears at first sight to be fully optimized.

Simulation of cells with localized back contacts

The efficiency of cells with localized back contacts of varying size has been explored by Huang and Moroz [9], using the Sentaurus Device tool [3]. Their simulations allow for different reflectivities (Fig. 12) and different surface recombination

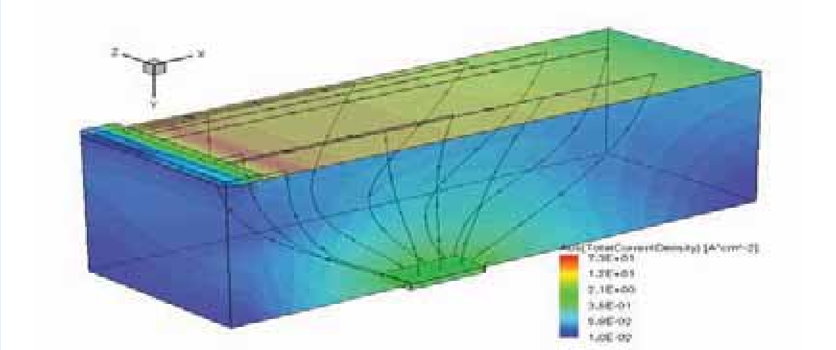

Image courtesy of V. Moroz, Synopsys.

Figure 13. Streamtrace plot showing the current flow between front and rear contacts. The cell dimension (L×H×W) is 500μm×150μm×350μm. In this simulation the rear contact size is 70μm×70μm, and is 130μm away from the edge of the top contact. The substrate doping is $2.0\times10^{16}cm^{-3}$.

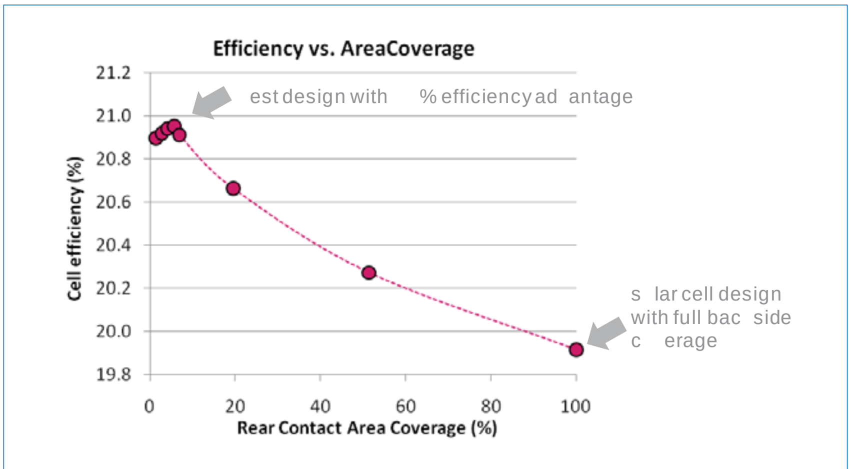

Figure courtesy of V. Moroz, Synopsys.

Figure 14. Simulated efficiency as a function of rear-contact area coverage. The cell with local contacts covering 5% of the back surface is 1% larger in efficiency than a cell with an unpatterned back side (100% coverage).

velocities for carriers at the back contacts and surrounding nitride passivation, and the effects of current crowding and contact resistance at the back contacts.

The simulated total current distribution arising from these conditions is shown in Fig. 13. Current flows three-dimensionally towards the back contact. To assess the impact of the back-contact area coverage, this is varied in a series of simulations from 100% down to about 1%. Fig. 14 shows the efficiency as a function of rear-contact area coverage. The efficiency peaks at 5% coverage, reflecting trade-offs between several physical mechanisms. The resulting power conversion efficiency is a full 1% higher than for the conventional cell with 100% coverage.

Simulation of emitter wrap-through based architectures

This section looks briefly at TCAD simulation for cell architectures currently being developed for production at a number of cell manufacturers. We outline applications to EMT and MWT cell architectures – these being current examples where TCAD can strongly accelerate introduction and optimization of higher efficiency solar cells from research and development to production.

A first discussion of EWT cell operation supported by 3D TCAD analysis has given insight into via resistance effects in the EWT cell [10]. Here we illustrate the application of 3D TCAD to evaluate trends in cell efficiency as functions of cell geometry and via processing (EWT versus MWT) [6].

A simplified EWT unit cell structure surrounding a single wrap-through cylindrical via of radius *r* is shown in Fig. 15. The simulation geometry represents one quarter of the repeating structure in a wrap-through cell, taking advantage of reflection symmetry about the x- and y-axes passing through the rows of vias. In the figure, only the silicon part of the cell is shown, viewed at an angle allowing the back-side diffusions to be shown. The emitter doping is shown in red and the base doping in blue.

This region is simulated using ~10^6 finite elements, leading to random-access memory requirements for efficient simulation of ~10^{10} byte. Typical cpu times on a PC-based processor cluster with sufficient available memory are a few times 10^5 seconds for a single I-V characteristic. Figs. 16 and 17 show the simulated hole current density and electron current density in the cell under AM1.5 front-side illumination. The current flow in the top-side emitter region is approximately radial (electrons flowing towards the via) while in the back-side region, holes flow towards the base contact and electrons flow towards the back-side emitter contact. In the region around the via, current flow is fully three-dimensional, with electrons flowing from the front-side emitter to the back side and more complex flows of electrons and holes in the via surroundings. Efficiency

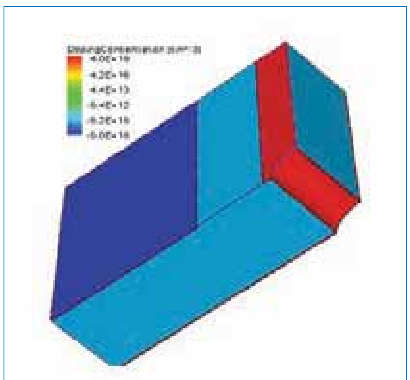

Figure 15. Quarter unit-cell of the EWT structure, inverted to show the back-side contacts.

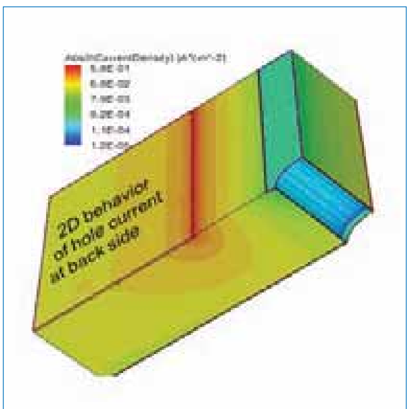

Figure 16. Simulated hole current density in the cell.

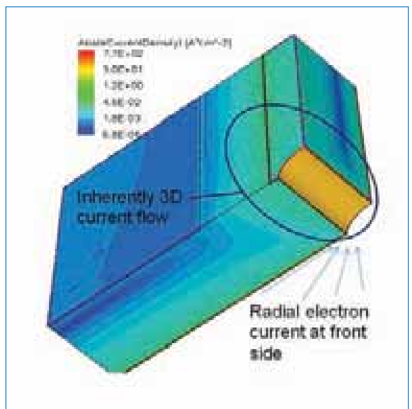

Figure 17. Simulated electron current density in the cell.

can be significantly limited by the rate of flow of electrons along the via to the back contact.

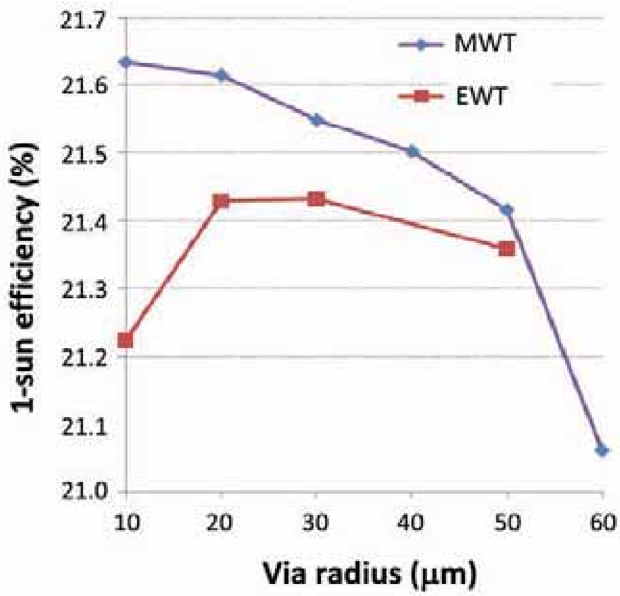

Figure 18. Efficiency versus via radius for the EWT and MWT. The EWT efficiency peaks at *r* ~ 20µm due to a trade-off between shadowing and via resistance. The MWT efficiency (assuming perfectly conductive metal fill) continues to increase towards smaller via radii.

Efficiency as function of cell geometry and via technology

Fig. 18 shows the dependence of efficiency on via radius for (a) emitter wrap-through technology where electron current along the via passes through the surrounding emitter doping, and (b) metal wrap-through technology where current flows through the metal fill. In the metal wrap-through case we have assumed that the metal acts as a perfectly conducting contact with no break in continuity. In the emitter wrap-through case (without metal fill), efficiency peaks at an intermediate via radius, found here to be ~20µm, while in the metal wrap-through case, efficiency rises towards smaller via radii. The optimal radius is determined by a trade-off between via resistance and optical shadowing, and depends on the emitter doping characteristics.

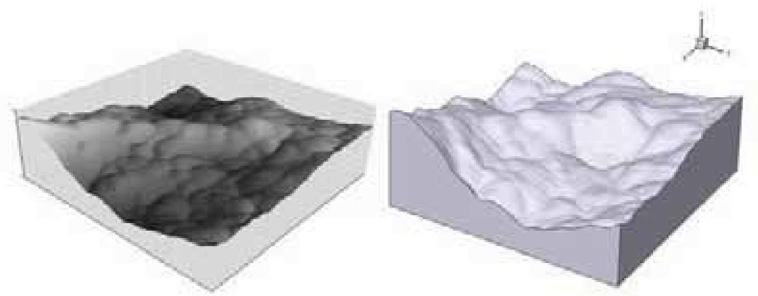

Figure 19. Transfer of TCO (SnO_2:F) topography measured by AFM (left) to simulation software (right).

Images courtesy of J. Lacombe, Next Energy.

Optical generation in textured thin films

This section takes a brief look at recent developments in simulation of light trapping and absorption in textured solar cell structures. The finite-difference time-domain (FDTD) method implemented in the Sentaurus Device has been used, together with imported atomic-force microscopy (AFM) data (Fig. 19) to simulate optical effects in glass/TCO/a-Si stacks – a key component of a-Si-based thin-film cells [11].

The simulated carrier generation rate in the a-Si film, deposited on textured TCO/glass, is shown in Fig. 20. Significant variations arise from interference and reflections at the rough topography. The absorption rate averaged over the simulation volume is substantially higher than for a planar structure. Such work will soon be combined with electronic simulations, as described in earlier sections of this paper, to enable highly realistic predictions of cell performance.

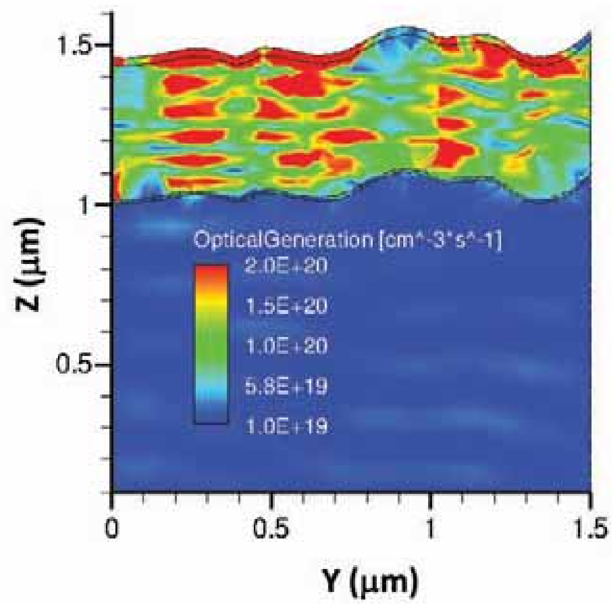

Figure 20. Optical generation rate in the a-Si:H absorber layer for λ = 640nm and perpendicular incidence. The lower part of the figure is the TCO layer, which has been deposited on glass (not shown).

Figure courtesy of J. Lacombe, Next Energy

Summary and conclusions

TCAD is an essential component of semiconductor research, development and manufacturing. It is pervasive in the IC industry and large-area electronics and is now penetrating the PV industry via research institutes and start-up companies. This paper has reviewed how TCAD, using physically accurate process and/or device simulation, can be applied to a range of wafer-based and, increasingly, thin-film solar cell technologies. Simulations of an established LGBC process show good agreement with observed efficiency trends as functions of processing conditions, and further potential improvements have been identified. 3D device simulations have been presented for cells with back-side passivation and for wrap-through cells with and without metal vias. Finally, we have reviewed some recent results on optical absorption in thin-film cell structures.

While experimentation is always required, TCAD can efficiently substitute for the very extensive in-line experiments and cell characterization studies needed to obtain equivalent insights without simulation. This approach will support faster development of advanced PV technologies from the imagination of inventors, through the laboratory scale into pilot and full production. Integrated TCAD – validated by process experiments – will become a critical component of future efficiency improvement roadmaps in the PV industry.

Acknowledgements

We would like to thank G. Letay, N. Zographos, C. Zechner, V. Moroz, J. Huang and S. Odermatt (Synopsys); A. Cole, K. Heasman, K. Drew and L. Brown (Narec); and J. Lacombe (Next Energy) for making available PV modelling and characterization results.

References

[1] FP6 ATOMICS Project Final Public Report [available online at http://www.iisb.fraunhofer.de/en/arb_geb/atomics/PublicFinalReport2.pdf].

[2] International Technology Roadmap for Semiconductors [available online at http://www.itrs.net/Links/2009ITRS/2009Chapters_2009Tables/2009_Modeling.pdf].

[3] Synopsys TCAD pages [available online at http://www.synopsys.com/Tools/TCAD/Pages/default.aspx].

[4] Basore, P.A. & Clugston D.A. 1997, "32-bit solar cell modeling on personal computers", *Proc. 26th IEEE PVSC*, Anaheim, California, USA.

[5] Altermatt, P.P. et al. 2009, "Highly predictive modelling of entire Si solar cells for industrial applications", *Proc. 24th EU PVSEC*, Hamburg, Germany.

[6] Ahn, C. et al. 2010, "Integrated process and device TCAD for enhancement of c-Si solar cell efficiency", *Proc. 25th EU PVSEC*, Valencia, Spain.

[7] Lölgen, P. et al. 1994, "Boron doping of silicon using coalloying with aluminum", *Appl. Phys. Lett.*, Vol. 65, p. 2792.

[8] Gee, J.M. et al. 1999, "Boron-doped back-surface fields using an aluminum alloy process", Sandia Nat. Lab. Report SAND99-0591C.

[9] Huang, J. & Moroz, V. 2010, "Mono-crystalline silicon solar cell optimization and modeling", *Electrochem. Soc. Proceedings*, Vol. 33, p. 33.

[10] Ulzhoefer, C. et al. 2009, "VIRE effect: Via-resistance induced recombination enhancement – the origin of reduced fill factors of emitter wrap through solar cells", *Proc. 24th EU PVSEC*, Hamburg, Germany.

[11] Lacombe, J. et al. 2010, "Optical modeling of light trapping in thin film silicon solar cells using the FDTD method", *Proc. 35th IEEE PVSC*, Hawaii, USA, pp. 1535–1539.

About the Authors

Nick Cowern is a physicist and works as a professor at Newcastle University, UK, where he currently heads the nanomaterials and electronics research group. His research interests involve experiments and theory of defects and diffusion in electronic materials and TCAD for nanoelectronic devices and photovoltaics. He previously held a principal scientist position at Philips Research Laboratories, Eindhoven, The Netherlands.

Chihak Ahn is a physicist and electrical engineer. He received his Ph.D. from the University of Washington, USA, and took a postdoctoral position at Newcastle University, UK, specializing in multiscale modelling of defects and diffusion in silicon-based materials, and TCAD for nanoelectronic devices and photovoltaics. He has just joined Samsung Information Systems America.

Enquiries

School of Electrical, Electronic and Computer Engineering, University of Newcastle-upon-Tyne,
NE1 2EQ, UK
Tel: +44 (0) 191 222 5636
Email: nick.cowern@ncl.ac.uk
Website: www.ncl.ac.uk/eece

Removal of trace metals using a biodegradable complexing agent

Helmuth Treichel[1], Avery Goldstein[1], Mark George[1], David Bohling[1], Jochen Rentsch[2], Antje Oltersdorf[2], Martin Zimmer[2], Sara Ostrowski[3], Ian Mowat[3], Larry Wang[3] & Werner Kern[4]
[1]Sunsonix, California, USA; [2]Fraunhofer Institute for Solar Energy Systems (ISE), Freiburg, Germany; [3]Evans Analytical Group, California, USA; [4]Werner Kern Associates, New Jersey, USA

ABSTRACT
Processing silicon substrates for PV applications involves texturing, cleaning and/or etching wafer surfaces with chemical solutions. Depending on the cleanliness of the industrial equipment and the purity of the chemical solutions, surface contamination with metals or organic residues is possible [1]. The presence of trace contamination at PV junctions leads to both mid-level traps and photonic defects, which ultimately cause reduced efficiency and rapid cell degradation. Metallic impurities have a greater impact on PV cell lifetime due to their deeper energy levels in the silicon band gap [2]. On the other hand, non-metallic impurities may modify the electrical activity of PV cells because these species involve complex interactions with the host silicon lattice and its structural defects. In other words, very small amounts of contamination can result in poor PV efficiency. This paper presents an overview of the effects of adding a biodegradable complexing agent in cleaning and rinsing baths to minimize surface contamination and thereby enhance solar cell efficiency.

Introduction

Conventional approaches in the solar industry for cleaning silicon have historically used either standard equipment and/or chemicals derived from semiconductor processing [3, 4]. These approaches, although effective in deep submicron processing common in semiconductor technologies, can be both dramatically over-engineered and ineffective for PV processing due to the inherent differences between solar cells and microelectronic devices. An effective approach to remove metal contamination during solar cell processing could aid manufacturers in meeting or exceeding solar cell efficiency and performance goals.

Standard wet chemical processes in industrial cell processing

Several wet chemical process steps, including surface preparation prior to junction diffusion and oxide etching following diffusion, are critical components of the silicon solar cell manufacturing sequence. Table 1 provides an overview of currently used wet chemical etching and cleaning steps within the front-end of a standard production sequence for c-Si solar cells based on screen printing.

Pre-cleaning of wafers, prior to texturing, is gaining importance due to the removal of organic residuals and metallic contamination from the wafering step which improves the homogeneity of the subsequent texturing step. Mostly alkaline cleaning solutions are utilized for texturing single crystalline wafers. These are similar to the common SC1 (standard clean 1 – NH_4OH/H_2O_2), known from semiconductor processing [5]. Texturing of multicrystalline wafers takes advantage of wafer saw damage in an aqueous acidic etch utilizing a combination of HNO_3 to oxidize the wafer and HF to etch the oxide. Significant metal contamination can build up in these baths as the bulk of the wafer is etched away [6].

Prior to emitter diffusion, any remaining alkali metal contaminants from the single crystal texturing process are removed by a second, additional cleaning step. Further on in the process, especially for subsequent inline diffusion processes, where e.g., diluted phosphoric acid or phosphooxychloride ($POCl_3$) is deposited on the wafer, the cleaning step also acts as a 'conditioner' to create a hydrophilic wafer surface. This ensures sufficient wetting of the wafer with the phosphoric acid. Therefore, HCl and HF 'dips' are used for the cleaning after texturing, and the surface is made hydrophilic by applying either gaseous ozone or rinsing with ozonated DI water [7].

During emitter diffusion a thick layer of a phosphorous silicate glass (PSG) is created on the wafer surface. This PSG layer can contain a significant concentration of metallic impurities that have been 'gettered' from the wafer bulk as the metallic contaminants can segregate preferentially into this layer. It is important that during the removal of the PSG, metals which are liberated from this layer do not redeposit on the wafer surface from the bath. For additional surface preparation prior to SiN_x antireflection coating, ECN developed a specialized, highly alkaline, not biodegradable selective etching mixture (commercial products are nowadays available from companies like Avantor or BASF), which removes the highly P-concentrated top surface emitter layer (so-called 'dead layer') especially observed after inline diffusion processes [8]. Similar performance levels can also be obtained using the already mentioned

Pre Clean	Removal of particles, slurry residues
Texturing	Surface structuring
Pre diffusion clean	Removal of surface metal, particles, native oxide
Diffusion (inline/batch)	
Rear emitter removal	Edge isolation
PSG removal	Oxide removal, gettered metal removal
Post diffusion clean	Native oxide and metal removal

Table 1. Overview of currently used wet chemical etching and cleaning steps within the front-end of a standard production sequence for c-si solar cells.

SC1 mixture or HF/ozone treatments. This removal results in a better blue response and typically slightly higher V_{oc} and J_{sc} values of the final solar cells. The process is not a drop-in replacement of current cleans; it requires a separate step, which means additional capital equipment cost.

Depending on the industrial equipment or purity of chemicals used, contamination of the surface with metals or organic residues is possible. Reduced efficiency and rapid cell degradation share common roots, being trace contamination at the photovoltaic junctions leading to both mid-level traps and photonic defects. The extremely high fields that exist at p-n junctions during operation of the finished device can also give rise to surface migration of ionic impurities if they are not removed. The effects of these contaminants may result in uncontrolled drifts of the surface potential, changes in the minority-carrier lifetime at the surface, surface recombination velocity, and the formation of inversion or accumulation layers. These effects can lead to increased and erratic reverse leakage current in devices [2].

Impact of metal contaminants on solar cell devices

The main issue with standard processing sequences (in production at most mc-Si and c-Si manufacturing facilities: see Table 1) is the lack of a consistent chemical method to remove Cu from wafer surfaces and cleaning baths. There are two approaches to control the electrically active impurity concentration in silicon solar cells:

1) Minimize contamination of the silicon base material by purification to provide the highest value of diffusion length possible in the wafers from which cells are made; and

2) Maintain or improve the initial diffusion length by chemical or thermochemical impurity 'gettering' techniques during the cell processing itself.

In the first method, the intent is to eliminate impurities; in the second, they may be removed from the device itself or made electrically inactive. In the solar cell industry, the cleaning of silicon wafers before different passivation and texturization treatments has not yet been studied intensively in detail. The most frequently used cleaning sequence is the RCA-clean (Radio Corporation of America), but the cleaning effect and the influence on solar cell parameters are not completely understood. Questions concerning the required bath purity (or loading) and subsequent silicon surface contamination can only be answered empirically. The contamination for which the Sunsonix clean (adding of a biodegradable complexing agent to aqueous cell processing solutions) has been developed, is that of metallic cations liberated from the substrate surfaces into the wet processing baths. The contamination of the substrate surfaces usually occurs as a result of physical or chemical adsorption by electrolytic action or by exchange of surface atoms with impurity ions in the cleaning solution [2]. Cu contamination is likely a result of the wafering process, since standard wires used to slice Si ingots are made of a metallic composite (e.g. a stainless steel core surrounded by a bronze or copper layer).

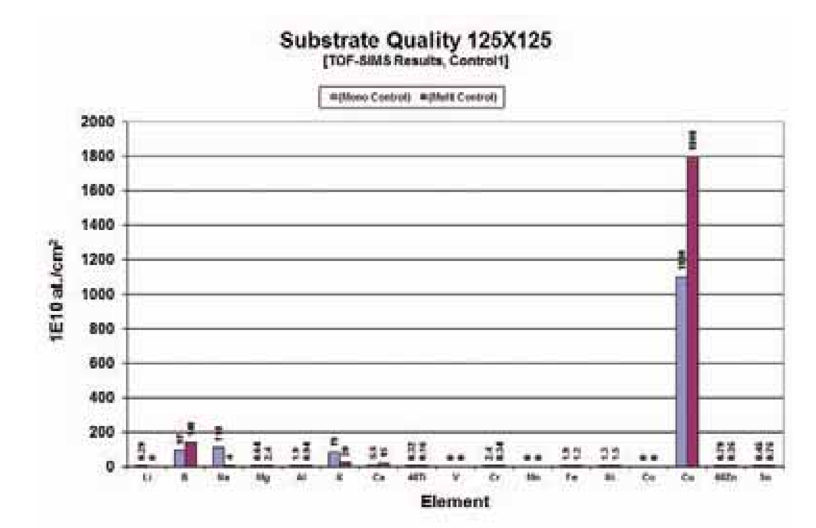

Figure 1a. As-received prime silicon substrates (mc-Si and c-Si); TOF-SIMS results.

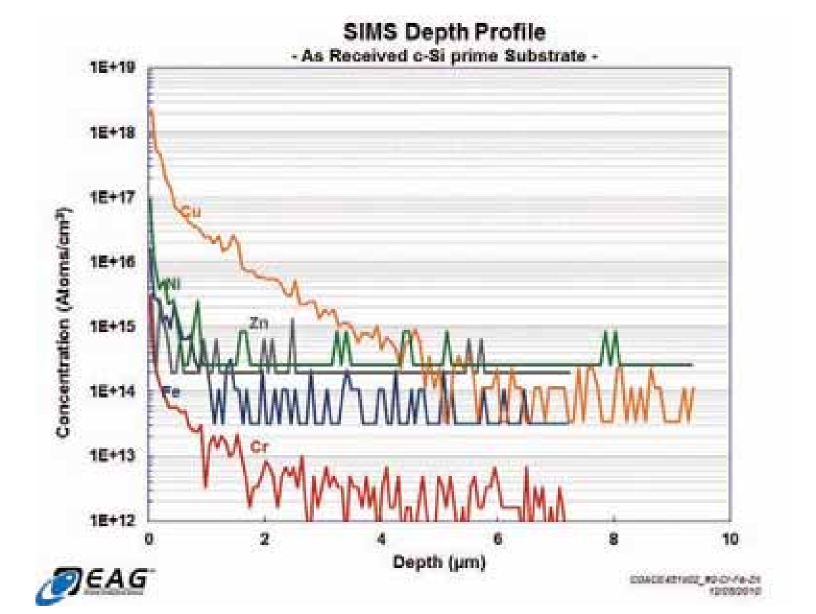

Figure 1b. SIMS depth profile of Cu, Fe, Ni, Cr and Zn; pristine c-Si substrate.

Time of flight secondary ion mass spectrometry (TOF-SIMS) analysis of solar-grade mc-Si and c-Si wafers detected 1.1-1.8 × 10^{13} atoms/cm^2 of Cu from the samples on the surface and Dynamic SIMS (D-SIMS) analysis detected 5 × 10^{16} atoms/cm^3 in the bulk at 1µm depth (Fig. 1a & Fig. 1b).

All impurities were detected at the surface region. Shapes of Cr, Fe, Ni and Zn profiles are most likely sputtering artifacts caused by surface roughness. High levels of Cu were detected both at the surface and a few micrometers into the sample. Bulk detection limits for this analysis are (in atoms/cm^3): Cr<3×10^{12}, Fe<3×10^{13}, Ni< 2×10^{14}, Cu<1×10^{14} and Zn<2×10^{14}.

Impurity effects

Defects or dislocations in the silicon lattice are sites where recombination centres can occur. Recombination results in the loss of photo-generated carriers (e.g., electrons drop from the conduction band back into the valence band and holes do the opposite) and significantly degrades the photovoltaic quality of the device.

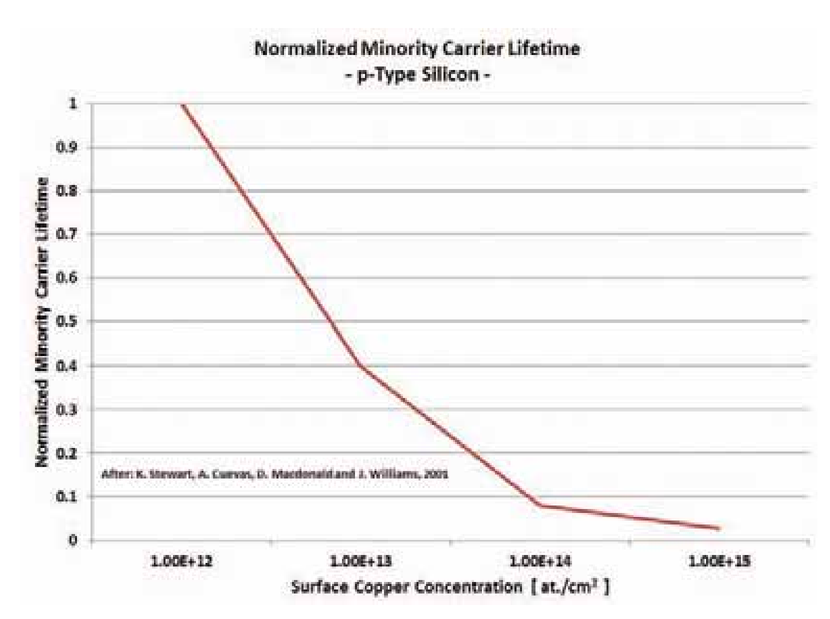

Figure 2. Impact of increasing copper contamination on the normalized minority carrier lifetime [7].

Diffusing trace metals lead to displacement damage (dislocations, stacking faults, precipitates etc.), and deep recombination centres reducing the minority carrier diffusion length. There are numerous metal species which introduce deep-level traps that stimulate the recombination of photogenerated carriers in silicon. Cu and Ni impact junction degradation, and Nb, Ti, V, Ta, W, Mo, Pd, Au, Zr, Mn, Al, and Sn, the removal of which has a great influence on carrier diffusion length reduction. Fe, Cr, Co and Ag have detrimental effects on both of these loss mechanisms. The presence of metallic impurities in the photovoltaic material is responsible for the formation of hot spots by metal agglomeration that are particularly problematic since they are responsible for creating localized increase of the electric field, inducing avalanche breakdown that leads to non-uniform current densities.

> "Copper can easily diffuse through the thickness of a solar cell within a few hours at room temperature."

Such effects will decrease the open-circuit voltage V_{oc}, short-circuit current density (J_{sc}) and fill factor, which represents the relationship, or balance, between current and voltage for effective power output. Of particular interest in this paper is the near ubiquitous presence of copper in 'solar-grade' silicon wafers. Copper can easily diffuse through the thickness of a solar cell within a few hours at room temperature [9]. Formation of Cu precipitates in the area of the p-n junction may shorten it and decrease the overall efficiency of the cell [4]. The carrier lifetime in Cu-contaminated Si is lower in n-type than in p-type Si (see Fig. 2) [10, 11]. Furthermore, copper diffuses in Si as a positively charged interstitial ion. The intrinsic diffusivity is $2.4\times10^{-7}cm^2\cdot s^{-1}$ at room temperature. Positively charged Cu ions pair with the negatively charged acceptor atoms which tends to concentrate the copper near the depletion region of the p-n junction where the fields are enhanced. This may be one mechanism for the known degradation of crystalline silicon solar cells of about 0.5% per year.

Analysis of trace metals during wet chemical processing of silicon wafers

We have identified why many industrial manufacturers have overlooked the influence of copper contamination on PV wafers. Standard methods of analyzing surface contamination are ICP-MS (Inductively Coupled Plasma Mass Spectrometry), ICP-AES (inductively coupled plasma atomic emission spectroscopy), and ICP-OES (inductively coupled plasma optical emission spectroscopy). These methods use an acid wash, usually based on HF or HF/HCl, of the wafer surface where it is assumed that the acid solution effectively removes all metallic contamination from the wafer surface. The solution is then concentrated and injected into the plasma of the spectrometer. In our work we determined that the standard ICP-MS solution did not effectively remove Cu and gave a false negative value for Cu concentration since metals are known to electrochemically plate out from an HF solution onto a bare silicon surface. The direct surface measurement by techniques such as TXRF (total reflection X-ray fluorescence spectroscopy) suffer from accuracy and detection limit due to stray reflection on the rough morphology of the PV substrates. Other direct methods utilize sputtering of the sample surface to liberate analyte ions which are detected by mass spectrometric techniques. SurfaceSIMS (surface secondary ion mass spectrometry, a type of dynamic SIMS), and TOF-SIMS [16, 17] are two such methods with the detection limits required for our PV application. TOF-SIMS was chosen as the method of choice in the current study for a number of reasons:

- It can detect all of the typical metal elements of interest in survey mode without the need to pre-select species of interest.
- The information depth of the measurement is very low, typically in the 10–20Å range.
- It is not adversely affected by the potential presence of particle contamination, or sample roughness.
- It has excellent detection limits, i.e. in the 1×10^9 at/cm² range for many transition elements, and substantially lower for alkali or alkali earth elements [16–18].
- No sample preparation is required and it is a direct analytical method, unlike VPD-ICP-MS/AAS which requires the use of appropriate chemistry and equipment to dissolve the surface of interest and concentrate it for analysis [19–22].

For the analysis performed for this work a Ga+ primary ion source was operated in pulsed, bunched mode with a beam energy of 15kV and with a 20nA beam current, in order to maximize sensitivity for elemental species in the positive ion mode. The instrument conditions were optimized for high mass resolution (typically 8000 at m/z 41) and abundance sensitivity to enable the best sensitivity for elemental ions.

Working principle of SX-E complexing agent

Over the past three years, novel, proprietary, biodegradable and biocompatible (i.e., green) cleaning chemistries and processes have been developed for the removal of detrimental trace metal contamination, e.g. from solar cell substrates during cell manufacturing processes. In testing performed by a variety of academic institutions, independent research labs,

industry equipment providers and solar cell manufacturers, this technology has been demonstrated to deliver a direct improvement of crystalline silicon (c-Si or mc-Si) absolute efficiency. The use of this type of cleaning not only enables improving and controlling the material quality, but participates actively to the process cycle by limiting the need for pre- and postdiffusion cycles aimed at gettering the minority carrier lifetime killing metallic impurities. Because its use is not limited to wafer type Si-based substrates, it also offers a scalable and extendable solution for any type, size or shape of substrates and participates to increase total cell efficiency and to reduce cell lifetime degradation. These chemistries/processes can be seamlessly incorporated into existing production lines at four process steps: silicon ingot reclaim, wire saw (wafering), substrate cleaning and texturing. The target cleaning agent used in this study, SX-E, is chemically compatible with almost all standard semiconductor and PV processing sequences and chemicals.

Contamination of Si surfaces by metallic impurities from reagent solutions is particularly severe in aqueous HF which strips the protective layer of natural oxide without etching the semiconductor. The large difference between the oxidation potentials of the Si and the metal ions in solution therefore becomes effective over the entire surface leading to large quantities of electrochemically deposited metals, in particular Cu (see Fig. 1a) [2, 3].

An ideal reagent would keep the metals in solution (i.e. to dissolve metals) and prevent oxidation/reduction reactions between Si and metal ions. It has been found that oxidation/reduction reactions can be prevented by increasing the redox potential of solutions and/or by injecting surfactants or chelating agents [12].

There are four deposition mechanisms when metallic impurities contaminate the Si wafer surface in solutions:

1) Electrochemical deposition: metal is deposited on the surface due to an electrochemical reaction between the metal ion and Si.

2) Precipitation: as some of the metals form metal hydroxides in alkali solutions, their deposition is attributed to precipitation of metal hydroxides on the substrate surface.

3) Film inclusion: metallic impurities close to the Si surface are included into the oxide as the Si surface is chemically oxidized by oxidizing agents, such as dissolved oxygen and H_2O_2.

4) Chemisorption: weakly bonded metal hydrate or halide that can be incorporated as described in mechanism (3).

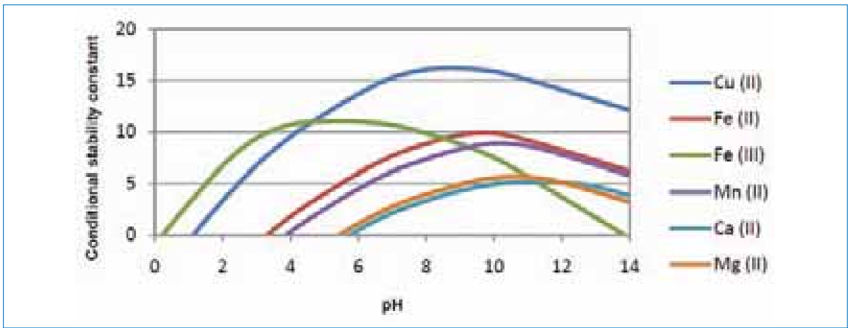

Figure 3. Conditional stability constant of the precursor for SX-E.

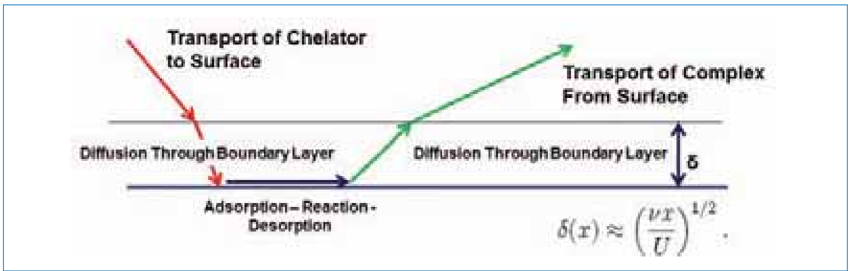

Figure 4. Metal removal by chelating agents.

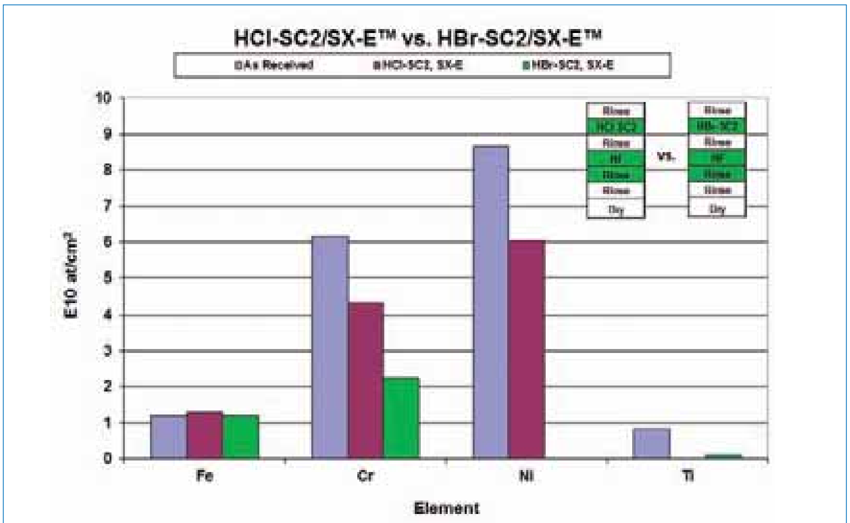

Figure 5a. Cleaning efficiency using SX-E - HCl-SC2/SX-E vs. HBr-SC2/SX-E; Fe, Cr, Ni and Ti results.

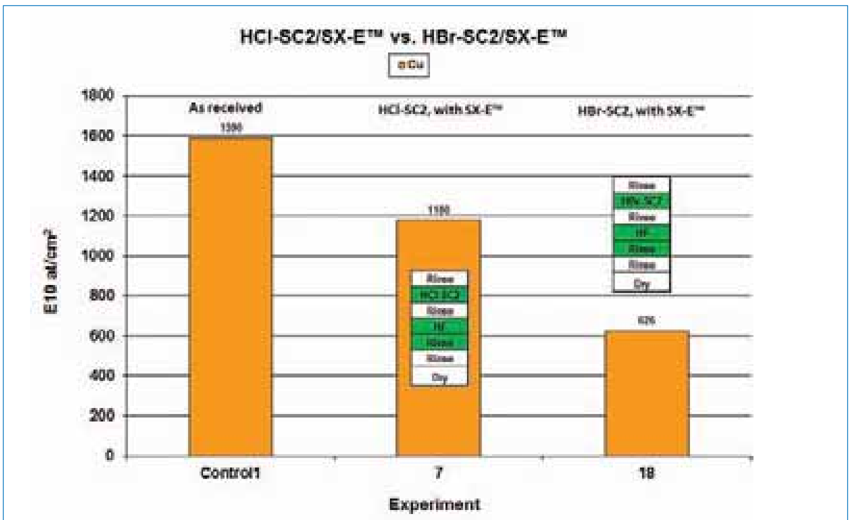

Figure 5b. Cleaning efficiency using SX-E - HCl-SC2/SX-E vs. HBr-SC2/SX-E; Cu results.

The contamination for which the SX-E clean has been developed is that of metallic cations liberated from the substrate surfaces into the wet processing baths. The contamination of the substrate surfaces usually occurs as a result of physical or chemical adsorption by electrolytic action or by exchange of surface atoms with impurity ions in the cleaning solution [2]. The unusual property of this specific cleaning agent is its ability to solvate metal ions in 1:1 metal-to-SX-E complexes. As the cleaning agent solvates the cations, the number of recombination sites is reduced and the conversion efficiency of light energy into electrical energy is augmented. If not removed, the metallic ions (positively charged ions in silicon) in the depletion region can pose an opportunity for electron-hole recombination sites that degrade the conversion efficiency of the solar cell as explained earlier.

> "The unusual property of this specific cleaning agent is its ability to solvate metal ions in 1:1 metal-to-SX-E complexes."

It is common for SC2 chemistry to remove post-texturing residue. The low pH of the SC2 bath caters mostly to the removal of iron and leaves the copper contamination at the initial level (see also Fig. 5a). The substitution of HCl in the SC2 solution by HBr is suggested (see Fig. 5a & 5b). Using HBr instead of HCl results in significant removal of all metals of interest compared to as-received values.

The fully deprotonated form (all acidic hydrogen removed) of SX-E binds to the metal ion. The equilibrium or formation constants for most metals, especially the transition metals, are very large (see Fig. 3); hence the reactions are shifted to the solvated metals.

Many of the reactions are pH-dependent. The conditional constant gives a relationship between the concentrations of the solvated complex formed (MeZ), the concentration of the unreacted metal (Me), and the concentration of the unreacted cleaning agent (Z). These constants pass for all metal complexes through a maximum as a function of the pH value [12]. At the thermo-dynamic equilibrium, the complex formation is selective. The most preferred metals being complexed are those with the highest conditional complex-forming constants. With increasing concentrations, other metal ions are complexed successively (Fig. 4). As shown in Fig. 7 and 8, the range of pH over which the SX-E precursor exhibits stability is consistent with the aqueous process steps used in PV manufacturing.

SX-E can only remove trace metals in ionic form. Therefore, the metal residuals from the wire sawing need to be oxidized in order to be removed.

Concentrations:		Temp [°C]	Grade
HF	10:1 (5.14%)	RT	48%, Class 10 Grade
HF/H_2O_2	3:1:20	RT	
HCl	2.06%	RT	38%, Class 10 Grade
HBr	2.06%	RT	48%, SemiGrade, 99.5% Minimum Purity
H_2O_2	1.58%	RT	30%, Electronic Grade
SC2 (HCl or HBr based)	1:1:20 @ 60 deg.C	60	
DIW		RT	16.84 MΩ
DIW/SX-E™	SX-E ~ 300 ppm	30	
N_2 (Drying)			bottled high purity

Table 2. Chemicals used for laboratory testing.

	Fe Expected	Cr Expected	Ni Expected	Ti Expected	Cu Expected
Standard	⇧	⇔	⇘	⇩	⇩
Test 1	⇩	⇩	⇩	⇩	⇩
Test 2	⇩	⇩	⇩	⇩	⇩
Test 3	⇘	⇩	⇧	⇘	⇘
Test 4	⇩	⇩	⇩	⇩	⇩
Test 5	⇘	⇩	⇗	⇩	⇩

Table 3. Expected trends of cleaning chemistry impact on trace metal removal. Every line constitutes a cleaning sequence with one step changed; arrows 'up' are suspected to be a sign of re-plating of metal from any one of the cleaning chemistries (other than SX-E); see also [2].

	Fe Is	Cr Is	Ni Is	Ti Is	Cu Is
Standard	⇘	⇩	⇩	⇩	⇗
Test 1	⇘	⇩	⇩	⇩	⇩
Test 2	⇧	⇩	⇩	⇩	⇩
Test 3	⇩	⇩	⇩	⇩	⇧
Test 4	⇧	⇩	⇩	⇩	⇩
Test 5	⇩	⇩	⇩	⇩	⇧

Table 4. TOF-SIMS results on cleaning sequences used.

Cleaning kinetics using HBr

The copper contamination on the sawn substrates from the wafering process is largely present as copper metal. This is so by direct inspection of the electrochemical half cell reaction of either Cu(I) or Cu(II) in contact with silicon. Given the extremely high rates of copper diffusion in silicon it is not surprising that the copper is not only present on the wafer surface but also present in significant concentrations in the bulk of the wafer. In either mc-Si or c-Si the texturing process results in baths with a high loading of copper where the copper represents a significant surface contaminant.

The use of the SC2 bath (composed of HCl and peroxide or ozone) to remove critical transition elements like Fe is not as effective on Cu. It is well known in the plating industry that HBr is more effective in dissolution of Cu than HCl. The electron affinities for $CuCl_2$ and $CuBr_2$ have been determined to be identical, 4.35+/-0.05eV. Both the anions and neutral CuX_2 species are linear with only a slight bond length variation between the charged and neutral species [23]. However, Br^- is a softer ion than Cl^- in the Lewis acid base theory.

Cell Processing

Electron affinity falls down the Group 7 elements in the periodic table. The affinity for copper on silicon follows the same trend when exposed to these acids.

CuX_2 species are expected to therefore complex at rates similar to those of SX-E. HBr dissolves copper quicker than HCl to form $CuBr_2$. This reaction is in equilibrium with formation of adsorption layer of Br^-. Whether this chelation occurs on the surface (before $CuBr_2$) is solvated and leaves the surface or occurs in solution is unknown. At the operational pH and the SX-E configurations available the copper-bromide chemistry is favored. Either way, oxidation of copper metal to Cu^+/Cu^{++} appears to be rate limiting. The rate limiting difference between HCl and HBr precedes formation of CuX_2. The addition of a strong oxidizer like H_2O_2 facilitates the complete oxidation of formed Cu_2O. SX-E complexes the species by making a mixed thermodynamically favoured Cu(X)SX-E complex (with higher stability when X=Br), stabilizing that intermediate against re-reaction/reduction with the silicon surface.

Cell Processing

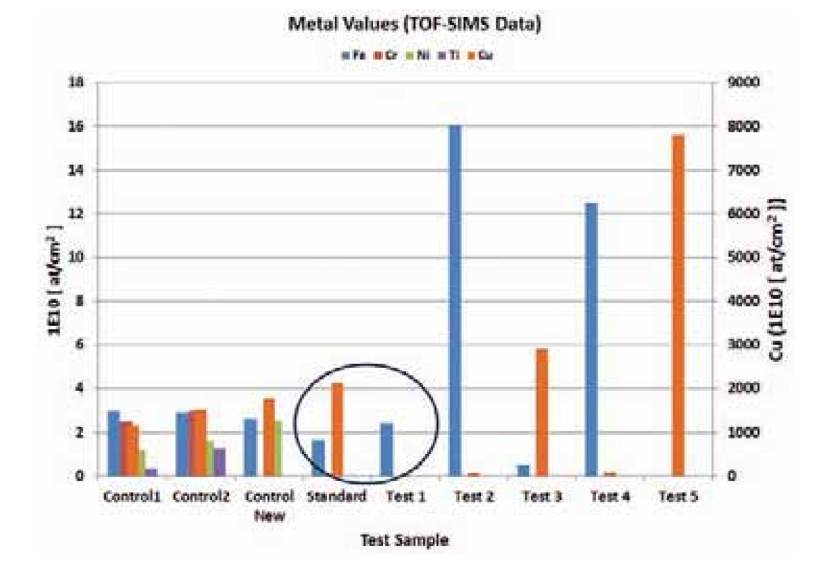

Figure 6. Optimized cleaning sequence (Test 1) vs. Standard Clean; TOF-SIMS results.

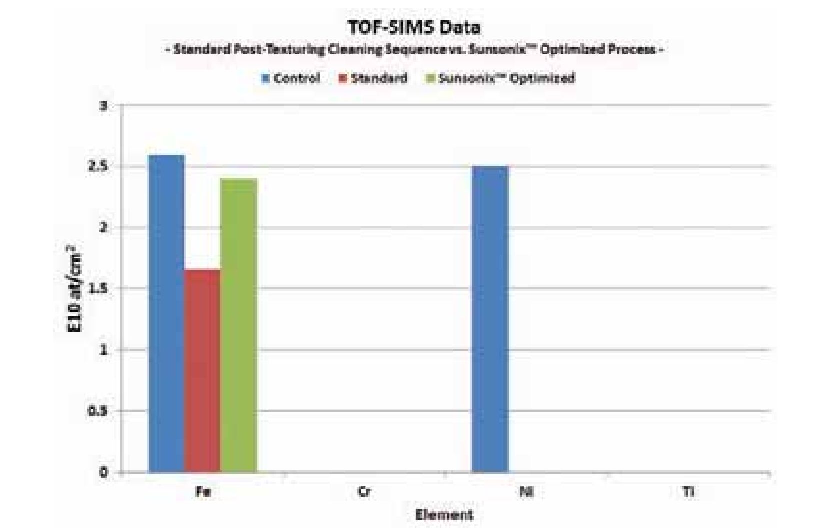

Figure 7. Comparison of standard post-texturing cleaning sequence to best process sequence (Test 1); TOF-SIMS results for Fe, Cr, Ni and Ti.

Reduction of metal contamination using SX-E

Laboratory testing

Environmental awareness has traditionally motivated the research of renewable energy sources. The technical investigation in this phase proves that biodegradable chelating chemistry is effective in controlling trace metals on silicon surfaces. The tests simulate a standard pre-diffusion cleaning sequence and use the contamination test as a dependent response. The experiments for this portion of the technology are designed to optimize the process treatments for various factors, for example SX-E application in various steps, time in the bath, temperature, and chemicals used, for specific applications to establish the factors to achieve the optimum low trace metal level (Table 2–4; Fig. 6 & 7).

> "The experiments for this portion of the technology are designed to optimize the process treatments for various factors."

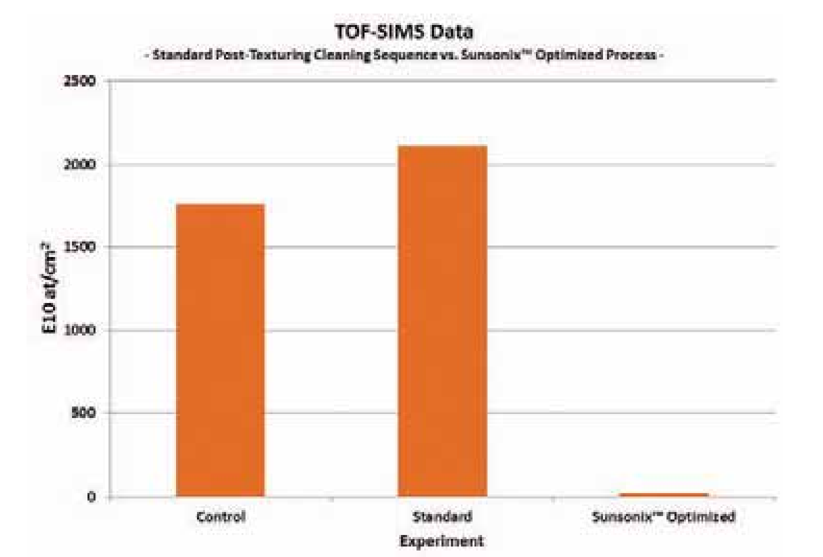

Figure 8. Comparison of standard post-texturing cleaning sequence to best process sequence (Test 1); TOF-SIMS results for Cu.

Critical success factors are expressed in the results that are obtained from the analytical chemical tests, presenting trace metal levels in atoms/cm^2. All test sequences performed were compared to as-received substrates and against standard cleaning sequences used in a manufacturing environment. The

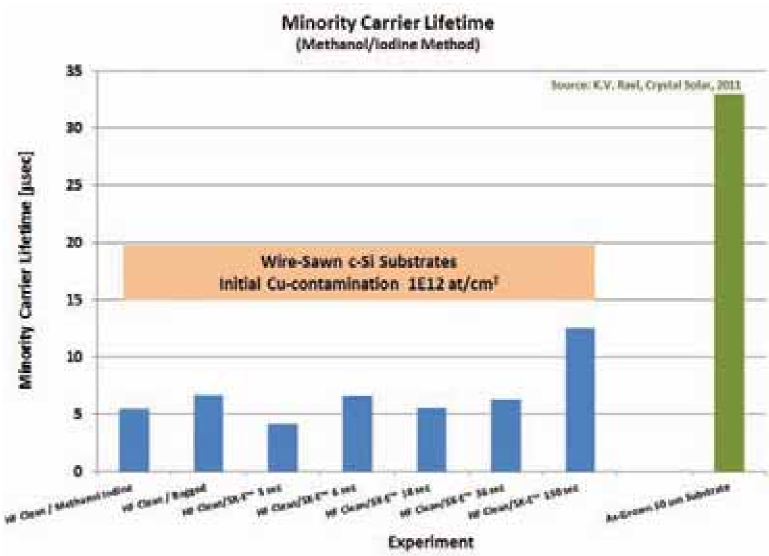

Figure 9. Impact of rinse time on minority carrier lifetime initial decay (see Fig. 14).

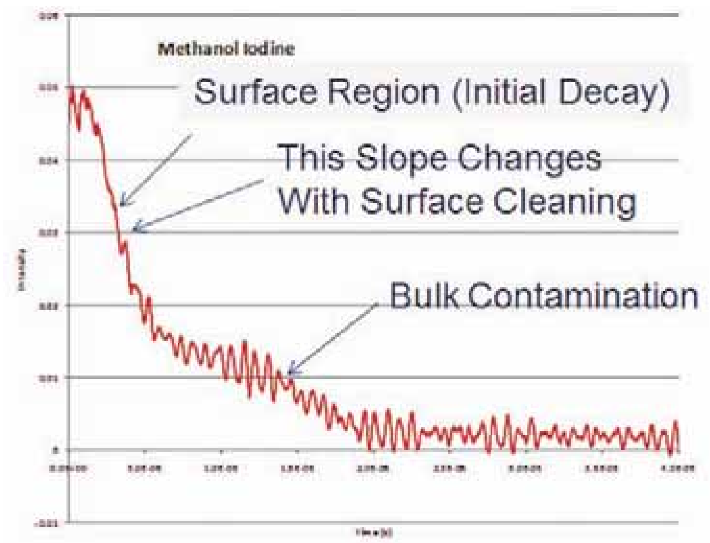

Figure 10. Bi-modal decay indicative of both sub-surface bulk recombination centres.

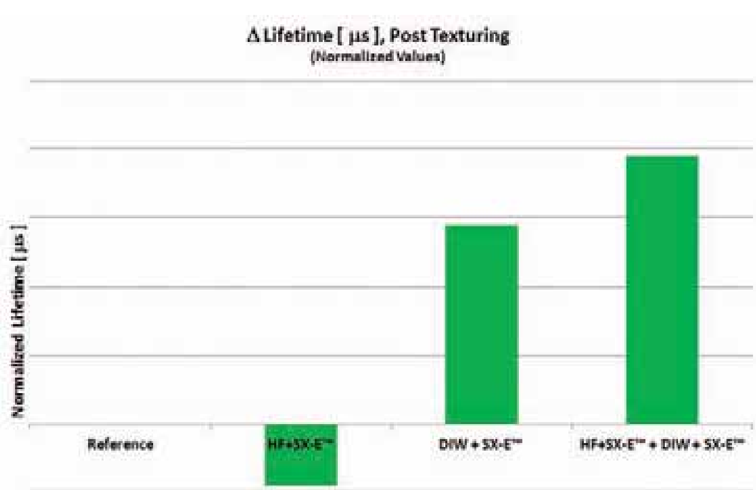

Figure 11a. Customer data; impact of SX-E addition and cleaning sequence on solar cell performance (normalized values post texturing).

in-house process evaluations, using cell manufacturer-supplied production test substrates (mc-Si and c-Si), have provided proof of successful cleaning of trace metals from the surfaces.

The various tests performed narrowed the applicable process sequence for optimum trace metal removal as compared to a standard process sequence (Table 4).

The resulting TOF-SIMS data confirmed that the standard processing shows an overall good removal of trace metals like Fe, Cr, Ni and Ti, but cannot reduce the copper contamination versus the incoming values (Table 4, Fig. 10). Detailed results are depicted in Fig. 7 and Fig. 8.

The careful tailoring of the process sequences, however, removes detrimental trace metal contamination below the detection limits of the analytical methods at hand (TOF-SIMS; see Fig. 8). Of particular note is the Cu level, which is reduced by three orders of magnitude.

> "Biodegradable chelating chemistry is effective in controlling trace metals on silicon surfaces."

High minority carrier lifetime is the key factor when striving for a good operational performance of solar cells. Lifetime influences the open circuit voltage, the short circuit current as well as the fill factor. Lifetime improvement is directly related to the reduction of metallic impurities in silicon, as-received or induced by diffusing metal atoms. It has been determined that effective removal of metal complexes from wafer surfaces is limited by a kinetic step in the aqueous process (Fig. 9). In customer tests, batch processing resulted in cell efficiency gains of 0.2 to 0.3% absolute, compared to no measured improvement for the in-line process. In order to further study this effect, cleaning experiments were conducted on production wafers and the minority carrier lifetime response was measured. As shown in Fig. 9, a doubling of the carrier lifetime was observed at rinse times of 150 seconds or greater. Not surprisingly, the batch process uses a 240-second rinse time, while that of the in-line process uses a bath contact time of 15 seconds.

The measured bimodal decay mechanism observed (Fig. 10) is a direct result of both sub-surface and bulk contamination as shown in Fig. 1b.

Field tests at cell manufacturer sites

Using the data obtained through optimization work on a lab scale, best cleaning practices were defined that provided augmented solar cell efficiency.

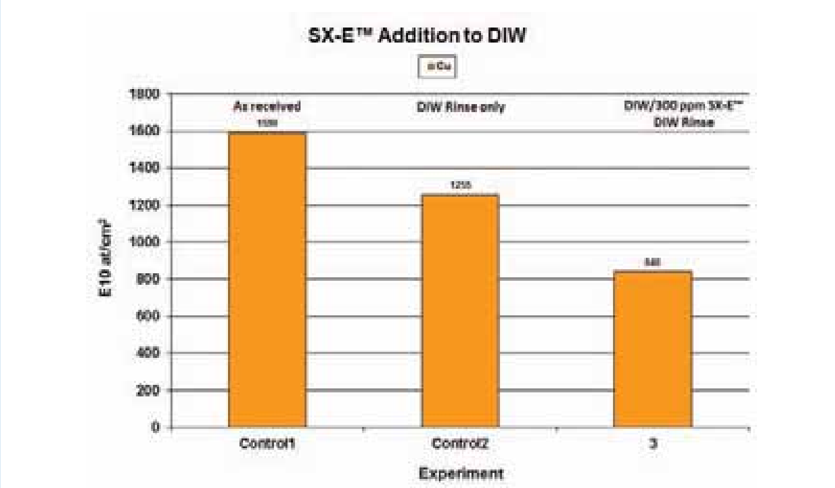

Figure 11b. Addition of SX-E to DIW only reduces the Cu level by about 50%.

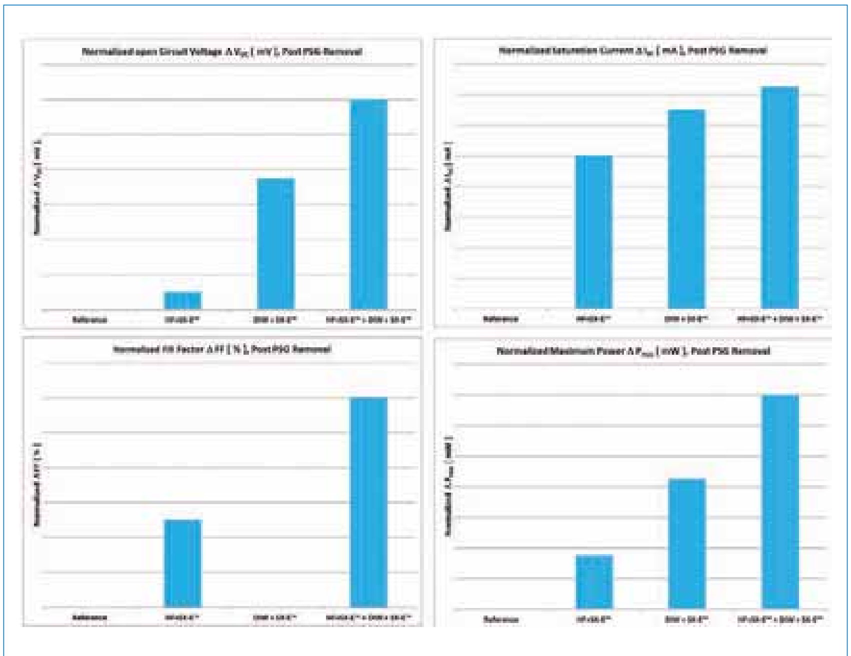

Figure 12. Customer data; impact of SX-E addition and cleaning sequence on solar cell performance (normalized values post PSG-removal).

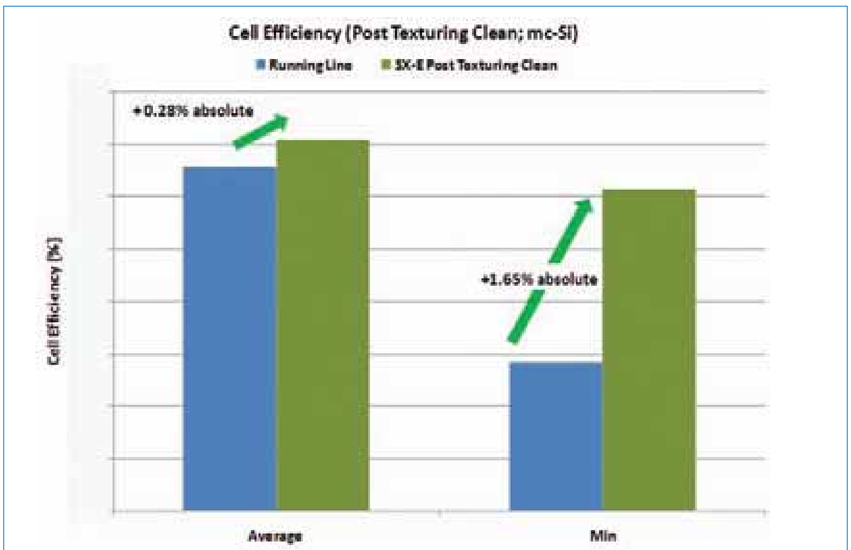

Figure 13. Cell efficiency (post texturing clean; mc-Si); running line vs. SX-E post-texturing clean.

Solar cell manufacturers and substrate manufacturers implemented industrial-scale trials using the best practices developed. These results obtained for both post-texturing clean and post PSG-removal clean correspond to TOF-SIMS data showing:

- Addition of SX-E to HF can be 'hit-and-miss' for effective removal (see also [3], Fig. 11a and Fig. 11b).
- Addition of SX-E to DIW reduces Fe, Ni and Cr levels marginally. The Ti-level is not impacted; copper is reduced by 50% as compared to the as-received level (Fig. 11b).
- Addition of SX-E to both DIW and HF shows an accumulative beneficial effect (Fig. 12a, Fig. 12b).

Metallic impurities close to the Si surface are included into the oxide as the Si surface is chemically oxidized by oxidizing agents, such as dissolved oxygen and H_2O_2.

"Narrowing the distribution of cell efficiencies translates to a reduction in mismatch losses when connected into a final PV module."

Solar cell efficiency distribution in a typical cell line follows a Gaussian type of response. Depending on the sophistication of the manufacturing process, among other parameters, the trail end to lower efficiencies represents a significant financial loss and imposes logistical efforts that can be significantly minimized. Narrowing the distribution of cell efficiencies translates to a reduction in mismatch losses when they are connected into a final PV module. Accounting for mismatch losses ultimately affects the module cost per watt [25]. In earlier manufacturing tests [1], an absolute efficiency increase of 0.2 to 0.3% was reported. In addition, the efficiency spread improved substantially. In fact, the lowest yielding cell efficiencies increased in average by 1.65% (Fig. 13).

Summary

Various promising cell concepts from research and development are currently under investigation for commercialization [15]. Standard cleaning processes that have been transferred from the microelectronics industry into PV manufacturing cannot solve the copper contamination issue. Instead of avoiding impurities by 'creative'

or 'intelligent' cleaning, the solar cell industry uses various impurity gettering and removal steps which are marginal and add to the overall operating costs. Effective removal of metal complexes from wafer surfaces has been determined to be limited by a kinetic step in the aqueous rinse process. The first indication of this dependency arises from split lot tests in both batch and in-line processing baths. Trace copper (Cu) impurities are frequently observed from solar-grade Si, which is most likely a result of the wafering process, since standard wires used to slice Si ingots are made of a metallic composite. TOF-SIMS analysis of bare mc-Si and CZ-Si wafers detected 1.1-1.8 × 10^{13} atoms/cm^2 of Cu from the samples on the surface. Starting with these contamination levels, further treatment of the metals by use of the complexing agent SX-E, for example, is gaining importance. With the addition of this material to various cleaning process options a reduction of most metallic contaminants from the wafer surfaces is observed. Quantification using TOF-SIMS analysis demonstrates a reduction of copper by *three orders of magnitude* as compared to the as-received level using an optimized process sequence.

In earlier trials, best-of-class cleans have been conducted that increase – in manufacturing split lot trials for both batch and in-line wet cleaning tools – the cell efficiency by 0.3% absolute on multi-crystalline Si wafers [1] and on the lowest yielding cells by 1.65% absolute.

Acknowledgements

This work was generously supported by PCT Systems, Fremont CA, USA, in particular by Sharyl Maraiov and Hank Miranda. A special thank you to Harald Moder (Merconics) and Jean-Marie Doris (CCS). This project was supported by the US Department of Education and the Arizona Governor's Office of Economic Recovery.

References

[1] Bohling, D. et al. 2010, "Crystalline silicon solar cell efficiency improvement by advanced cleaning technology", *NSTI-Nanotech*, Vol. 3, pp. 704–707.

[2] Weber, E.R, October 2001–December 2004, 2005, "Efficiency improvement of crystalline solar cells", *NREL Final Subcontract Report*.

[3] Kern, W. 1970 "Radiochemical Study of Semiconductor Surface Contamination", *RCA Review*, Vol.31, pp. 207–264.

[4] Morinaga, H. et al. 1996 "A Model for the Electrochemical Deposition and Removal of Metallic Impurities on Si Surfaces", *IEICE Transactions on Electronics*, Vol. E79-C, No.3, pp. 343–362.

[5] Kern, W. 1993, "Handbook of semiconductor wafer cleaning technology", *Noyes*, Vol. 623, Park Ridge, New Jersey.

[6] Oltersdorf, A., Zimmer, M. & Rentsch, J. 2009, "Analysis of metal impurities in wet chemical processes by ICP OES and AAS", *Proc. 24th EU PVSEC*, Hamburg, Germany.

[7] de Smedt, F. 2000, "Fundamental study of the behaviour of ozone in water: application in the cleaning of semiconductor devices", *Ph.D thesis*, Katholieke Universiteit Leuven, Belgium.

[8] Tool, C.J.J. et al. 2006, "Almost 1% absolute efficiency increase in mc-si solar cell manufacturing with simple adjustments to the processing sequence", *21st EUPVSEC*, Dresden, Germany.

[9] Istratov, A.A. et al. 1998, "Intrinsic diffusion coefficient of copper in silicon", *Phys. Rev. Letters*, Vol. 81, p. 1243.

[10] Yli-Koski, M. et al. 2005, "Measurement of Copper in p-Type Silicon Using Charge-Carrier Lifetime Methods", *Solid State Phenomena*, 108–109, pp. 643

[11] Stewart, K. 2001, "Influence of copper on the carrier lifetime of n-type and p-type silicon", *Proc. 11th Workshop on crystalline silicon solar cell materials and processes*, Estes Park, Colorado, pp. 212–215.

[12] "Environmental Risk Assessment of Complexing Agents", 2001, UCC Umweltchemie Consulting on behalf of Umweltbundesamt, Berlin, Germany.

[13] Hopkins, R.H. 1985, "Impurities in Silicon Solar Cells", *NTRS*, Westinghouse R&D Center, pp. 215–233.

[14] Fishman, O.S. 2008, "Solar silicon Part II. (POWERING THE FUTURE)", *Adv. Materials & Processes.*

[15] Taguchi, M. et al. 2000, "HIT TM Cells -High-Efficiency Crystalline Si Cells with Novel Structure", *Prog. Photovolt. Res. Appl*, pp. 503–513.

[16] Brundle, C.R., Evans Jr., C.A. & Wilson, S. (eds), 1992, *Encyclopedia of materials characterization - surfaces, interfaces, thin films*, Butterworth-Heinemann.

[17] Vickerman, J.C. & Briggs, D. (eds), 2001, *ToF-SIMS – Surface analysis by mass spectrometry*, SurfaceSpectra.

[18] Mowat, I., Lindley P., & McCaig, L. 2003, "A Correlation of TOF-SIMS and TXRF For the Analysis of Trace Metal Contamination on Gallium Arsenide", *Applied Surface Science* pp. 203–204 & 495–499.

[19] Gloudenis Jr, T.J. 2000, "Silicon wafer surface metals characterization by vapor phase decomposition inductively coupled plasma mass spectrometry (VPD-ICPMS)", *Agilent Appl. Note*, pp. 1–6.

[20] Wang, J. et al. 2000, "Analytical techniques for trace elemental analyses on wafer surfaces for monitoring and controlling contamination", Stanford Publications, pp. 1–9.

[21] Walsh, A. 1955, "The application of atomic absorption spectra to chemical analysis", *Spectrochim. Acta,* Vol. 7, no. 108.

[22] Welz, B. & Sperling M. 1999, *Atomic Absorption Spectrometry*, Wiley-VCH, Weinheim, Germany, pp. 1–941

[23] Wang, X.B. et al. 2001, "The electronic structure of $CuCl_2$ and $CuBr_2$ from anion photoelectron spectroscopy and ab initio calculations", *Journal of Chemical Physics*, Vol. 114. No 17. pp. 7388–7395.

[24] van den Berg, C.M.G. & Kramer, J.R., 1979, "Determination of complexing capacities and conditional stability constants for copper in natural waters using MnO_2" *Analytica Chimica Acta*, Vol. 106, No. 1, pp. 113–120.

[25] Ristow, A., Begovi, M. & Rohatgi, A. 2004, "Numerical approach to uncertainty and sensitivity analysis in forecasting the manufacturing cost and performance of pv modules", *19th EUPVSEC*, Paris, France, pp. 2178–2181.

About the Authors

Helmuth Treichel is a chemical engineer whose experience spans semiconductor capital equipment; thin films for electronics and optics; ALD, oxidation and CVD; and semiconductor (silicon and compound semiconductor) processes. Helmuth has collaborated on more than 32 different patents, presented 31 invited and 14 contributed lectures, and published more than 56 papers internationally.

Dr. David A. Bohling is a technology innovator whose experience includes 25 years in Stage Gate, NPI, PDP, and systems engineering. He holds 11 US Patents; seven of which were in advanced semiconductor cleaning technologies, and was involved in 68 publications in technical journals, trade journals and conference proceedings.

Dr. Mark A. George has 20 years of experience in product, process and business development of or related to thin-film manufacturing technologies. He has authored or co-authored 65 technical papers and is the holder of eight US and two European Patents with several patents pending.

Avery Goldstein received his Juris Doctor degree from Wayne State University in

1998. He is admitted to practice before various State courts and received a doctoral degree in chemistry from the University of California, Berkeley in 1993. He holds numerous patents, was the editor of The Handbook of Nanophase Materials, and currently is editor of Patent Law for Scientists and Engineers.

Antje Oltersdorf studied process engineering at TU Hamburg-Harburg. During her diploma thesis at Fraunhofer ISE, she investigated ion chromatographic and titration methods for acidic texturization. She is working on her Ph.D. thesis on trace element analytics in wet chemical processes.

Martin Zimmer graduated in 2005 with a diploma in chemistry from the Ruprecht-Karl's University in Heidelberg. He joined Fraunhofer ISE in 2006 and is currently pursuing a Ph.D. in the field of wet chemical analysis and process development within Fraunhofer ISE's department for Wet Chemical and Plasma Technologies.

Jochen Rentsch is head of the wet chemical and plasma technologies/process transfer department at Fraunhofer ISE. He received his degree in physics in 2002 from the Albert-Ludwigs University of Freiburg, Germany. His Ph.D. research at Fraunhofer ISE was conducted in the field of plasma etching technologies.

Larry Wang is vice president and scientific fellow of SIMS services at Evans Analytical Group, headquartered in Silicon Valley. Dr. Wang received his Ph.D. in physics from University of Wisconsin in 1990. He has over 20 years' experience with variety of analytical techniques for material analysis.

Ian Mowat is director of sales for the surface analysis and materials characterization division of Evans Analytical Group (EAG). He joined EAG in 1996, working as an analyst in the TOF-SIMS group. Since then, he has worked in various other analytical groups including SIMS and FTIR, moving into a sales role in 2008.

Dr. Sara G. Ostrowski is a materials characterization scientist at Evans Analytical Group (EAG), where she specializes in time-of-flight secondary ion mass spectrometry (TOF-SIMS), scanning probe microscopy (SPM), and optical profilometry (OP). Sara earned a B.A. in chemistry from Franklin & Marshall College in 1999 and a Ph.D. in analytical chemistry from Pennsylvania State University in 2005.

Werner Kern is the president of Werner Kern Associates. From 1959-1987, he was a scientist at the RCA David Sarnoff research center in Princeton, New Jersey where he developed the RCA Standard Clean Process for silicon wafer cleaning and in 1988 he joined Lam research corporation as a senior scientist, concurrently opening his own consulting company. Werner Kern is the holder of 11 US patents and is the author and co-author of over 150 scientific publications. He is the editor of four technical books and has received numerous awards.

Enquiries

Sunsonix
859 Pheland Ct.
Milpitas
CA 95035
USA
Tel : +(408) 515-8585
Email: helmuth@sunsonix.com

Fraunhofer Institute for Solar Energy Systems (ISE)
Heidenhofstr. 2
D-79110 Freiburg
Germany

Evans Analytical Group
810 Kifer Rd.
Sunnyvale
CA 94086
USA

Werner Kern Associates
22 Greenways Ln.
Lakewood
NJ 08701
USA

Progression of n-type base crystalline silicon solar cells

L.J. Geerligs, **N. Guillevin** & **I.G. Romijn**, ECN Solar Energy, Petten, The Netherlands

ABSTRACT

This paper reviews the status of solar cell technology based on n-type crystalline silicon wafers. It aims to explain the reasons behind the strong and increasing attention for n-type cells, including the inherent advantages of n-type base doping for high diffusion length, and for the industrialization of designs with good rear-side electronic and optical properties. The focus will be on cells using diffused junctions.

Introduction

Most industrial crystalline silicon solar cells are based on p-type wafers. Applying a phosphorous-diffused emitter and a back-surface field created by aluminium-silicon alloying, results in the common multicrystalline or monocrystalline silicon solar cells used in the vast majority of PV modules. The exceptions to this rule have been (for many years) the cells and modules produced by Sanyo and Sunpower, who are using n-type wafers for their high-efficiency cells. Recently, Yingli Solar has also taken high-efficiency 'Panda' cells based on n-type wafers into production. In addition, practically all major research organizations and several companies, including Bosch and Suniva, have started to report activities in cell processing from n-type wafers. This paper aims to explain the reasons behind the strong and increasing attention for n-type cells, including the inherent advantages of n-type base doping for high diffusion length.

Heterojunction (HIT) solar cells will not be discussed in this article, as the principles of the low-temperature heterojunction cell processes are very different from diffused junctions. Of course, differences in p- and n-type wafer properties apply irrespective of whether or not the cell process is based on HIT or diffused junction technology although changes in wafer properties due to high temperature process steps will be absent in HIT processes.

Differences in properties of p-type and n-type wafers

One of the most important characteristics of wafers used for solar cells is the minority carrier diffusion length, which is directly dependent on the minority carrier recombination lifetime or 'lifetime'. A long diffusion length and high lifetime allow for higher efficiencies. A characteristic of n-type doped crystalline silicon is that it generally reaches (much) higher lifetimes than p-type silicon. This is one of the reasons for the interest in n-type wafers for solar cell production. In the following we briefly review why the lifetime in n-type wafers is generally higher, but also mention several nuances.

Boron-doped p-type Czochralski (Cz) wafers show lifetime degradation due to formation of a boron-oxygen related metastable defect, upon illumination or in general upon minority carrier injection. Since boron (dopant) and oxygen (growth process impurity) are abundant in typical p-type Cz wafers for solar cells, the effect is very important. The lifetime degradation has been parameterized [1]; 15 or 20ppma of oxygen (the range typical for Cz wafers) limit the lifetime in a 1Ωcm wafer to 20 or 12µs, respectively (diffusion length 250 or 190 micron), though 2 to 3× higher lifetimes are possible for optimized thermal processing. While these diffusion lengths are still longer than typical wafer thicknesses, they severely limit the potential cell efficiency in high-efficiency cell designs [2].

Absence of boron or oxygen in wafers will avoid this boron-oxygen related lifetime reduction [3]. Oxygen reduction can be realized by magnetic Cz (MCz), for example, or floatzone (FZ) ingot growth; however these techniques are not yet available for low cost production. Boron can be avoided altogether by switching to Ga doping (Al-doping results in defects [4]). Ga-doped Cz for example is applied by Suntech in its high-efficiency Pluto cells [5]. A technique to remove the boron-oxygen defect is so-called regeneration [6], which does not yet appear to be applied commercially. Obviously, switching to n-type wafers will entirely avoid the boron dopant and the associated lifetime reduction [7].

In the last decade, another reason for higher lifetime in n-type wafers has become clear: the reduced impact of typical transition metal impurities [8]. In particular, the impurities which have donor-type character (i.e., toggle between positive and neutral states when they cause recombination) will, due to their charged state, have an increased capture rate for minority carriers in p-type wafers (electrons), but not for minority carriers in n-type wafers (holes). Such impurities happen to be the faster diffusing impurities. This means that process-induced contamination such as Fe causes typically (much) more recombination in p-type wafers than in n-type wafers. Cr is a relevant exception it is an impurity which diffuses relatively fast, and can be a relevant process impurity, but causes quite similar recombination in p-type and n-type wafers [9]. Acceptor-type impurities will show the opposite behaviour: they cause recombination in n-type rather than p-type wafers;

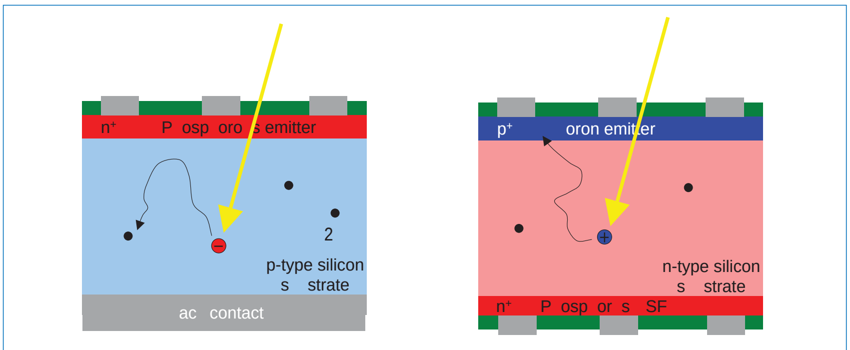

Figure 1. Schematic representation of the differences in recombination at impurities for p-type versus n-type solar cells. Typical transition metal impurities are donor-type, resulting in a large capture cross-section for electrons, but a much smaller one for holes. Therefore they are effective minority carrier recombination centres in p-type cells, but not in n-type cells. In addition, in p-type Cz, boron-oxygen-related defects are present, which are important recombination centres.

They also typically diffuse very slowly. Such impurities which are harmful in n-type rather than p-type wafers are, for example, Au and Zn.

In practice, lifetimes of many milliseconds are readily obtained in n-type Cz. Even in n-type mc-Si, very high lifetimes have been measured [10]. However, the crystal defects in mc-Si appear to reduce the carrier lifetime more or less equally for n-type and for p-type [11]. It is not currently clear whether there is a significant diffusion length advantage of n-type mc-Si over p-type mc-Si (however, other advantages of n-type cell architecture, which will be discussed below, remain applicable).

> "The crystal defects in mc-Si appear to reduce the carrier lifetime more or less equally for n-type and for p-type."

For n-type Cz reduction of the diffusion length due to oxygen-induced crystal defects has been reported [12,13], but it also that this can be minimized by suitable design of the cell thermal processing [12].

In conclusion, for very high-efficiency cell concepts (requiring very long diffusion lengths, such as back-junction back-contact, or having exceptional surface passivation, such as HIT), n-type silicon as a base material has clear benefits. Nevertheless, it is possible that for particular cell designs (e.g., a diffused emitter on the front and dielectric passivation on the rear) and with particular care to avoid process-induced contamination, similar efficiencies can be reached in Ga-doped or MCz p-type, as in n-type silicon. After all, UNSW still holds the cell efficiency record with a cell based on a p-type FZ base [14].

Differences between n-type and p-type cell processing

The reasons for the current industrial emphasis on p-type cells are manifold. Martin Green gives an historic perspective [15], mentioning aspects such as the convenience of phosphorous gettering, and aluminium-silicon alloying to create a back-surface field (BSF), which applies to p-type substrates, and the complications of boron diffusion as a technology to form an emitter on an n-type substrate.

Until recently the passivation of a boron emitter was also considered a bottleneck, with only thermal oxidation available as a high quality passivating step, with some doubts about its long-term stability [16]. Silicon nitride typically does not provide practical passivation for boron emitters [17]. Also, the complexity and therefore cost of creating and isolating two separate diffusions (emitter and BSF) on either face of the cell may have been considered to be a bottleneck. In this respect the standard p-type cell process is very simple with only eight or nine process steps, and every additional process step means a cost increase that has to be paid for by increased cell efficiency.

However, for all these bottlenecks there has been much progress in recent years, and therefore interest and activities in n-type cells have increased dramatically. For passivation of the boron emitter there are now at least five methods that seem to work well, with coating by Al_2O_3 via atomic layer deposition (ALD) – probably the best documented [18]. Several companies are actively developing equipment for the PV industry to deposit Al_2O_3. Industrial boron emitters have now been reported with emitter recombination currents (J_{oe}) below 30fA/cm^2 [19,20] based on a variety of passivation layers, which compares favourably with industrial phosphorous emitters for which typical numbers appear to be somewhat higher [21]. Incidentally, this low J_{oe} shows that the boron emitter of n-type cells does not need to be influenced much by recombination due to impurities (e.g. Fe or boron-oxygen defect), or crystal defects induced by boron diffusion [22]. It may be fortunate in this respect that the gettering of Fe by a boron emitter is not very good [23]. We refer to an earlier article from this journal for more details on (boron) emitter diffusion [24]. Notably, since that publication more results have been published for implanted boron emitters [25].

A practical aspect of concern for n-type cell processing might be the resistivity variation through an n-type ingot, which will be larger than for a p-type ingot due to the different segregation coefficients of the dopants phosphorous (k≈0.3) and boron (k≈0.7). However, for high-efficiency cell designs, the typical resistivity variation in a phosphorous-doped ingot is acceptable.

Opportunity for bifacial n-type cells and modules

N-type cells, when using a full area-diffused BSF, offer the possibility of a bifacial layout – where light is collected from the rear as well as the front. This is a distinct difference with conventional p-type cells. Bifaciality results can be excellent (e.g. 90% in [20]). A recent review of bifacial technology lists results of a *30% and higher gain* in power yield for bifacial modules with suitable installation of modules ('suitable' meaning for example painting the base surface below the modules white)[26]. The paper also mentions the advantage of a reduced operating temperature. However, not all cell architectures are suitable for bifacial application. The use of a locally diffused BSF on the rear probably requires a fine pitch of contact points which will allow little bifaciality, and also IBC cells are only moderately suitable for bifacial application [27].

Basic n-type cells

In this section we describe the most basic n-type cells, with full-area emitter on front or rear, and contact grid on the front. They are:

1. The cell with emitter on front and BSF on rear (BSF cell, or p$^+$nn$^+$ cell). It normally has a boron-diffused emitter and a phosphorous-diffused BSF.

2. The Al rear-emitter cell with a front-surface field (FSF cell, or n$^+$np$^+$ cell). It normally has a phosphorous-diffused FSF, and is also known as PhosTop cell.

Both cell types have a variant with local junction formation on the rear, either local BSF or local emitter.

BSF n-type cell

Many variations of this cell have been published, including the following types:

- bifacial BSF type cell (Fig. 2): full area emitter on front and full area BSF on rear, which are contacted by contact grids. Front and rear-passivating dielectric coatings.

- PERT: passivated emitter rear totally-diffused. Can be identical to the above, but

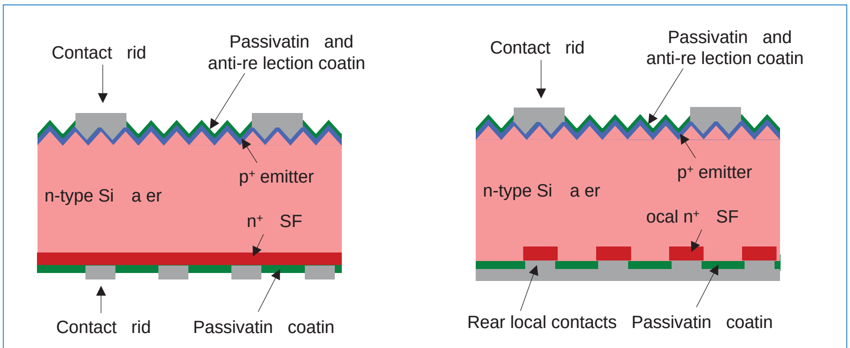

Figure 2. Left: p$^+$nn$^+$ bifacial BSF type cell. Right: Local BSF (PERL) cell structure. Variations such as selective diffusion and mixtures of the two cell types are possible.

typically has rear point contacts with local heavier BSF diffusion, and a full-area metal layer to interconnect the point contacts.

- PERL (Fig. 2): passivated emitter rear locally-diffused; most of the rear area is undiffused. Local BSF diffusion under the rear contacts. Typically a full area metal layer to interconnect the point contacts.
- PERC: passivated emitter rear contact. Rear undiffused. Typically high density of rear point contacts, and a full area metal layer to interconnect the point contacts. This will not yield a high efficiency unless the rear point contacts are passivated (for p-type this can be done by using aluminium point contact metallization where a local BSF is created by alloying).

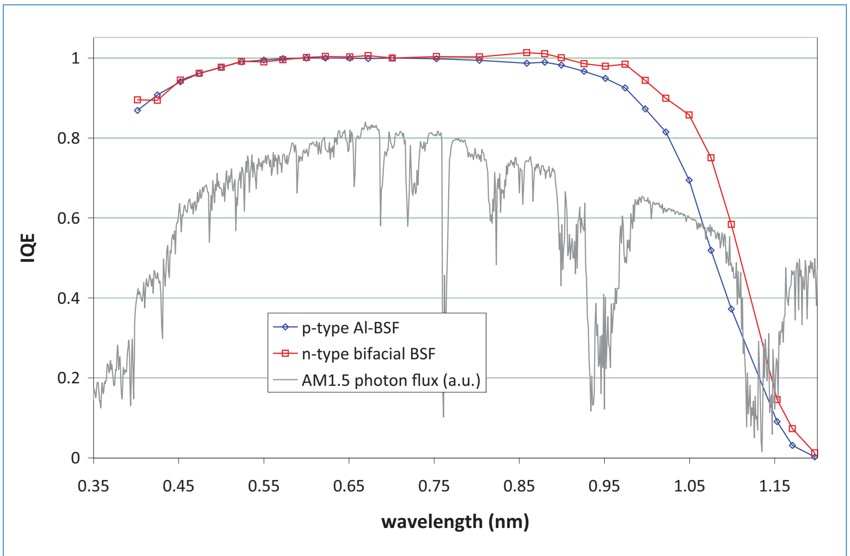

Figure 3. example of internal quantum efficiencies (normalized at 700nm) of industrial-type p^+nn^+ bifacial BSF type cell (red) and conventional Al-BSF p-type cell (blue). The gain in the infrared is due to improved diffusion length, improved internal rear reflection, and improved rear surface passivation. Photon flux versus wavelength in AM1.5 (grey) shows the importance of the IR wavelength region.

In 1978, Sandia labs published excellent results for p^+nn^+ cells (probably not bifacial; the BSF appears to have been fully covered by metal contact) [28]. The Sandia paper explains the advantages of the structure: a transparent emitter; gettering as well as passivation by the BSF; and a long hole diffusion length in the base.

In recent years the development of p^+nn^+ bifacial cells using simple industrial techniques such as screen-printing was pursued by many institutes [2,19,20,29-31]. Yingli Solar has adopted and piloted the technology in a joint project with ECN and Amtech [32] and subsequently commercialized the concept, so far reporting a best cell efficiency in trial production of 19.5% (independently confirmed) [33] and in production of 19.9% [34]. Other companies like Bosch and Suniva have made public that they work on production technology of p^+nn^+ type cells. Suniva reported 19.1% (independently confirmed) using implantation in cooperation with Varian [35].

In addition to the cells with nearly 20% efficiency made by industrial techniques, there have also been efforts on laboratory cells, demonstrating new processes, materials and the potential of particular cell designs. In particular ISE has reached very high cell efficiencies upto 23.9% for a cell structure with full-area BSF, using emitter passivation by Al_2O_3 (pioneered in collaboration with University of Eindhoven) [36]. Comparisons of different emitter profiles were reported. PERL [37] as well as PERT [16] laboratory cells have been reported. The rear-side recombination seems to be only marginally different between these two cell types, as their V_{oc}s are very similar.

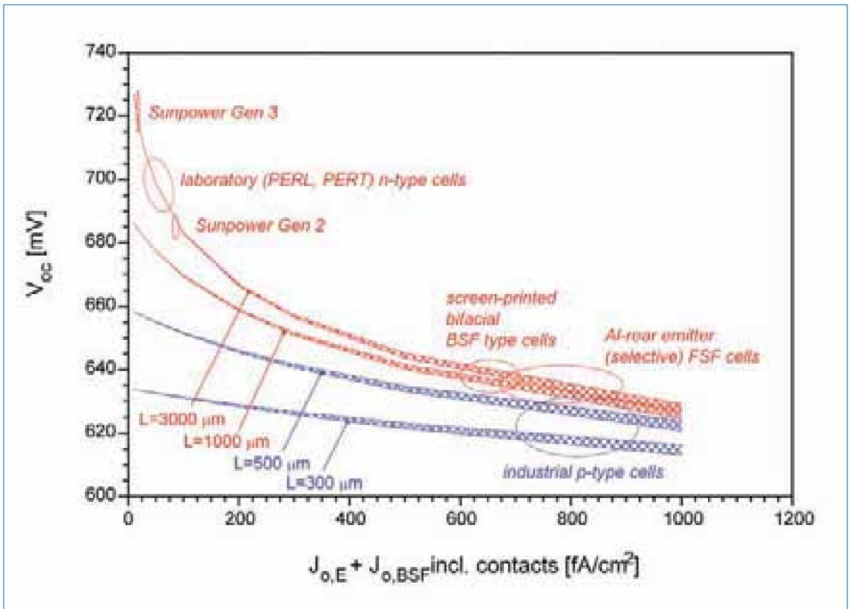

Figure 4. Model calculations of the dependence of V_{oc} on recombination current *Jo* in emitter and BSF (including contact recombination) and on minority carrier diffusion length L in the base. Typical ranges for L in n-type wafers (red, lifetime approx. 1–10ms) and p-type (blue, lifetime approx. 30–100µs) have been taken. The hatched areas cover a variation of the ratio $J_{o,E}/J_{o,BSF}$ between 1/3 and 3. Ellipses roughly indicate the estimated present parameter ranges for the various cell types (Sunpower data from [12]). Reducing the emitter and BSF recombination and, in particular, the contact recombination will move the bifacial BSF type cell performance towards the lab cell performance.

Compared to conventional p-type Al-alloyed BSF cells, the high efficiencies obtained with p^+nn^+ cells are due to several factors. Ranked by approximate importance they are:

1. Improved light trapping due to much better internal rear reflection than an Al-BSF provides.
2. Improved diffusion length in the base.
3. Improved rear-passivation due to BSF with passivating dielectric coating.
4. Low emitter recombination current, probably somewhat better than for comparable phosphorous emitters on p-type wafers.

Fig. 3 illustrates the impact of improved bulk recombination, rear-surface recombination, and improved rear-side optical performance for measured internal quantum efficiencies (IQEs) of industrial-type n-type and p-type cells made at ECN. The difference in IQE accounts for a difference in I_{sc} of close to 4%.

Fig. 4 illustrates by model calculations how V_{oc} depends on recombination current at the front and rear of the cell, and the bulk diffusion length, according to the following equations [38]:

$$V_{oc} \quad \frac{kT}{q} \quad \left(\frac{J_{sc}}{J} \quad \right) \qquad (1)$$

with, assuming low level injection (LLI) in the base,

$$J \quad J_{oe} \quad \frac{J_{o,BSF} \quad W/L \quad \frac{qDn_i^2}{LN_d} \quad W/L}{W/L \quad \frac{J_{,BSF}\, LN_d}{qDn_i^2} \quad W/L} \qquad (2)$$

which for the BSF uses the relation between J_o and S_{eff}, valid for LLI:

$$S_{eff} \quad \frac{J \;\; N_d}{qn_i^2} \qquad (3)$$

N_d, D, L are dopant density, diffusion constant, and diffusion length in the base, respectively. J_{oe} and $J_{o,BSF}$ are the emitter and BSF recombination current densities, respectively, which are a function of recombination current densities at the various diffused and passivated surfaces and at the contacts. FF will typically slowly increase with increasing V_{oc} [38]. The resistivity used in the calculations for Fig. 4 is 2Ωcm.

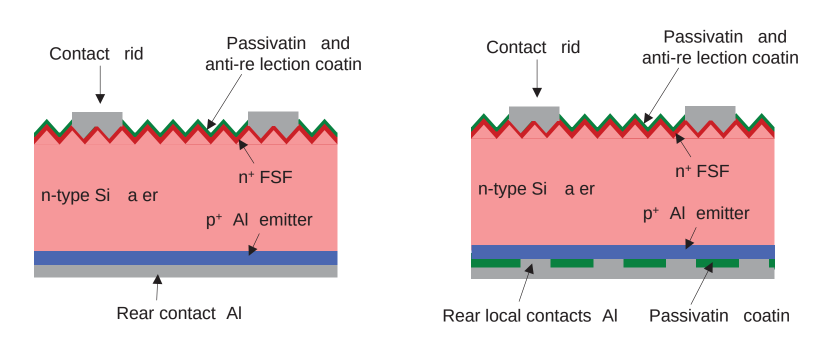

Figure 5. n+np+ FSF Al back-junction cell. Right: variations with selective diffusion, local emitter regions, etc., are possible.

Together, these two figures illustrate the difference in IV parameters between n-type and p-type cells.

> "When applying a boron-diffused BSF, maintaining a high diffusion length in a p-type wafer might be challenging."

For this cell structure, with two differing diffused layers on both faces of the wafer, the diffusion process is more complex than for p-type cells. For example, the use of both BBr_3 and $POCl_3$ tube furnace diffusions has been described [20], use of BCl_3 instead of BBr_3 and use of PECVD SiO_x diffusion barrier [31], etc. Also, diffusion sources such as spin-on or printed layers [29] have been used.

A valid question is whether or not with comparably more complex processing than the standard p-type cell process, it is also possible to create a p-type bifacial BSF cell (n^+pp^+ cell) with comparable advantages. One of the challenges in that case would be to obtain wafers with high diffusion length (e.g. Ga-doped or magnetic Cz), and maintain this high diffusion length during processing. Especially when applying a boron-diffused BSF, maintaining a high diffusion length in a p-type wafer might be challenging. The high temperature for boron diffusion easily contaminates a

Type	Area (cm^2)	Metallization	V_{oc} (mV)	Efficiency (%)	References
bifacial BSF	239	screen printed	641/-	19.49/19.89	[33]/[34]
PERL, laboratory	4	evaporated front grid, rear full area evaporated	705	23.9	[2]
PERT, laboratory	4	evaporated front grid + plating, rear full area evaporated	695	21.9	[16]
Al-rear emitter, selective FSF	6" Cz	screen printed	639/641	18.5/18.5	*[45,46]/[49]
Al-rear emitter, Al_2O_3 passivated, laboratory	4	evaporated	649	19.8	**[43]

* Obtained 18.6% on a 5" FZ wafer.

** An efficiency of 20.0% was actually obtained with a-Si rear side passivation, but judging from the V_{oc} the potential of Al_2O_3 passivation seems to be better.

Table 1. Results of the various n-type cell concepts (non-back contact).

wafer with Fe, which is a severe lifetime killer for p-type wafers but not for n-type wafers. Siemens worked on p-type cells with boron BSF until several years ago [39]. For p-type high-efficiency designs, it is more common to omit the full-area BSF and apply a PERC or PERL cell design, but this requires a finely spaced rear-contact grid for low series resistance losses, and therefore requires low recombination (high quality local BSF) under these contacts.

Aluminium rear-emitter cell

An alternative process to create n-type cells by a relatively simple process is by applying phosphorous front diffusion and Al-alloying on the rear, i.e., very close to the current industrial p-type cell process [40–46] (see Fig. 5).

In its basic form this process has the disadvantage that it lacks the efficiency improving factors one, three and four of the bifacial BSF cell of the previous section. Without removal of the Al and Al-Si alloy layers on the rear, the V_{oc} of such cells is limited by the emitter recombination to about 640mV [41]. In addition, conventional cell interconnection is impossible since the complete rear surface area should be Al-doped, as the commonly used Ag interconnection pads would be large areas with high recombination loss ('electrical shading' areas). Alternative interconnection might resolve this problem [44, 47].

Despite the limited rear surface passivation, an efficiency of up to 19.3% was recently obtained on FZ material by using a plated front grid and SiO_x/SiN_x front-surface passivation, and with full rear-area Al coverage (i.e., cutting off the cell edges on which emitter is absent) [46].

To improve the rear recombination and enable conventional interconnection, cell processes have been developed where, after Al-Si-alloying to create the emitter, the remaining Al layer and the Al-Si alloy are removed by wet chemistry, and the rear surface is coated with a passivating layer such as a-Si, Al_2O_3, or SiO_x [43, 46]. This can improve the cell efficiency to a level more comparable to the bifacial BSF type cell, as reported efficiencies well over 19% demonstrate. However, for lab cells the V_{oc}s are still significantly lower than for a B-emitter; this shows that the emitter recombination current is significantly higher (J_{oe}=160–180fA/cm^2 is reported in [48]) than for a well-passivated B-emitter. A quick estimate shows that free carrier absorption in the Al-emitter is probably roughly the same as in the B-emitter.

A variation of the Al rear-emitter cell that has been explored is based on the laser-fired contacts scheme [46]. Here a dielectric rear-side passivation is applied with only local Al-emitter areas, created by laser-firing of an Al layer through the dielectric. However, for this elegant process scheme so far the results are lagging behind the full-area rear Al-emitter cells, due to non-optimal junction quality.

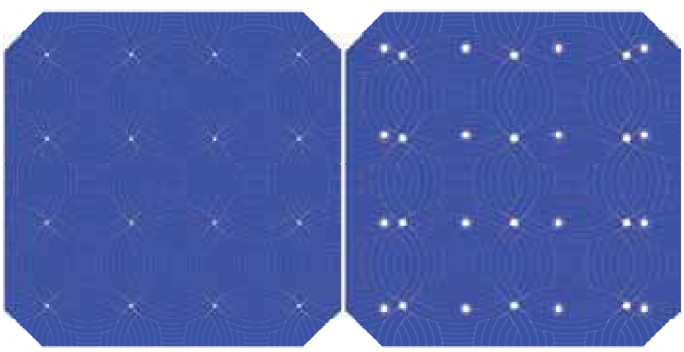

Figure 6. n-type bifacial MWT cell developed by ECN [55]. Left: front of cell; right: rear of cell.

Back-contact n-type cells

Back-contact n-type cells require more complex processing but offer the significant advantages of reduced shading losses (higher cell efficiency) and lower losses in module interconnection.

Back-contact cells have the major advantage that interconnection in a module will be on one side of the cells only. This will reduce the stress exerted by the interconnection on the cells. It allows the use of thinner cells, or cells larger than six inches. Back-side interconnection also has efficiency advantages. The interconnection conduits can be optimized for best series resistance losses without the constraints related to normal front-to-back tabbed interconnection: shadow loss (i.e. width of tab) and stress on cells (i.e. thickness of tab). The reduction of series resistance losses at the module level can result in a significant reduction of efficiency loss from cell to module, compared to standard interconnection; for example, the FF loss can be reduced to 2%, about 1.5% better than for traditional tabbed modules [52].

Only Sunpower is commercially producing back-contact n-type cells, of the back-junction back-contact type (also often referred to as interdigitated back-contact or IBC cells, although that term is rather ambiguous). Metal wrap-through (MWT) and emitter wrap-through (EWT) cells (cells where the back-contact is realized by connecting a front emitter to the back of the wafer through holes in the wafer) are in research phase.

N-type metal wrap-through and emitter wrap-through cells

MWT and EWT cells have been under development for p-type cells for more than 10 years [53]. Typically the cell process requires laser drilling of a small number (MWT) or a large number (EWT) of holes in the wafer. For MWT the front grid connects

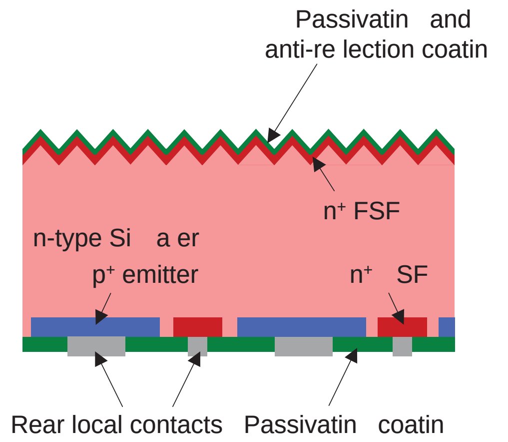

Figure 7. Schematic of an interdigitated back contact cell, such as is produced by Sunpower and is in development at many institutes and several companies. This cross-section of an n-type IBC cell made at ECN shows on the front side an n+ FSF which is coated with a passivating and anti-reflection coating. The p+ emitter and n+ BSF are located at the rear side and contacted using screen-printing. Contacts can of course be made with other methods, while also variations like point contacts or multiple emitter contacts are possible.

through these holes to contact pads on the rear, while for EWT there is no front grid, but the emitter is wrapped through these holes to contact pads on the rear. N-type EWT cells have to our knowledge not yet been reported. In principle, cell processing used for high efficiency p-type EWT cells such as RISE [52] might be applicable to n-type base material.

The authors have reported bifacial n-type MWT cells [53] (see Fig. 6). Depending on the front grid design and the number of holes, a cell efficiency gain of several tenths of a percentage point can be obtained [61]. ECN have obtained up to 19.75% cell efficiency with low-cost industrial techniques on 156mm-size Cz wafers. This means that current technology allows low-cost back-contact cells of efficiency close to 20% or higher. Together with the possibility of using thinner wafers, and the benefit for module interconnection and efficiency, this is a promising route to low-cost high-efficiency modules. An advantage of MWT back-contact technology is that it should allow bifacial modules with quite good bifaciality, whereas IBC cells due to the requirement for finer grids on the back result in modules with rather low bifaciality [27].

Back-junction back-contact cells

IBC cells on n-type wafers have been around for more than 50 years. High efficiencies can be achieved on IBC cells because all current collecting contacts are located at the rear, eliminating all front shading losses (Fig. 7). At the same time, the rear structure can be optimized for maximum collection efficiency and minimal resistive losses. However, as the minority carriers need to travel to the emitter contacts on the rear of the cell, the cells are very sensitive to wafer quality. Furthermore, the device structure needs excellent surface passivation on both sides. Currently the most successful approach is that used by Sunpower with cell efficiencies of over 24% [12].

Recently, several institutes have published work on IBC cells [54–57] using low cost methods to fabricate the p^+nn^+ junctions and contacts at the rear surface. These methods range from screen-printing and laser processing [54] to the RISE concept which is based on laser ablation and self-aligned metallization by a single evaporation step [55]. Efficiencies up to 21.3% have been reached on n-Cz [54] and up to 22% on p-FZ [55]. The latter process can be applied to n-type without a change in design [55]. Most institutes so far demonstrated high efficiencies on relatively small areas ($4cm^2$). ECN has worked in collaboration with Siliken to achieve 19.1% efficiency on larger area IBC cells applying low-cost methods like wet chemistry and screen-printing

Type	Area	Metallization	V_{oc}	Efficiency	References
MWT	239	screen printed	644	19.65	[61]
IBC	155		721	24.2	[12]

Table 2. Best results for n-type back contact cell concepts.

[58]. Another lower cost cell approach that has been published is the use of a screen-printed Al-alloyed emitter which also reached 19.1% on n-Cz wafers [56,57].

On the front-side of IBC cells, the front surface field (FSF) serves not only to reduce recombination but the FSF (together with the bulk resistivity) also has to improve the lateral transport of majority carriers. The latter is important when the contact pitch on the rear becomes large [54], which can be the case if lower cost methods like screen printing are used to define the contact structure. Besides the FSF, the cell design requires the highest resolution patterning possible, within the patterning method used, to minimize lateral transport losses. On the rear side of IBC cells, the p^+nn^+ structure needs to be well passivated with appropriate dielectrics. Traditionally, high-quality silicon oxides have been used for this purpose which benefit from a low density of fixed charges and low interface state density. Lower cost methods like deposition of dielectric layers by for example PECVD are under investigation by several groups including ECN [58, 56].

Conclusions

This article has reviewed recent directions and results in solar cell technology based on n-type crystalline silicon wafers. Clearly, it is recognized in research and industry that n-type silicon offers advantages for creating very high efficiency cells, which is of high importance for reducing costs per Wp. Therefore, in addition to the very high-efficiency cells that Sunpower and Sanyo have been producing for a number of years, there are many new exciting developments and results of n-type cell technology, and it is very likely that n-type solar cells will rapidly gain a larger market share in the coming years.

Acknowledgements

The authors acknowledge the many colleagues and project partners inside and outside ECN with whom they have had the pleasure of collaborating on science and technology of this exciting field.

References

[1] Bothe, K., Sinton, R. & Schmidt, J. 2005, "Fundamental Boron–Oxygen-related Carrier Lifetime Limit in Mono- and Multicrystalline Silicon", *Prog. Photovolt: Res. Appl*, Vol. 13, pp. 287–296.

[2] Glunz, S. et al. 2010, "N-type silicon - enabling efficiencies >20% in industrial production", *Proc. 35th IEEE PVSC*, Honolulu, Hawaii, USA, pp. 50–56.

[3] Saitoh, T. et al. 2000, "Suppression of light-induced degradation of minority carrier lifetimes in low-resistivity Cz-silicon wafers and solar cells", *Proc. 16th EU PVSEC*, Glasgow, UK, pp. 1206-1209.

[4] Schmidt, J. 2003, "Temperature- and injection-dependent lifetime spectroscopy for the characterization of defect centers in semiconductors", *Appl. Phys. Lett*, Vol. 82, pp. 2178–2180.

[5] Suntech general information [http://www.suntech-power.com].

[6] a) Herguth, A. et al. 2007, "Investigations on the Long Time Behavior of the Metastable Boron–Oxygen Complex in Crystalline Silicon", *Prog. Photovolt: Res. Appl*, Vol. 16, pp. 135–140.
b) Lim, B. et al. 2008, "Permanent deactivation of the Boron-oxygen recombination center in silicon solar cells", *Proc. 23rd EU PVSEC*, Valencia, Spain, pp. 1018–1022.

[7] Schutz-Kuchly, T. et al. 2010, "Light-Induced-Degradation effects in Boron–phosphorus compensated n-type Czochralski silicon", *Appl. Phys. Lett.* Vol. 93, p. 093505.

[8] Macdonald, D. & Geerligs, L.J. 2004, "Recombination activity of interstitial iron and other transition metal point defects in p- and n-type crystalline silicon", *Appl. Phys. Lett*, Vol. 85, pp. 4061–4063.

[9] Schmidt, J. et al. 2008, "Recombination activity of interstitial chromium and chromium-Boron pairs in silicon", *J. Appl. Phys.*, Vol. 102, p. 123701.

[10] Cuevas, A. et al. 2002, "Millisecond minority carrier lifetimes in n-type multicrystalline silicon", *Appl. Phys. Lett*, Vol. 81, pp. 4952–4954.

[11] Geerligs, L.J. et al. 2007, "Precipitates and hydrogen passivation at crystal defects in n- and p-type multicrystalline silicon", *J. Appl. Phys.* Vol. 102, p. 093702.

[12] Cousins, P.J. et al. 2010, "Generation 3: improved performance at lower cost", *Proc. 35th IEEE PVSC*, Honolulu, Hawaii, USA, pp. 275–278.

[13] Edler, A. et al. 2010, "High lifetime on n-type silicon wafers obtained after Boron diffusion", *Proc. 25th EU PVSEC*, Valencia, Spain, pp. 1905–1907.

[14] Zhao, J., Wang, A. & Green, M.A. 1999, "24.5% Efficiency Silicon PERT Cells on MCZ Substrates and 24.7% Efficiency PERL Cells on FZ Substrates", *Prog. Photovolt: Res. Appl*, Vol. 7, pp. 471–474.

[15] Green, M. 2000, "Silicon solar cells at the crossroads", *Prog. Photovolt: Res. Appl*, Vol. 8, pp. 443–450.

[16] Zhao, J. et al. 2003, "Performance instability in n-type PERT silicon solar cells", *Proc. 3rd WCPEC*, Osaka, Japan.

[17] a) Chen, F.W., Li, T.A.P. & Cotter, J.E. 2006, "Passivation of Boron emitters on n-type silicon by plasma-enhanced chemical vapor deposited silicon nitride", *Appl. Phys. Lett*, Vol. 88, p. 263514.
b) Altermatt, P.P. et al. 2006, "The surface recombination velocity at Boron-doped emitters: comparison between various passivation techniques", *Proc. 21st EU PVSEC*, Dresden, Germany, pp. 647 –650.

[18] Hoex, B. et al. 2008, "On the c-Si surface passivation mechanism by the negative-charge-dielectric Al_2O_3", *J. Appl. Phys.*, Vol. 104, p. 113703.

[19] Mihailetchi, V.D., Komatsu, Y. & Geerligs, L.J. 2008, "Nitric acid pretreatment for the passivation of Boron emitters for n-type base silicon solar cells", *Appl. Phys. Lett*, Vol. 92, p. 063510.

[20] Mihailetchi, V.D. et al. 2010, "Screen-printed n-type silicon solar cells for industrial application", *Proc. 25th EU PVSEC*, Valencia, Spain, pp. 1446–1448.

[21] Hilali, M.M. et al. 2006, "High-efficiency (19%) screen-printed textured cells on low-resistivity float-zone silicon with high sheet-resistance emitters", *Prog. Photovolt: Res. Appl*, Vol. 14, pp. 135–144.

[22] Jellet, W. et al. 2008, "The effect of Boron diffusions on the defect density and recombination at the (111) silicon-silicon oxide interface", *Appl. Phys. Lett*, Vol. 92, p. 122109.

[23] Phang, S.P. & Macdonald, D. 2010, "Boron, phosphorus and aluminium gettering of iron in crystalline silicon: Experiments and modelling", *Proc. 35th IEEE PVSC*, Honolulu, Hawaii, USA, pp. 352–356.

[24] Bultman, J. et al. 2010, "Methods of emitter formation for crystalline silicon solar cells", *Photovoltaics International*, Vol. 8, pp. 69–80.

[25] a) Benick J., Bateman, N. & Hermle, M. 2010, "Very low emitter saturation current densities on ion implanted Boron emitters", *Proc. 25th EU PVSEC*, Valencia, Spain, pp. 1169–1173;
b) Janssens, T. et al. 2010, "Implantation for an excellent definition of doping profiles in Si solar cells", *ibid.* pp. 1179–1181.

[26] Cuevas, A. 2005, "The early history of bifacial solar cells", *Proc. 20th EU PVSEC*, Barcelona, Spain, pp. 801–805.

[27] Campbell, M.P. et al. 2007, "High-efficiency back contact solar cells and application", *Proc. 20th EU PVSEC*, Milan, Italy, pp. 976–979.

[28] Fossum, J.G. & Burgess, E.L. 1978, "High-efficiency p^+-n-n^+ back-surface-field solar cells", *Appl. Phys. Lett.*, Vol. 33, pp. 238–240.

[29] Hoces, I. et al. 2010, "Fully industrial bifacial solar cells with selective emitters", *Proc. 25th EU PVSEC*, Valencia, Spain, pp. 1974–1977.

[30] Buck, T. et al., 2006, "Industrial screen printed n-type Silicon solar cells with front Boron emitter and efficiencies exceeding 17%", *Proc. 21st EU PVSEC*, Dresden, Germany, pp. 1264–1267.

[31] Veschetti, Y. et al. 2010, "High efficiency n-type silicon solar cells with novel diffusion technique for emitter formation", *Proc. 25th EU PVSEC*, Valencia, Spain, pp. 2241–2244.

[32] Burgers, A.R. et al. 2010, "19% efficient n-type Si solar cells made in pilot production", *Proc. 25th EU PVSEC*, Valencia, Spain, pp. 1106–1109.

[33] Yingli press release Oct 20, 2010.

[34] Yingli press release Feb 18, 2011.

[35] Suniva press release Feb 15, 2011.

[36] Benick, J. et al. 2009, "High efficiency n-type silicon solar cells with front side Boron emitter", *Proc. 14th EU PVSEC*, Hamburg, Germany.

[37] Suwito, D. et al. 2010, "Industrially Feasible Rear Passivation and Contacting Scheme for High-Efficiency n-Type Solar Cells Yielding a V_{oc} of 700mV", *IEEE Trans. Electron Devices,* Vol. 57, pp. 2032.

[38] a) Green, M. 1986, *Solar Cells*, UNSW Press, Section 4.8.
b) Aberle, A. 1999, *Crystalline Silicon Solar Cells, Advanced Surface Passivation and Analysis*, University of New South Wales, Section 3.1.2.

[39] Münzer, K.A. et al., 2006, "Over 18% industrial screen printed silicon solar cells", *Proc. 21st EU PVSEC*, Dresden, Germany, pp. 538–543.

[40] Meier, D.L. et al. 2001, "Aluminium alloy back p-n junction dendritic web silicon solar cell", *Solar Energy Materials & Solar Cells*, Vol. 65, pp. 621–627.

[41] Cuevas, A. et al. 2003, "Back junction solar cells on n-type multicrystalline and Cz silicon wafers", *Proc. 3rd WCPEC*, Osaka, Japan, pp. 963–966.

[42] Veschetti, F. et al. 2010, "High efficiency solar cells by optimization of front surface passivation on n-type high efficiency solar cells by optimization of front surface passivation on n-type rear Al alloyed emitter structure", *Proc. 25th EU PVSEC*, Valencia, Spain pp. 2265–2267.

[43] Bock, R. et al. 2010, "N-type Cz silicon solar cells with screen-printed aluminium-alloyed rear emitter", *Proc. 25th EU PVSEC*, Valencia, Spain, pp. 1449–1452.

[44] Kopecek, R. et al. 2010, "Aluminium rear emitter large area n-type Cz-Si solar cells for industrial application", *Proc. 25th EU PVSEC*, Valencia, Spain, pp. 2381–2386.

[45] Book, F. et al. 2010, "Large area n-type silicon solar cells with selective front surface field and screen printed aluminium-alloyed rear emitter", *Proc. 25th EU PVSEC*, Valencia, Spain, pp. 1465–1468.

[46] Schmiga, C. et al. 2010 "Aluminium-doped p+ silicon for rear emitters and back surface fields: results and potentials of industrial n- and p-type solar cells", *Proc. 25th EU PVSEC*, Valencia, Spain, pp. 1163–1168.

[47] Schneider, A., Rubin, L. & Rubin, G. 2006, "The Day4 electrode - a new metallization approach towards higher solar cell and module efficiencies", *Proc. 21st EU PVSEC*, Dresden, Germany, pp. 230–233.

[48] Bock, R. et al. 2010, *Appl. Phys. Lett.*, Vol. 96. No. 263507.

[49] Rohatgi, A. & Meier, D. 2010, "Developing novel low-cost, high-throughput processing techniques for 20%-efficient monocrystalline silicon solar cells", *Photovoltaics International,* Vol. 10, pp. 87–93.

[50] Lamers, M. et al. 2011, "Metal-wrap-through mc-Si cells resulting in module efficiency of 17.0%", *Prog. Photovolt: Res. Appl.*, Vol. 19, Issue 3.

[51] Van Kerschaver, E. & Beaucarne, G. 2006, "Back-contact Solar Cells: A Review", *Prog. Photovolt: Res. Appl.* Vol. 14, pp. 107–123.

[52] Harder, N.-P. et al. 2009, "Laser-processed high-efficiency silicon RISE-EWT solar cells and characterisation", *Physica Status Solidi C,* Vol. 6, pp. 736–743.

[53] Guillevin, N. et al., 2010, "High efficiency n-type metal wrap through Si solar cells for low-cost industrial production", *Proc. 25th EU PVSEC*, Valencia, Spain, pp. 1429–1431.

[54] Granek, F. et al. 2009, "Enhanced Lateral Current Transport Via the Front Nþ Diffused Layer of N-type High-efficiency Back-junction Back-contact Silicon Solar Cells", *Prog. Photovolt: Res. Appl.*, Vol. 17, pp. 47–56.

[55] Engelhart, P. et al. 2007, "Laser Structuring for Back Junction Silicon Solar Cells", *Prog. Photovolt: Res. Appl.* Vol. 15, pp. 237-243.

[56] Gong, C. et al. 2010, "High efficient n-type interdigitated back contact silicon solar cells with screen-printed Al-alloyed emitter", *Proc. 35th IEEE PVSC*, Honolulu, Hawaii, USA, pp. 3145–3148.

[57] Bock, R. et al. 2010, "Back-junction back-contact n-type silicon solar cells with screen-printed aluminium-alloyed emitter", *Appl. Phys. Lett.* Vol. 96, No. 263507.

[58] Castaño, F.J. et al. 2011, "Industrially feasible >19% efficiency IBC cells for pilot line processing", *Proc. 36th IEEE PVSC*, Seattle, Washington, USA.

[59] Guillevin, N. et al. 2011, "Development towards 20% efficient n-type Si MWT solar cells for low-cost industrial production", *1st International Conference on Silicon Photovoltaics*, Freiburg, Germany.

About the Authors

L.J (Bart) Geerligs is a researcher at ECN Solar. He holds a Ph.D. from Delft University of Technology for research on nanoscale quantum electronic devices and has been at ECN Solar since 2000. Since 2003 he has been involved in the development of n-base silicon solar cells, including silicon heterojunction technology, and occasionally also in scientific research on n-type doped silicon.

Ingrid G. Romijn studied physics at the Leiden University where she received her Ph.D. on metal-insulator transitions in conducting polymers and composite materials. She joined the ECN-Solar group in 2004, where she started working as a researcher on passivating (SiN_x) layers. At present her work focuses on new solar cell concepts.

Nicolas Guillevin is a researcher at ECN Solar in the device architecture and integration group. He joined ECN in 2007, where he started his research activities on development of n-type base silicon solar cells. He studied at the National Engineering School of Industrial Ceramics in Limoges (France) where he received a Master degree in the field of material science and processes.

Enquiries

ECN Solar Energy, Westerduinweg 3,
1755 LE Petten, The Netherlands,
Tel: +31 22456 4761
Email: solar@ecn.nl
Web: www.ecn.nl

Monitoring and controlling possibilities in wet chemical etching processes for c-Si solar cell production

Jochen Rentsch, Katrin Birmann, Tobias Dannenberg, Jan Nievendick, Antje Oltersdorf & Martin Zimmer,
Fraunhofer Institute for Solar Energy Systems (ISE), Freiburg, Germany

ABSTRACT

Quality assurance and process control are becoming increasingly important in the industrial production chain to the manufacturing of silicon solar cells. There are a number of relevant wet chemical processes for the fabrication of standard screen-printed industrial solar cells, mainly for texturization and cleaning purposes. While one-component systems like pure HF for oxide-removal are easy to monitor, i.e., by conductivity measurements, typical texturization processes are much more complex due to the number of constituents.

For acidic texturization of multicrystalline silicon wafers, typical mixtures involve amounts of hydrofluoric acid (HF), nitric acid (HNO_3) and water. It has also been documented that mixtures can be found where additional additives like phosphoric acid (H_3PO_4), acetic acid (HOAc) and sulphuric acid (H_2SO_4) have been used [1, 2]. In alkaline random pyramid texturization for monocrystalline wafers, a base like potassium hydroxide (KOH) or sodium hydroxide (NaOH) and organic additives like 2-propanol (IPA) are used [3]. In addition to these processes, recently developed high-efficiency cell concepts require several additional wet chemical process steps like advanced cleaning processes, chemical edge isolation or single side oxide removal processes [4].

In order to obtain continuously stable and reproducible process results and to overcome process operations based on operator experience, a reliable monitoring of the bath concentrations is essential. Such quality control has the potential for significant cost reductions due to optimized durations between replacements of bath mixtures or shortening of processing times. In this context, the application of on-line analytical methods, either by means of chemical, optical or electrical measurement techniques, is of particular interest.

Introduction

Wet chemical etching processes represent standard procedures in modern batch or inline-based production lines for crystalline silicon solar cells. However, continuous and accurate process monitoring is still not widely used, while physically measurable parameters like temperatures, gas flows or process pressures are continuously measured.

Similar to other relevant production steps, significant cost reduction might be achieved by continuous process monitoring resulting in:

- an increase in process quality and stability which results in an increased overall production yield; and
- optimized durations between replacements of bath mixtures or shortening of processing times.

Process monitoring in the case of wet chemical processes necessitates the use of inline (or even online) bath analysis methods, which would overcome modern typical operation based on operator experience. As an example of the importance of an elaborate process control, chemical consumption data for a typical acidic texturing process can be taken; assuming an average industrial bath operating time of around 80h, the amount of dosed HF and HNO_3 during that time period accumulates to a factor of 10 to 15 higher than the original amount of HF and HNO_3 used for the fresh bath make-up. These figures demonstrate that basically the overall process performance is mainly driven by an accurate dosing of the consumed chemicals and therefore their exact determination is of great importance.

Additionally, from a more scientific point of view, a better understanding of the underlying mechanisms especially for the texturing processes could be achieved, which will ultimately support further process optimization.

> "Continuous and accurate process monitoring is still not widely used."

Only a few applications exist for process monitoring, already exist, mainly for the alkaline or acidic texturing processes, an overview is given in Table 1. Titration is a very robust and widely used method for the determination of acids and bases, but also allows the concentrations of oxidizing agents like hydrogen peroxide are measurable [5, 6]. Maintenance and calibration costs are quite low, since most of the used stock solutions are commercially available. The measurement cycle is in the range of 10 to 15 minutes. A constraint for the usage of the titration is the limited number of components that can be detected simultaneously. For example, the acidic texturization involves the inclusion of additional titration steps for the analysis of all components. The determination of organic components like 2-propanol is not possible.

A more fast and flexible method is chromatography, where inorganic acids and bases and organic additives are measurable, with measurement cycles are commonly shorter than 10 minutes [7]. Commercially available high-end equipment has a high automation level, which reduces the running costs to a minimum.

A real inline system is shown via NIR spectroscopy [8]. Since NIR spectroscopy is a non-selective method, interactions between the measured components as well as the influence of varying temperatures have to be included into the calibration dataset. This leads to a high workload for the calibration, but calibration models for most purposes in photovoltaic industries are commercially available. After setting up a calibration model, there is very little need for further maintenance. Modern FT-NIR (Fourier Transform) instruments reach a measurement cycle of 30 seconds so that NIR-spectroscopy enables a real-time process control.

For surface active components like 2-propanol, determination of the air-to-

	Detectable species in acidic etching mixtures	Detectable species in alkaline etching mixtures
Titration	HF, HNO_3, H_2SiF_6 [Henßge 2007] / [Weinreich 2007]	KOH, $K_2Si(OH)_2O_2$, K_2CO_3 [Grosvenor 1982]
HPLC/IC	HF, HNO_3, H_2SiF_6, HNO_2	2-Propanol
Surface tension		2-Propanol
NIR-Spectroscopy	HF, HNO_3, H_2SiF_6, HNO_2* *addition of UV/Vis channel	KOH, $K_2Si(OH)_2O_2$, 2-Propanol

Table 1. Overview of existing inline/online analysis techniques for wet chemical process baths.

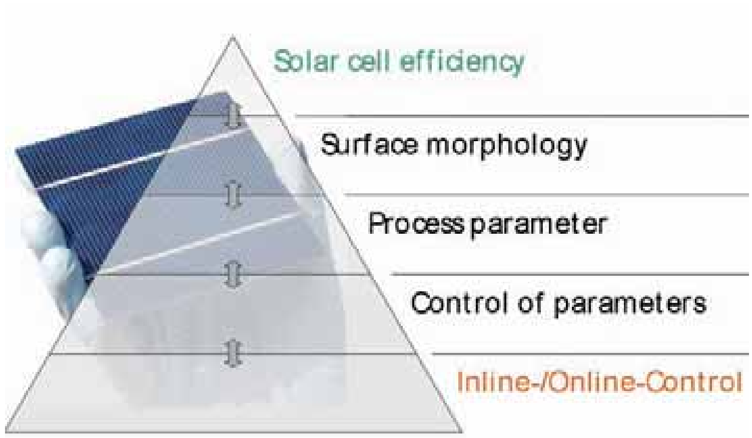

Figure 1. Overview of measurement categories for complete analysis of wet chemically textured silicon surfaces. The different techniques can be carried out either by means of inline or offline measurement tools.

liquid surface tension represents a viable measurement method [9].

In order to establish a closed-loop process control methodology, all relevant interdependencies between chemical bath compositions and effects on the final solar cell performance, have to be determined. Fig. 1 represents the step-by-step methodology for final optimization of the solar cell's output performance, which is based on an exact inline/online control of the most important process parameters. Such a procedure is principally transferable to any kind of technology step; in our study we applied this approach to wet chemical texturing processes. In order to reach an optimized texturing process, first of all the most suitable surface morphology of the designated surface texture has to be determined. This includes structural information about the resulting surfaces (reflectance, feature homogeneity and sizes, roughness) as well as information on the resulting electrical quality of the surfaces. All relevant process parameters (e.g. concentrations, process time, temperature, etc.) influencing the final surface morphology need to be identified and control strategies for these parameters need to be defined. For continuous process control in modern production lines, especially online measurement, techniques are of special interest. When measuring the chemical bath components, inline chromatography or spectroscopic methods are usually applied. Optical control of the textured surfaces is performed by means of surface reflectance measurements or simple optical scanning of the wafer surface. Electrical analysis involves either lifetime measurements of the textured surfaces (typically only local information) or camera-based analysis techniques like PL (photoluminescence) imaging [10].

In the following sections we will focus on inline/online control possibilities of the main bath components for alkaline and acidic texturing processes, and will discuss how concentration variations influence the final texturing result.

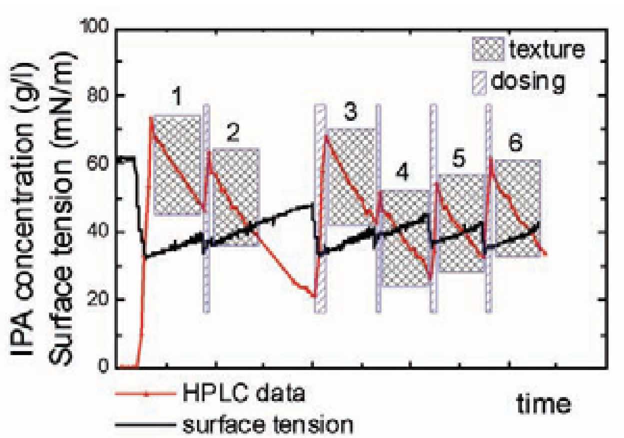

Figure 2. IPA concentration analyzed online by HPLC and surface tension in alkaline texturing solution during six texturing runs with incorrect IPA redosing amount.

Alkaline texturing process

Alkaline etching with sodium hydroxide (NaOH) or potassium hydroxide (KOH) has different etch rates for different crystallographic orientations. Hence this anisotropy results in small pyramids with a square base randomly distributed over the wafer surface for monocrystalline silicon wafers with <100> orientation. To improve the lateral uniformity and the anisotropy of the etching process, isopropyl alcohol (IPA) is added to the etching solution. After texturing the wafers are typically cleaned in hydrochloric (HCl) and hydrofluoric (HF) acid with intermediate rinsing in DI water. Alkaline texturing is typically performed within batch processes, where wafers are held in carriers that allow chemicals to wet the entire surface. For standard process control, the carriers are weighed before and after etching to determine an average etching depth. Typical process temperatures range between 70 and 80°C, which is close to the boiling point of the IPA (82°C). Constant evaporation of IPA occurs during the etching process, which represents a major process uncertainty and results in the need for regular redosing. In order to simplify the redosing of the additive and to get a higher reproducibility of the initial IPA concentration, it should be measured and controlled.

The concentration of organic molecules like alcohols in aqueous solutions can be analyzed by high-performance liquid chromatography (HPLC). The IPA concentration of an alkaline wet chemical bath used during a solar cell process can be measured directly without dilution by HPLC. The alkaline sample is separated while IPA is retarded and the inorganic components are accelerated compared to water. The IPA peak area is used to relate to the IPA concentration.

IPA is a surface active compound which lowers the surface tension of air in the liquid. When surface tension and IPA concentration of the bath solution are measured during a texturing process, the surface tension follows the IPA concentration reciprocally proportionally. The surface tension of an alkaline texturing bath solution increases with decreasing IPA concentration. The decreases in IPA concentration can be seen in Fig. 2 as the surface tension increases during a texturization process [9].

"The evaporation rate depends not only on the concentration but also on the etch rate."

In order to reach the initial IPA concentration, the IPA has to be redosed. Different dosing amounts were tested. The IPA redosing is lower for run four than for run six in Fig. 2, resulting in a lower IPA concentration. As the incorrect amount of IPA is redosed, the initial IPA concentration is different for different runs. The reflection of KOH/IPA textured wafers is usually high as the surface tension of the etching solution and the etch rate are also high. However if the correlation between IPA concentration and surface tension are known, the exact amount of IPA can be dosed while knowing the actual surface tension. The initial IPA concentration can be reached for several runs as IPA is redosed in the correct amount (Fig. 3, run two to six). The target concentration was the initial IPA concentration of run two. The IPA bath condition is well reproducible for several runs (Fig. 3).

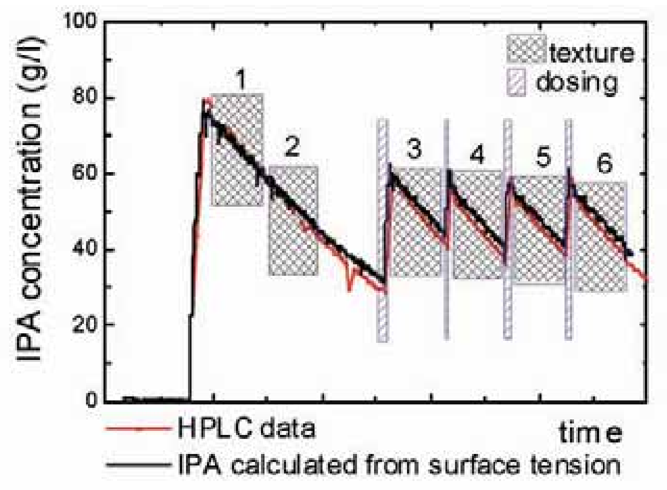

Figure 3. IPA concentration analyzed by HPLC and IPA concentration calculated from surface tension in alkaline texturing solution with correct IPA dosing.

Rather than redosing per run, redosing per time is also possible. As the time in between redosing gets shorter, the IPA concentration stays constant or increases because the evaporated IPA is replaced; however it is difficult to dose IPA accurately without a real online control parameter. The evaporation rate depends not only on the concentration but also on the etch rate. This means that a wrong redosing leads to high concentration variations. Therefore an IPA redosing was developed that was dependent on the surface tension (Fig. 4) [9]. The IPA dosing is controlled by a proportional-

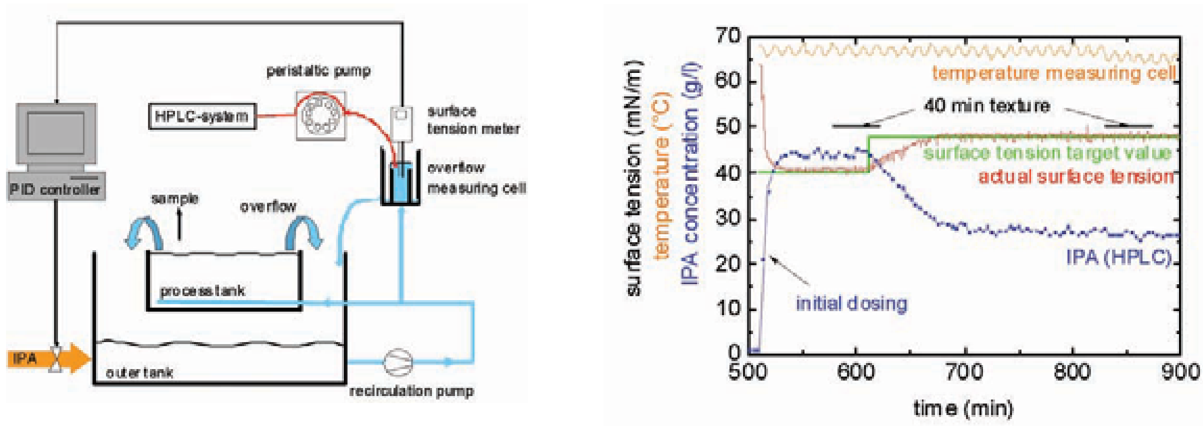

Figure 4. Surface tension measurement set-up. Right: HPLC as reference measurement.

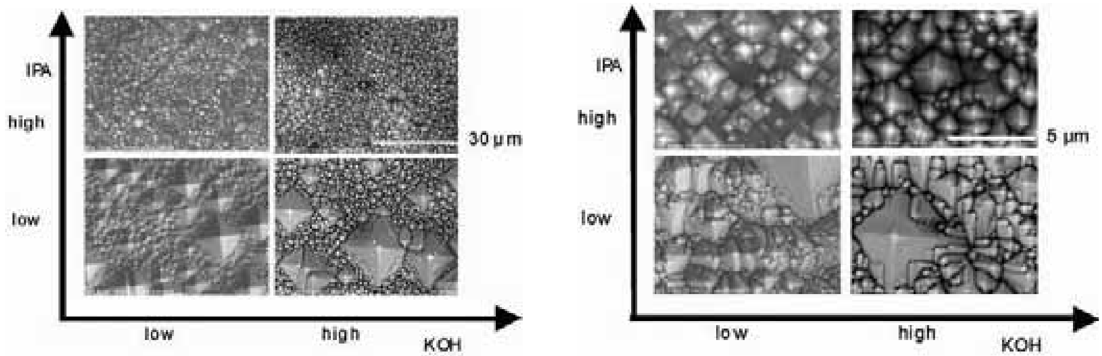

Figure 5. Pyramids on initially saw-damage etched wafers in SEM (1.8k left picture, 11k right picture). These wafers resulted from low and high KOH and IPA in bath solution and were textured at constant IPA concentration (75°C, 40 min).

integral-derivative (PID) controller, reading a constant IPA level during a texturing process as shown by the HPLC data in Fig 4. When the surface tension target value was changed to a higher value, the dosing stops until the actual surface tension value corresponds to the target surface tension.

The following texturization results were obtained using the IPA controller for a constant IPA concentration in the bath solution. Different KOH and IPA levels during texturization reveal different textured surfaces (Fig. 5). A low IPA concentration level leads to small pyramids with a few big pyramids in between. A low KOH concentration in the bath solution coupled with a high constant IPA concentration results in some flat pyramids and a high weighted reflection of the wafer surface is high (ca. 25%, Fig. 5, right).

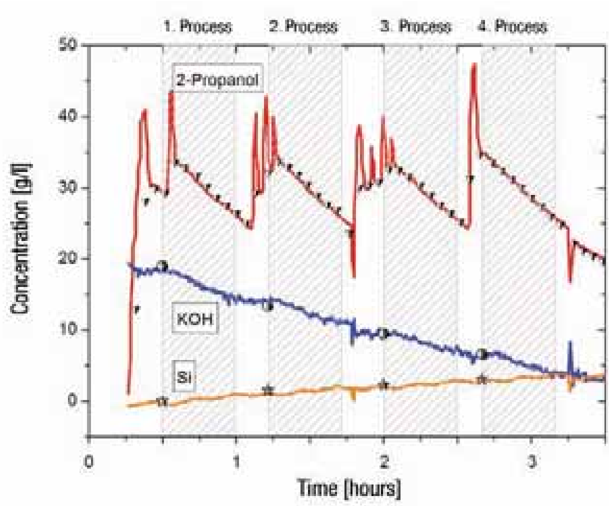

Figure 6. Concentration development measured with NIR spectroscopy in the alkaline texturization bath during the texturization of four batches with 100 wafers each. Reference measurements were done with titration (KOH, Si) and HPLC (isopropanol).

The flat parts between the pyramids lead to this high reflection. For a high KOH concentration, the standard deviation of the height data taken from confocal microscope pictures is higher than for low KOH concentration (2.0μm vs. 1.6μm). A high KOH and IPA concentration results in more homogeneous pyramids sizes. The pyramids on the textured wafer surface are relatively small (< 5μm wide and < 3μm high, Fig. 5, right).

In order to control all components of the alkaline etching bath with one measurement method, an NIR spectroscopy model has been developed for this process [11]. In contrast to most inorganic components like KOH, IPA has a separate –CH-group with separate vibration modes, which enables a very precise calibration for this component [16]. The model was created in a temperature range from 60°C up to 80°C under laboratory conditions. The transfer to the process tool required an offset for IPA and silicate as well as a slope and bias adjustment for the KOH concentration.

The IPA concentration measured with NIR spectroscopy shows the expected good correlation with the IPA concentration from the online HPLC-measurements. The concentration increases in the beginning of the process due to the initial IPA dosing and

decreases during the process to a level of 70% of the initial concentration (Fig. 6).

Acidic texturing process

Acidic texturization, as an isotropic process, does not depend on the crystallographic orientation and thus is most suitable for multicrystalline silicon. Typically, a solution of HF, HNO_3 and water is used on an industrial scale either in batch or inline type production equipment. For the more common inline application, the wafers move horizontally on rolls through different tanks. A typical sequence involves the texturing itself, lowly concentrated KOH for porous silicon removal, HCl and HF clean and air drying, between chemical treatments. Spray rinses are used to minimize cross-contamination and to stop chemical reactions.

The concentrations of HF, HNO_3 and H_2SiF_6 are accessible by titration in two steps. The first step is an acid-base titration, which delivers the total acid amount as well as the concentration of dissolved silicon. This is followed by a precipitation titration. The concentrations of free HF and HNO_3 are calculated from the total fluoride concentration, the total acid concentration and the dissolved silicon. The detection of dissolved N(III)-species is not possible.

A more flexible measurement technique for the analysis of components in acidic texturization baths is ion chromatography. After the separation of the ionic species in the chromatographical column, fluoride, nitrate and nitride ions are measured in a conductivity channel; the detection of dissolved silicon is not possible by conductivity measurement. Therefore a post-column derivatization with sodium molybdate was used in order to form a yellow reaction product that can be measured in a UV/Vis-detector.

An advantage of ion chromatography in contrast to titration is the ability to monitor the concentration of N(III)-species. A detection of these species is also possible with spectroscopic methods, when the instrument allows an extension to the UV/Vis range, where the nitrogen oxides occur in the range of 340nm–400nm.

Near-infrared (NIR) spectroscopy is a suitable method for the concentration monitoring of acidic texturization baths. The method is based on the observation of overtone and combination vibration bands of water. The position as well as the shape of these bands is influenced by the temperature and by the presence and concentration of ionic species like HF, HNO_3 and H_2SiF_6.

A partial least squares (PLS) model was built for the determination of the HF-, HNO_3 and H_2SiF_6 concentration. The measurement accuracy of the model was estimated from a cross validation. The standard error of validation was 1.8g/l for HF, 3.5g/l for HNO_3 and 1.8g/l for H_2SiF_6. This model was used to determine the bath composition of the acidic texturization bath twice a minute.

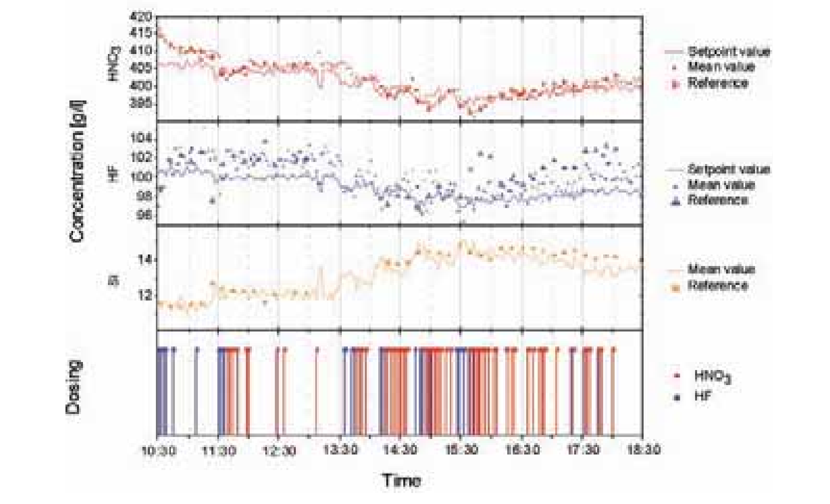

Figure 7. Inline processing of 736 mc-Si wafers with a total amount of 812g silicon etched. Dosing volumes were determined as 500ml HF and 250ml HNO_3 per dosing step. References were realized by inline ion chromatography.

The control algorithm was written in LabVIEW and the communication to the FT-NIR spectrometer was achieved via OPC protocol. The dosing events were transferred to the PLC of the process tool via an optocoupler interface card. A rising edge on the PLC triggers the dosing of a variable volume of the selected chemistry. The PLC responds a signal indicating the business of the dosing unit.

The used NIR model was validated with reference measurements achieved by inline ion chromatography. Over a time period of one week, a slight change in the offset was observed, which necessitated a further optimization of the NIR hardware. The developed dosing algorithm was used to control the concentrations of HF and HNO_3 in dependence of the etched silicon amount over one process day (Fig. 7). The algorithm was able to stabilize concentrations the resulting in a deviation of the etching rate of only 2% relative.

The main influencing parameters on the texturization quality are the educt concentrations as well as the concentration of the hexafluorosilicic acid (H_2SiF_6) that is generated during the etching process. H_2SiF_6 is an acid that enlarges the oxidation potential of HNO_3 by moving the chemical equilibrium between N_2O_3 and NO^+ towards the nitrosyl cation. H_2SiF_6 also etches silicon dioxide, leading to the conclusion that the increasing

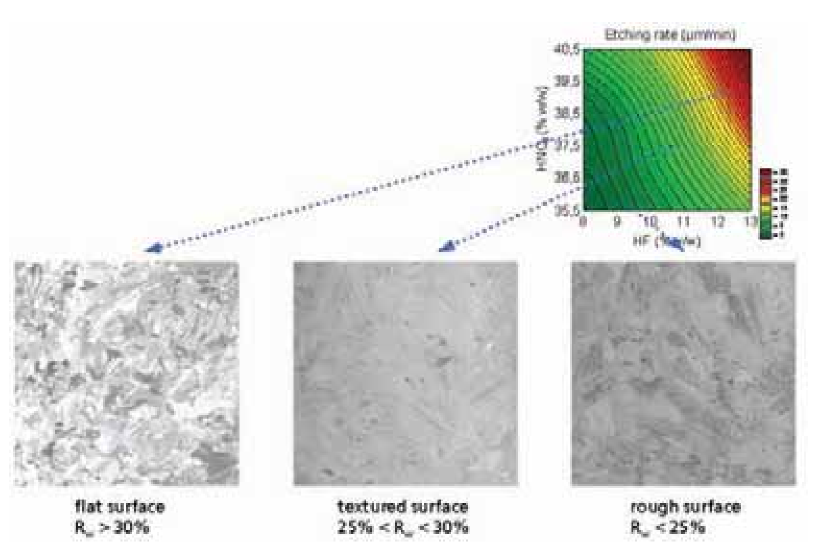

Figure 8. Correlation between total acid concentration, resulting etch rates and surface morphologies. High acid concentrations result in flat, more polished surface structures, whereas lower acid concentrations result in a surface roughening with preferential etching of crystal defects.

concentration of H_2SiF_6 has to be compensated by a decrease of the HF- and HNO_3 concentration (Fig. 7).

Too high an acid concentration leads to a smooth surface with a high reflectance, while too low concentrations result in very rough surfaces that are difficult to passivate. A reason for the low efficiencies at low reflection might be the presence of etch attacks at grain boundaries (GBs), which tend to occur strongly, under the etching conditions that are needed for a low reflecting texture. Due to these etch attacks, v-shaped trenches are formed at GBs. These trench structures are barely deeper than ordinary etch cavities, but they are very steep, while still being narrow (ca. 3µm). Because of the steepness of their facets, incident light is reflected to the opposite side leading to another chance for absorption (double-bounce effect). Therefore, trench structures appear as dark lines on the wafer surface; on a macroscopic scale, these lines appear in ball-of-wool-like clusters.

Trench structures are more preferably formed at a low etch rate than at a high etch rate. Therefore one possibility for reducing the fraction of the surface area covered by trench structures is to implement an accurate control of the etch activity, e.g. etch rate, of the texturing bath.

The appearance of trench structures on the wafer surface has been mentioned in earlier publications and is often recognized as harmful to solar cell performance. Trench structures could lead to shunts after firing as the passivation-layer inside them is thinner. Furthermore, the solar cell surface area is enhanced by trench structures leading to more surface recombination. Wafer breakage is also increased by the appearance of trench structures [12]. On the other hand, trench structures offer an impressive reduction of surface reflection which might compensate some of their negative effects.

A method for in-line measurement of preferred grain boundary etching caused by acidic texturization (trench structures) uses a line camera to scan wafers moving on a conveyor belt [13]. The system provides the required diffuse illumination and still measures sharp and contrast-rich images [14].

The number of trench structures on these images is quantified by a newly developed automatic algorithm (Fig. 9, left). The algorithm uses a threshold value to distinguish trench structures from the surrounding texture. All pixels that have a grey value below the threshold value are counted as trench structures, the other pixels as texture. As the threshold value is linearly dependant on the wafer reflection/ brightness, it had to be determined via an appropriate calibration with a set of texturized wafers.

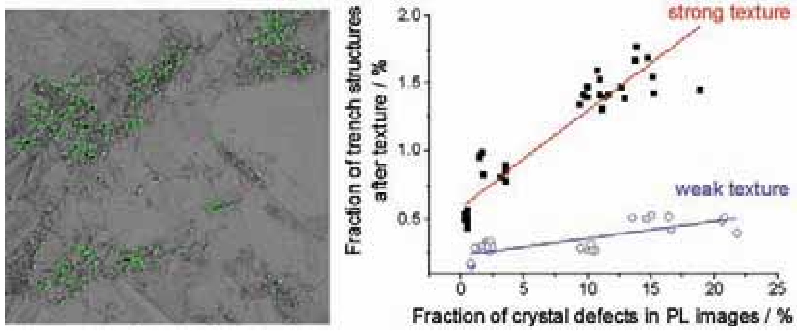

Figure 9. Left: Marked rift structures determined by a colour vision system on a textured multicyrstalline silicon wafer. Right: Relation between material quality and texture: the fraction of rift structure area f_R on the wafer surface as well as the fraction of crystal defect area determined by as-cut photoluminescence images has been quantified using a newly developed algorithm.

By regarding the measurement method in detail, it could be shown that the true area fraction of trench structures (*fT*) only lies between 0.3 and 1.8%. This is only 15% of the value expected from looking at the wafer or from camera images. The size of trench structure areas seems to broaden because the camera system has a much lower resolution (a pixel has a length of 130µm) than the width of trench structures (<5µm). The measurement method, as well as the algorithm, were tested by measuring *fT* for 150 multicrystalline wafers with a broad variety in the number of trench structures and comparing the results to manually obtained results. The variety in the number of trench structures was obtained by choosing wafers representing a typical cross-section of industrially available mc-Si materials and texturizing them with two different textures: an acidic texture with strong etch attacks and an acidic texture with weak etch attacks. The number of trench structures strongly depends on the number of crystal defects in as-cut wafers and on the texture strength (Fig. 9, right). The fact that the expected correlation could be reproduced well indicates the viability of the measurement method.

The strong dependence of *fT* on material quality and texture strength indicates that the number of trench structures can be reduced by choosing an appropriate texture, e.g. an adjustment of the chemical concentrations. If trench structures are as harmful as reported, their prevention could result in an increase in solar cell efficiency.

Conclusion

An online process control of acidic and alkaline wet chemical texturization processes was successfully demonstrated with different analysis methods. In the case of alkaline texturing processes, the online bath control was directly utilized to control the dosing of 2-propanol during the process. By stabilizing the 2-propanol concentration, more homogeneous pyramidal surface structures as well as a higher process-to-process reproducibility was achieved.

In the case of acidic texturing processes, either inline ion-chromatography or near-infrared spectroscopy might be used for online bath control. Beside the accurate control of the chemical concentrations, optical as well as electrical analysis of the resulting surface morphologies is necessary in order to obtain an optimized texturing process. Depending on the original material quality (especially the appearance of crystal defects), the etching solution has to be adjusted to avoid the formation of rift structures. A closed-loop process control therefore necessitates the material analysis by means of photoluminescence imaging prior to the texturization process and the control of the chemical components during, as well as an optical analysis of the resulting surfaces after, the process itself.

References

[1] Nishimoto, Y., Ishihara, T. & Namba, K. 1999, "Investigation of acidic texturization for multicrystalline silicon solar cells", *Journal of the Electrochemical Society*, Vol. 146, No. 2, pp. 457–61.

[2] de Wolf, S. et al. 2000, "Towards industrial application of isotropic texturing for multi-crystalline silicon solar cells", *Proc. 16th EU PVSEC*, James & James, London & Glasgow UK.

[3] Vazsonyi, E. et al. 1999, "Improved anisotropic etching process for industrial texturing of silicon solar cells". *Solar Energy Materials and Solar Cells* Vol. 57, No.2, pp. 179–88.

[4] Rentsch, J. et al. 2009 "Wet chemical processing for C-Si solar cells – status and perspectives", *Proc. 24th EU PVSEC*, Hamburg, Germany.

[5] Henßge, A. & Acker, J. 2007, "Chemical analysis of acidic silicon etch solutions I. Tritrimetric

determination of HNO_3, HF, and H_2SiF_6", *Talanta*, Vol. 73, pp. 220–6.
[6] Weinreich, W., Acker, J. & Gräber, I. 2007, "Determination of total fluoride in HF/HNO_3/H_2SiF_6 etch solutions by new potentiometric titration methods", *Talanta*, Vol. 71, No. 5, pp. 1901–5.
[7] Oltersdorf, A. et al. 2008, "Analytical research of the acid etching bath by ion chromatography", *Proc. 23rd EU PVSEC*, Valencia, Spain.
[8] Zimmer, M. et al. 2008, "Spectroscopical inline analysis of wet chemical processes", *Proc. 23rd EU PVSEC*, Valencia, Spain.
[9] Birmann, K., Zimmer, M. & Rentsch, J. 2009, "Controlling the surface tension of alkaline etching solutions", *Proc. 24th EU PVSEC*, Hamburg, Germany.
[10] Glatthaar, M., et al. 2010 "Luminescence imaging for quantitative solar cell material and process characterization", *Proc. 25th EU PVSEC*, Valencia, Spain.
[11] Zimmer, M. et al. 2009, "Nir-spectroscopical process control for wet chemical processes", *Proc. 24th EU PVSEC*, Hamburg, Germany.
[12] Mathijssen, S. et al. 2009, "Survey of acid texturing and new innovative acid processes for mc solar wafers", *Proc. 24th EU PVSEC*, Hamburg, Germany.
[13] Krieg, A., Wallach, J & Rein, S. 2009, "Impact of surface structures on the inline vision inspection of antireflection coatings", *Proc. 24th EU PVSEC*, Hamburg, Germany.
[14] Korte, L., Bastide, S. & Lévy-Clément, C. 2008, "Fast measurements of effective optical reflectivity using a conventional flatbed scanner", *Proc. 23rd EU PVSEC*, Valencia, Spain.
[15] Haunschild, J. et al. 2010, "Quality control of as-cut multicrystalline silicon wafers using photoluminescence imaging for solar cell production", *Solar Energy Materials & Solar Cells*, Vol. 94, No. 12, pp. 2007–12.
[16] Zimmer, et al. 2010, "Online process control of alkaline texturing baths with near-infrared spectroscopy", *Vibrational Spectroscopy*, Vol. 53, pp. 269–273.

About the Authors

Jochen Rentsch is head of the wet chemical and plasma technologies/ process transfer department at Fraunhofer ISE. In 2005 he received his Ph.D. in physics from Albert-Ludwig's-University of Freiburg, Germany. Current research activities at Fraunhofer ISE focus on innovative wet chemical- and plasma technologies and their application for industrial solar cell processing.

Katrin Birmann studied geoecology and process engineering at TU Bergakademie Freiburg. She worked at Fraunhofer ISE for her diploma thesis in the field of alkaline texturing and its analytics. She is now focusing on wet chemical processes at ISE.

Tobias Dannenberg worked on his diploma thesis at Fraunhofer ISE in 2010. He graduated with a degree in environmental engineering from the Hamburg University of Applied Sciences (HAW). He works at Fraunhofer ISE on automation and analytical control of wet-chemical processes.

Jan Nievendick has a diploma in chemistry from the Philipps-University, Marburg, specializing in theoretical and physical chemistry. He joined Fraunhofer ISE in 2009 and is currently pursuing a Ph.D. in the field of controlling and improving the texturing of multicrystalline silicon solar cells.

Antje Oltersdorf studied process engineering at TU Hamburg-Harburg. During her diploma thesis at Fraunhofer ISE, she investigated ion chromatographic and titration methods for acidic texturization. She is now working on her Ph.D. thesis on trace element analytics in wet chemical processes at ISE.

Martin Zimmer received his 2005 diploma in chemistry from the Ruprecht-Karl's-University, Heidelberg. He joined Fraunhofer ISE in 2006 and has just finished his Ph.D. in the field of wet chemical analysis and process development at ISE.

Enquiries

Fraunhofer-Institut für Solare Energiesysteme (ISE)
Heidenhofstr. 2,
79110 Freiburg,
Germany
Tel: +49 (0) 761 4588 5199
Email: jochen.rentsch@ise.fraunhofer.de
Web: www.ise.fraunhofer.de

Thin Film

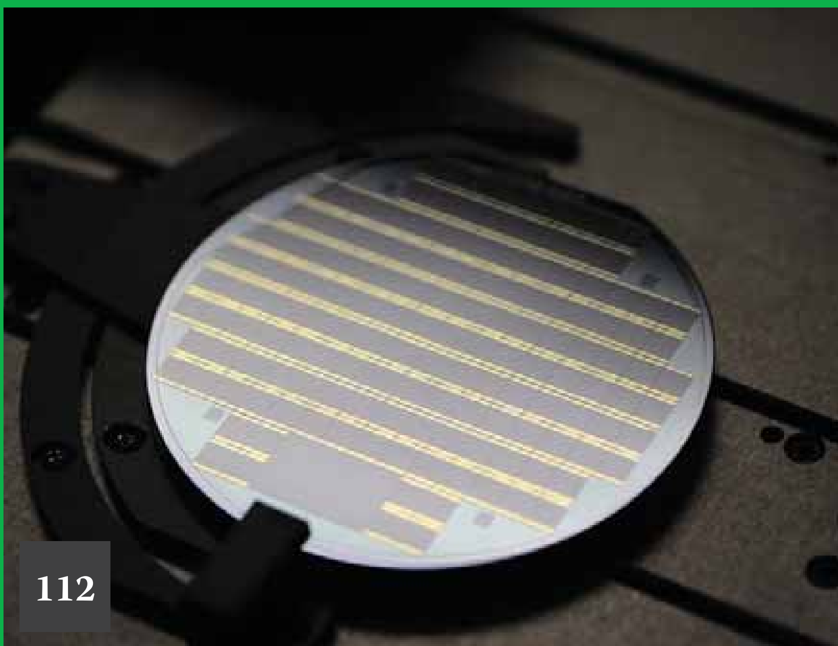

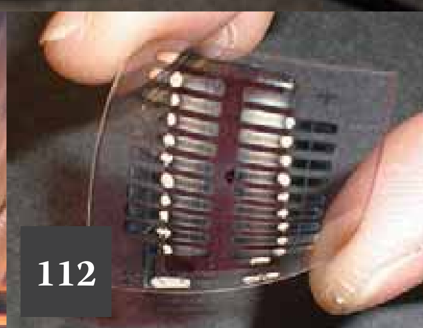

MiaSolé taps Intel for CIGS thin-film production ramp

Semiconductor market leader Intel has signed an agreement with CIGS thin-film start-up MiaSolé to help it ramp from 50MW to 150MW per annum capacity by the end of 2011. Intel's Technical Manufacturing Services practice has been awarded the contract, which includes such services as strategic consulting, operational knowledge and training to MiaSolé as well as customized manufacturing services and systems, though specifics were not disclosed.

"The engagement is part of Intel's broader strategy to partner promising high tech innovation with Intel's world class manufacturing and Copy Exactly! Methodology," noted Brian Krzanich, senior vice president and general manager of Intel's Manufacturing and Supply Chain. "This will enable companies like MiaSolé to scale to high-volume manufacturing cheaper, faster, and better."

MiaSolé is following in the footsteps of First Solar, which employed several key manufacturing experts from Intel to ramp to gigawatt scale. First Solar recently announced that its president of operations, Bruce Sohn, whom had previously been Intel's first 300mm fab manager, was leaving the company. Sohn assisted First Solar in recruiting a number of key Intel personnel as the company planned its major capacity expansions a few years ago.

Image: Miasolé

MiaSolé manufactures each of its solar modules from start to finish at its two manufacturing facilities.

Testing and Certification News Focus

NexPower obtains PAS 2050 and ISO/CD 14067-1 carbon footprint verification

Taiwan-based thin-film PV module manufacturer NexPower claims to be the first thin-film producer to receive carbon footprint verification under PAS 2050 and ISO/CD 14067-1 standards. NexPower's multi-junction PV modules were verified by DNV (Det Norske Veritas) in February 2011, a verification process that took approximately four months.

NexPower's product carbon footprint report contains data from the product's greenhouse gas emission life cycle in raw material mining, component manufacturing, parts transportation, product manufacturing and product delivery. The company's thin-film capacity stands at 120MW and NexPower reached module efficiencies of 10% in 2010.

NexPower Technology was founded by semiconductor foundry, UMC in 2005. NexPower also claims to be the first Taiwanese company to begin thin-film PV mass production and the first to attain IEC 61646, IEC 61730 certification and UL 1703 listing.

Solar Frontier's CIS modules granted UL certification

Showa Shell Sekiyu's subsidiary, Solar Frontier, revealed that its SF130 150W CIS module series has been certified by Underwriters Laboratories (UL) for sale in the Americas. UL tested the design and safety of the modules, which are suited for commercial, residential and utility-scale applications. Solar Frontier noted that its modules have previously been certified for the performance and safety by both Japanese and European standards organizations.

Image: Solar Frontier

Solar Frontier's CIS modules have recently received UL certification for sale in the Americas.

NREL confirms world-record 43.5% efficiency on Solar Junction's CPV cell

Solar Junction's concentrated photovoltaic (CPV) cell has achieved a world-record efficiency of 43.5%. The company reported that the US Department of Energy's (DOE) National Renewable Energy Laboratory (NREL) confirmed the commercial-ready production cell efficiency under their Measurement and Characterization Laboratory.

Solar Junction's 5.5mm × 5.5mm production cell received support from the DOE's PV Incubator Program and beat the current CPV cell efficiency record by 1.2%. Furthermore, the company maintains that the CPV cell's average efficiency gain is higher than that achieved by any prior record holders.

The company's CPV cell was calculated to have a peak efficiency of 43.5% at greater than 400 suns and preserved efficiency as high as 43% out to 1,000 suns. Solar Junction pointed out that over the past four years world-record CPV cell efficiencies typically saw improvements of 0.4% annually. The company's new world record comes only two months after the

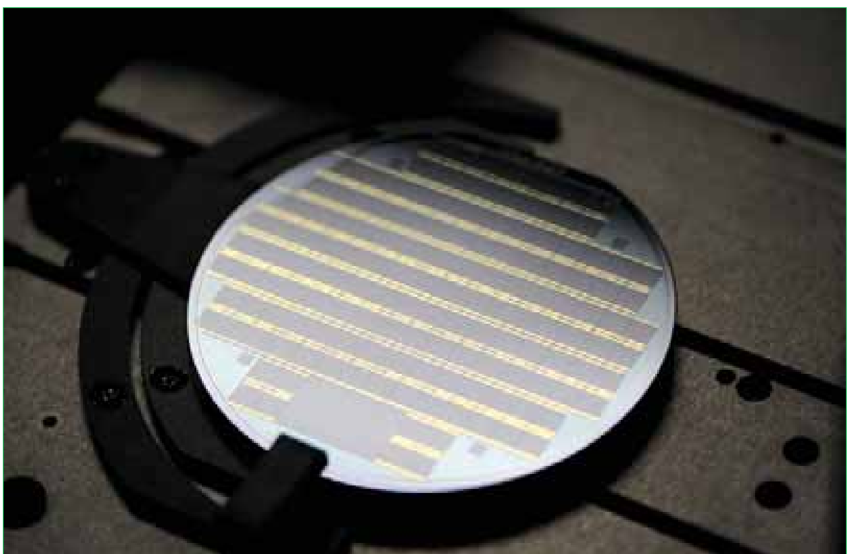

Image: SolarJunction

Solar Junction's CPV cell wafer.

NREL confirmed 41.4% efficiency under the PV Incubator program.

Inventux's silicon thin-film modules certified non-toxic and climate friendly by TÜV Rheinland

Inventux Technologies' silicon thin-film modules have been newly certified as toxic free and environmentally friendly by TÜV Rheinland, who bestowed its restriction of hazardous substances (RoHS) certificate on the company's modules. TÜV Rheinland grants the RoHS certificate after concluding that the products tested are free from toxic heavy metals such as cadmium and lead. Inventux had previously volunteered to have the European RoHS Directive and the German Electrical and Electronic Equipment Act check its modules for toxic-free conformity.

Image: SolarJunction

Inventux's X-Series Micromorph modules consist of an amorphous and a microcrystalline silicon layer.

Inventux states that it can now guarantee non-toxic, climate-friendly modules with the RoHS confirmation. Additionally, the certification also allows for the company's modules to be more easily disposed of once they reach their end of service life. Since the silicon thin-film modules are catalogued as conventional building glass, they should be able to be recycled without the need for extensive chemical processing.

Delta Energy inverter lines certified for compatibility with First Solar modules

Delta Energy Systems' inverter lines have been certified for compatibility with First Solar's latest FS-Series 2 and FS-Series 3 thin-film modules. First Solar's System Design and Application certification covers both Delta's Solivia 2.5, 3.0, 3.3 and 5.0 EU G3 string inverters and its central inverter line.

The process ensures the performance, safety and reliability of its modules is optimised when they are used in conjunction with other equipment and in varying conditions.

The Solivia string inverters can be used with the majority of module types,

Image: Delta Solivia

Delta Energy Systems' Solivia 5.0 inverter has been certified for compatibility with First Solar's latest FS-Series 2 and FS-Series 3 thin-film modules.

even with rear-side contact modules and thin-film modules that require positive or negative DC grounding.

Business News Focus

Bruce Sohn to step down as First Solar's president of operations

The man who brought semiconductor manufacturing know-how and discipline to First Solar and led the company's push to gigawatt-scale production will be moving on. Bruce Sohn, the thin-film PV firm's president of operations, left the organization effective April 30. He will not be replaced, with the current group of senior executives continuing in their roles and reporting to CEO Rob Gillette.

Sohn has played an integral role at First Solar since early in the 2000s, working as an engineering, operations, and managerial consultant and serving on the company's board from 2003-2009. After a long career at Intel, he joined the executive team in 2007 as president, and since then has been responsible for technology, operations, and supply chain for module production, as well as for the engineering, procurement, and construction and operations and maintenance groups.

Image: First Solar

Bruce Sohn, First Solar's president of operations, has left the organization.

"I am proud of what we have accomplished at First Solar so far and remain confident in the company's future," said Sohn. "Not only have we achieved our cost and manufacturing milestones, but we also have positioned a new generation of leaders to take First Solar into the next phase of growth."

As for the top-level reporting reorganization, the following executives will be running their respective units and report to Gillette: Tymen DeJong, SVP of operations; Doug Duval, VP of supply chain; Heinrich Eichermueller, SVP of plant replication; and Jim Lamon, SVP of EPC.

TSMC forms TSMC Solar subsidiary

The recently formed solar business unit of TSMC is being transferred into a wholly-owned and incorporated subsidiary to be called TSMC Solar Ltd. TSMC said in financial filings with the Taiwan Stock Exchange (TSE) that the value of its solar business unit had been pegged at NT$12.5 billion or US$433.1 million.

The semiconductor foundry also noted that the transfer to a subsidiary was intended to motivate entrepreneurship within TSMC Solar and to facilitate business specialization in order to become competitive in the PV market.

Auria Solar and Mitsubishi plan joint venture 'micromorph' thin-film PV module operations

Taiwan-based Auria Solar is in negotiations with Mitsubishi Heavy Industries (MHI) to establish a 65.3MW 'micromorph' thin-film PV module production line in Taiwan. Auria Solar originally used Oerlikon Solar's micromorph technology to establish a 60MW line in Taiwan in June 2009. The potential collaboration with MHI would include equipment and processes developed by both parties that could achieve 11% effective cell efficiencies.

Auria claims to be fabricating cell efficiencies of 10.5% (1.1m × 1.3m) and module efficiencies of 10%. Emphasis was also placed on the cost reduction benefits the partnership could bring.

Veeco partners with CNSE on DOE's SunShot initiative

The announcement by the US Department of Energy (DOE) to invest US$457 million in solar technology development under the moniker of the SunShot Advanced PV Manufacturing Partnerships Program has given the industry a welcome boost. With the recent payout to the College of Nanoscale Science and Engineering (CNSE), news has emerged that Veeco has partnered with the CNSE for technology

News

The US Department of Energy is investing US$457 million in solar technology development under the title of the SunShot Advanced PV Manufacturing Partnerships Program.

development and reduction of costs associated with CIGS technologies.

The SunShot Initiative aims to reduce the total costs of photovoltaic solar energy systems by about 75% with the ultimate goal of rendering CIGS thin film cost-competitive with other forms of energy by the end of the decade. CNSE is partnering with the US Photovoltaic Manufacturing Consortium (PVMC) which, along with California-based Bay Area PV Consortium (BAPVC) and SVTC Technologies, recently received a DOE grant of US$112.5 million for development of the technology.

Veeco's role in this effort will involve the company's contribution to the establishment of a full-scale CIGS centre enabling collaboration along the whole PV supply chain. In February, the company received a US$4.8 million DOE R&D grant to help speed its CIGS equipment development. Veeco has a small-scale pilot production line for CIGS development in Greater Albany.

OPV revenues to reach US$387 million by 2016, claims NanoMarkets report

The organic photovoltaics (OPV) industry is set to experience a near-sixfold increase in size over the next five years, according to a new report from industry analysts NanoMarkets. The report, entitled *Materials, Applications and Opportunities in Organic Photovoltaics*, claims that OPV, which is expected to generate revenues of US$56 million in 2011, will be worth US$387 million by 2016.

Since NanoMarkets issued its last report on OPV in 2010, not only has its performance efficiency been transformed but there has been a growing realisation that, as a niche technology, OPV should shift its focus towards smaller sectors in the solar industry; it is forecast that the portable power and BIPV glass sectors will account for US$250 million and US$113 million of the OPV industry by 2016.

NanoMarkets believes the interest in and growth of the sector will be facilitated by an improved supply of materials. This materials market alone will grow in size to US$200 million by 2016, with half of these revenues coming from encapsulation and substrate materials.

R&D News Focus

Oak Ridge National Lab develops 3-D nanocone solar cell with high efficiency potential

Jun Xu and his team of researchers at the Oak Ridge National Laboratory have created a 3-D nanocone-based solar cell, which is said to enhance the light-to-power conversion efficiency by almost 80%. The solar cell is constructed using n-type nanocones made from zinc oxide, which perform as the junction framework and electron conductor, and are enveloped by a p-type semiconductor consisting of polycrystalline cadmium telluride, which act as the principal photon absorber channel and hole conductor.

"To solve the entrapment problems that reduce solar cell efficiency, we created a nanocone-based solar cell, invented methods to synthesize these cells and demonstrated improved charge collection efficiency," said Xu, a member of ORNL's chemical sciences division.

Using this technology, Xu and his team are said to have reached a light-to-power conversion efficiency of 3.2%, compared to the 1.8% efficiency of the traditional planar structure from the same materials. The researchers point to the solar material's distinctive electric field distribution, which allows for an efficient charge transport, the combination of nanocones using economical proprietary methods and the reduction of defect and voids in semiconductors as important features of the technology that allow for the enhanced conversion rate. Interestingly, the team maintains that due to the efficient charge

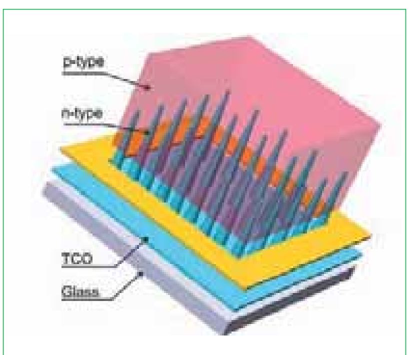

Nanocone-based solar cell consisting of n-type nanocones, p-type matrix, transparent conductive oxide (TCO) and glass substrate.

transport, the new solar cell is said to be able to endure defective materials and therefore lessen the cost of producing next-generation solar cells.

New Energy enters CRADA with NREL for SolarWindow technology

New Energy Technologies has entered a cooperative research and development agreement (CRADA) with the US Department of Energy's National Renewable Energy Laboratory (NREL) for the advancement of New Energy's SolarWindow technology.

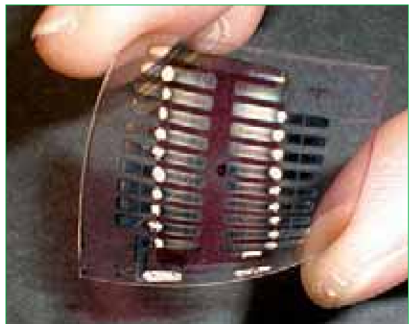

Image: New Energy Technologies

New Energy Technologies' SolarWindow technology.

The CRADA will see NREL and New Energy researchers utilizing each other's intellectual property to reach specific goals, including ramping up SolarWindow's efficiency and transparency and increasing its electrical power output. The agreement will also aim to enhance the application of the active layer coatings, which allow the SolarWindow technology to produce electricity on glass surfaces.

Natcore awarded patent for nanostructured flexible thin-film solar cell technology

Natcore Technology has been awarded a patent by the US Patent Office for its solar cell structure, which uses carbon nanotubes for enhanced cell performance. This patent is based off three earlier foundational patents, the first of which was issued to Rice University and licensed to Natcore. The first patent involved a liquid phase deposition (LPD) process for growing inorganic films on silicon.

The remaining two foundational patents, which Rice University and Natcore jointly own, include a patent for the growth of silicon dioxide on carbon nanotubes and a patent for the growth of inorganic semiconductors, such as cadmium telluride and cadmium selenide, on carbon nanotubes.

Chuck Provini, Natcore's president and CEO, commented: "The near-term module efficiency using this technology is projected to be equivalent to commercial silicon modules at 15% to 16%, and the longer-term improvements could raise the efficiency to 20% or more."

The new patent is wholly owned by Natcore and encompasses the use of inorganic semiconductor-coated nanotubes for the production of high-efficiency thin-film solar cells. Natcore is in talks with Eastman Kodak and Phono Solar of China for the commercialization of the technology on equipment that was once used to manufacture photo film before digital photography developed into a more burgeoning market.

The company also recently settled upon the Kodak Research Laboratories in Eastman Business Park, Rochester, New York as the site for its Natcore Research and Development Center. At the moment, the company conducts its research at three separate locations: Ohio State University, Rice University and at its JV in China.

The Kodak Research facility will have two equipped labs, a cleanroom and administrative offices. Furthermore, it will contain Natcore's first production model of its intelligent LPD processing station for growing an antireflective coating on silicon wafers in the process of manufacturing solar cells.

Fraunhofer ISE produces prototypes of largest screen-printed dye-solar-cell PV module

Over the past few years, Fraunhofer ISE has been working on the development of dye solar cells, with an ultimate goal of being able to fully integrate the solar modules into the face of a building. One of the main challenges the researchers have faced is bringing the technology out of the lab and putting it into the industrial field. Lately, Fraunhofer ISE researchers have started to overcome this dilemma, specifically with the production of a 60 × 100cm^2 dye solar cell module on a continuous substrate material.

The large-area dye solar module prototypes have been manufactured on glass with a zigzag-like design. The glass frit sealing was applied by a screen printing process and holds claims to be stable over the long-term. "For the first time, we were able to show that an integrated series connection of cells is possible on a module area of 60 × 100cm^2 using screen-printing technology," explains Dr. Andreas Hinsch of Fraunhofer ISE. "This avoids a complex external connection of the submodules. With this prototype, we have achieved a decisive step towards cost-effective up-scaling and paved the way for the transfer to the industrial level."

The prototype modules were created using applicable industry procedures and machines. The dye and electrolyte were applied with help from Fraunhofer IAO – providing the essential in-house development – who worked with Fraunhofer ISE to create a station that automatically filled and sealed the modules. Fraunhofer ISE is looking to continue using this new mechanism towards the creation of demonstration modules and a pilot processing line.

Image: Fraunhofer ISE

Prototype of a 60 × 100cm^2 dye solar cell module manufactured at Fraunhofer ISE using a screen-printing process.

OPEL Solar Asia nabs its first order with a 5MW contract from a Chinese power company

OPEL Solar International, the joint venture between OPEL Solar and Ecotech Environmental Technology, has been awarded its first order, just over three months after its formation. The company will provide 5MW of its HCPV panels and dual-axis trackers to one of China's electric power companies. OPEL Solar International initially expected the order to be for 2MW, but looks at the doubled purchase order as a way for it to break into the HCPV market in East Asia. Deliveries should start in the second quarter of 2011 and be completed during 2012.

Air Liquide signs contracts with leading cell manufacturers

Air Liquide has consolidated its position as one of the leading gas suppliers to the solar industry by signing 15 long-term contracts with a range of Asian and European manufacturers. Among these new partners are six of the seven leading c-Si cell and module manufacturers and the world's premier c-Si wafer producer, all of whom are based in China. Contracts were also signed c-Si and CIGS companies in Germany, Japan and Taiwan.

Schiller wins contract to provide facility automation to Chinese thin-film PV plant

Schiller Automation has won a contract for a new factory automation facility in China, which, as sources confirmed to PV-Tech, is a silicon thin-film factory. It is expected that the new automation facility will utilize Schiller's BackBone concept, which allows for full-size glass substrates to be handled in a central control area and then distributed to multiple process steps. Additionally, the installation of a ProLoad station, which handles the substrates as they are being processed in one step, and Schiller's line control (LC) software system, will implemented. Schiller's LC software is already being used in eight thin-film module factories, allowing for continuous operation to be maintained at the facilities.

Solar Frontier signs thin-film CIS distribution, installation agreement with Albatech

Solar Frontier has signed a contract with Albatech for the distribution and installation of its thin-film CIS module range nationwide. This agreement marks the company's expansion of its European-wide distribution network, and will help in strengthening the company's product range on the Italian market.

Bürkle supplies Ypsator lamination line to CdTe start-up in US

Perrysburg, Ohio-based CdTe thin-film start-up Willard & Kelsey Solar Group (also known as WK Solar) has purchased a module lamination system from Bürkle. The equipment order reflects the company's move to begin volume production and is claimed by Bürkle to be the first tool of its type in the North American market.

Ampulse books development tool from Roth & Rau for c-Si thin-film PV work at NREL

Crystalline-silicon thin-film PV company Ampulse has ordered a cell process development tool from Roth & Rau MicroSystem. The system, scheduled for delivery in the first half of this year, will be installed at the National Renewable Energy Laboratory's Process Development and Integration Laboratory in Golden, Colorado.

The AK1000 tool on order consists of a modular line of process chambers which can be combined in any number and order to form flexible inline processing systems. It can accommodate large substrates up to 480mm wide or batches of wafers, and can be configured with a variety of sources, including plasma, ion beam, sputter magnetron, and hot-wire CVD. Processes developed on the AK inline systems may be easily scaled up to high-volume production platforms.

Heliatek buys two Dr. Schenk metrology systems for OPV production line

Heliatek has placed an order for two Dr. Schenk SolarInspect roll-to-roll metrology systems that will be placed in its organic photovoltaics (OPV) line located at the company's Dresden, Germany, facility. Delivery of the two systems is expected to occur midway through this year.

XsunX signs production line supply contract with Globe Future Technology

XsunX has signed a contract to supply Globe Future Technology Development with its thin-film production systems. Under the agreement, XsunX will provide Globe Future with its baseline production system and an additional 30MW CIGSolar cell production system.

The contract will also see the companies collaborate on tailoring the CIGSolar system's specifications to ensure its meets Globe Future's specific needs. Once this has been completed, Globe Future will post a letter-of-credit for the payment of the systems.

Abound Solar closes sales deal with Solarsis, enters Indian market

Abound Solar is making its entrance into the Indian market under a long-term sales agreement with Solarsis. The companies aim to promote Abound's thin-film CdTe modules to project developers in the country's burgeoning solar market. Additionally, Solarsis will create a test facility catering to the enhancement of balance of system (BOS) designs that center on Abound's modules.

Specifics about the financial terms of the agreement or the amount and timing of module shipments were not revealed.

Other News Focus

Solyndra forms international subsidiary in Switzerland

US solar system manufacturer Solyndra has signalled its intent to increase its worldwide presence by founding Solyndra International. The subsidiary will be based in Baar, Switzerland, with Clemens Jargon taking on the role of chairman.

"With new sales offices in Italy, France and the Czech Republic and our representative in the Middle East, we are establishing strong local capabilities to meet customer needs," said Jargon. "We are evaluating additional offices in the UK and Benelux as well."

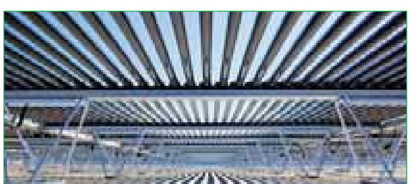

Solyndra's cylindrical CIGS modules.

United Solar earns US patent for nanocrystalline silicon thin-film deposition technology

Subhendu Guha, Jeff Yang and Baojie Yan of thin-film solar module manufacturer United Solar, a subsidiary of Energy

Uni-Solar's triple-junction amorphous-silicon thin-film PV laminates.

Conversion Devices, have been granted US Patent 7,902,049 by the United States Patent and Trademark Office for their "method of depositing high-quality microcrystalline semiconductor materials." The patent was granted to the company just a few months after it announced that the US Department of Energy and the National Renewable Energy Laboratory (NREL) had conducted testing resulting in a 12% initial conversion of the nanocrystalline technology.

Mark Morelli, president and CEO of Energy Conversion Devices, commented: "The proprietary technology covered in this patent will enable us to achieve our 12% aperture-area conversion efficiency in 2012, as outlined in our technology roadmap. The direct result of this is that we will be able to harness the sun's energy in a more cost-effective manner."

This is the latest patent for United Solar, which has been awarded almost 70 US patents in its 25 years of operation.

First Solar, juwi sign sponsorship deal with cycling team

First Solar and juwi solar have become the latest names in the solar industry to enter into the world of sports sponsorship after they signed a joint contract with an amateur US road cycling team. The move comes just a few months after Yingli Green secured a three-year contract to sponsor German football club Bayern Munich. The First Solar-juwi team will compete nationally and is made up of 10 world-class cyclists, including two-time US champion Michael Olheiser.

The four-day Redlands Bicycle Classic, which took place on March 31, saw the cyclists pass First Solar's proposed 850MW Stateline and Desert Sunlight projects.

Ascent Solar inks European distribution deal with Sunload Mobile Solutions

Sunload Mobile has signed an agreement to become an authorized dealer of Ascent Solar's thin-film CIGS modules for electronic integrated photovoltaics (EIPV) applications in Europe. Ascent Solar anticipates that the distribution deal will develop further opportunities in the European off-grid battery charging and portable power markets.

This is the third distribution deal that Ascent Solar has signed since February. Ascent Solar and SW Solarwatt signed a distribution deal for BIPV projects in Greece and Cyprus in February, which was preceded by a reseller deal that Ascent Solar signed with Polymeur Sun.

Product Reviews

Tosoh SMD

Tosoh SMD's sputtering targets support 18% thin-film efficiencies

Product Outline: Tosoh SMD has introduced new transparent conducting oxide (TCO) sputtering targets that are said to achieve higher solar cell efficiency than standard targets. Available in planar and rotary configurations, the targets are composed of either traditional indium tin oxide (ITO) or aluminium zinc oxide (AZO) and doped with performance-enhancing additives, such that thin films deposited from these targets have improved optical properties, in particular increased transparency.

Problem: TCO targets for leading-edge thin-film solar applications require a stringent combination of optical, electrical and mechanical properties and the durability to meet manufacturers' lifetime expectations.

Solution: Tosoh's new ITO and AZO TCO targets produce films that are highly transparent, especially in the visible to infrared range, and that feature high thermal stability, including under humid conditions. The targets enable the deposition of textured surfaces that feature enhanced light-trapping capability. Compared with thin-films from conventional TCO targets, a single-junction thin film deposited by a Tosoh AZO TCO target in a silicon solar cell shows a one-point gain in conversion efficiency. Thin films achieve a similar gain in a CIGS-based solar cell. The company claims that the new targets will contribute to achieving 18% energy conversion efficiency with a focus on low-cost and large-scale production.

Applications: Thin-film sputtering.

Platform: Tosoh SMD's products are compliant with ISO/TS-16949:2000 and are currently registered to ISO-9001:2000 and ISO-14001:2004.

Availability: Tosoh is engaging customers in North America and Europe for the beta testing.

StellarNet

Black-Comet-HR spectrometer from StellarNet offers enhanced spectral analysis

Product Outline: StellarNet has introduced the Black-Comet-HR spectrometer, which is available for measurements in two ranges – UV (200–600nm) and visible (380–750nm). The spectrometer is said to achieve resolving resolutions of 0.4nm.

Problem: Surface roughness is the primary source of grating-generated stray light. In the standard Czerny Turner design, grating scatter is collected and focused by the mirror toward the exit port. When additional optical components like collimating and focusing mirrors are used in the instrument design, it is more likely that light may be re-diffracted and scattered.

Solution: One of the main advantages of the Black-Comet is its ability to reduce straylight levels by 0.02% at 435nm and 0.2% at 200nm – claimed to be the lowest values yielded by any field spectrometer. By design, the holographic grating has a smoother surface than the normal ruled gratings used in competing spectrometer models. The Black-Comet spectrometers utilize a holographic concave grating with aberration correction to provide improved spectral imaging, significantly improving spectral shapes by reducing comma and astigmatism found in all other plane grating miniature spectrometer designs. The flat field spectrograph architecture does not utilize mirrors and therefore drastically reduces stray light effects while providing uniform resolution across the entire spectral range.

Applications: A range of uses for thin-film analysis of solar cells.

Platform: This 16-bit concave grating spectrometer is USB-2 powered, shock-proof and vibration tolerant with no moving parts.

Availability: Currently available.

Sentech Instruments

Sentech Instruments's SenSol Haze offers quality control of TCO films

Product Outline: Sentech Instruments, a manufacturer of advanced quality control instrumentation for thin-film metrology applications, has developed a transparent conductive oxide (TCO) inspection tool that offers uniformity mapping of film thickness and spectrally resolved haze (λ) on glass sheets of all standard glass sizes.

Problem: In order to increase the optical absorption capacity of thin-film solar cells, typical TCO glass must increase the scattering capacity of transmission light, a capacity that is referred to as haze. Haze is the cloudy or muddy appearance of transparent or translucent materials on the surface that are caused by light diffusion.

Solution: The SenSol Haze is designed for quality control of TCO films in PV manufacturing of thin-film solar cells. It comprises the computer-controlled conveyor transport system and the sensor platform for haze and film thickness. The special design of the system allows measurements at every position of the glass sheet, especially at the edges. Glass sheets can be loaded and unloaded manually or by robot, while the high measurement speed allows integration of the system into a manufacturing line.

Applications: Uniformity mapping of film thickness and spectrally resolved haze on glass sheets of all standard glass sizes.

Platform: The system can be offered with additional sensors for the measurement of sheet resistance, optical constants and band gap (spectroscopic ellipsometer), current voltage characteristics and quantum efficiency.

Availability: Currently available.

Astronergy pushes toward gigawatt scale, with silicon thin film set to play a major role

By **Tom Cheyney**

HANGZHOU, CHINA – Liyou Yang started in the thin-film game in 1985 with BP Solar, where he eventually ran the company's amorphous-silicon research efforts. "Once you get into it," he smiled, "you get hooked." During the course of our conversation at Astronergy's headquarters, the Rutgers-educated president/CEO would often reference his time at the old company, using his early experiences as reminders of just how far the technology and the solar industry in general have come since those pioneering days in the 1980s and '90s.

"The macroenvironment was totally different then," with no "industrial base for solar – we incubated the whole thing ourselves," he recalled. BP's in-house R&D and equipment teams were largely on their own trying to figure things out, designing the tools and the processes, and working with equipment builders to transform the concepts into functioning systems and nascent production lines.

Now running one of China's fast-growing photovoltaics enterprises, Yang and his team have aggressive plans to bring Astronergy to gigawatt production scale and beyond over the next few years. Benefitting from the support of the Chint Group, its deep-pocketed corporate parent, he told me that the not-quite-five-year-old solar company is adding or will soon be adding both crystalline-silicon and tandem-junction amorphous-silicon manufacturing capacity in four locations – Hangzhou, Shanghai, Wenzhou and Jiuquan.

As one of a handful of PV firms continuing to promulgate c-Si and a-Si product lines, Astronergy (also called Chint Solar) plans to dedicate about two-thirds of its production focused on crystalline and one-third on thin film, according to Yang.

Liyou Yang, president/CEO of Astronergy.

Astronergy's 30MW line is highly automated, employing a stocker-based approach.

Photos courtesy of Astronergy

A new 50MW TFPV line in Hangzhou starts production in Q2 2011, supplementing the existing Oerlikon-supplied 30MW fab. Another 100–150MW is coming online by year's end at the headquarters campus and the Wenzhou site several hours drive south of the lakeside resort city, where building construction will be done in September, and the tools installed by December, he said.

Plans call for an additional several hundred megawatts of thin-film factory capability to be available by 2012 – pushing the total to 730MW – with 200MW of that coming from a new Jiuquan location in northwest China. Astronergy's crystalline capacity should increase to 800MW this year – most of that growth will come from its Shanghai facility – with a total of 1200MW ramped by 2012, he noted.

Altogether, Astronergy hopes to see its total capacity rise to almost 2GW in 2012, before continuing its expansion and passing another milestone the following year. "We want to be at two-and-a-half gigawatts by 2013," the chief executive said.

Once the Chinese factories have been built, the company will site its first production facility outside the home country – a highly automated silicon thin-film fab located in the United States. "We do believe the US market will become prominent," he added, noting the importance of putting factories close to key end-markets. (This distributed-manufacturing strategy also played a role in the decision to build the moduling plant in Jiuquan, near the 1GW of solar farms backed by a partnership of Chint and government entities planned for Gansu province.)

Written off by some as an inadequate or doomed technology with little or no future, silicon thin-film PV has been seeing a bit of a resurgence of late, thanks to companies like Sharp and Astronergy as well as the continued envelope-pushing efforts of equipment and process supplier Oerlikon.

After a couple of tough years riding out the financial crisis and fending off the blowback of Applied Materials' failed SunFab venture, the company cofounded by Yang is now capacity constrained, unable to keep pace on its single production line with the prodigious demand for its 9%-plus-efficient tandem-junction micromorph panels.

"We can't make enough panels," he said. "We're in a difficult situation: how do you turn customers down? We could take three times more orders. It feels like if we really put the squeeze on, we can win every bid. But since we don't have enough capacity, we don't go after every single deal."

Much of the business is coming from southern Asian countries like India and Thailand, including five sizeable orders from the region landed so far this year, he related.

"We are focusing on large customers, going into different markets, especially emerging ones like India, getting our name out, working on bankability. We've found that it's most efficient going through the big guys, and they really help us. We concentrate on that with the small line so far, to get the most out of it."

The combination of Astronergy's c-Si reputation, the built-in financial clout of Chint, and high-quality, low-cost, relatively efficient panels have provided the key components of what Yang sees as the company's competitive "sweet spot" with its silicon thin-film efforts.

"One of the advantages we have is that we already have 500MW of crystalline capacity, so we have some loyal customers who are also doing thin film," he underscored. "We have not seen one customer so far that we supply who specializes in thin film, so that's a plus for us."

Eschewing the prevalent strategy of many companies of starting with a single-junction

A dual-source solar simulator, with carefully tuned spectral balance, tests the tandem-junction panels.

amorphous silicon turnkey line and then progressing to a tandem-junction design after that, Astronergy chose to go directly to the twin-junction architecture, with the help of its equipment partner, Oerlikon.

"Thin film with 6%-plus efficiencies was never going to make it, except maybe for a short time when polysilicon was so expensive," Yang said, highlighting how he uses the generic term regularly as shorthand for "silicon thin film." "Since I knew thin film struggled long before, because of its lower efficiency, I believe that you really can't compete ultimately."

"We decided that we wanted to go directly to tandem-junction structures at that time [2008], from 8% to 9% range," he continued. "We struggled for many quarters, but we got past the financial crisis, and right now I believe that for thin film to become sufficiently competitive with crystalline products, the efficiency needs to be around 10% and the cost structure needs to be below 75 cents US. If you can't do that, you are in a relatively weak position."

"We've held [up] the expansion of thin film for the last two years; we've not done things aggressively because we just simply couldn't. But we have been doing a lot of technology development in the meantime, and we've been building very strong teams.

"After about two years of development, I feel that we are about to make a breakthrough this year, so that we can really hit what I call that threshold for true competitive thin film at 75 cents and 10% efficiency. From there, we're working with Oerlikon to push the envelope for efficiency – 11% is pretty doable, though beyond that I don't know."

Already producing 110–135W panels achieving north of 9% aperture-area efficiency at a cost basis of about 95–98 cents US per watt on the first line, Astronergy is implementing the new process recipe into production on its second line in Hangzhou. After successfully piloting it on a single-chamber R&D tool, the 10% process "can be rolled out when the certification process is done by the middle of the year," Yang said.

The boss wouldn't say which "knobs" were turned to achieve the improvements, pointing out that he could not even share the general categories where they occurred, "because once you mention that, then people would know. Interestingly, in this tandem-junction stack, with something like 20 layers all the way down, there are a number of things that in the past people have been looking into, but to implement them in the production environment, I think this is the first time."

The yield and capacity utilization data from the initial Hangzhou line are impressive. Yang provided charts showing the yield numbers hitting in the 98–99%-plus range continuously since June 2010, with that 30MW of current manufacturing capacity sustaining run rates of about 94% since October.

"We have been running month after month at a yield level that is astonishing – not just the high nineties, it's really close to 100%!" he exulted. "I think there are some intrinsic fundamental factors that are associated with the whole process flow, but there's also the equipment reliability and so on. At BP Solar, we struggled for two years, *two years* to get 80%, so you can see how happy I am."

Yang believes by increasing panel efficiencies and improving throughputs – two areas of development focus at Astronergy and Oerlikon, individually and jointly – more capacity can be squeezed out of the 30MW line. "By achieving 10% efficiency as well as implementing other productivity enhancements, we can increase the line capacity by at least 10%. Right now, we are not even achieving nameplate, running at about 28MW. We will be above 30MW when it's done."

The high level of automation becomes quickly apparent when you walk through Astronergy's tandem-junction production factory floor. Train-like AGVs run along a central chase area and big-armed material-handling robots glide back and forth, slinging the hefty, glass panels in and out of the cassette carriers and various process tools with little or no human intervention on most of the line.

The layout is a serial-batch stocker configuration not unlike that seen in modern semiconductor and flat-panel display fabs. ""The systems are all built around the stocker, so they're pretty flexible. If an individual tool is down, the rest of the process can operate," Yang explained.

The thin-film veteran described the inner workings of the all-important plasma-enhanced chemical vapor deposition tool. "The Oerlikon line's system is built with a single vacuum chamber with 10 individual plasma boxes inside, which operate independently. There is very little interaction between the boxes, and it's pretty reproducible and uniform.

"The system takes about 20 plates at a time for simultaneous deposition, and it takes about a half hour for 20 plates to be processed," he said. The total cycle time on the line, from bare glass in to finished module out, is about 3–4 hours, although "there are some queue times between the production steps."

As the decibels of production throb and whir enveloped us, Yang talked about several aspects of Astronergy's technology and manufacturing as well as offering some teachable moments on the intricacies of certain silicon thin-film behavior and characteristics.

One element of the company's film stack that he sees as a differentiator is its use of zinc oxide rather than tin oxide as its front

A youthful workforce helps keep Astronergy's silicon thin-film fab running at high yields and capacity utilization.

contact layer, materials he is well familiar with from his days at BP.

"Zinc oxide is the superior transparent conductive oxide, yet because of its electrical properties, you need some engineering to get around some problems. Otherwise, even though you get higher, superior light transmission, the open-circuit voltage typically will be lower. But Oerlikon has found a process that does it well. Another difference is that we use zinc oxide on the back-side as well, not using a metal back contact."

He commented on how far the laser technology used in the trio of scribing tools deployed in the fab had come since the old days, when the crystals used in the UV lasers needed to scribe the TCO film were expensive and the process difficult. Now the quartet of tunable-wavelength parallel beams sweep across the glass, quickly separating the films into serially connected cells.

Applied bursts of concentrated photonic energy will also play an increased role on future Astronergy lines, as the trimming of excess material from the panels' edges now done by what he called "sandblasting" will be replaced with laser ablation.

When the subject of one of the banes of amorphous-silicon PV performance – light-induced degradation – came up, Yang took on a professorial air, noting he had written some 10 papers on that very subject. He informed me that tandem-junction structures have intrinsic advantages in reducing LID.

"One factor that influences the LID is material quality," he explained. "If you do a very fast deposition, you can have very strong degradations. Second is the film stack. If you make the junction thinner, so the electrical field within the junction is much stronger; it's not as sensitive to the light-induced defects."

"With tandem junction, for one thing, the junction gets thinner, especially the top junction, where it's more the silicon that is subject to light degradation, while the microcrystalline material on the back-side is mostly stable. Also, that front junction is very, very thin, only about <1000 angstroms. So the total degradation of a panel's junction device is limited to 10-15%, rather than for single junction, where you can have around 25% or more."

Once Astronergy has exhausted the various knobs it can turn to get the most out of its current tandem-junction design, the addition of a third junction to the stack – which would decrease the LID effect even more – is squarely on the company's roadmap. But don't expect a fourth or fifth junction down the proverbial road.

"The general understanding is that triple junction is the most you want to go to; even with the trouble you have, it's still worth doing," he said. Because of diminishing performance returns and increasingly complex engineering challenges, "four-junction is not."

The depth of Oerlikon's involvement in Astronergy's ambitious technology development and capacity ramp plans remains an open question. The new 50MW line entering production status features a different mix of equipment suppliers than the initial, more turnkey line.

"We want to have our own capability of integrating, because that's the way the semiconductor industry has developed, where nobody buys turnkey lines, and eventually solar will go that direction as well. We will continue to work with Oerlikon, all the way from pieces of equipment to a fully integrated fab, depending on the timing, what makes sense at the time, speed, cost, all of that."

A different configuration will help boost the new line's nameplate to 50MW to go along with the targeted 10% efficiencies and 75 cents per watt cost basis, he said.

"If you look at the technology mix that you can bring in, Oerlikon is one configuration, and we have looked at other options. We are very confident we can reach 75 cents by Q2 this year, and that's been done by opening up all of the technology options. You can look at various suppliers and can significantly reduce costs, even though the line is still mostly imported equipment.

"I think our cost structure is still much better compared to an Oerlikon turnkey line, from a capex point of view. We're looking at domestically-produced equipment, which is also still in its infancy stage, yet it has some potential to further reduce capex. We are working with European, US, Taiwanese and domestic equipment on the new line. It's an interesting choice of vendors but it's a painful process of qualifying all of them."

Despite the growing pains experienced by Astronergy, the presence of its flush parent company makes its future prospects trend toward the brighter portions of the spectrum. Yang laid out several advantages of having a "big daddy."

"At the development stage with a big parent company behind you, it really helps in terms of financing. Another reason is that setting up a factory here in China is not an easy thing, even for regular Chinese. When I came back and got a group of technologists together and tried to start a company, it was not as easy. In that regard, the parent company has helped quite a bit in terms of getting the right government support and so forth. Third, there is some access to the parent's global sales network.

"Fourth, there is the synergistic advantage of having complimentary products (Chint is a major player in the power transmission and distribution industry), so we are now pushing in the direction of a total solution together with the parent company," he continued. "Eventually it's the total system that counts; with lower costs you really have to consider everything. Together we can not only optimize the system design and the solution path, but also really leverage the low-cost manufacturing infrastructure in China, with scale and expertise, to really make the PV systems as inexpensive as they could be."

Another not-to-be-discounted factor is what Yang calls the "top level of connections" enjoyed by Chint company head Cunhui Nan, who he describes as "charismatic" and "visionary."

"Our chairman is a member of the People's Congress. He's one of the most well-known businesspersons in China. There are seven guys in the Politburo, and very few businesspeople that all seven would know. And our chairman is one of them. In terms of connections, we probably enjoy one of the best."

This article is the original version of a two-part blog that appears on PV-Tech.

Tom Cheyney is senior editor, North America, for *Photovoltaics International* journal and writes blogs and news for PV-Tech.org.

Polarized light metrology for thin-film photovoltaics: research and development scale processes

R.W. Collins[1], **Jian Li** [2], **Michelle N. Sestak**[1] & **Sylvain Marsillac**[3],
[1]Center for Photovoltaics Innovation & Commercialization and Department of Physics & Astronomy, University of Toledo, Ohio; [2]National Renewable Energy Laboratory, Golden, Colorado, and Department of Electrical Engineering & Computer Science, University of Michigan, Ann Arbor, Michigan; [3]Department of Electrical & Computer Engineering, Old Dominion University, Norfolk, Virginia, USA

ABSTRACT
Optical probes based on polarized light spectroscopy, including spectroscopic ellipsometry (SE) and polarimetry, have been applied in research and process development for the three major thin-film photovoltaics technologies, including thin-film hydrogenated silicon (Si:H), cadmium telluride (CdTe), and copper indium-gallium diselenide ($CuIn_{1-x}Ga_xSe_2$). Real-time SE during materials fabrication has provided insights into the nucleation, coalescence, and structural evolution of these thin films. These insights have led, in turn, to guiding principles for PV performance optimization, as well as future directions for real-time process control. The optical properties deduced simultaneously with the layer thicknesses using real-time SE have been applied to characterize the phase composition of materials (amorphous versus crystalline), the mean free path and grain size, and the relative free carrier concentration. As a result, analytical formulae for the optical properties of PV materials have been developed with free parameters that are linked to basic materials properties. This paper shows how the formulae and associated parameter-property relationships can serve as a database for analyzing complete PV stacks, with future prospects for mapping layer thicknesses and basic materials properties in on-line monitoring applications for large-area PV plates and modules.

Introduction

Non-destructive and non-invasive measurement and monitoring tools are needed at all stages of thin-film photovoltaics development; in research laboratories, in scale-up of processes, and in production [1, 2]. Maturation of thin-film technologies has led to a growing demand for such probes particularly for on-line monitoring and control of manufacturing lines. Depending on the technology, optimized thin-film PV device fabrication may require the deposition of a dozen or more major layers, with the possibility of additional intentionally-graded and inadvertent transition layers between major layers. Some transition layers may be as thin as a few atomic distances, or one nanometer (nm), and the major layers may be as thick as 10 microns (µm). Substrates on which these multilayers are fabricated can range in size from cm^2 or less for specialized substrates – designed for exceptional crystalline quality in thin film form – to m^2 for glass plates, designed for low cost production of amorphous, nanocrystalline, or polycrystalline thin films. As a result, in thin-film PV the thickness d for each layer and its uniformity over the substrate area collectively represent a critically-important starting point in the evaluation of the overall performance of the multilayer PV stack.

At the next level of detail in component layer evaluation, the spectral dependence of the index of refraction and extinction coefficient (n, k) and their uniformity are also critically important, as these spectra, in conjunction with the set of d, enable the calculation of the internal quantum efficiency (QE) of the PV device at a given location on its surface. The internal QE describes the number of electron-hole pairs generated within the active material component of the device per unit area per unit time – given as a ratio of the incident photon flux. The differences between the calculated internal QE and the measured QE provide insights into the spectral dependence of electronic losses. Further analysis of the deduced (n, k) spectra can also yield more fundamental optical parameters of critical point (CP) amplitudes, CP energies or bandgaps and CP widths. These can provide information on material density, temperature, composition, strain, grain size, and defect density, assuming that the appropriate parameter-property relationships are established.

> "Polarized light spectroscopies have served as non-invasive optical probes of thin films and multilayers in a wide variety of technologies."

In this article, the application of polarized light spectroscopy will be described for the determination of thicknesses and (n, k) spectra toward the analysis and optimization of PV fabrication processes on the research and development scale. Polarized light spectroscopies, which encompass ellipsometry and polarimetry – both performed in reflection – have served as non-invasive optical probes of thin films and multilayers in a wide variety of technologies (see Fig. 1) [3-7]. Polarized light spectroscopies achieve a significant advantage over reflectometry through the additional measurement of a phase difference. Reflectometry exploits the change in real irradiance I upon reflection; however, the technique of ellipsometry exploits the change in a complex polarization state parameter ξ, which includes both a relative amplitude $|\xi|$ and a phase difference δ: $\xi = |\xi|\exp(i\delta)$ [3]. In turn, the relative amplitude $|\xi|$ is the ratio of two orthogonally-directed, linearly-polarized optical field amplitudes, and δ is the phase difference between the two orthogonal components. The irradiance change upon reflection is characterized by the reflectance $R = I_r/I_i$, the ratio of the reflected (r) to incident (i) beam irradiances, whereas the polarization state change is defined analogously, but as a complex number $\rho = \xi_r/\xi_i = (|\xi_r|/|\xi_i|)\exp\{i(\delta_r - \delta_i)\}$.

Thus, ellipsometry provides two angles, one defined (historically) in terms of a ratio of the relative amplitudes $|\xi|$ by $\psi = \tan^{-1}(|\xi_r|/|\xi_i|)$, and the second described as a shift (upon reflection) in the phase difference δ given by $\Delta = \delta_r - \delta_i$ [3]. Ellipsometry is less sensitive to surface defects and macroscopic roughness that may scatter power out of the optical beam because, ultimately, it is based on the measurement of the shape (not the size) of the polarization ellipse – characterized by tilt and ellipticity angles (Q, χ). It can also be made less sensitive to small variations in alignment that would require recalibration in a reflectance experiment. The ellipsometry angle Δ exhibits extraordinary sensitivity to film thickness. High precision ellipsometers can detect the formation of fractions of a monolayer, 0.01nm in effective thickness, while providing the (n, k) spectra for thin films at the level of a few monolayers [8].

Thin Film

Applications in the three major thin-film technologies of hydrogenated amorphous and nanocrystalline silicon [a-Si:H and nc-Si:H], cadmium telluride [CdTe], and copper indium-gallium diselenide [$Cu(In_{1-x}Ga_x)Se_2$, or CIGS] will be described at research and development scales. In some cases, detailed insights into process optimization have been obtained; in others, a foundation for in-depth process development is being established. A second goal of the R&D scale activity is the development of an optical property or (n, k) database including analytical formulas and associated parameter-property relationships for all the major thin-film PV materials, from metallic and transparent conducting oxide contacts to the n-type, p-type, and intrinsic semiconductors [9]. Such a database is particularly useful for on-line and off-line analysis of materials on a manufacturing scale. A description of these analysis efforts is beyond the scope of the present article.

Polarized light measurements

Spectroscopic ellipsometry

The simplest ellipsometry measurement is that of a bare isotropic substrate, or its optical equivalent, an opaque ideal, isotropic thin film. If the dielectric function ε_a of the ambient medium (typically air or vacuum) and the oblique angle of incidence θ_i are both known, then (ψ, Δ), as defined in the previous section, provide directly the real and imaginary parts (ε_{1s}, ε_{2s}) of the complex dielectric function of the substrate (or opaque film) for the given optical wavelength λ of measurement (or photon energy of measurement: $E = hc/\lambda$; where c is speed of light and h is Planck's constant) [3]. The complex dielectric function of the substrate $\varepsilon_s = \varepsilon_{1s} + i\varepsilon_{2s}$ is obtained from its complex index of refraction $N_s = n_s + ik_s$, simply according to $\varepsilon_s = N_s^2$, so that $\varepsilon_{1s} = n_s^2 - k_s^2$ and $\varepsilon_{2s} = 2n_sk_s$, where (n_s, k_s) are the index of refraction and extinction coefficient of the substrate, respectively. For a non-absorbing ambient medium, $k_a = 0$ and so $\varepsilon_{1a} = n_a^2$ and $\varepsilon_{2a} = 0$. This measurement capability provides the unique opportunity for spectroscopic ellipsometry to measure directly the wavelength or photon energy ($E=\hbar\omega$) dependence of the complete optical properties of a substrate or an opaque film, either in the form of ε_s or N_s. Thus, spectroscopic ellipsometry enables development of a reference set of material dielectric functions [9] that can then be applied to assist in the analysis of ellipsometry data on single thin films and multilayers.

> "Spectroscopic ellipsometry enables development of a reference set of material dielectric functions."

The next step in the progression of ellipsometric measurement and analysis involves determination of the thickness d and the real and imaginary parts of the complex dielectric function (ε_{1f}, ε_{2f}) of a single unknown, ideal, isotropic thin film on a known isotropic substrate. Because there are three unknowns: {d, (ε_{1f}, ε_{2f})}, in a single photon energy problem and only two data values: (ψ, Δ), then multiple measurements are required [3]. As spectroscopic ellipsometry is powerful in its own right (as described in the next paragraph), this same multiple measurement approach is also the most desirable for solving the single film data analysis problem. For spectra consisting of M photon energies, there are $2M + 1$ unknown parameters, including M pairs of (ε_{1f}, ε_{2f}) as well as one d value, but only $2M$ measured (ψ, Δ) values. In spite of this, it is still possible to solve the single film problem using a single pair of (ψ, Δ) spectra, in a process called artifact minimization [10]. Even greater success results, however, from measuring and analyzing multiple spectra at different times during film growth, through the methods of real-time spectroscopic ellipsometry [11]. If spectra with M photon energies are collected at N different times, associated with different values of d during deposition of a film with a constant dielectric function versus d, then there are $2M + N$ unknowns and $2MN$ data values. For typical values used in real time spectroscopic ellipsometry, with state of the art instrumentation, M and N are each on the order of 10^2 – 10^3, and the analysis solution is greatly over-determined.

The dielectric function (ε_1, ε_2) of a substrate or thin film, versus photon energy, can be described as an analytical function of lineshape parameters, including amplitudes A_n, energies E_n, and broadening parameters Γ_n , which provide information on physical characteristics [12,13]. For example, A_n reflects material density; E_n reflects material temperature, composition, and strain; and Γ_n reflects defect density, grain size or ordering, depending on the structure (crystalline, polycrystalline, or amorphous, respectively). In many cases, such information cannot be determined directly and must be established through correlations of optical data with direct measurements that enable development of parameter-property relationships. If ε_f can be expressed accurately as an analytical function of lineshape parameters, then the single film analysis problem can be reduced to least-squares regression or determination of only $\hbar\omega$-independent parameters. The validity of the best-fit model for (ε_{1f}, ε_{2f}) is evaluated using the mean square error between the best-fit simulation and the experimental (ψ, Δ) spectra [14].

A single thin film on a substrate can rarely be modelled adequately assuming a single layer between the semi-infinite ambient and substrate. Film surfaces and interfaces are microscopically rough to at least some degree, with possible film/substrate interdiffusion as well. Microscopic roughness, i.e., roughness having an in-plane scale much smaller than the light wavelength, can be incorporated into the optical model as one or more layers. The complex dielectric functions of these layers are modelled assuming effective media of the underlying and overlying materials. The Bruggeman approximation has been applied most widely for determining ε for microscopic mixtures based on the dielectric functions and volume fractions of the components [15,16]. Consequently, roughness regions can be incorporated into least squares regression through the addition of $\hbar\omega$-independent thickness parameters [14].

> "A single thin film on a substrate can rarely be modelled adequately assuming a single layer between the semi-infinite ambient and substrate."

The final step in the progression of ellipsometric measurement and analysis capability involves characterization of a full multilayer stack [3,14]. In this case, a single pair of (ψ, Δ) spectra can be useful under two circumstances. First, if all dielectric functions in the problem are known, or if some are known and others can be expressed in terms of a few wavelength independent lineshape parameters [e.g., (A_n, E_n, Γ_n)], then least-squares regression can provide the thicknesses of the bulk, surface roughness and interface roughness layers as well as the dielectric function parameters. Second, if only one dielectric function is unknown and one to three thicknesses are unknown, then the artifact minimization method is possible. The best solution, however, is real-time

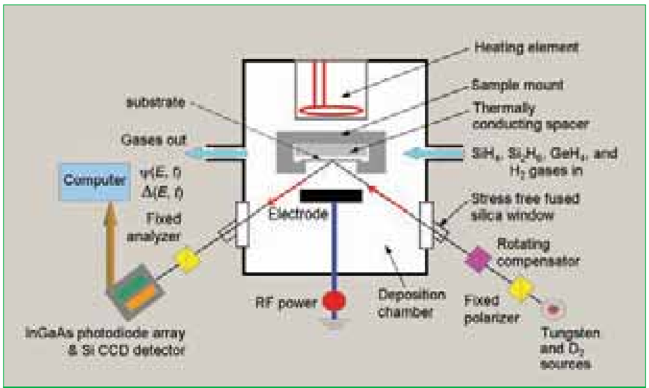

Figure 1. Schematic of a commercially-available, rotating-compensator multichannel ellipsometer (J.A. Woollam Co., M2000-DI) integrated with a system for thin-film silicon preparation by plasma-enhanced chemical vapour deposition.

spectroscopic ellipsometry, which can overdetermine the thickness and optical properties of each layer as it is deposited. In such a case, very fine details of the film structure related to interactions with the substrate, surface roughness development, and even optical property evolution can be incorporated into the deposition models.

Spectroscopic polarimetry

The presence of a variety of non-idealities in thin-film structures motivates spectroscopic polarimetry. This technique involves generating an optical beam with a known four-component Stokes vector ($\mathbf{S}_i$), reflecting that beam from a surface, and detecting the four-component Stokes vector ($\mathbf{S}_r$) after reflection [17], such that both generation and detection are spectrally resolved and characterized. The Stokes vector describes not only the polarization ellipse shape (Q, χ), but also the beam irradiance I and degree of polarization p. Changes in the ellipse shape (Q, χ) upon reflection can provide the angles (ψ, Δ), as in ellipsometry. Changes in I upon reflection can provide information on macroscopic roughness, whose in-plane scale is on the order of the wavelength and scatters irradiance out of the beam. Finally, changes in p upon reflection can provide information on non-uniformities that lead to a distribution of thickness or optical properties over the probed area: typically 0.1 – 1cm^2. The non-uniformities in turn lead to a distribution of reflected beam polarization states, or depolarization of the incident polarized beam, yielding $p < 1$. By expanding spectroscopic polarimetry to the measurement of the sample's 4 × 4 Mueller matrix $\mathbf{M}_S$, which describes how the sample modifies any incident 4 × 1 Stokes vector upon reflection [17], anisotropic systems can be characterized – including the thicknesses and principal axis complex dielectric functions of substrates and films [14].

Applications of polarized light spectroscopy in photovoltaics

Applications of real-time spectroscopic ellipsometry (RTSE) in the three major thin-film photovoltaic technologies will now be discussed in order of maturity of the technology, which parallels the level to which the RTSE capability has been advanced in each case. For thin-film hydrogenated silicon (Si:H), significant progress has been made in understanding the growth mechanisms using RTSE, and in developing guiding principles for the optimization of both amorphous silicon (a-Si:H) and nanocrystalline silicon (nc-Si:H) solar cells [18]. For thin-film CdTe, RTSE studies currently explore the relationships between the nucleation and growth dynamics of as-deposited CdTe and CdS and the resulting solar cell performance, and the ability of the dielectric functions to provide information on temperature, strain and grain size in these materials [19]. In this case, the complexity of such relationships is enhanced as a result of the post-deposition $CdCl_2$ treatment. Finally, for CIGS, RTSE studies are at an early stage, and the initial effort requires developing dielectric function database components of the relevant phases and compositions of the materials.

Fig. 1 shows an apparatus used for real time spectroscopic ellipsometry in the rotating-compensator configuration. The commercial instrument shown here (J.A. Woollam Co., M2000-DI) consists of a broadband light source incorporating both D_2 and filament lamps for a spectral range of 0.75 to 6.5eV. A collimated light beam from the source passes through a polarizer and a continuously rotating compensator. Upon transmission of the beam, the compensator imposes a shift in the phase difference between two orthogonal linear polarization components, resolved along the fast and slow axes of the device, thus generating elliptically polarized light in general. The beam then passes through a strain-free window into the chamber, reflects from the growing film, and exits the chamber. After passing through the second strain-free window, the light is analyzed with a second polarizer and spectroscopically resolved and measured using a pair of linear array detectors. The deposition system shown schematically in Fig. 1 is designed for the fabrication of thin-film Si:H from silane or disilane and hydrogen gases by plasma-enhanced chemical vapour deposition (PECVD), although the same spectroscopic ellipsometer can also be mounted onto deposition systems used for CdTe and CIGS.

Thin-film hydrogenated silicon (Si:H)

Thin-film Si:H is the most extensively studied of the thin-film solar cell materials since it encompasses prototypical amorphous and nanocrystalline semiconductors [20]. The best small area solar cells from multijunctions of these materials exhibit a factor of two lower efficiency than the corresponding best c-Si solar cells. In spite of this, the thin-film Si:H does present certain advantages such as relaxed crystal momentum conservation (hence strong absorption for a much reduced thickness), abundant non-toxic materials, and a potential for low production costs [20]. The Si:H materials are deposited by plasma-enhanced chemical vapour deposition in low temperature processes (< 300°C) using SiH_4 or Si_2H_6 and H_2, making these solar cells excellent candidates for fabrication on flexible substrates in roll-to-roll processes. By altering the deposition parameters, most notably the *R* value (the ratio of H_2 to SiH_4 or Si_2H_6 gas flows), a thin Si:H film can be made amorphous, mixed-phase or nanocrystalline. These forms of thin-film Si:H have been studied in detail using RTSE [18, 21].

Fig. 2 compares the deduced dielectric functions of purely amorphous and purely nanocrystalline phases of Si:H (a-Si:H and nc-Si:H, respectively) measured at a calibrated substrate temperature of 200°C [21]. Although the overall shapes are similar, the nc-Si:H dielectric function shows two features near 3.4 and 4.2eV, which are the broadened critical points characteristic of crystal Si [22]. In contrast, the a-Si:H dielectric function shows a single, much broader feature due to complete loss of long-range order. This loss leads to a relaxation of crystal momentum (or electron **k**-vector) conservation and as a result, a larger imaginary part of the dielectric function is observed just above the band gap (1.8eV) for a-Si:H than for nc-Si:H. Thus, stronger absorption is obtained over much of the photon energy range of the visible spectrum, from 2 to 3eV. It is these differences that enable one to distinguish readily between the two phases and to characterize the evolution of mixed-phase materials using RTSE as shown in Fig. 3 [21].

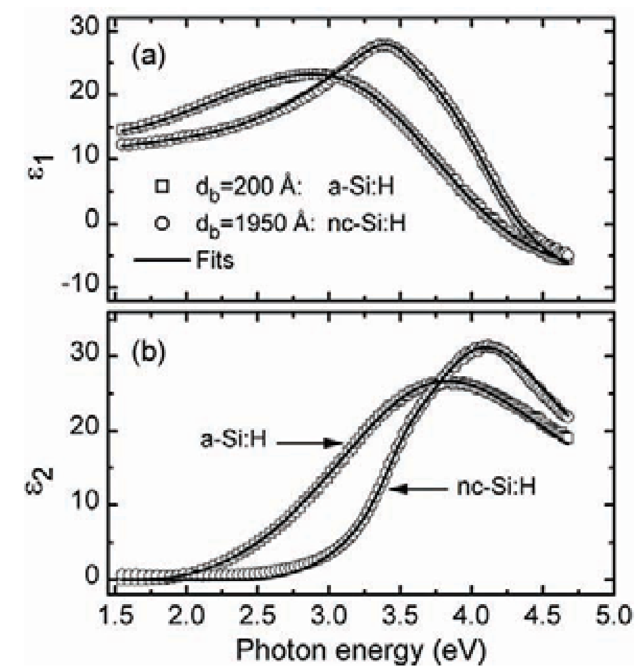

Figure 2. The real (a) and imaginary (b) parts of the dielectric functions of intrinsic amorphous and nanocrystalline Si:H (a-Si:H and nc-Si:H, respectively), measured at 200°C in RTSE studies of 20 and 195nm thick films (points). The solid line results have been calculated from oscillator models using best-fit lineshape parameters appropriate for a temperature of 200°C [21].

Fig. 3 presents the RTSE-deduced depth profile of the volume fraction of nanocrystalline phase (f_{nc}) in a mixed-phase Si:H intrinsic layer (*i*-layer), obtained as the PECVD film evolves in thickness under fixed conditions: a nominal substrate temperature of 200°C and *R* = 150 [18]. RTSE can be used to calibrate the actual substrate temperature, and the result in this case (110°C) is considerably lower than the nominal value (200°C). The substrate is an a-Si:H *n*-layer film, which starts the layered configuration used for a standard amorphous *n-i-p* solar cell. The results of Fig. 3 are obtained by applying to the RTSE data the virtual interface analysis technique including a pseudo-substrate approximation in order to extract the dielectric function of

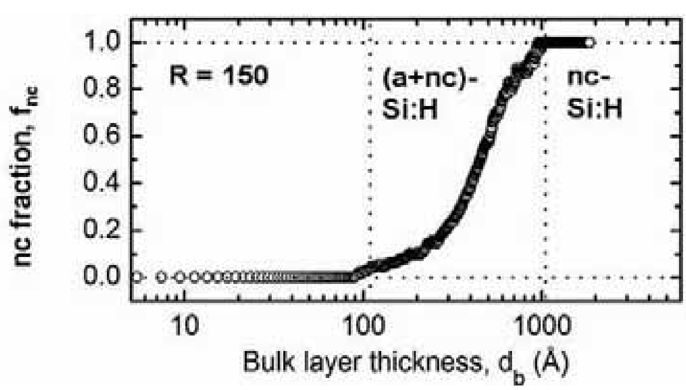

Figure 3. Depth profile in the nanocrystalline volume fraction (f_{nc}) from the substrate (left) to the surface (right) for a mixed-phase Si:H *i*-layer deposited under fixed conditions with a nominal substrate temperature of 200°C and *R*=150 on top of an a-Si:H *n*-layer [18].

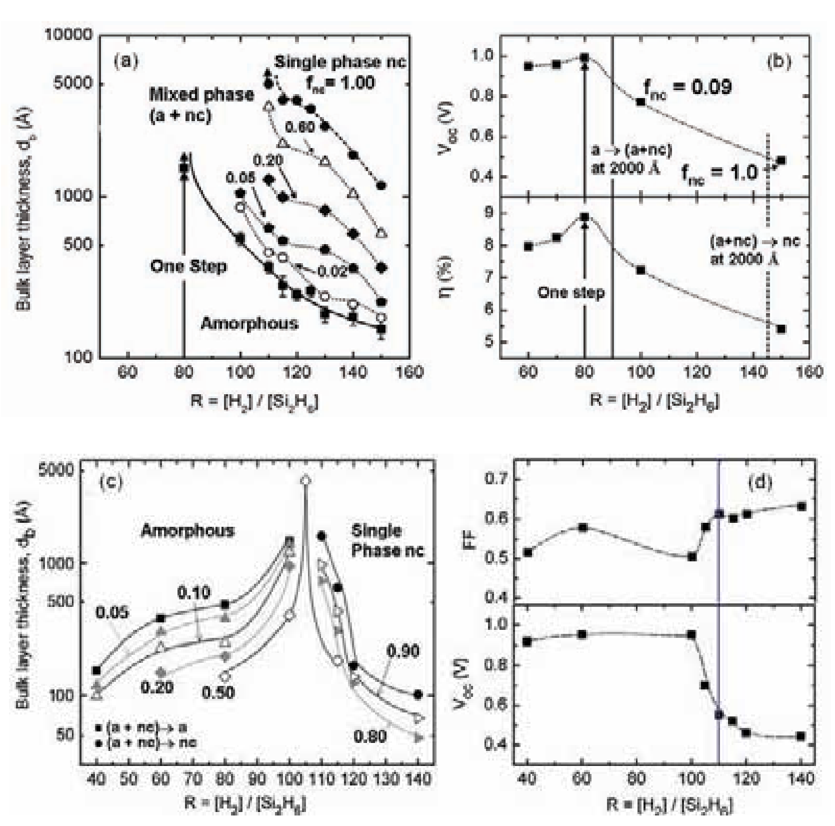

Figure 4. Deposition phase diagram (a) for a Si:H *i*-layers deposited on top of purely a-Si:H *n*-layers in the *n-i-p* configuration used for a-Si:H solar cells (contours on the diagram indicate f_{nc} values); (b) V_{oc} and efficiency versus the Si:H *i*-layer *R* value for single-junction solar cells [18]. Figure 4 (c) shows a deposition phase diagram for Si:H *i*-layers on nc-Si:H *n*-layer substrate films. These *i*-layers are designed for incorporation into nc-Si:H solar cells [18] (contours on the diagram indicate f_{nc} values); (d) V_{oc} and FF versus *R* for intended nc-Si:H solar cells in which case nc-Si:H *n*-layers are used. The vertical line identifies the optimum nc-Si:H solar cell performance [18].

the top ~ 1nm. In this way, a depth profile in the volume fraction of nanocrystallites, f_{nc}, can be obtained by applying the Bruggeman effective medium approximation [16] to the deduced dielectric function assuming a microscopic mixture of fully amorphous and fully nanocrystalline phases. For this deposition, the Si:H *i*-layer film nucleates on the *n*-layer as amorphous Si:H, undergoes an amorphous-to-nanocrystalline transition after a thickness of ~ 10nm, and then becomes fully nanocrystalline after a thickness of ~ 100nm.

Similar depth profiles obtained as a function of *R* from *R* = 80 to 150 have been used to construct a deposition phase diagram for the PECVD films as in Fig. 4(a) [18]. In this case, the Si:H *i*-layer films grown on a-Si:H *n*-layer films remain amorphous throughout the first ~200nm of bulk layer growth when $R \leq 80$. For higher *R* ($R \geq 100$), the Si:H *i*-layer films initially nucleate as a-Si:H, but then undergo an amorphous-to-nanocrystalline transition at a thickness that shifts from above 200nm to lower thicknesses with increasing *R*. Performance parameters of single-junction solar cells fabricated using a thickness of ~ 200nm for the Si:H *i*-layer, and different *R* values are shown in Fig. 4(b) [18]. The optimum V_{oc} and efficiency for this series of cells occurs when *R* = 80, which is the maximum *R* value possible such that the *i*-layer remains fully amorphous throughout its thickness. For a larger value of *R* = 100, the fraction of nanocrystallites in the near-surface of the final *i*-layer is small (~0.09), but these nanocrystallites apparently degrade V_{oc} due to their presence at the *i-p* interface in the completed device. This concept of maximum hydrogen dilution developed by RTSE is being applied widely to optimize the efficiencies of a-Si:H solar cells [21]. RTSE has suggested extensions of this concept using multistep and continuously variable dilution ratios *R* for improvements over simple single-step processes.

Another deposition phase diagram determined by RTSE is shown in Fig. 4(c), in this case for Si:H *i*-layers which are deposited on intended nanocrystalline Si:H (nc-Si:H) *n*-layers at the same nominal temperature of 200°C [18]. This is the layer structure used for a standard nanocrystalline *n-i-p* solar cell, and the resulting diagram exhibits significantly different behaviour than that of the Si:H *i*-layers on a-Si:H *n*-layers shown in Fig. 4(a). Initial stage mixed-phase Si:H growth results from a template effect due to the underlying nc-Si:H *n*-layer, which is itself mixed-phase, consisting of ~ 0.5/0.5vol. fraction ratio of a-Si:H/nc-Si:H. At lower dilution levels (*R* < 105), the mixed-phase *i*-layers evolve to a-Si:H due to a preference for amorphous growth. In this range of *R*, the mixed-phase nanocrystalline to amorphous [(a+nc) → a] transition shifts to larger thickness with increasing *R*. At higher dilution levels (*R* > 105), the initial mixed-phase material rapidly evolves to fully nc-Si:H due to the strong preference for nanocrystalline growth. In this range, the (a+nc) → nc transition shifts to lower thickness with increasing *R*. Fig. 4(c) reveals a bifurcation value of *R*=105, which divides the ultimate phase of the film between fully amorphous and fully nanocrystalline, even though the film nucleates as mixed-phase Si:H independent of *R*.

In the case of relatively thin 0.4–0.6µm nc-Si:H *i*-layers used in solar cells with performance shown in Fig. 4(d), the optimum one-step deposition process occurs on the basis of the phase diagram at the minimal value of *R* = 110, i.e., the smallest *R* value possible such that the *i*-layer evolves to dominantly nc-Si:H during its growth [18]. At *R* = 100 the (a+nc) → a transition occurs at a thickness of 150nm, and it is clear from the V_{oc} value of 0.95V in Fig. 4(d) that the top of the film is a-Si:H. At *R* = 120 the (a+nc) → nc transition occurs at a thickness of 20nm, and in this case, it is clear from the V_{oc} value of 0.46V that the top of the film is nc-Si:H. The highest performance nc-Si:H i-layer in Fig. 4(d) is observed at *R* =110, just before a more rapid drop in fill factor associated with the bifurcation region. For a higher substrate temperature, in which case the maximum nc-Si:H solar cell fill factor is larger, the rapid drop is even more dramatic. The continued lower fill factor for the low *R* Si:H films in Fig. 4(d) relative to those of Fig. 4(b) is attributed to the nc-Si:H phase at the bottom of the *i*-layer (about 40nm-thick for *R* = 60). Overall, these results demonstrate clear correlations between structural evolution from RTSE and solar cell performance that enable single-step, multi-step, and graded layer optimization.

CdTe

CdTe is used widely in thin-film photovoltaics as a *p*-type semiconductor serving as the active layer, along with CdS as its *n*-type heterojunction partner serving as a window layer. Thin films of CdTe can be produced by several different methods including vapour transport deposition (VTD), close-space sublimation (CSS), and rf magnetron sputtering [23]. The work reviewed here focuses on the use of RTSE to study thin films deposited by magnetron sputtering [24]. Although the sputter deposition rates of CdTe are generally slower, this deposition method is of interest because it allows one to fabricate efficient solar cell devices in a relatively low temperature process, limited by the temperature of the post-deposition treatment (~ 400°C). Also, by controlling sputtering parameters such as the temperature, pressure, and power, the growth mechanisms can be controlled, including the surface mobility of the deposited species, the bombardment energy and directionality of incident species, and the deposition rate/kinetics, respectively. These mechanisms determine the nano/microstructure of the sputter-deposited film [25, 26].

Fig. 5(a) shows the dielectric functions for bulk single crystal CdTe (c-CdTe) and an as-deposited polycrystalline CdTe film sputtered to 100nm thickness at 188°C [19]. Fig. 5(b) compares the room temperature dielectric functions of polycrystalline CdS films 50nm-thick fabricated at substrate temperatures of 145°C and 310°C [19]. All thin-film measurements were performed at room temperature by in-situ spectroscopic ellipsometry under vacuum before exposure of the freshly-deposited film to laboratory air. CdTe exhibits four critical points (CPs) over the energy range of 0.75 < E < 6.5eV and CdS exhibits three CPs. In general, the CP amplitudes depend on the density of the material, the CP energies depend on the strain and the measurement temperature, and the CP widths depend on the grain size and measurement temperature. The lowest-energy CP, denoted E_0, represents the fundamental bandgap. For CdTe, the very broad dielectric function features for the thin film relative to c-CdTe are due to its fine grained structure. The blue-shifted E_0 energy for the polycrystalline CdTe film relative to c-CdTe is due to strain in the film. In addition, from the results for CdS, one can conclude that the grain size of this material increases with increasing substrate temperature.

The effects due to strain and grain size can be quantified by modelling the dielectric function as a sum of direct interband resonances at the band structure CPs using the parabolic band approximation with Lorentzian broadening. The nth CP generates the following lineshape in the complex dielectric function ε [13,22,27,28]:

$$\varepsilon(E) = A_n \exp(i\phi_n)\,[E - E_{0n} + i(\Gamma_n/2)]^{\mu n}, \quad (1)$$

where E is the photon energy, A_n is the nth CP amplitude, E_{0n} is the associated CP energy, Γ_n is the broadening energy, ϕ_n is the phase, and μ_n is the exponent. Considering as an example, a sample-dependent grain radius R, which controls the mean free path λ of the excited carriers associated with the nth CP, the following applies:

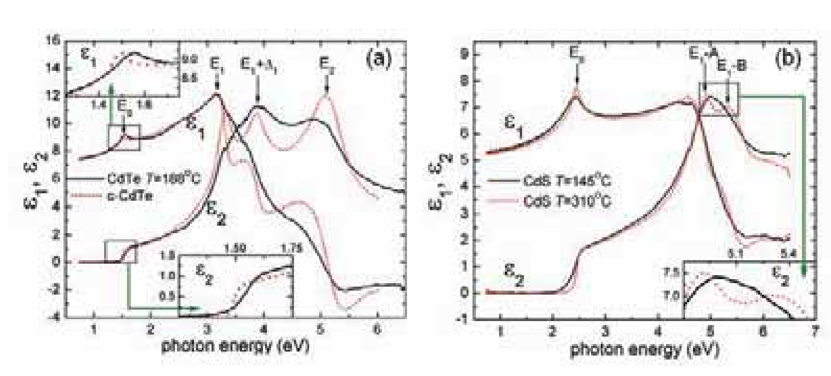

Figure 5. (a) Comparison of the room temperature dielectric function of an as-deposited polycrystalline CdTe thin-film magnetron sputtered at 188°C with that of c-CdTe [19]; (b) comparison of the room temperature dielectric functions of polycrystalline CdS thin films magnetron sputtered at 145°C and 310°C [19].

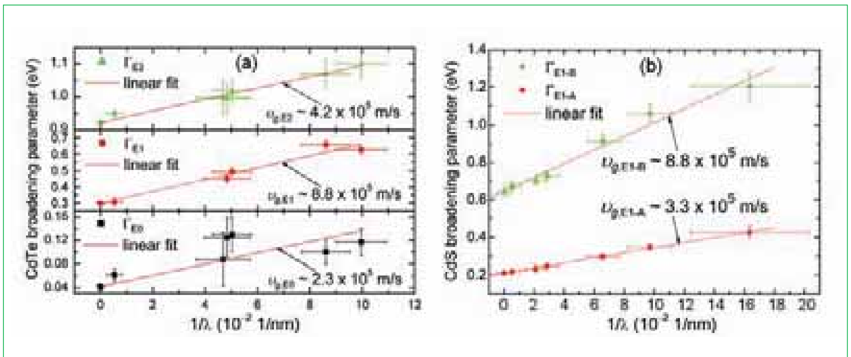

Figure 6. Broadening parameters plotted as functions of the reciprocal of the deduced mean free path for (a) CdTe and (b) CdS. The group speeds of excited carriers are calculated from the slopes of the linear fits using Equation 2 [19]. The poorer linearity for the CdTe E_0 is due to the large penetration depth, which leads to an averaging of the film structure at different depths.

$$\Gamma_n = \Gamma_b + (h v_n/\lambda), \quad (2)$$

where λ ~ R as a result of grain boundary scattering [19]. This expression is derived from the energy-time uncertainty principle, such that Γ_b is the single crystal CdTe broadening parameter, h is Planck's constant, and v_n is the group speed of the excited carriers. The mean free path λ can be extracted from the Γ_n values for the dominant CPs of CdTe and CdS, using estimates of v_n for these CPs derived from the band structure. Then, the other Γ_n values can be plotted versus 1/λ to evaluate the validity of the above relationship [19].

The results for the CPs of CdTe and CdS for two sets of samples fabricated at different substrate temperatures are shown in Fig. 6(a) and (b), respectively [19]. The points at 1/λ = 0 for CdTe are results for c-CdTe, and the nearby point is a $CdCl_2$ treated CdTe thin film. The linearity of the data for each of the higher energy critical points demonstrates consistency with Equation 2. These results have two implications: (i) that a meaningful mean free path can be extracted from the full set of CP broadening parameters for a given CdTe or CdS thin-film material; and

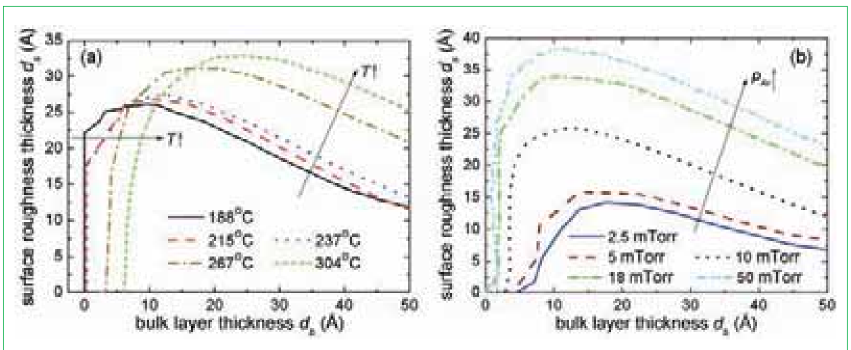

Figure 7. (a) Surface roughness evolution for CdTe thin films sputtered at different substrate temperatures [29]; (b) surface roughness evolution for CdTe thin films sputtered at different Ar pressures [30].

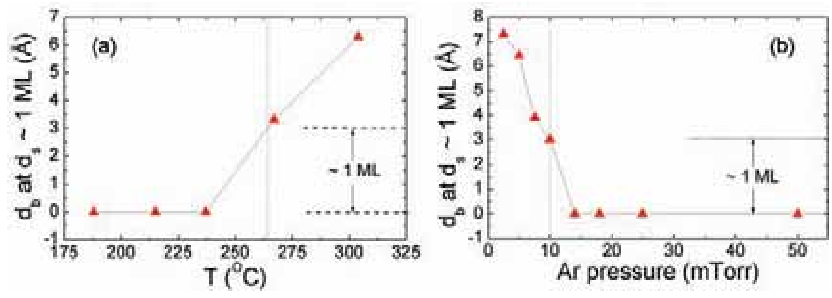

Figure 8. Bulk layer thickness d_b at a surface roughness layer thickness d_s of 1ML for CdTe thin films sputtered at different (a) temperatures and (b) Ar pressures.

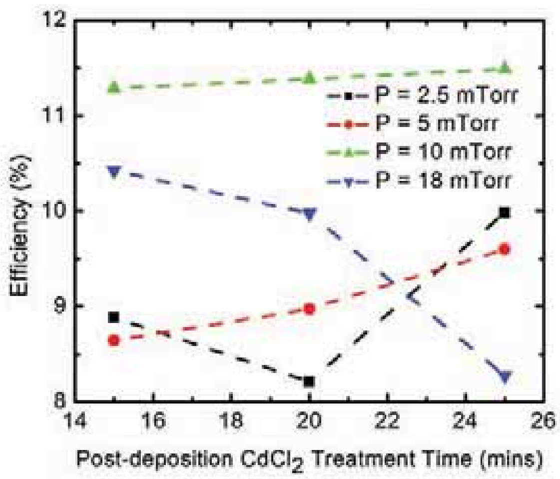

Figure 9. Efficiency of CdTe solar cells prepared at different Ar pressures as a function of the post-deposition $CdCl_2$ treatment time [30].

(ii) that in modelling dielectric functions of either CdTe or CdS, and accounting for their dependences on processing, one can replace the full set of broadening parameters Γ_n by a single mean free path that controls all of them, once the appropriate group speeds are available. For CdTe, for example, this reduces by three the number of lineshape parameters needed to model the dielectric function. A similar approach can be used to model strain, in which case each critical point energy E_{on} is controlled by strain, again reducing the number of lineshape parameters by three.

In further RTSE analyses of CdTe thin films, the nucleation and growth dynamics have been characterized as a function of the substrate temperature T and Ar pressure p_{Ar} [29,30]. These films were deposited onto silicon wafers covered with native SiO_2 due to their smoothness, reproducibility and well-known optical properties. Figs. 7(a) and 7(b) show the surface roughness thickness evolution for the temperature and pressure series, respectively, for the first ~ 5nm of growth [30]. In this case, for T < 267°C and for p_{Ar} >10mTorr, it is clear that surface roughness develops before a bulk-like layer is formed, which can be interpreted in terms of initial cluster growth, followed by bulk-like layer growth. In contrast, for T ≥ 267°C and p_{Ar} ≤ 10mTorr, a thin bulk-like layer is formed before surface roughness starts to develop, interpreted in terms of initial layer growth followed by cluster growth. These different initial growth modes are more pronounced when viewing plots of the bulk-like layer thickness at a cluster layer thickness of ~ 1 monolayer (ML), as shown in Figs. 8(a) and 8(b) for the temperature and pressure series, respectively.

These results from RTSE were also considered in view of CdTe solar cell performance. Thus, several devices were produced at different CdTe Ar pressures [30]. Each device underwent $CdCl_2$ post-deposition treatment for times ranging from 15 to 25 minutes and the resulting efficiency for each device is shown in Fig. 9. This figure shows that films deposited at low pressure appear to require longer treatment times for higher efficiency, whereas films deposited at high pressure (p_{Ar} = 18mTorr) appear to require shorter times. The best devices were obtained for p_{Ar} = 10mTorr, where the efficiency is not strongly dependent on treatment time. It has been suggested that this pressure is consistent with the transition in initial growth mode as observed by RTSE, and that a microstructure for optimum $CdCl_2$ treatment may be obtained in this transition region.

CIGS

The I-III-VI_2 chalcopyrite alloy system $Cu(In_{1-x}Ga_x)Se_2$ (CIGS) and related absorber material systems represent one of the most promising second-generation thin-film technologies for photovoltaic applications [31]. The very rough surfaces of such thin films at the thicknesses (1–2μm) used in photovoltaic devices imply that optical analysis can be challenging due to the reduction in irradiance of specularly transmitted and reflected light beams via scattering. Because the surface roughness increases in thickness during film growth, one way to avoid this problem is to perform measurements during film growth and to extract the dielectric function at a bulk layer thickness in the range of ~ 40–100nm. In general, such an approach enables an accurate surface roughness correction and avoids post-deposition oxidation, as well. This general approach was also utilized to obtain the dielectric functions for the CdTe and CdS films in Fig. 5 of the previous subsection. Such high accuracy dielectric functions deduced versus measurement temperature using this methodology can be expected to serve in future RTSE analyses, not only for analyzing the growth dynamics of alloy layers as in this article, but also for on-line monitoring in a manufacturing environment.

The CIS and CIGS thin films studied here were grown by codeposition on

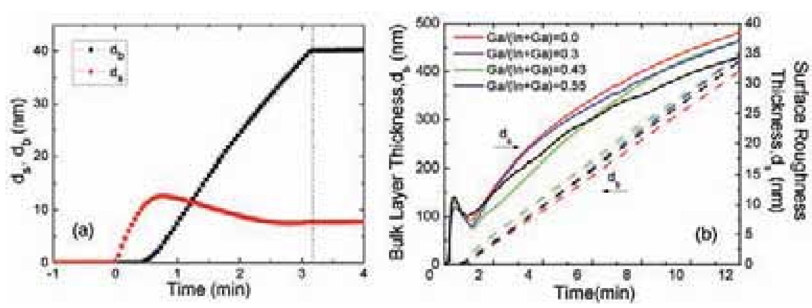

Figure 10. (a) Time evolution of surface roughness layer thickness d_s and bulk layer thickness d_b in the initial stages of growth for a thin $CuInSe_2$ film; (b) similar results over a wider time range highlighting the surface roughening for CIS as well as for CIGS with x = 0.30, 0.43 and 0.55. In (b) the solid lines correspond to d_s and the broken lines to d_b.

Si(100) substrates held at a temperature in the range from 550 to 570°C. The CIS exhibited an average composition of Cu = 22%, In = 23%, and Se = 55%, a total thickness of ~50nm, a root mean square surface roughness of ~10nm, and a single α-phase with a slight preference in (112) orientation, as reported by a variety of *ex situ* measurements.

Fig. 10(a) shows the typical time evolution of both the surface roughness layer thickness (d_s) and the bulk layer thickness (d_b) deduced from RTSE data collected in the initial stages of the growth of a thin CIS film [32]. The Cu, In and Se shutters were opened and closed simultaneously at time zero and after 3.2 minutes of codeposition, respectively. Initial growth of the film is observed in the form of islands which increase to 11nm in thickness before the onset of bulk layer growth. The islands continue to grow until the onset of coalescence, as indicated by a decrease in d_s with an associated more rapid increase in d_b. Thereafter the film continues to smoothen as d_b increases approximately linearly with an average rate of 15nm/minute until shutter closure (dashed vertical line). The final values of surface roughness (d_s = 7.7nm) and total thickness ($d_b + d_s$ = 47.9nm) are in good agreement with those from *ex-situ* measurements. A weak upturn in d_s visible near three minutes in Fig. 10(a) represents the onset of roughening which is explored in greater detail in Fig. 10(b). This latter figure shows corresponding results over a longer time duration for CIS and CIGS with x = 0.30, 0.43, and 0.55.

For each deposition in Fig. 10(b), the dielectric functions of the bulk layer can be determined at the deposition temperature. As an example, dielectric functions of the CIS bulk layer of Fig. 10(a) are shown in Fig. 11(a). Two representative results are displayed; one was obtained from real-time data acquired at the growth temperature of 550°C whereas the other was obtained from data acquired *in-situ* after cooling to 20°C. For further interpretation of these dielectric functions, an optical averaging effect in the polycrystalline films may be taken into account due to the anisotropy of single-crystal CIS [33-37]. Given the uniaxial nature of the tetragonal chalcopyrite crystal structure of CIS and the lack of a strong orientation of the studied films, however, it is expected that the dielectric functions of Fig. 11(a) more closely resemble the ordinary component of the single crystal dielectric function [34].

A comparison of the results in Fig. 11(a) reveals characteristic red shifts of the CP energies and increases in CP broadening parameters with increasing temperature. These can be quantified by modelling each of the dielectric functions as a sum of direct interband resonances at the band structure CPs according to Equation 1. A sum of up to 12 CPs was used to simulate the convolved dielectric functions of the polycrystalline CIS thin films along the ordinary and extraordinary rays. The CP energies obtained with such fits were found to agree well with results reported for single crystals [33], whereas three high-energy transitions at 5.11, 5.41 and 5.91eV have been identified for the first time in the RTSE study. With the availability of 12 CP energies, it may be possible in the future to track composition, sample temperature and possibly strain from the RTSE data, assuming the appropriate database components have been established.

Due to the complexity of the CIGS material system as well as the solar cell stack itself, many other opportunities exist for RTSE in the evaluation and possible control of the CIGS growth processes. For example, Fig. 11(b) (lower panel) compares the imaginary parts of the dielectric functions of a CIGS layer extracted at various times for a thin film grown by a two-stage process from a Cu-rich film to a Cu-poor film. Fig. 11(b) (upper panel) shows corresponding results for a CIGS film grown from Cu-poor to Cu-rich. Below the onset of the band gap in both cases, the magnitude of the imaginary part of the dielectric function ε_{2f} scales with Cu content [38]. Thus in a transition from Cu-rich to Cu-poor, there is a monotonic decrease in ε_{2f} below the band gap. This effect is the result of a decrease in free carrier concentration which can be modelled with a Drude contribution to the dielectric function, given by:

$$\varepsilon = -A_D^2 (E^2 + i\Gamma_D E)^{-1} \qquad (3)$$

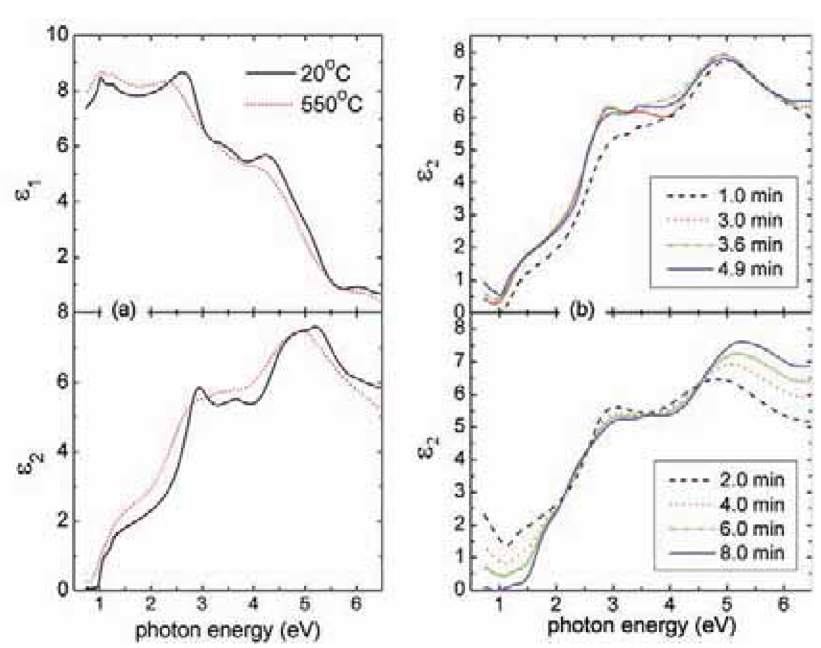

Figure 11. (a) CIS bulk layer dielectric functions at 550°C and 20°C; (b)the imaginary parts of the dielectric functions of a CIGS layer extracted at various times for a thin film grown by a two-stage process from a Cu-rich film to a Cu-poor film (lower panel); results for a CIGS film grown from Cu-poor to Cu-rich (upper panel) [38].

where A_D and Γ_D are Drude amplitude and broadening parameters. The free electrons in Cu-rich CIGS film are suspected to arise from a conducting $Cu_{2-x}Se$ semimetal phase at the grain boundaries and on the surface [39]. The presence of a conductive phase was also confirmed at the end of the deposition by a sheet resistance measurement, which was 5kΩ/☐ for the Cu-rich films of Fig. 11(b) (top panel) and 70MΩ/☐ for the Cu-poor films of Fig. 11(b) bottom panel [38]. Although the magnitude of these ε_{2f} variations appear small in Fig. 11(b), the large thickness of film amplifies the effect in the (ψ, Δ) data, leading to the ability to control the Cu content simply on the basis of the RTSE output versus time at low energy.

The Cu-poor films of Fig. 11(b) (bottom) were grown after a Cu-rich phase, whereas the Cu-poor films of Fig. 11(b) (top) were grown before the Cu-rich phase, with an initial growth comparable to a one-stage process [38]. Determination of Γ_n values show that films that are Cu-poor at the end of the deposition (Fig. 11(b), bottom) have a longer mean free path than those that are Cu-rich at the end of the deposition (Fig. 11(b), top). XRD measurements and AFM images taken after film growth reveal a larger grain size for the final films that are Cu-poor. Thus, the longer mean free path determined for those films reflects the process of grain boundary scattering, and demonstrates that the CP widths are providing key processing information towards optimum CIGS materials for device applications.

Summary and future directions

Polarization spectroscopies, in particular optical methods based on spectroscopic ellipsometry, are becoming increasingly popular as the interest in developing, optimizing and scaling up thin-film photovoltaic devices has grown. Real-time spectroscopic ellipsometry (RTSE) allows one to study the characteristics of thin-film growth processes ranging from the initial nucleation and coalescence stage to the final film structural depth profile. A sampling of information that can be extracted from RTSE has been provided in this article and includes: (i) phase diagrams that can guide optimization in the case of Si:H thin films; (ii) material quality and growth mode determination in the case of CdTe thin films; and (iii) Cu content and final material quality in the case of CIGS thin films. These examples provide insights into why solar cells deposited under different conditions result in varying efficiencies, and overall, they help in process development for thin films deposited by different techniques including plasma-enhanced chemical vapour deposition, magnetron sputtering and multi-source evaporation.

As shown in this article, RTSE is well established for the characterization of thin-film photovoltaic materials in a research and development environment; however, excellent prospects also exist for expansion to the pilot and full-scale production environments. For example, RTSE can be applied to monitor solar cell fabrication on flexible substrates in roll-to-roll processes. In this case, one can track the initial start-up of the deposition process and the stability at a particular thickness point in the process. Also, using a dielectric function database obtained from RTSE measurements, one can characterize completed solar devices *ex-situ* for relevant information such as component layer thicknesses and compositions. For superstrate modules deposited on glass, the glass/film-stack interface is generally smoother than the film back-side, and this motivates the technique of through-the-glass ellipsometry. The interest in studying large-area partially or fully completed modules from production lines motivates mapping spectroscopic ellipsometry, in which case thickness and compositional maps can provide insights into process uniformity.

Acknowledgments

The authors gratefully acknowledge support from DOE Grants No. DE-FG36-08GO18067 and DE-FG36-08GO18073 and from the State of Ohio Third Frontier's Wright Centres of Innovation Program. Prof. André Ferlauto, Prof. Nikolas Podraza, Dr. Vikash Ranjan, Dr. Simon Cao, Lila Dahal, Naba Paudel and Jason Stoke contributed to the research described herein.

References

[1] Luque, A. & and Hegedus, S. (eds.), 2003, *Handbook of Photovoltaic Science and Engineering*, John Wiley & Sons, Somerset, NJ.

[2] Herman, I. P. 1995, *Optical Diagnostics for Thin Film Processing*, Academic, New York.

[3] Azzam, R. M. A. & Bashara, N. M. 1977, *Ellipsometry and Polarized Light*, North-Holland, Amsterdam.

[4] Tompkins, H.G. 1992, *A User's Guide to Ellipsometry*, Academic, New York.

[5] Fujiwara, H. 2007, *Spectroscopic Ellipsometry: Principles and Applications*, John Wiley & Sons, West Sussex UK.

[6] Tompkins, H.G. & Irene, E.A. (eds.), 2005, *Handbook of Ellipsometry*, William Andrew, Norwich NY.

[7] (a) Boccara, A.C., Pickering, C. & Rivory, J. 1993 (eds.), *Proc. 1st ICSE*, Elsevier, Amsterdam (also published as Thin Solid Films, pp. 233–234).
(b) Collins, R.W., Aspnes, D.E & Irene, E.A. (eds.) 1998, *Proc. 2nd ICSE*, Elsevier, Amsterdam (also published as Thin Solid Films, pp. 313–314).
(c) Fried, M., Humlicek, J. & Hingerl, K. (eds.) 2003, *Proc. 3rd ICSE*, Elsevier, Amsterdam.
(d) Arwin, H., Beck, U. & Schubert, M. (eds.), 2007, *Proc. 4th ICSE*, Wiley-VCH, Weinheim, Germany.
(e) Tompkins, H.G. et al. (eds.) 2011, *Proc. 5th ICSE*, Elsevier, Amsterdam, in press.

[8] Aspnes, D.E. & Studna, A.A. 1975, "High precision scanning ellipsometer",

Appl. Opt. Vol. 14, pp. 220.
[9] (a) Palik, E.D. 1985, *Handbook of optical constants of solids*, Academic, New York.
(b) Palik, E.D. 1991, *Handbook of optical constants of solids II*, Academic, New York.
[10] Aspnes, D.E. 1976, "Spectroscopic ellipsometry", in Seraphin, B.O. (ed.), *Optical Properties of solids: new developments*, North-Holland, Amsterdam, p. 799.
[11] Collins, R.W. et al. 2005 "Multichannel ellipsometry", in Tompkins, H.G. and Irene, E.A. (eds.), *Handbook of ellipsometry*, William Andrew, Norwich NY, p. 481.
[12] Wooten, F. 1972, *Optical properties of solids*, Academic, New York.
[13] Collins, R.W. & Ferlauto, A.S. 2005, "Optical physics of materials", in Tompkins, H.G. & Irene, E.A. (eds.), *Handbook of ellipsometry*, William Andrew, Norwich NY, p. 93.
[14] Jellison, Jr., G.E. "Data analysis for spectroscopic ellipsometry", in Tompkins, H.G. & Irene, E.A. (eds.), 2005 *Handbook of ellipsometry*, William Andrew, Norwich, NY, p. 237.
[15] Aspnes, D.E. 1982, "Optical properties of thin films", *Thin Solid Films*, Vol. 89, p. 249.
[16] Fujiwara, H. et al. 2000, "Assessment of effective-medium theories in the analysis of nucleation and microscopic surface roughness evolution for semiconductor thin films", *Phys. Rev. B*, Vol. 61, p. 10832.
[17] Hauge, P. S.1980, "Recent developments in instrumentation in ellipsometry", *Surf. Sci.*, Vol. 96, p.108.
[18] Stoke, J.A. et al. 2008, "Optimization of Si:H multijunction n-i-p solar cells through the development of deposition phase diagrams", *Proc. 33rd IEEE PVSC*, New York, Art. p. 413.
[19] Li, J., Podraza, N.J. & Collins, R.W. 2007, "Real time spectroscopic ellipsometry of sputtered CdTe, CdS, and $CdTe_{1-x}S_x$ thin films for photovoltaic applications", *Phys. Stat. Sol. (a)*, Vol. 205, p. 91.
[20] Deng, X. & Schiff, E.A. 2003, "Amorphous silicon-based solar cells" , in: A. Luque and S. Hegedus (eds.), *Handbook of photovoltaic science and engineering*, John Wiley & Sons, Somerset, New Jersey, p. 505.
[21] Collins, R.W. et al. 2003, "Evolution of microstructure and phase in amorphous, protocrystalline, and microcrystalline silicon studied by real-time spectroscopic ellipsometry", *Solar Energy Materials and Solar Cells*, Vol. 78, p.143.
[22] Lautenschlager, P. et al. 1987, "Temperature dependence of the dielectric function and interband critical points in silicon", *Phys. Rev. B*, Vol. 36, p. 4821.
[23] McCandless, B.E. & Sites, J.R. 2003 "Cadmium telluride solar cells", in Luque, A. & Hegedus, S. (eds.), *Handbook of Photovoltaic Science and Engineering*, John Wiley & Sons, Somerset, New Jersey, p. 617.
[24] Compaan, A.D. et al. 2009, "Magnetron sputtering for II-VI solar cells: thinning the CdTe", *Mat. Res. Soc. Symp. Proc.*, Paper M09-01, Vol. 1165, MRS, Warrendale, PA.
[25] Messier, R., Giri, A.P. & Roy, R.A. 1984 "Revised structure zone model for thin film physical structure", *J. Vac. Sci. Technol. A*, Vol. 2, p. 500.
[26] Mirica, E., Kowach, G. & Du, H. 2004, "Modified structure zone model to describe the morphological evolution of ZnO thin films deposited by reactive sputtering", *Crystal Growth and Design*, Vol. 4, No.157.
[27] Lautenschlager, P. et al. 1987, "Interband critical points of GaAs and their temperature dependence", *Phys. Rev. B*, Vol. 35, p. 9174.
[28] Aspnes, D.E., in Balkanski, M. (ed.) 1980, *Handbook on semiconductors*, North-Holland, Amsterdam, Vol. 2, Chap. 4A.
[29] Li, J. et al. 2006, "Real-time spectroscopic ellipsometry of sputtered CdTe: effect of growth temperature on structural and optical properties", *Proc. 4th World Conf. Photovolt. Energy Conv*, p. 392.
[30] Sestak, M.N. et al. 2009, "Real-time spectroscopic ellipsometry of sputtered CdTe thin films: effect of Ar pressure on structural evolution and photovoltaic performance", *Mat. Res. Soc. Symp. Proc.*, MRS, Warrendale PA, Vol. 1165, Paper M09-02.
[31] Repins, I. et al. 2008, "19.9%-efficient $ZnO/CdS/CuInGaSe_2$ solar cell with 81.2% fill factor", *Prog. Photovolt.*, Vol. 16, p. 235.
[32] An, I. et al. 1990, "Microstructural evolution of ultrathin amorphous silicon films by real time spectroscopic ellipsometry." *Phys. Rev. Lett.* Vol. 65, p. 2274.
[33] Alonso, M.I. et al. 2001, "Optical functions and electronic structure of $CuInSe_2$, $CuGaSe_2$, $CuInS_2$, and $CuGaS_2$", *Phys. Rev. B*, Vol. 63, p. 75203.
[34] Alonso, M.I. et al. 2000, "Optical properties of chalcopyrite $CuAl_xIn_{1-x}Se_2$ alloys" *J. Appl. Phys.*, Vol. 88, p. 5796.
[35] Paulson, P.D., Birkmire, R.W. & Shafarman, W.N. 2003, "Optical characterization of $CuIn_{1-x}Ga_xSe_2$ alloy thin films by spectroscopic ellipsometry", *J. Appl. Phys.*, Vol. 94, p. 879.
[36] Kawashima, T. et al. 1998, "Optical constants of $CuGaSe_2$ and $CuInSe_2$", *J. Appl. Phys.*, Vol. 84, p. 5202.
[37] Kreuter, A. et al. 2001, "Anisotropic dielectric function spectra from single-crystal $CuInSe_2$ with orientation domains", *Appl. Phys. Lett.*, Vol. 78, p.195.
[38] Marsillac, S. Et al. 2008, "In-situ study of CIGS dielectric function as a function of copper content", *Proc. 35th IEEE PVSC*, p. 866.
[39] Schock, H.W. 2004, "Properties of chalcopyrite-based materials and film deposition for thin-film solar cells", Y. Hamakawa, (ed.), *Thin-film Solar Cells: Next Generation Photovoltaics and its Applications*, Springer, Berlin, p.163.

About the Authors

Dr. Robert W. Collins is a professor and NEG endowed chair in the department of physics and astronomy at the University of Toledo, Ohio. He co-directs the Center for Photovoltaics Innovation and Commercialization and has been involved in research and development of thin-film photovoltaics since 1976.

Dr. Jian Li received his Ph.D. from the University of Toledo, Ohio in 2010 and is currently a post-doctor at the National Renewable Energy Laboratory, Colorado. His research interests involve the development and application of spectroscopic ellipsometry.

Dr. Sylvain Marsillac is an associate professor in the department of electrical and computer engineering at Old Dominion University, Virginia. He specializes in the science and engineering of solar cell fabrication and characterization. He has authored more than 100 papers in peer-reviewed journals and conference proceedings.

Michelle N. Sestak is currently a doctoral student at the University of Toledo, Ohio. Her thesis research includes application of spectroscopic ellipsometry for the study of II-VI thin-film photovoltaic materials.

Enquiries

Center for Photovoltaics Innovation & Commercialization and Department of Physics & Astronomy, University of Toledo, Toledo, Ohio 43606, USA
Tel: +1 419 530 3843
Email: robert.collins@utoledo.edu

National Renewable Energy Laboratory, 1617 Cole Boulevard, Golden, Colorado, 80401, USA

Department of Electrical & Computer Engineering
Old Dominion University, Norfolk, Virginia 23529, USA

CdTe thin-film modules: basic developments, optimizing performance and considerations in module design

Frank Becker & **Hubert-Joachim Frenck**, Calyxo GmbH, Bitterfeld-Wolfen, Germany

ABSTRACT

A growing number of thin-film photovoltaic module producers are either trying to keep up with the current cost leader or aiming to differentiate on product design. Calyxo is dedicated to both keeping the pace in the US$0.50/Wp race and introducing new product generations, therefore delivering more value to the customer. We have tried to improve the methodology and approaches for knowledge building in the individual process steps, by learning the relevant interactions between them, as well as ramping volume and lowering manufacturing cost in the first production line. Developing and building the deposition equipment suited to the high process temperatures of approximately 1000°C at atmospheric pressure took some time, but the technology itself now enables Calyxo to benefit from significant cost savings both on capital investment and operational cost – compared to some well-known vacuum deposition methods. Besides the continuous decrease in manufacturing costs, even early on in building the manufacturing capacity, the ability to design the product itself according to the needs of the customers proved itself to be a decisive factor in ensuring competitiveness. This paper aims to give an insight into some of the basic design features of a new product generation and how the so-called new CX3 product will generate more watts by improved performance: delivering better customer value by decreased voltage to save on BOS costs and ensuring further increased field durability through an optimized package design.

Introduction

There are numerous accounts on the details of transferring scientific results to production and ramping up thin-film PV manufacturing lines. This paper will add to these considerations the notion of a holistic approach to PV module design criteria, covering aspects from manufacturing to special package consideration, and how it will affect the process of transfer and eventual ramp-up of a new technology. The process used by Calyxo will serve as an example.

Established in 2005 and based on a technology invented by SolarFields (Perrysburg USA), Calyxo has since developed a unique deposition method for thin-film CdTe solar cells known as atmospheric pressure physical vapour deposition (APPVD). This sets forward certain specific boundary conditions for the process steps to complete a solar module, as the knowledge regarding the individual process steps – as well as the relevant intermediary interactions – needed to be developed while also ramping up production.

This study will report on this unique deposition method and give an account of some of the major aspects of thin-film solar module process development. The specifics of package and device design will be discussed in some detail. One particular focus will be on the fact that our CdTe modules are manufactured using the so-called superstrate technique, giving rise to advantages in solar module design. An account is given of common features of thin-film PV developments

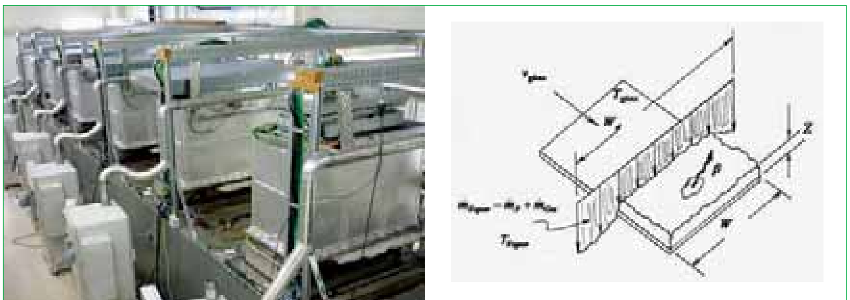

Illustration by Kenneth R. Kormanyos.

Figure 1. Evaporation and powder feed units at an APPVD furnace. The left-hand picture was taken during ramp-up of the furnace. The right-hand schematic illustrates the principle of APPVD film formation.

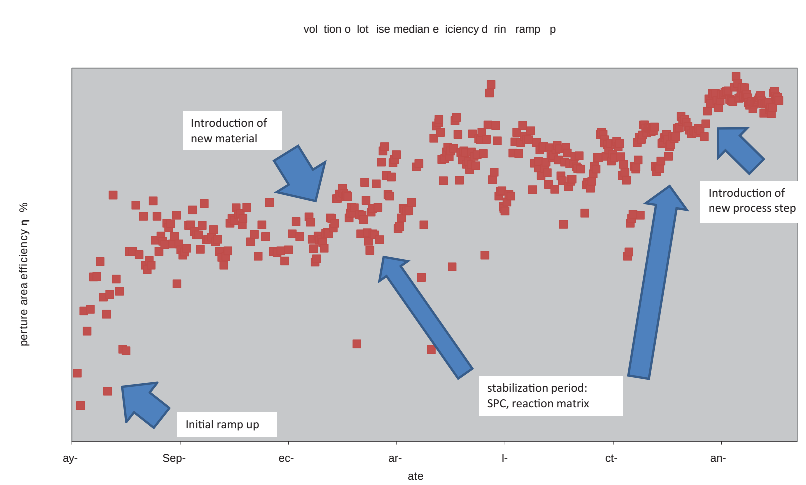

Figure 2. Evolution of lotwise efficiencies during ramp-up of a CdTe production process. Each lot is 1,000 modules strong. The arrows mark the parts of the ramp-up that are discussed in detail in the text.

and some of the specifics of the CdTe technology employed are highlighted.

APPVD process for CdTe semiconductor deposition

With any thin-film deposition process there are numerous competing approaches to successfully deposit CdS/CdTe films for solar applications. These include sputtering [1], close-space-sublimation (CSS) [2], vacuum-transport-deposition [3] or APPVD [4], to name but a few. Among those, the APPVD approach has received some attention because of its potentially intrinsic low costs for initial expenditure as well as high material utilization rates [6], although it is deemed difficult to both establish a reliable process and transfer into mass production [7].

Atmospheric processes differ from the more widely used thin-film vacuum technologies in a number of respects. The mean free path of particles hitting any surface is substantially shorter than with vacuum technologies. While this is challenging because it may lead to nucleation in the deposition – which in turn may lead to dust formation in the deposited films in case of the solid-gaseous two-phase system – there is also the incentive that potentially dynamic deposition rates exceed those of comparable vacuum technologies. These two processes compete in any atmospheric thin-film processes. It is necessary to design process and machinery in such a way that the balance of film formation on the substrate is favourable for thin-film nucleation. The parameters to be controlled to this end are temperature, gas flow and mixture.

Since the dynamic deposition rate is the parameter that determines the rate at which a work piece can be transported through a given set of machinery, it eventually lowers the limits of expenditure necessary for a thin-film deposition apparatus. Therefore, Calyxo has always chosen the atmospheric process as the core process for CdS/CdTe deposition [4].

Fig. 1 shows a purpose-built APPVD furnace for commercial manufacturing of CdS/CdTe semiconductor thin films. The furnace shown in Fig. 1 features six vaporizer stations which can either be run in parallel to achieve a high throughput or run alternately to achieve a maximum MTBM (mean-time-between-maintenance) for the APPVD furnace as a whole. This way, a maximum MTBM of 1,200h with dynamic deposition rates of the order of 1µm/s has been demonstrated in full-scale production. The deposition rate is realized by a very small effective area of deposition. This is illustrated by the schematic drawing on the right-hand side of Fig. 1. As a positive by-effect, any parasitic effects due to process-substrate-deposition reactor interactions are also minimized, since the necessary temperatures for deposition are achieved in the deposition zone only.

The following section will discuss some of the basic considerations that determine this optimization process.

Ramping up a novel thin-film production line

While thin-film processes have been known and explored for a long time [5] and have found widespread application in such diverse industries from car-making to nanoelectronics, the challenge of transferring thin-film technologies from lab to pilot scale and then to full production still remains. Most of this challenge originates in the fact that the task of transferring opens a multi-parameter space in all terms, from process limitations to manufacturing requirements. Hence, it is obviously beyond the scope of a technical paper to give a detailed account of the transfer process and every detail that needs to be considered. Nevertheless, it is worthwhile to note that common features can apply to any transfer process. There is much to be learned for future upgrading steps or introduction of new and potentially disruptive technologies by looking at the broader picture and analysis of the basic motivation for major developments.

Fig. 2 shows the median efficiencies of distinct production lots during the ramp-up phase. The data on the production result

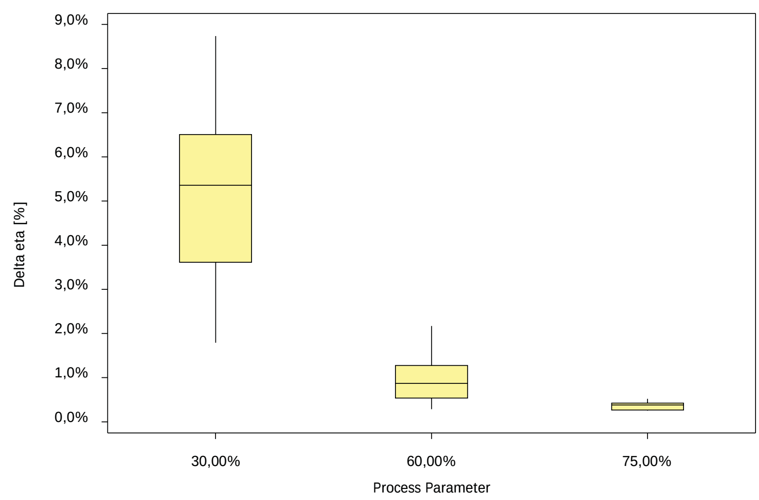

Figure 3. Example for reduction of variability of a production process by adjusting specific process parameters.

stretches over a significant period of time (and thus hundreds of thousands of modules), representing a good portion of a ramp-up scenario. From the data in Fig. 2 it may be concluded that ramping up a novel production of thin-film modules is characterized by several distinct phases if the major output variable, module efficiency, is taken as a measure. Initially, improvements in efficiency are easy to achieve. These improvements are mainly the result of replacing manual production steps by industrial machinery. Not only do the process parameters set forth on the lab scale need to be transferred, but also the geometric dimensions and interaction are altered. The machinery introduced also ensures that the variation is reduced, and parameters may be controlled far more effectively, thus increasing the efficiency as well. Therefore faults and errors (e.g. miscalculated transfer ratios of process parameters) are obvious, found quickly and tend to contribute significantly.

> "These improvements are mainly the result of replacing manual production steps by industrial machinery."

Still, it can be seen clearly in Fig. 2 that variation in efficiency remains comparatively large throughout this period.

The second event noted in Fig. 2 is the introduction of a new raw material into the production process. While in earlier experiments the positive effect was clearly identified, it is almost invisible because of the large fluctuation of net output at that time. This example is to illustrate one of the most imminent dangers during ramp up; a major analytical effort was necessary to stick with the introduction since at first glance the experimental result did not show itself in production volume. This is quite often the case on introducing new process steps and/or materials, and this is a pitfall that needs to be safely avoided. To avoid this, some 2,500 data sets from 13 individual process steps were continuously monitored. Included were machine parameters, process settings, film properties and module readings. From the sheer number of data sets monitored, it is clear that a great understanding of the underlying technical and physical processes is necessary to separate the parameters from having major second-order effects. It is impossible to discuss the influence of every single data set or process step, so the effect of tuning specific process parameters will be discussed with one example. It is shown that both optimizing maximum efficiency of the devices produced, as well as reducing noise, is achievable.

It is shown in Fig. 2 that the next step is mainly characterized by reducing the variation of the efficiencies of the modules produced. A reduction of noise can be achieved through a variety of measures. These include, among others:

- Introduction of an SPC-based production system, preferably based on an automated MES system.
- In-line control systems with short and frequent feed-back loops. These feed-

	CX1 design	CX3 design
V_{max} Inverter	600V	600V
V_{oc} Module	90V	60V
Max No. of modules in string	6	10

Table 1. Sample calculation of maximum string length in a solar array.

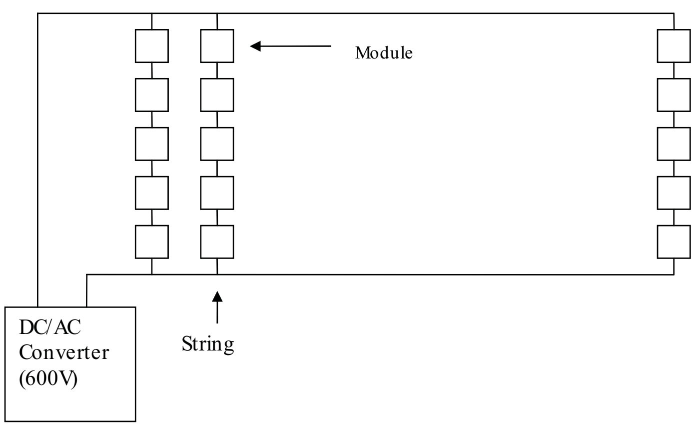

Figure 4. Schematic drawing of a PV array.

Figure 5. Schematic drawing of the monolithic serial connection of individual cells in a thin-film module.

back loops may be automated, but in a ramp-up situation it is more important to establish the right correlations first.

- Specialized reactions matrices to deal with deviations anytime, anyplace.
- Reduced noise in the individual process steps.

As obvious as the last point may be, it is often overlooked. Fig. 3 gives an example of the improvement of a specific process step. One specific process parameter was investigated. At one particular point it was noted that fluctuation was at a high level. In the experiment represented in Fig. 3, the setting of this process parameter in the production flow was adjusted during ramp-up. Results were compared to the maximum efficiency of the champion cell of the basic process as established in small-scale experiments before ramp-up. It can be seen from Fig. 3 that at a low level the overall result is low, but the noise is high. By adjusting the process parameter, both the overall result as well as the noise were improved considerably.

Having introduced this package of measures as well as having improved the performance of the major processing steps in thin-film solar module production, the efficiency of the modules produced was significantly stabilized – as can be seen in Fig. 2. The next step noted was the introduction of a new process step. While at an experimental level this new process step should have yielded lower impact than the introduction of the new raw material introduced earlier, the effect was more clear cut.

Thus it may be concluded that for optimum performance, stabilization of the line output – both in terms of volume and efficiency of the solar modules produced – needs to take first priority in any ramp-up or major redevelopment project.

Thin-film PV module design

Upon designing a photovoltaic system there are numerous considerations to be taken into account. Among them is the fact that the maximum DC voltage for today´s inverters is between 600–1000V. This limit is due to technical and safety considerations of an inverter with the American UL 1703 (flat-plate PV modules and panels) setting the limit of installations at or on buildings to 600V DC. The maximum DC voltage of the inverter in turn determines the maximum number of PV modules to be put serially in a string. The maximum number of modules can easily be determined if the V_{oc} (open circuit voltage) of the PV module is known. A sample calculation is shown in Table 1.

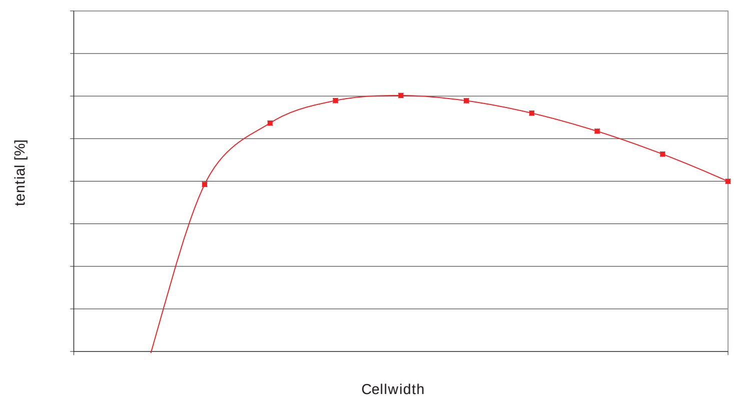

Figure 6. Schematic drawing showing the optimum width of a cell in a thin-film module.

It can be seen from the calculation in Table 1 that the maximum length of a string roughly follows the open circuit voltage of a PV module: the lower the module's V_{oc}, the larger the number of modules in a string. This way, connecting the modules to an array (see Fig. 4) is much simpler and requires less material (including cables, protecting diodes and auxiliary facilities), thus reducing the BOS costs of a PV power station by as much as 4%. Since eventually the BOS costs are the main factors in determining the price of PV electricity, there is a drive in the market towards lower module voltages.

> "By adjusting the cell width, the efficiency of the thin-film module is also optimized."

With thin-film PV modules there is another incentive driving the development for modules with a lower V_{oc}. Thin-film modules are usually monolithic serial connections of individual cells (see Fig. 4). Thus, the structuring of individual cells into the thin-film design is, for the majority of thin-film technologies, the easiest (and in some cases the only) way of adjusting the open circuit voltage of the module.

It comes as a welcome additional benefit that by adjusting the cell width, the efficiency of the thin-film module is also optimized. The width of the individual cells is a compromise; it both minimizes the losses due to serial resistance in connecting the individual cells and minimizes the area between cells and the area of the module. These areas are consumed by the scribes themselves – which do not contribute to power generation, hence the term 'dead area'. The wider each cell, the lower these losses. On the other hand, the wider the cells, the more current is generated in each cell leading to increased serial losses due to:

$$P = R \times I^2 \tag{1}$$

The current in a cell is given by

$$I = j \times l \times z \tag{2}$$

where j is the current density (essentially determined by the specific number of carriers generated by the photoeffect), l the width of the cell given by the modules outer dimensions in one direction and z is the width of the cells given by scribe distances as shown in Fig. 5. From these

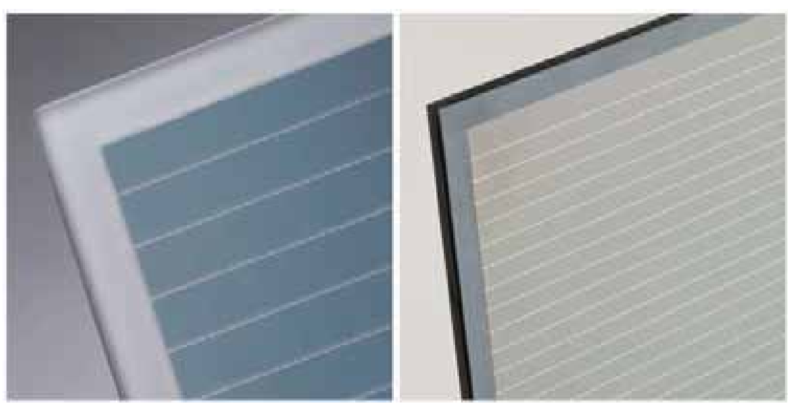

Figure 7. Picture of a CX1 module (left-hand picture) in comparison to a CX3 module (right-hand side) featuring optimized cell widths and improved package design. Details discussed in the text.

basic considerations it can be calculated that for a given set of materials (TCO, n-p diode, back contact) there is a specific optimum width of a cell in a thin-film solar module, as can be seen in Fig. 6.

Fig. 6 gives a representative calculation for one particular thin-film set. The maximum is rather broad, so for minor deviations of the cell width, negligible losses are expected. It has to be pointed out that for a different set of PV cell materials the maximum efficiency is yielded at different cell width. Since making the cells smaller implies the use of more advanced technologies, in positioning and referencing the scribes and materials included in the PV cell, they are also subject to manufacturing variability. It is common to choose a design cell width larger than the optimum width.

"Package design in PV technology is not yet considered as part of the technology roadmap."

A comparison between a conventional thin-film module and a thin-film module with optimized cell width is shown in Fig. 7. The overall appearance of the module with optimized cell width is much more uniform. This aspect is further underlined by the use of an all-black sealing material. The comparison in Fig. 7 is an example for a specifically designed package. Being a comparatively new industry, package design in PV technology is not yet considered part of the technology roadmap. In the last paragraph we will point out some aspects whereby this largely uncharted territory can be exploited with CdTe thin-film modules.

On the whole, thin-film PV modules are distinguished by the order in which the individual layers are deposited. With substrate technology, the back contact is deposited as the first layer, followed by the semiconductors and the front contact, respectively. The advantage of this approach is that the substrate material is to be chosen either to account for processing needs or to comply with PV modules' system specifications. The range of substrate materials currently employed covers plastics as well as thin metal foils for large-area roll-to-roll deposition. With substrate technology, the final processing step is the encapsulation of the thin-film solar cell material, so the encapsulating material has to be applied to the 'sunny side' of the module. Therefore, careful choice of the encapsulation material and its durability upon UV exposure, for example, is imperative.

In contrast, with the so-called superstratetechnology, the first layer to be deposited is the transparent front contact followed by the semiconductor layers and the back contact. CdS/CdTe thin-film modules are usually deposited using superstrate technology. This is done primarily for historic reasons (most of the CdTe module manufacturers have deep roots in the glass manufacturing industry), and partially due to issues with high temperature properties of the back-contact metals that are being employed. With superstrate technology, attention has to be paid to the choice of glass substrate. This approach allows use of established inexpensive deposition technologies employed in large volumes by the glass manufacturing industry. In addition, there are several other advantages. The encapsulation material is not exposed to UV radiation, so the major property prone to degradation with currently used materials like EVA is of minor importance. The encapsulation design can be done placing the focus on diffusion barrier properties, appearance or matching expansion coefficients. Also, the overall efficiency of the module is enhanced since there is one layer less facing towards the sun, reducing the overall optical transmission [8].

The newly designed package CX3 shown in Fig. 7 is an example of this approach. Here, the encapsulation is designed for maximum durability leading to long-life modules.

Summary and conclusion

In this article we have given an overview of considerations in designing modern thin-film PV modules together with their respective manufacturing technology. We have pointed out that from the offset all aspects of module design, from electrical to mechanical to optical specifications, need to be taken into account. We have demonstrated this with the example of ramping a novel CdS/CdTe thin-film production with a novel deposition technology combined with new approaches in module and package design. The manufacturing process needs to be effective and fast, while at the same time ensuring high utilization rates of the equipment. Ramping up a thin-film line follows distinct patterns which need to be accounted for in the ramp up plan. From the start, all specifications for the PV module need to be laid out in order to put forward the specifications for the production systems. This way, high efficiency, long-term stability, economically attractive and optically pleasing modules are produced. The success of this approach is shown with the CX3 module, presented to create customer value in the US\$0.5/W_p race.

References

[1] Compaan, A. et al. 2009, "Fabrication and physics of CdTe devices by sputtering", NREL/SR-520-45398.

[2] Maack, S. 2006, "Herstellung und Charakterisierung von CSS CdTe Dünnschichtsolarzellen", Dissertation, Jena, Germany.

[3] Powell, R. et al. 1998, "Apparatus and method for depositing a semiconductor material", US Patent 6037241.

[4] Johnston, N.W. et al. 1978, "Atmospheric pressure CVD", US Patent 7674713.

[5] Vossen, J.L. & Kern, W. 1978, "Thin film processes", Academic Press, New York.

[6] Woods, L. & Meyers, P. 2002, "Atmospheric pressure CVD and Jet vapor deposition of CdTe for high efficiency thin film PV devices", NREL/SR-520-32761.

[7] Gessert, T.A. 2008, "Review of photovoltaic energy production using CdTe thin film modules", *Workshop on physics and chemistry of II-VI materials*, Las Vegas, US.

[8] Huld, T.H. et al. 2010, "Mapping the performance of PV modules, effect of module type and data averaging", *Solar Energy*, Vol. 84, pp. 324–338.

About the Authors

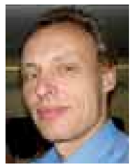

Dr. Hubert-Joachim Frenck studied physics at the University of Münster. Under Prof. Kassing at Kassel he concluded his Ph.D. on "Molecular engineering in PE-MOCVD thin film deposition" in 1988. In 1999 he joined Ikarus Solar and worked at Viessmann SA from 2005 until 2007, when he joined Q-Cells, being responsible for the vacuum division of the process development department there. In November 2009 he was appointed head of production at Calyxo where he is also responsible for semiconductor process improvement.

Frank Becker studied electrical engineering at the University of Saarland, where he specialized in semiconductor and sensor technology. In 1997 he became manager of the Siemens Fiber Optics Group in Japan and the business unit manager of the Fiber optics, USA in 1999. He joined the start-up company Mergeoptics in 2002, followed by Q-Cells in 2007 as department head of the metallization group. Since 2008 Frank Becker has been head of development in the technical management team at Calyxo.

Enquiries

Werksleiter Calyxo
Sonnenallee 1a
D-06766 Bitterfeld-Wolfen
Germany
Tel: +49 3494 3689 80176
Email: j.frenck@calyxo.com

PV Modules

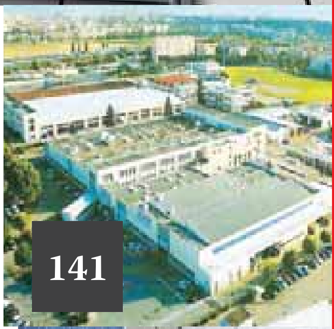

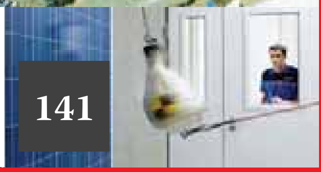

Bosch brings 150MW crystalline-silicon PV module production line to Vénissieux, France

Bosch is taking its PV module production international by establishing a 150MW manufacturing facility for its crystalline-silicon solar modules in Vénissieux, France. Although the company did not disclose the full amount of its investment, it did reveal that the set-up of its production facility in Vénissieux is a "low eight-figure amount". Over 200 jobs will be secured once production starts in January 2012.

"This investment will secure the future viability of the location, as well as the jobs of our Vénissieux associates," said Guy Maugis, the president of Robert Bosch France. "At the same time, Bosch is expanding its product portfolio in France to include the innovative field of renewable energy."

The Vénissieux location currently houses Bosch's diesel pump manufacturing and hydraulic component manufacturing. Bosch advised that the plants would be merged into one organizational unit with one plant manager.

Bosch's diesel pump and hydraulic component manufacturing facility in Vénissieux, France will be the location for the company's new 150MW PV module facility.

Testing and Certification News Focus

Burns & McDonnell to help set up solar test bed at Southwest Solar research site in Phoenix

Burns & McDonnell Engineering and Southwest Solar Technologies have agreed to research and test a 3.5kW PV test system at the 18-acre Southwest Solar Research Park in Phoenix, Arizona. The facility, just outside of Sky Harbor Airport, is home to a 75-foot diameter concentrating solar dish, which is said to be the largest commercial solar dish in North America.

Burns & McDonnell has joined forces with Abound Solar, Suntech Power Holdings and Power-One for the 3.5kW solar test system. Three solar arrays will make up the test system, all of which will be outfitted with test instrumentation so that researchers can determine the effect of different types and amounts of cooling on the solar array. The solar arrays will be adjustable so that testing can be conducted at different tilt angles and will use thin-film and crystalline silicon solar modules, allowing for a comparison of the different modules' performances in relation to the varying environmental conditions. Information on the long-term performance data for modules and inverters will be assembled during testing.

Intertek-tested PV products earn J-PEC recognition and eligibility for Japanese government subsidies

Under a new recognition by Japan's Department of Energy and its Japanese Photovoltaic Expansion Center (J-PEC), Intertek's CB reports on PV products distributed to the Japanese market will be eligible for consumer subsidies. The recognition allows for a more streamlined operation whereby a manufacturer that has its PV products tested and certified by Intertek will not need any supplementary certifications or approvals when entering the Japanese market.

This recognition by J-PEC complements Intertek's partnership with the US Department of Energy, Natural Resources Canada and the International Electrotechnical Commission (IEC) for test reports used by national, international and state-level governments worldwide.

Hanwha SolarOne's crystalline solar modules receive UL, MCS and TÜV Rheinland certification

Hanwha SolarOne's crystalline solar modules have received certification from three global entities: US-based Underwriters Laboratories, UK-based Microgeneration Certification Scheme (MCS) and Germany's Technical Inspection Association (TÜV Rheinland). The certification for the US, UK and German markets is essential for Hanwha's modules to be sold in the countries as preferred options, and they may even receive financial incentives in certain circumstances. Certifications were granted for its X-tra serial and Black Diamond modules as well as modules from its standard line.

Image: TÜV Rheinland

PV Module testing at TÜV Rheinland.

CFV Solar Test Laboratory in New Mexico opens for business

CFV Solar Test Laboratory, a PV certification test company owned by the CSA Group, VDE Testing and Certification Institute, Fraunhofer Institute for Solar Energy Systems (ISE) and Fraunhofer USA Center for Sustainable Energy Systems, has officially opened its doors in Albuquerque, New Mexico. The centre will offer solar panel manufacturers in North America and international markets worldwide certification services from one location.

The CFV lab has complete certification and non-certification testing services for PV technologies including flat panel, thin-film and concentrating PV (CPV) testing. The centre's laboratory can certify solar panels for use in several countries while meeting the standards for each location.

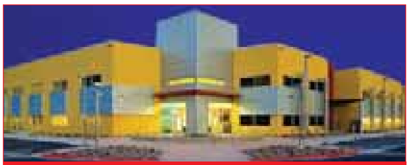

Image: CFV Solar

The CFV Solar Test Laboratory in Albuquerque, New Mexico.

The 25,000 square-foot indoor facility has climate chamber for thermal cycling and humidity freeze up of panels to 4m × 2.5m, a large-area AAA+ rated solar simulator with temperature controlled enclosure for performance measurements and a five-acre outdoor testing area with single and double-axis trackers.

PVEL introduces third-party flash testing service

PV Evolution Labs (PVEL) has debuted its new fast turn-around third-party flash testing services for solar project developers. The company asserts that its assessment as a third party will help project developers cut risks when it comes to selecting a panel supplier and keep in line with tight project timelines.

PVEL operates its own test system facility in Berkeley, California. The company maintains that its new service can help developers select a solar panel supplier that not only suits the solar project, but will perform under high standards.

Scheuten Solar gives Multisol Vitro modules 30-year linear power warranty

Extended warranties have been applied to Scheuten Solar Multisol Vitro modules sold from May 2011 onwards. Warranty conditions for Multisol Vitro now include a 30-year linear power warranty coupled to a 12-year product warranty. Scheuten Solar first introduced a linear power warranty in 2009.

The company claims that the modules are resistant to acid or salt, with a very high mechanical strength and an improved resistance against snow and wind loads. The use of solarfloat HT glass and an innovative quartz-based hard anti-reflection coating (ARC) is said to improve power output and energy yield.

Image: Scheuten Solar

Multisol Vitro modules from Scheuten Solar now have a 30-year linear power warranty.

TÜV Rheinland adds North American ANSI/UL1703 solar safety mark to portfolio

TÜV Rheinland has been given the go-ahead from the US Occupational Health and Safety Administration (OSHA) to provide certification for ANSI/UL1703, which is the required North American solar safety mark. The ANSI/UL 1703 certification, which is the latest accreditation in TÜV Rheinland's portfolio of testing and photovoltaic certifications, is currently one of the pivotal regulatory requirements to launch photovoltaic products in the US marketplace.

Image: TÜV Rheinland

TÜV Rheinland's solar testing lab.

"We are very pleased by the accreditation of our North American certification body from OSHA. The elevation of status as a Nationally Recognized Test Laboratory (NRTL) for TÜV Rheinland PTL will give TÜV Rheinland Group another of the key pieces to service our clients globally," said Richard Bozicevich, North American business field manager for solar services. "With this accreditation we can leverage the expertise and geographic reach of the TÜV Rheinland network to better service clients across the globe."

TÜV Rheinland operates test laboratories for solar modules and systems in six locations worldwide, which together employ approximately 200 experts specializing in solar technologies.

Canadian Solar awarded ISO14001, REACH certifications

Canadian Solar's CS6 series modules have been certified with two industry standards: the ISO 14001 and the EU'S REACH (registration, evaluation, authorization and restriction of chemicals) program. The achievement of the ISO standard is achieved when companies like Canadian Solar have an established corporate environmental policy, goals associated with the policy and an environmental program.

Canadian Solar's certification by the European Union's REACH directive means that the company's CS6 series modules comply with REACH's adherence that substances used in the production of modules are free from substances of high concern. Canadian Solar's modules were analyzed by the SGS group who confirmed that substances of high concern, such as carcinogenic or mutagenic substances, were not used in the CS6 series module's production.

Business News Focus

China Sunergy enters UK market

PV module manufacturer China Sunergy has obtained the UK's much sought-after Microgeneration Certification Scheme certification, which allows the company to market its modules in the country. The certification was granted by BABT (British Approvals Board for Telecommunications).

Mr. Stephen Cai, CEO of CSUN, commented, "This is not only a recognition of our product quality, but also a great opportunity for CSUN to step into the UK, an emerging yet strategically important market for our solar products."

Trina Solar strengthens presence in Australia

Trina Solar, active in Australia since 2009, has strengthened its presence in the country by opening a sales and business development office in Sydney. The PV manufacturer recently announced an R&D collaboration with the Australian National University (ANU). The new office aims to grow Trina's customer base and develop new business opportunities in the region.

Last year, Trina appointed RF Industries, Australia's largest renewable energy distributor, as its main agent.

Day4 Energy cuts workforce at Burnaby facility

Solar module manufacturer Day4 Energy has cut the workforce at its Burnaby production facility by 30 people. The Burnaby site will now focus on research and development, with sales, customer care and supply chain management being outsourced to Day4's European offices in Germany and Italy.

Day4 will provide employees affected by the redundancies with severance pay and human resource support. There will be a restructuring charge recorded in Q2 2011.

Suntech becomes world's leading solar module supplier, according to IMS Research

Suntech has usurped First Solar as the world's leading PV module supplier after topping IMS Research's 2010 module


Image: Suntech

Inspection of a Suntech Pluto solar cell.

sales table. The switch in positions was inspired by Suntech's 130% year-on-year rise in module shipments; First Solar saw sales rise by less than 50% despite the total market value more than doubling.

Other firms that capitalized on the market boom were Chinese tier-one suppliers Canadian Solar and Hanwha SolarOne, both of whom gained two places in the rankings, and REC Solar, which moved up to 11th in the IMS global list.

"2010 was an outstanding year for everyone in the PV industry. Module suppliers were able to benefit from the strong demand, which lasted all year, and make great increases in their shipments; five of the top 10 suppliers more than doubled them, some even increased them by more than 150%," IMS Research's PV market analyst Sam Wilkinson said.

Last year was also one to remember for China's JA Solar, which expanded production levels by 180% to become the

JinkoSolar signs 50MW module supply deal with BULL PowerTech

BULL PowerTech, a business segment of BULL Holding AG, has signed a module supply deal with JinkoSolar. Under the terms of the agreement – the first between the two companies – JinkoSolar will supply the PV products supplier and project developer with 50MW of co-branded modules during 2011. BULL Holding Group recently reported revenue surpassed the €100 million level for the first time in 2010.

MAG to supply 30MW turnkey system for Polish company Solar Energy

MAG has disclosed that its renewable energy division will supply Solar Energy, based in Poland, with a 30MW turnkey system for the production of crystalline silicon PV modules. The €3 million contract will see the system assembled at MAG's Schaffhausen, Switzerland facility and delivered to Solar Energy. The first PV modules are expected to roll off the system this summer.

MAG advised that its turnkey system would encompass all production steps necessary for the production of PV modules. Furthermore, as the modules that will be manufactured by MAG's system will be sold to eastern and western European customers, the company maintains that the modules will have UL and IEC certification.

GP Joule places order for 97MW of Canadian Solar's PV modules

Canadian Solar and GP Joule are continuing their work partnership with a new supply agreement signed between the two companies. Under the agreement, Canadian Solar will supply GP Joule with 97MW of its solar modules, which will be delivered before December 31. Financial details from the contract were not revealed.

Canadian Solar signs 100MW module supply contract with Fire Energy Group

Canadian Solar has signed a 100MW solar module supply contract with Fire Energy Group. Under the terms of the agreement, Canadian Solar will deliver modules throughout 2011, with prices adjusted on a quarterly basis.

"Under our latest agreement, we will be using Canadian Solar's 60-cell CS6P and the CS6V large-format module for a variety of rooftop and ground-mounted applications. As Fire Energy Group continues to expand across Europe, it is critical we have a proven partner working alongside us. Canadian Solar is that proven partner," added Fire Energy chairman John Liu.

Yingli Green signs exclusive module distribution agreement with Japanese firm

Yingli Green Energy has signed an exclusive module distribution agreement with YHS. Under the terms of the contract, YHS will purchase modules totalling 10MW and take on the role of Yingli's sole Japanese residential market distributor. The agreement was signed in March and will run until December, with the first shipment of modules due to be delivered in the second half of the year.

Trina Solar extends RFI supply deal

Trina Solar subsidiary Changzhou Trina Solar Energy has extended its national distribution agreement with RF Industries (RFI). Initially signed in January 2010, the ~40MW deal, which recognizes RFI as Trina's exclusive distributor in Australia, will now run until December 31, 2012.

Silfab Ontario signs 9.3MW module supply deal with Agris for Ontario microFIT projects

Agris Solar Co-Operative will be deploying 9.3MW of PV modules made in Silfab Ontario's new production facility for 10kW and smaller micro feed-in tariff projects in the Canadian province. The first tranche of monocrystalline-silicon panels will be delivered in April, with shipments continuing until April 2012.

EC's Ispra joint research center to get Spire solar simulator for module testing

Spire has been selected to supply its Spi-Sun Simulator 4600SLP to the European Commission's Joint Research Center in Ispra, Italy (JRC ISPRA), which will use the simulators for its PV module testing.

Roger Little, chairman and CEO of Spire, said, "With a Class AAA rating, Spire's Simulators have become the industry standard for PV module testing, as demonstrated by utilization in over thirty test labs worldwide. Our proprietary method of controlling the Simulator's pulse length, its large irradiance range, and its superior spectral control provide test labs with a powerful tool for assessing PV module performance during development or qualification.

Qsolar sells record number of Spraytek panels

Canada's Qsolar shipped a record number of its proprietary Spraytek79 solar panels to European customers during the final quarter of 2010. The final sales total of US$600,000 was a more than 100% increase on the Q3 figure.

This success has carried on into 2011, with Qsolar already securing letters of intent covering the full production capacity of the contracted manufacturing facility. The panels are produced in China using its patented Spraytek manufacturing process.

The Spraytek panels were sold with positive tolerance, meaning that customers will get a guaranteed output which can be up to 5% more than the specified figure. Contrastingly, most of Qsolar's competitors were bringing panels to market with tolerances ±3% of the official output.

JinkoSolar signs 6MW module deal with Lumos for US market

JinkoSolar has signed a one-year supply PV module agreement with Lumos Solar, a US-based solar design, development, and distribution company. Terms of the deal call for the vertically integrated Chinese manufacturer to produce 6MW of frameless LSX modules as well as traditional Lumos-framed modules under a cobranded label "Lumos powered by Jinko" to be shipped in the second quarter of 2011. Financial terms of the deal were not disclosed.

Arturo Herrero, CMO of Jinko, commented, "The LSX technology can not only be applied in the US but also in Europe where commercial and residential segments often require fully integrated solutions for PV roofing systems."

Spire signs deal to supply 20MW PV module line to Tecnometal Equipamentos of Brazil

Spire recently released that it will be delivering a 20MW solar PV module line to Tecnometal Equipamentos of San Paulo, Brazil. Details involving delivery date and pricing of the deal were not disclosed. In mid-February, Spire won a 20MW turnkey module line deal with Bangladesh firm Rahimafrooz Renewable Energy, which was followed by a 50MW automated PV module line deal with Mage Solar in March.

world's largest manufacturer of PV cells; in 2009 the company was fifth on the IMS list. Despite this success across the board, IMS is predicting a slowdown in the industry in 2012, as many major European markets contract in response to adjustments to feed-in tariff initiatives.

US solar panel prices set to drop in 2011

Solar panel prices in the US are set to drop by US$0.20 per watt in 2011, according to SolarCity CEO Lyndon Rive. Such a fall would bring the average panel price down to US$1.40 per watt – 12.5% below the predicted price for 2011.

Prices for solar panels have declined by around 75% in the past 10 years and now contribute less than half the total installation cost of an average rooftop system. Despite a spate of recently-announced feed-in tariff cuts, most major solar panel manufacturers are raising their output this year in an attempt to increase market share. However, this could result in a surplus of panels on the market, thus tightening margins at companies such as Trina Solar and First Solar.

SolarWorld begins production of Sunmodule Plus polycrystalline solar panels

SolarWorld has launched the new polycrystalline Sunmodule line, which is being fabricated at its Oregon and California production facilities. The polycrystalline solar panels are now available in 230W and 240W peak power concentrations and, like their monocrystalline Sunmodules, SolarWorld's Sunmodule Plus poly panels are offered with a 25-year linear performance guarantee.

Image: Suntech

SolarWorld's Sunmodule Plus multicrystalline panels come with a 25-year linear performance guarantee.

Eclipsall signs PV module supply deal with Honeybee Solar, MOU with Sustainable Energy

Ontario-based PV firm Eclipsall Energy has signed a module supply deal with distributor Honeybee Solar as well as an agreement with inverter company Sustainable Energy to design, package, and market 'solar power kits' for the province and the rest of the North American market.

The company has also created Eclipsall Financial Services, which offers equity and debt financing program for Ontario solar projects through a joint venture with Canada Green ESCO.

The memorandum of understanding with Sustainable Energy calls for the production of at least 10MW of solar kits based on a combination of Eclipsall's modules and the Sunergy inverter, beginning in Q3 2011. The partnership will allow both companies to bundle the inverters and panels directly into turnkey packages for the installer community in Ontario, especially those serving the under 10kW micro-FIT market.

Product Reviews

Adhesives Research

Adhesives Research's new pressure-sensitive adhesive tapes offer greater manufacturability

Product Outline: Adhesives Research (AR) has launched new pressure-sensitive adhesive tapes (PSAs) for bus bar, solar cell junction box, and encapsulation barrier applications in crystalline and thin-film PV module applications.

Problem: As an alternative to traditional bonding methods, such as soldering for electrical interconnects and liquid epoxies for encapsulation, new PSA technologies can remedy issues that tend to cause problems in this step, such as handling, continuous roll formats, and messy clean-ups.

Solution: The ARclad 92446 and ARclad 92709 combine advancements in adhesive and foam technology that are die-cuttable and can be laminated to the junction box. The tapes create a bond directly to the glass, producing a long-term, reliable bond, which outperforms other bonding products in accelerated aging and damp heat tests. Specifically developed for use in flexible thin-film PV modules, the barrier technology is claimed to offer less mess, ease of handling and more rapid throughput. A benign, low-outgassing, non-corrosive and electrically clean adhesive, this PSA becomes active at an industry low of 100°C (industry standard is 140–150°C), according to the company.

Applications: Pressure-sensitive adhesive tapes for bus bar, solar cell junction box and encapsulation barrier applications in crystalline and thin-film PV module applications.

Platform: AR also offers a range of PSA products to complement ARclad 90038, a 2.4-mil, highly conductive PSA tape featuring a 1oz tin-plated copper foil backing. The range covers electrical interconnections, wire management, bonding, assembly and encapsulation.

Availability: Currently available.

Q-Cells

Q-Cells develops polycrystalline module with an efficiency rating of 17.84%

Product Outline: Q-Cells has used new cell technology to break the world record in the field of polycrystalline solar modules. The ESTI (European Solar Test Installation) confirmed independently that the module has a record efficiency rating of 17.84% in relation to the aperture area, with an output of 268W.

Problem: Increasing the conversion efficiency of solar cells reduces the cost per watt. New techniques are required that are both performance boosting but feasible to manufacture at cost competitive levels, while maintaining high quality for long-life operation.

Solution: The base material for the high-efficiency solar cells used in the module is conventional, 180µm-thick polycrystalline silicon wafers, which were metallized on the back side and passivated in Q-Cells' in-house research centre with functional nanolayers. This new type of structure for the back side consists of dielectric layers combined with local contacts, which is said to improve the solar cell's aesthetic and electrical characteristics and boost its output as compared to the BSF (back surface field) approach. Fraunhofer ISE's calibration laboratory confirmed that these high-efficiency cells have a peak efficiency rating of 18.45%.

Applications: Modules for residential, industrial and utility-scale installations.

Platform: The Q-Cells module contains 60 high-efficiency polycrystalline cells with dimensions of 156 × 156mm^2, produced in-house and arranged in a conventional layout. The module tested achieved a 17.84% efficiency rating on an area of 1.492m^2 (aperture area); V_{oc}: 38.86V; J_{sc}: 9.04A; module output: 268W.

Availability: Pilot production is underway. Volume production will take place at Q-Cells' facility in Malaysia.

ADCO Products

ADCO Products' HelioSeal PVS 800 j-box potting sealant offers significant reduction of moisture permeability

Product Outline: ADCO Products has developed a new PV sealant and j-box pottant that is claimed to offer a significant reduction in moisture permeability. The HelioSeal PVS 800 is a newly developed, hot melt pumpable butyl material. It is designed to seal the module's back hole – a drilled hole in the glass through which power wires and conducting tapes connect to the j-box – and to pot the j-box all at once, avoiding corrosion and preventing moisture vapour from passing through to the wire connections.

Problem: Permeability is the key factor in PV sealants, as corrosion and moisture vapour transmission can greatly affect module reliability.

Solution: Using HelioSeal PVS 800 for both back-hole and potting applications is said to allow PV module manufacturers excellent protection against moisture. HelioSeal PVS 800 is applied using industry available hot melt equipment. Standard hot melt bulk unloaders are recommended, which use optimum length heated hoses and a heated platen ram to achieve proper melt rate to allow for required flow rates. No hydraulic assisted ram plates nor vacuum de-gassing are necessary to achieve higher volumes. Typical system heat requirements of the hot melt bulk unloader are 275°F–325°F (135°C–163°C). Typical flow rates for this product of 400cc/minute can be reached under these conditions.

Applications: J-box sealing.

Platform: Rod displacement or metered gears are both acceptable dispensing technologies for the HelioSeal PVS 800, which is UL listed under QIHE2.

Availability: Currently available.

Spire Corp.

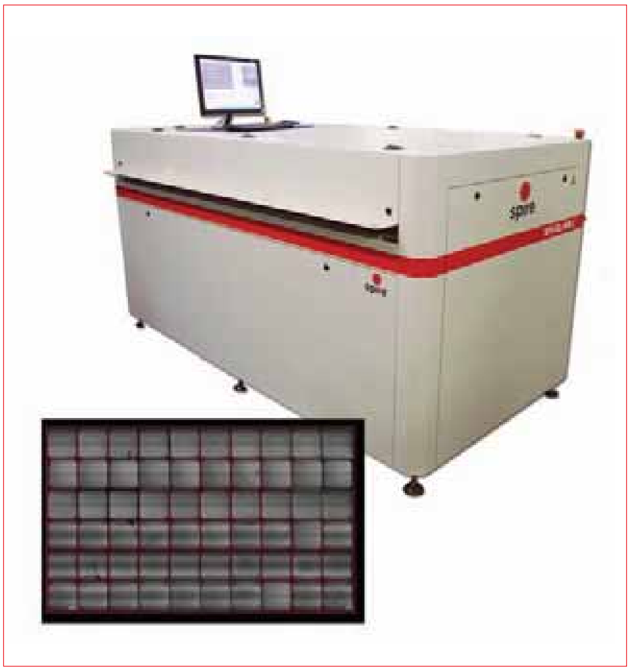

Spire's Spi-EL tester provides high-resolution inspection for solar modules

Product Outline: Spire Corp. has introduced a new advanced metrology platform, the 'Spi-EL' Electroluminescence Solar Module Tester. First debuted at the SNEC exhibition in Shanghai, China, the Spi-EL-HR (high resolution) and Spi-EL-MR (medium resolution) testers can be used for pre- and post-lamination of framed or unframed modules.

Problem: Microcracks and hard-to-see defects can reduce module performance and lifetimes. Microcracks can happen anywhere and anytime, during production, transportation or installation.

Solution: Two basic models, Spi-EL-HR and Spi-EL-MR, can be used for pre- and post-lamination of framed or unframed modules. The system can take the image of the entire module or take individual images of cells and combine them into an overall picture of the module. Combining the individual cells into an overall module picture will provide higher resolution. Image acquisition capture time can be less than 35 seconds for high resolution and 10 seconds for medium resolution. Systems can be standalone or inline; module loading and unloading can be short side or long side, including feed in/out conveyors on the same or opposite side of the system.

Applications: Inspection of PV c-Si modules.

Platform: The Spi-EL series of solar module testers use electroluminescence (EL) to identify microcracks and other invisible defects in modules. The testers utilize cooled near-infrared charge-coupled device camera technology to image each solar cell with resolutions less than 200μm per pixel, the equivalent of a 60 megapixel image for an entire module.

Availability: Currently available.

Research on power loss of solar cell modules

Wang Qi, **Zhichun Ni**, **Fangxing Ren**, **Jianhua Zhao** & **Aihua Wang**, China Sunergy (R&D) Co., Ltd., Nanjing, China

ABSTRACT
After the encapsulation step, a c-Si solar module's output is usually decreased, in comparison to its cells' power, which is referred to as 'power loss.' This paper focuses on the various factors that can impact power loss of solar modules, such as solar cell classification, encapsulation material, match of solar cells, the encapsulation process used, and so on. The conclusion indicates that power loss in solar modules can be significantly decreased with a resulting increment of a module's output by appropriately optimizing those factors.

Introduction

Solar cells must be connected in series or parallel and encapsulated into modules in order to obtain current, voltage, output power and to prevent them from mechanical or environmental damage. As a general rule, the output power of the encapsulated module (actual power) is less than the summation power of all the solar cells (theoretical power), which is known as 'power loss' and calculated as follows:

power loss = (theoretical power-actual power)/theoretical power. (1)

If the power loss is high and the output power of modules is lower than design value, this poses a major problem for customers. Complaints would have a bad impact on the module company and cause economic loss. Conversely, decreased power loss will cause an increment in the module's output which could increase revenue, lessen the cell efficiency needed for the module encapsulation and reduce the production costs indirectly.

After analysis and discussion of the possible factors that may impact power loss from the aspect of optical loss and electrical loss respectively, this paper shows some elementary conclusions which could provide reference for a module company to improve its product performance. This paper only aims at the study of power loss when modules are encapsulated, excluding the decrease of module output power caused by LID (light induced degradation) etc.

Analysis of power loss

A typical encapsulation scheme [1,2] of the crystalline silicon solar cell is shown in Fig 1. The components, from top to bottom, are tempered glass, sealant, crystalline silicon solar cell, sealant and back sheet.

We classify power loss according to optical loss and electrical loss. The impact factors will be discussed in detail in the following paragraphs.

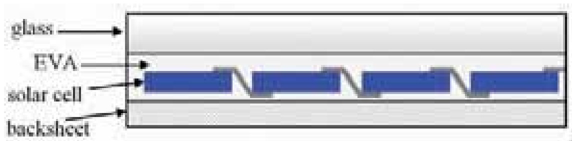

Figure 1. Structure of laminated module.

Optical loss

In theory, single crystalline silicon solar cells cannot convert all the light that strikes it into electric energy. The spectrum response of normal silicon solar cells ranges from 300nm to 1100nm approximately. As a result, the factors that reduce the light entering the solar cell will cause optical loss, which can be analyzed from the viewpoint of both light transmission and reflection.

"In theory, single crystalline silicon solar cells cannot convert all the light that strikes it into electric energy."

Transmitted from the module surface to the silicon inner, the light will pass through glass and sealant in turn (usually ethylene-vinyl acetate – EVA), both of which have impact on the light absorption. The higher the transmission rates of glass and EVA are, the lower the power loss of modules is. The transmission rate of regular ultra-white tempered glass is approximately 92%. However, the transmission rate of coated glass with anti-reflection film which has been sold on the market can be as high as 96%. Normally, the coated glass can improve the output power of modules by 1%. However, further research on the long-term stability and reliability is needed for this kind of glass.

Fig. 2 illustrates that the transmission rate of 3.2mm-thick tempered glass from different manufacturers changes with wavelength (300nm–1100nm). Sample D is coated glass and the other three are normal tempered glasses. It is clear

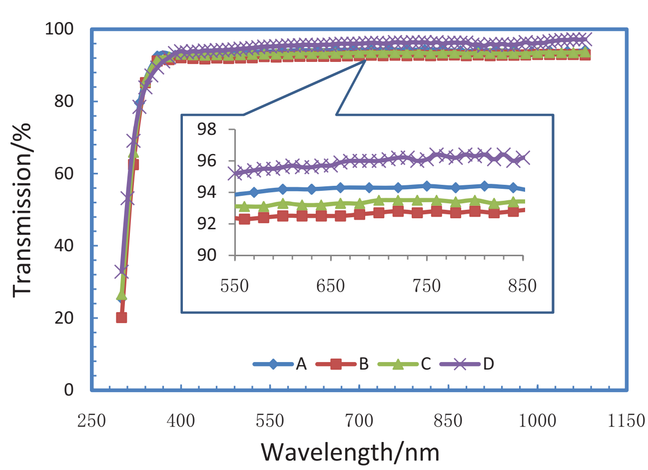

Figure 2. Transmission of glass (thickness 3.2mm). Samples A, B and C are normal tempered glasses from different manufacturers; sample D is coated glass.

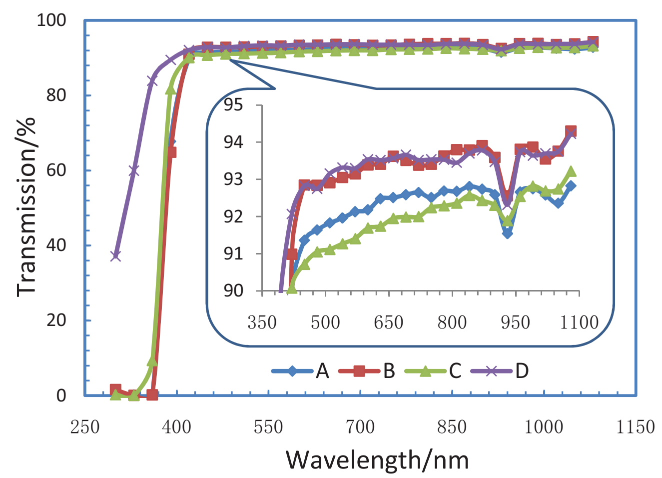

Figure 3. Transmission of EVA (thickness 1.5mm).

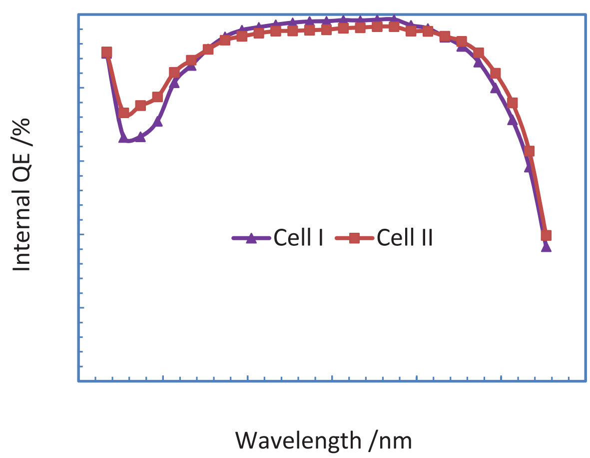

Figure 4. IQE curves of normal cell (Cell I) and high R_{sh} cell (Cell II).

that the transmission rates of glass from different manufacturers show a large variation. The higher the transmission rate, the more light can enter into the solar cell, and the output power of solar cell is proportional to light intensity. Assuming that solar cells and encapsulated material remain unchanged, the output power of modules will increase and power loss will decrease by using tempered glass with high transmission rates.

An anti-UV component can be added into EVA by manufacturers, which will result in the decrease of transmission rates for short wavelengths. Fig. 3 is a diagram demonstrating the transmission rate of EVA (1.5mm thick) produced by different factories. Sample D, the material without UV absorbency shows a transmission rate of 37.1% with 300nm wavelength. The other three EVA with the anti-UV component have no spectral response for light with wavelength shorter than 360nm. However, solar cell manufacturers are starting to use high sheet resistance and close finger processes to increase solar cell conversion efficiency. A solar cell with high sheet resistance (R_{sh}) has a different spectrum response from the conventional p-type solar cell.

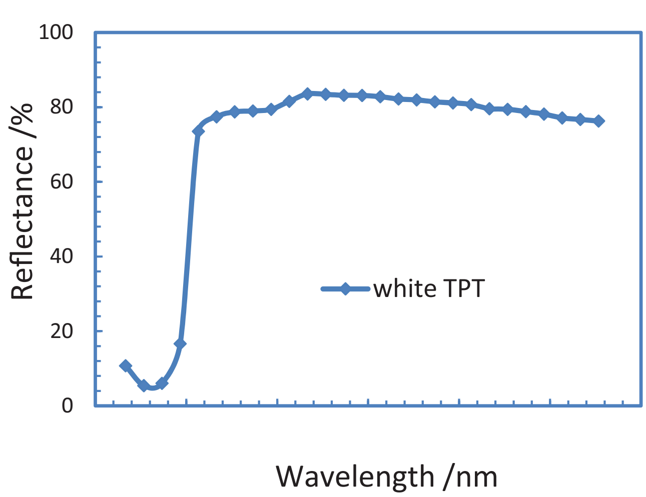

Figure 5. Reflectance of white TPT.

Fig. 4 illustrates different IQE curves of a normal cell (Cell I) and high sheet resistance cell (Cell II) with similar efficiency. The IQE of the high sheet resistance cell is higher than that of the normal cell at short wavelength (<450nm). However, on application of the kind of EVA that cannot work at short wavelengths, this short wavelength light cannot be absorbed by the high sheet resistance cell. Consequently, the power loss will be higher than that of normal cells with the same efficiency, illustrating why the selection of EVA should match the cell manufacturing process and balance the transmission rate and anti-UV characteristics, which may reduce the power loss without affecting the module reliability. Furthermore, some companies propose that transparent silica gel with a stable chemical property, anti-UV characteristics and high transmission rate, can be used as a module sealant to prevent problems such as yellowing of sealant which prevents the absorption of short wavelength light by the cell.

An anti-reflection coating of SiN_x is deposited on the solar cell surface with refractive index of 2.1, which is covered by EVA and tempered glass (the total refractive index of 1.48). The thickness of SiN_x, EVA and glass need to be optimized to maximize the module transmission rate, anti-reflection effect as well as the output power.

The module back sheet prevents vapour from entering the module. TPT (Tedlar-PET-Tedlar) film is often used as the back sheet. Fig. 5 shows the reflectivity curve of normal white TPT to EVA contact surface: the reflectivity is as high as about 80% at mid-long wavelength. White TPT film is able to reflect the sunlight which cannot be absorbed by the solar cell. This part of sunlight is reflected to the solar cell from the air-glass interface, thus increasing the utilization of light incident to the solar cells. Compared with black TPT, white TPT could improve the output power by 1%, which can contribute to reducing module power loss.

EVA is used to bind the glass, cell and back sheet. Due to its UV instability, long-

term irradiation by sunlight consisting of 6% UV light may result in its aging, cracking and yellowing. As a consequence, the transmission rate will be decreased, and those parts of the solar cells that are covered by ribbon cannot absorb the sunlight. Therefore, some ribbon companies produce light-reflecting ribbon which has grooves and silver plating on the top surface, which can reflect the light incident on the ribbon into the glass inner surface from some certain angles. The light then can be totally reflected from the glass-air interface to the cell surface. Theoretically, this light absorption is able to increase the module efficiency by approximately 2% [3].

Electrical loss

In practice, solar cells are rarely used individually. They are usually connected in series, parallel, or both, to form modules that satisfy current or voltage demand. Due to the mismatch of solar cells, the actual power output of the connected module is probably lower than the maximum output power of the component cells. When solar cells are connected in series, the total voltage is equal to the summation of the component cells' voltage, whereas the total current is limited by the smallest current of component cell. When solar cells are connected in parallel, the total current is equal to the summation of the component cells' current, and its voltage is the average of all component cells' voltage. The common module is connected by cells in series. If a 'bad' cell with low current is connected into the module, as discussed above, the output current of module is determined by this low current [4]. Consequently, the module output power will decrease and power loss will increase. In order to reduce this kind of power loss resulting from mismatched solar cells in module, solar cells with the same or similar electrical characteristics need to be selected to be connected into the module in series. Hence, a proper classification method is necessary when solar cells are sorted in order to prevent solar cell mismatch.

"Solar cells with the same or similar electrical characteristics need to be selected to be connected into the module in series."

Solar cells are connected by ribbon in modules. A solder strip is usually a copper ribbon with Sn plating on the surface. The Sn layer contains Sn/Pb, Sn/Pb/Ag or Sn/Pb/Bi, etc. The resistance of a solder strip is determined by copper ribbon. If the resistance is too high, parts of the module output power could be dissipated on the solder strip which causes electrical power loss. The metal resistance is yielded by multiplying resistivity by metal length divided by metal cross-section area. As the resistivity and length are fixed, the strip resistance can be reduced by increasing the width and thickness of the solder strip. However, the width of a solder strip cannot be increased because if the width of the solder strip becomes wider than the busbar of the solar cell, then the shading area will be enlarged and the solar cell efficiency will be reduced. Therefore, increasing the width of the copper ribbon needs to be considered, but a thicker solder strip can cause cell fragmentation when soldering. Accordingly, solder strips of suitable width and thickness should be chosen to be encapsulated into modules to prevent the module output power from dissipating on the solder strip.

The soldering process has a major impact on module output power. During the soldering process, errors such as cold solder joint and solder skips can occur, causing the contact resistance to go up and the module current to decrease. Improper soldering process can cause electrodes to fall off the wafer, which means that the current cannot be collected completely and the power loss escalates.

SiN_x thickness (nm)	Module No (pcs)	Avg. P_{max} (W)	Power loss (%)
70-75	5	95.95	2.05
80-85	5	95.99	1.60
90-95	5	96.00	1.57

Table 1. Power loss of solar cells of varying SiN_x thicknesses.

Experiment and discussion

Comparison of solar cells with different SiN_x thickness

We chose three groups of single crystalline S125-D165 (diagonal 165mm) silicon solar cells with different SiN_x thickness and efficiencies of 17.25% to be encapsulated into modules (4×9=36pcs of cells in series). During the PECVD process, the SiN_x thickness is adjusted as 70-75, 80-85 and 90-95 (nm) respectively. Each group of solar cells are made into five modules and all the other components remain unchanged. Theoretical module power output is 96.15W; Table 1 illustrates the results.

It is obvious from the collected data that modules with thicker SiN_x have a higher power output and a lower power loss, which can be attributed to optical loss. A possible explanation is that the match of thick SiN_x, EVA and glass is quite beneficial to anti-reflection, hence increasing the module output power.

Comparison of sorting by Eff and I_{ap}

Solar cells are usually sorted by efficiency (Eff). As discussed in earlier, currents of solar cells in series should be as equal as possible, so sorting by I_{ap} should be considered. Single crystalline silicon S156 solar cells with 17.75% efficiency are sorted by Eff and I_{ap} separately and encapsulated into modules (6×10=60 pcs of cells in series). The solar cells are manufactured by two different production lines and the theoretical output power of the resulting module is 254.4W. The average output power of the modules, standard deviation of each group of modules output power and average power loss of each group are calculated.

Table 2 shows that power loss of classification by Eff is 0.39% lower than classification by I_{ap} when the solar cells are produced in the same S156 production lines (line A); there are some differences between power losses of modules encapsulated by S156 solar cells sorted by I_{ap} from different production lines. I_{ap} classification has little impact on power loss, but brings about a smaller standard deviation.

Comparison of different solar cell production lines

Owing to the fact that there is a discernable difference between power losses of solar cells made by different production lines, S125 solar cells produced by two different production lines were selected. Modules (6×12=72pcs in series) were encapsulated with three groups of solar cells with 17.5% efficiency. One group is made by line A, the second group comprises line B and the last group is made by solar cells mixed from lines A and B. The theoretical output power of module is 195.08W. The standard deviation of each group of modules' output

Sorting type	Production line	No. (pcs)	Avg. P_{max}(W)	Deviation	Power loss (%)
Eff	line A	59	245.29	1.65	3.58
I_{ap}	line A	50	244.30	1.48	3.97
I_{ap}	line B	58	246.26	1.36	2.20

Table 2. Power loss of Eff & I_{ap} classification.


The same sun
that powers a PV module
can also
destroy it.
3M™ Scotchshield™ Film Backsheets
Real world performance against the elements.
Engineered with innovative fluoropolymer technology, 3M™ Scotchshield™ Film backsheets offer outstanding heat resistance, excellent UV stability and a low moisture vapor transmission rate. No other solar partner can match our more than 30 years of Renewable Energy solutions, powered by a century of 3M innovation.
Proven performance. Global reach. Unbeatable value. The power of 3M.
www.3M.com/ScotchshieldFilm
3M and Scotchshield are trademarks of 3M.
© 2011, 3M. All Rights Reserved.
3M

Production line	No. (pcs)	Avg. P_{max} (W)	Deviation	Power loss (%)
line A	13	189.40	0.45	2.93
line B	13	189.03	0.64	3.12
mixed line	14	188.64	1.04	3.32

Table 3. Power loss of modules comprising cells from different production lines.

Current (mA)	No. (pcs)	Avg. power (W)	Deviation	Power loss (%)
I_1	8	187.49	1.45	2.47
I_2	8	187.45	1.46	2.49
I_3	8	186.42	1.51	3.03
Ref	15	187.22	2.05	2.64

Table 4. Current subdivision.

power and the average power loss of each group are calculated.

From the results in Table 3, modules encapsulated by solar cells from the same production lines were seen to have a lower power loss and better output power uniformity than solar cells mixed from different production lines. The standard deviation of line A is smaller than that of line B, and line A also has a lower power loss than line B. These differences are most likely caused by the differences in equipment and calibration.

Subdivision of solar cells' current

Solar cells with 17.25% efficiency are divided into three groups by current, I_1:5.274~5.299mA, I_2:5.249~5.274mA, I_3:5.224~5.249mA. The current of the reference group is not subdivided. The theoretical output power of these four groups of modules is 192.3W.

Table 4 illustrates that the subdivision of current has little impact on power loss. However, the output power of the module changes gradually by current subdivision. Group I_1 has the largest output power while I_3 has the smallest. After encapsulation, the reference group (current non-subdivision) of modules was found to have the smallest standard deviation.

Impact of different ribbons on power loss

Ribbons with different specifications were used to form three groups of modules. The thickness by width are: 0.15 × 1.6, 0.18 × 1.6, 0.20 × 1.6 (mm). Referring to the previous discussion it is clear that the resistances of three groups are reducing. Solar cells with 17.50% efficiency are encapsulated into modules (6×10=60 pcs in series), the theoretical output power of which is 250.8W.

The data in Table 5 shows that the output power of the module increases with thicker ribbon, while the power loss is also lower. However, thick ribbon can lead to high cost and high fragment rates when soldered manually. Nevertheless, if the automated soldering line is used, any concerns about this high fragment rate by manual soldering is eliminated; thick ribbons will cause an incremental module output power and detrimental power loss. In the long run, thick ribbons are beneficial to controlling the quality of modules, increasing yield of modules and reducing the production cost.

Ribbon type (mm x mm)	No. (pcs)	Breakage (%)	Avg. power (W)	Power loss (%)
0.15 × 1.6	30	1.7	242.12	3.46
0.18 × 1.6	30	2.7	242.78	3.20
0.20 × 1.6	22	4.5	243.49	2.91

Table 5. Module encapsulation with different ribbons.

Conclusion

The power loss of modules can be divided into optical loss and electrical loss. The former contains losses resulting from limitation in the transmission rate of glass and sealant and extra power by the absorbtion of light reflected by ribbons and the back sheet. The latter contains losses caused by mismatch, ribbon resistance and current loss by bad soldering.

Solar cell classifications by efficiency or I_{ap} have little impact on the module output power. Similarly, subdivision does not have much impact on power loss, although it does contribute to the output power uniformity. The power loss of modules encapsulated by solar cells produced by the same production line is smaller than that of solar cells taken from different production lines.

The improved anti-reflection effect that results from optimization of matching the SiN_x film, EVA and glass is beneficial to increasing module output power.

Assuming there is no influence on the long-term stability and reliability, accessories should be chosen to increase the output power and decrease the power loss, such as glass/sealant with high transmission rate and soldered ribbons with high conductivity.

References

[1] Green, M.A. 1982, *Solar Cells-Operating Principles, Technology and System Application*, Prentice Hall Inc. Englewood Cliffs, pp. 161–164.

[2] Rulong, C. et al. 2003, "Encapsulation material after multi-Si solar cell module's output", *Acta Energiae Solaris Sinica*, pp. 28–30.

[3] Sachs, E.M. et al. 2009, "Light-capturing interconnect wire for 2% module power gain", *Proc. 24th EU PVSEC*, pp. 3222–3225.

[4] Garcla, A., Ruiz, J. M. & Chenlo, F. 2006, "Experimental study of mismatch and shading effects in the IV characteristic of a photovoltaic module". *Solar Energy Materials and Solar Cells*, pp. 329–340.

About the Authors

Wang Qi is supervisor of the A&T division in R&D, China Sunergy. He studied physics at Nanjing University and received his bachelor degree in 2007. He is currently working on the analysis and testing of solar cells and modules, as well as module reliability research.

Zhichun Ni is director of R&D for China Sunergy, which he joined in 2007 as senior researcher. Following a role as process engineer at Wuxi Suntech, he completed his Ph.D. at the Shanghai Institute of Applied Physics. He also has an M.Sc. from the Institute of Metal Research, and a B.Sc. in physics from the University of Inner Mongolia.

Dr. Jianhua Zhao is CTO and one of the founders of China Sunergy. From 2002 to June 2006, he was an associate professor of the Centre of Excellence for Advanced Silicon Photovoltaics and Photonics, at the University of New South Wales in Australia, and also served as its deputy director from 1999 to June 2006.

Enquiries

China Sunergy (Nanjing) Co., Ltd.
No.123 Focheng West Road
Jiangning Economic & Technical Development Zone
Nanjing 211100, China
Tel: +86 25 5276 6775
Email: zhichun.ni@chinasunergy.com

Mechanical properties of EVA-based encapsulants

Ulrich Eitner & **Sarah Kajari-Schröder**, Institute for Solar Energy Research Hamelin (ISFH), Emmerthal, Germany

ABSTRACT

Since the 1980s, ethylene-vinyl acetate (EVA) has been the standard encapsulation material for crystalline photovoltaic modules. From a mechanical point of view, the encapsulant takes the function of a compliant buffer layer surrounding the solar cells. Therefore, understanding its complex mechanical properties is essential for a robust module design that withstands thermal and mechanical loads. In the cured state after lamination, its stiffness features a high sensitivity to temperature especially in the glass transition region around -35°C, and a dependence on time which becomes obvious in relaxation and creep behaviour. This paper outlines the viscoelastic properties of EVA and the corresponding standard experimental methods, as well as the impact on the accuracy of wind and snow load test procedures for PV modules.

Introduction

The use of EVA as an encapsulation material for photovoltaic modules as shown in Fig. 1, dates back to the Flat Plate Solar Array Project at the Jet Propulsion Laboratory from 1975 to 1986 [1]. The purpose of this project was to commercialize photovoltaic energy production which included the initiation of module warranties and a high reduction of the production cost. The findings of the research project concluded that EVA-based encapsulants offered a low-cost material that meets the technical requirements for long-term stability and easy processability in a lamination step. Since this research was conducted, the vast amount of commercially deployed crystalline PV modules contain EVA encapsulants. By now, the failure modes and the reliability of EVA-based modules have been intensively discussed and have led to a number of standard accelerated aging tests, as well as to a continuous improvement of the EVA material composition [2–5].

Although promising alternative encapsulants with superior material properties have been introduced in recent years [6], EVA has remained the favoured material choice for crystalline PV modules. The reasons for the dominant position of EVA in the market are its low cost and the industry's 25 years of experience with EVA-based modules in the field. The latter point is important in order to understand the conservative attitude of module manufacturers towards new materials as they give warranties of up to 25 years on 80% of the initial output power for their product.

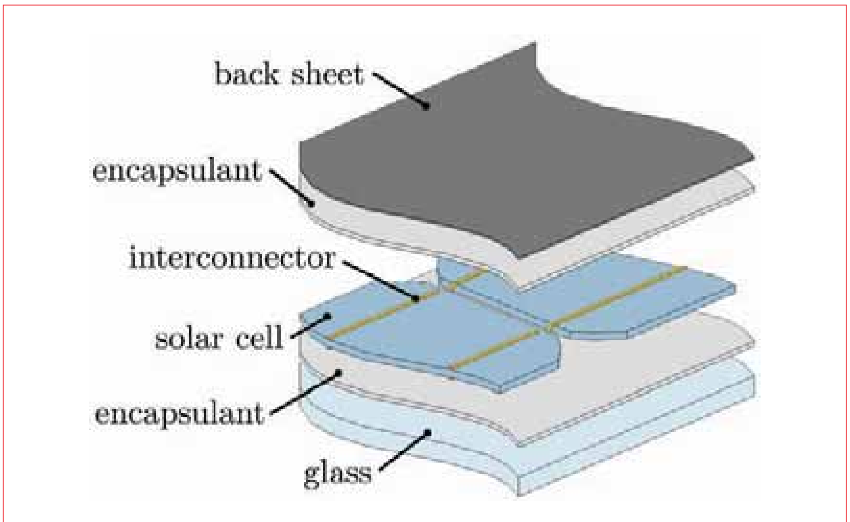

Figure 1. Lay-up of a PV module.

Structure

EVA is a thermoplastic material which becomes an elastomer after crosslinking. The crosslinking takes place during the lamination step at 150°C, where the thermoplastic polymer softens before covalent C-bonds between the formerly unconnected chain molecules are formed to create a polymeric network structure. In contrast to a purely thermoplastic material, this elastomeric macromolecule, obtained after crosslinking, cannot be melted in subsequent heating steps.

Elastomeric material behaviour

The chemical structure of the crosslinked EVA exhibits the typical mechanical properties of elastomers [7, 8]. These are closely related to the three different states: the glassy region, the glass transition region and the rubbery region. In the glassy region, which describes the polymeric behaviour at low temperatures and at high loading frequencies, the material is stiff and brittle. The macromolecular network structure is frozen so that a deformation causes the atoms to be shifted out of their energetic optimal position, resulting in a force response. When the deformation is relieved, the atoms move back into their energetic optimal positions. This kind of behaviour, found in the glassy state, is called energy-elastic.

Crosslinked EVA is in the rubbery state at room temperature. The chain segments of an elastomer are then free to rotate and to relocate so that they arrange in an optimal configuration of maximal entropy. Upon deformation, the material is stretched along the loading direction. Very high strains of up to several hundred percent are possible as the molecular chains are mobile. The reacting forces are driven by the molecular system's effort to get back into a state of maximal entropy. This behaviour is called entropy-elastic and explains the lower stiffness of the material in the rubbery state. The elastic moduli are two to three orders of magnitude lower than in the glassy state. The process of rearranging the chain segments into a configuration of maximal entropy does not occur instantaneously, and is known as relaxation or creep.

The transition between the glassy and the entropy-elastic states is not sharp but ranges over a temperature or a frequency interval, a region called glass transition. The glass transition temperature is used to quantify the centre of the transition region

Hermetically Sealed, Extra Lightweight, Extremely Flexible.

Glass-glass PV-modules ...

- Ultra thin and lightweight glass-glass modules
- Optimum performance
- More durable and more robust
- Absolutely diffusion-proof and UV-resistant
- Ideal for BiPV applications

...with LiSEC technology.

- Fully automatic line for any kind of solar cell or thin-film module
- Revolutionary, time-saving lamination process
- Reduced overall energy consumption of the manufacturing process

Glass-glass modules produced by LiSEC equipment are more robust and more flexible than traditional modules. Take advantage of their longer durability and benefit from the faster production process of this new generation of PV-modules.

LiSEC

CREATING VISIONS. PROVIDING SOLUTIONS.

www.lisec.com

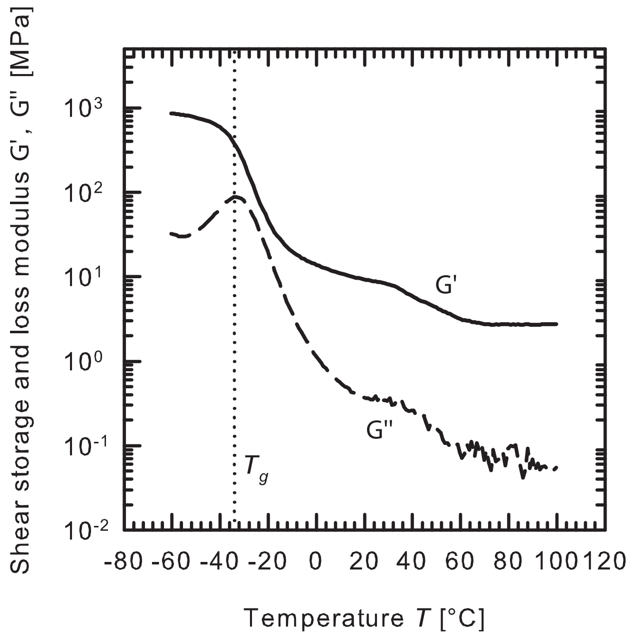

Figure 2. Dynamic mechanical analysis of EVA at 1Hz.

and is defined as the inflection point in the stiffness curve over temperature [8].

The rubbery region ends at temperatures where the elastomer is chemically decomposed. Crosslinked elastomers do not melt.

For an elastomer, the desired entropy-elastic properties of low stiffness and high deformability are given in the rubbery region. Elastomers should thus be used for applications with operating temperatures and loading frequences that fall into the rubbery region.

Mechanical testing

A common measurement method to determine the mechanical properties of a polymeric material is dynamic mechanical analysis (DMA). A specimen is dynamically loaded by applying a sinusodial strain or force and the material response in terms of force or stain are monitored. At the same time the temperature or the frequency is slowly changed at a constant rate. The measured response is plotted over temperature or frequency, split into the in-phase (elastic) signal and the off-phase (viscous) signal. The elastic part is called storage modulus G' while the viscous response is named loss modulus G''. The DMA analysis is applicable in tension, torsion or shear deformation. Results of DMA measurements of EVA can be found in various publication, for example in [9] and [10].

Fig. 2 shows a DMA of cured EVA at a constant frequency of 1Hz in torsional loading as given in [11]. The strong dependence on temperature is shown in terms of the storage modulus in shear which changes between 800MPa at -40°C and 0.2MPa at 100°C. The glass transition temperature is -35°C. A second phase transition is found at 40°C where semicrystalline parts in the EVA melt. The loss modulus G'' indicates the time dependence of the mechanical behaviour.

In order to assess the full time and temperature-dependence to set up a constitutive material law for EVA, additional experiments are necessary. It is either possible to perform the DMA as described above at various other frequencies or at different isothermal temperatures while sweeping over frequencies. Another alternative is to make use of relaxation and creep tests where a strain or stress is applied in an instantaneous loading step. Here, different isothermal temperatures are required for a full description of the mechanical behaviour.

At ISFH, relaxation and creep tests were carried out at constant temperatures between -40°C and 140°C. Specimens of cured EVA in the shape of the ASTM D638 standard (type I) were loaded in tension in a 2s elongation step of approximately 5% strain. The elongation was held constant for several hours to monitor a decreasing force signal of the sample. The longitudinal and transverse strain was recorded with a stereo camera system in conjunction with digital image correlation technique. The relaxation modulus, which is the fraction of stress σ and strain ε,

$$E(t) = \frac{\sigma(t)}{\varepsilon(t)} \qquad (1)$$

is shown in Fig. 3. Again, the time- and temperature-dependence become obvious. At high temperatures above 100°C the tensile relaxation modulus *E(t)* is below 1MPa whereas at -35°C it is between 60 and 800MPa. In creep experiments a step in stress was applied to the tensile specimen in order to monitor the increasing elongation in terms of longitudinal strain.

Viscoelastic material model

The purpose of a valid mechanical material model for EVA is to fully describe the relation between stress, strain, time and temperature. The model can then be used for direct evaluation of simple load cases or for complex Finite-Element-Analyses (FEM) of a complete module. The measured behaviour of EVA is time-

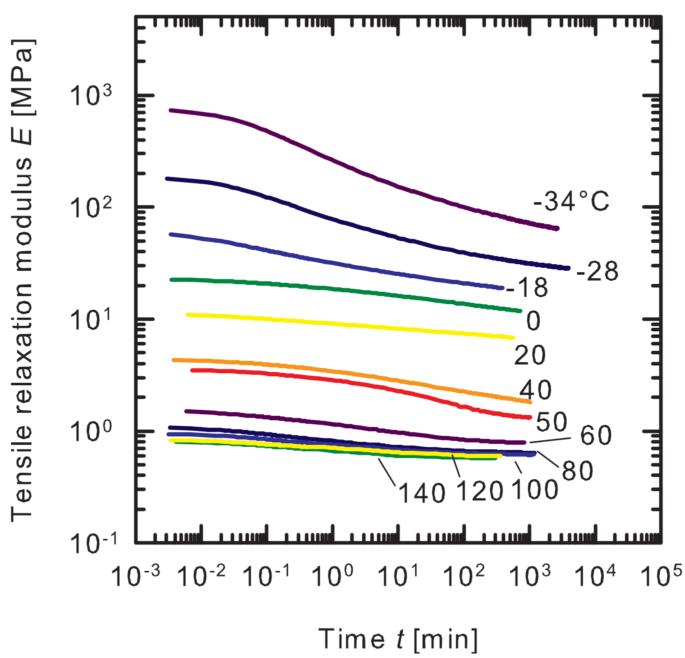

Figure 3. Relaxation curves of EVA.

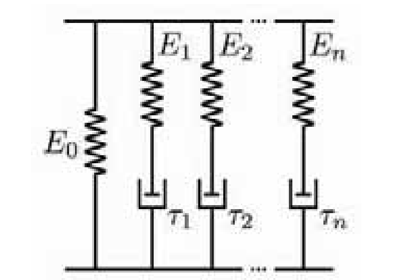

Figure 4. Generalized Maxwell model.

and temperature-dependent and can be described by a viscoelastic constitutive equation. For a constant temperature it is:

$$\sigma(t) = \int_0^t E(t-s)\dot{\varepsilon}(s)ds \qquad (2)$$

where $E(t)$ is the relaxation modulus at that temperature. The integral implies that the complete loading history is relevant for the actual stress state. The temperature-dependence is included with the help of the time-temperature-superposition. It is based on the observation that the isothermal relaxation curves (as shown in Fig. 3) overlap if they are shifted along the logarithmic time axis, resulting in a mastercurve. For each shifted curve the shift factor α expresses the amount of shifting and is formalized by the Williams-Landel-Ferry (WLF) equation:

$$\log_{10}(\alpha) = \frac{C_1(T-T_0)}{C_2+T-T_0} \qquad (3)$$

with T_0=-20°C, C_1=-48.4 and C_2=172.5 K. To complete the viscoelastic material model for EVA the mastercurve needs to be expressed in terms of the reduced time t. The standard procedure is to use a generalized Maxwell model that consists of springs and dashpot elements as illustrated in Fig. 4. The corresponding equation is the Prony series:

$$E(t) = E_0 + \sum_{i=1}^{n} E_i \exp\left(\frac{-t}{\tau_i}\right) \qquad (4)$$

.

The τ_i are set to one per decade while the E_i are treated as fit parameters; details of the modelling procedure are given in [11].

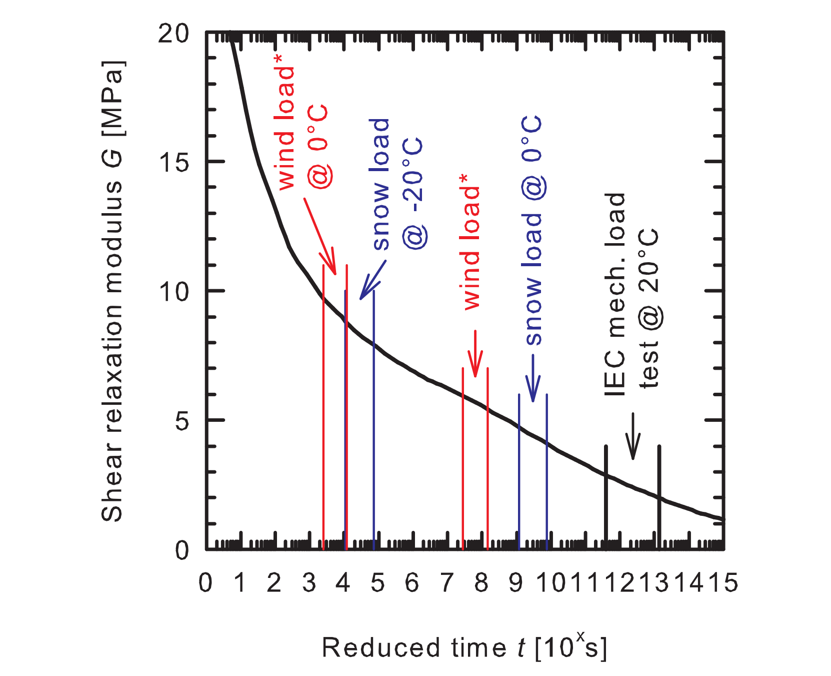

Figure 5. Behaviour of EVA in wind and snow load tests at different temperatures. *Time scales converted from [14].

Consequences for module design and standard testing

The fact that the mechanical properties of EVA depend on time and temperature has direct consequences for the module design and the standard tests. First it should be noted that the glass transition region lies within the operating temperatures that range from -40°C to 85°C. At around -30°C the shear storage modulus drops from 800MPa to 10MPa as measured with the DMA at 1Hz. As stated in the discussion of elastomeric properties, such an overlap between operation temperatures and the glass transition region should be avoided.

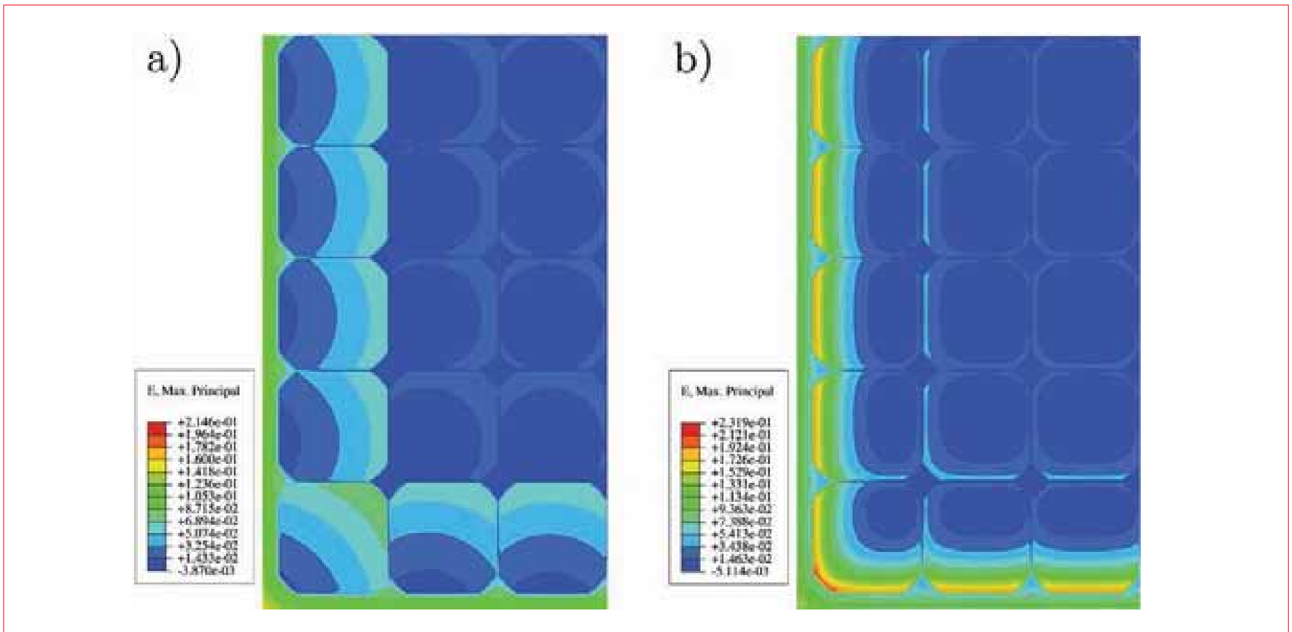

Figure 6. Simulated maximum principle strain in the EVA layer between glass and cells (a) and in the EVA layer between back sheet and cells (b) at -40°C. The lower left hand quarter of a 60-cell module is shown.

Of particular importance in regard to thinner cells that break at lower strains in the module, the compliant characteristics of the encapsulant have to be maintained for all thermomechanical loading conditions. The fact that the encapsulant creeps raises questions about the long-term deformation of modules as discussed in [12].

Second, the snow load and the wind load tests do not reflect the outdoor conditions as they do not imitate the correct temperature or loading frequency. Fig. 5 shows the stiffness of EVA over the reduced time and the testing conditions for the snow and wind load tests at different temperatures. In a worst-case scenario, the module survives the IEC 61215 load test at room temperature but fails with an equivalent snow load at -20°C as the EVA is not compliant enough to protect the cells from large strains. For PVB encapsulants, where the glass transition is around 25°C, the effect of less bending at lower temperatures due to higher stiffness of the encapsulant has been experimentally shown [13]. Another worst-case scenario is possible for the wind loads when relying on the frequencies reported in [14] as indicated in Fig. 5.

FEM-simulation of a module during thermal cycling

Along with accurate material models for all module materials, the viscoelastic model for EVA allows for a detailed simulation of a module during a thermal cycling test. When a 60-cell module with a 4mm-thick glass superstrate and 200µm-thick, 125 × 125mm^2 monocrystalline cells cools down from a stress-free initial state at 150°C lamination temperature, the largest deformation and stresses are found at -40°C. The reasons for this are the different coefficients of thermal expansion for the glass, the silicon solar cells and the back sheet. Fig. 6 shows the resulting strains at -40°C in the lower left-hand quarter of the module. The simulated strains exceed 20% which demonstrates that the EVA takes the function of a compliant buffer layer between glass, back sheet and solar cells. The deformation is higher between the back sheet and the cells than in the EVA layer between the glass and the cells due to the larger contraction of the back sheet compared to the glass. The maximum strain is found under the outer edges of the cells close to the module edges. The interconnects are not part of the simulation.

Conclusions

The complex mechanical properties of EVA-based encapsulants, i.e. the time- and temperature-dependence have been discussed in this paper. The elastic modulus of EVA was determined in DMA and relaxation/creep experiments to range from almost 1GPa at -40°C to below 1MPa at 140°C. Furthermore, relaxation and creep experiments reveal the time-dependent characteristics of EVA. The glass transition region overlaps with the operating modules' temperatures around -20°C, representing a possible weak point in the standard module design, especially when it comes to the encapsulation of thin fragile cells. Another direct consequence of the time- and temperature-dependence is the limited validity of the standard snow and wind load tests. The fact that they are usually performed at room temperature where the EVA is very compliant does not guarantee a correct operability at temperatures below 0°C where the stiffness of EVA increases by several orders of magnitude. The Finite-Element-Analysis of a module during thermal cycling demonstrates that the soft and compliant material properties of EVA are needed to provide a mechanical buffer layer between the glass, the crystalline solar cells and the back sheet. The simulated strains exceed 20% which are in general best borne by a polymeric material with entropy-elastic properties such as EVA in the rubbery state.

References

[1] Cuddihy, E. et al. 1986. "Flat-plate solar array project. Volume 7: Module encapsulation", Technical Report, DOE/JPL-1012-125-VOL-7.

[2] Czanderna, A.W. & Pern, F.J. 1996. "Encapsulation of PV modules using ethylene vinyl acetate copolymer as a pottant: A critical review", *Solar Energy Materials and Solar Cells*, Vol. 43(2), pp. 101–181.

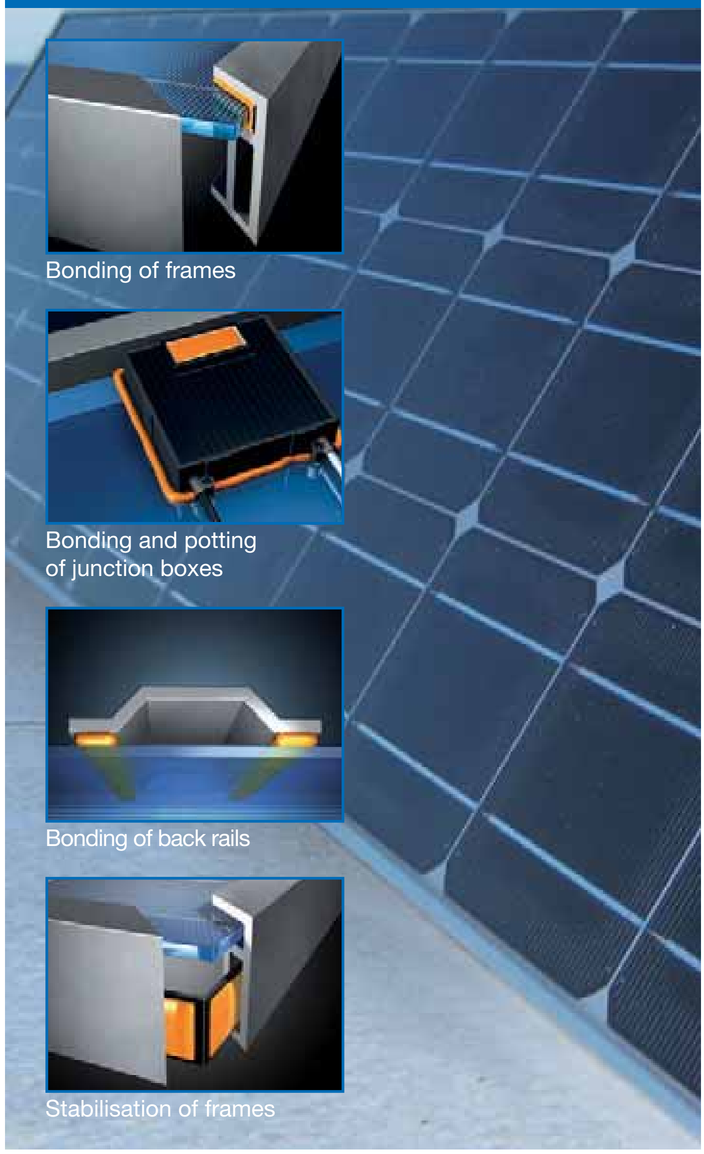

[3] Wohlgemuth, J. & Petersen, R. 1993. *"Reliability of EVA modules", Proc. 23rd IEEE PVSC*, pp. 1090–1094.

[4] Osterwald, C.R. & McMahon, T.J. 2009, "History of accelerated and qualification testing of terrestrial photovoltaic modules: A literature review", *Progress in Photovoltaics: Research and Applications*, Vol. 17. pp. 1133.

[5] King, D.L. et al. 2000, "Photovoltaic module performance and durability following long-term field exposure", *Progress in Photovoltaics: Research and Applications*, Vol. 8, pp. 241–256.

[6] Kempe, M. 2010, "Evaluation of encapsulant materials for PV applications", *Photovoltaics International*, Vol. 9, pp. 170–176.

[7] Menges, G., Haberstroh, E., Michaeli, W. & Schmachtenberg, E. 2002, *Werkstoffkunde Kunststoffe*, Hanser Fachbuch, Germany.

[8] Ehrenstein, G. 1999. *Polymer-Werkstoffe: Struktur Eigenschaften – Anwendung*, Hanser Fachbuch, Germany.

[9] Kempe, M.D. 2005, "Rheological and mechanical considerations for photovoltaic encapsulants", *DOE Solar Energy Technologies Program Review Meeting*, Denver, Colorado, USA.

[10] Stark, W. & Jaunich, M. 2011. "Investigation of Ethylene/Vinyl Acetate Copolymer (EVA) by thermal analysis DSC and DMA", *Polymer Testing*, Vol 30, pp. 236–242.

[11] Eitner, U. et al. 2010. "Non-linear mechanical properties of ethylene-vinyl acetate (EVA) and its relevance to thermomechanics of photovoltaic modules", *Proc. 25th EUPVSEC*, pp. 4366–4368.

[12] Miller, D. et al. 2010, "Creep in photovoltaic modules: Examining the stability of polymeric materials and components", *Proc. 35th IEEE PVSC*, pp. 262–268.

[13] Schubbert, C. et al. 2010, "Exemplary results of temperature-dependent mechanical load tests under variation of glass and foil parameters and investigation of different load types", *Proc. 25th EU PVSEC*, pp. 3981–3983.

[14] Assmus, M. et al. 2009, "Dynamic Mechanical Loads on PV-Modules", *Proc. 24th EU PVSEC*, pp. 3395–3397.

About the Author

Ulrich Eitner studied technical mathematics at the University of Karlsruhe (TH) and joined the PV module technology group at ISFH in 2006. He recently finished his Ph.D. thesis on thermomechanics of photovoltaic modules where he focused on mechanical testing, material modelling, Finite-Element-simulations, deformation experiments and optimization of back-contact module interconnection. He is currently a project leader at ISFH working on the mechanical characterization of novel module concepts and materials.

Sarah Kajari-Schröder is a scientist at the ISFH in the PV module technology group. She received her Ph.D. degree in physics in 2009 from the University of Ulm, Germany. Her current research interests include the mechanical properties of PV modules and their components with emphasis on crack formation in silicon solar cells and their influence on the power stability of PV modules under artificial ageing.

Enquiries

PV Module Technology - Mechanics
Institute for Solar Energy Research Hamelin (ISFH)
Am Ohrberg 1
D-31860 Emmerthal, Germany
Tel: +49 (0)5151 999 303
Fax: +49 (0)5151 999 400
Email: eitner@isfh.de


© Schweizer Solarpreis 2010/Solar Agentur Schweiz

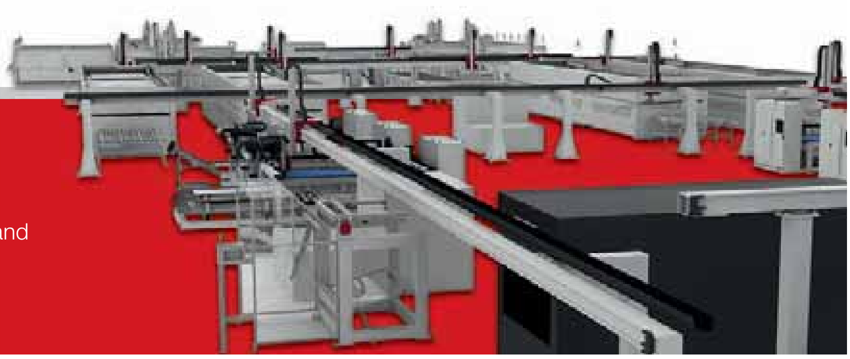

Snapshot of spot market for PV modules – quarterly report Q1 2011

pvXchange, Berlin, Germany

ABSTRACT
Solar enterprises will each be faced with the occasional surplus or lack of solar modules in their lifetimes. In these instances, it is useful to adjust these stock levels at short notice, thus creating a spot market. Spot markets serve the short-term trade of different products, where the seller is able to permanently or temporarily offset surplus, while buyers are able to access attractive offers on surplus stocks and supplement existing supplyarrangements as a last resort.

Prices are falling and falling, and the spot market for PV modules has said farewell to Q1 2011, which saw prices that that have never been so low. Whether the prices will rise again – as so often happens at the start of summer – is difficult to predict.

In this issue of *Photovoltaics International*, we present our market report using a slightly modified structure. With an ever-expanding share of products on the spot market coming from South Korea and Taiwan, we are incorporating more statistics from these regions than before. As price developments seen in some markets are almost identical, we have combined the four nations in two groups: China/Taiwan and Japan/Korea. We have also performed an accurate analysis of the European offers on the pvXchange spot market and have come to the conclusion that – for us at least – the relatively small offers being produced by the Spanish, Italian and Scandinavian markets are no more statistically relevant than these 'new' markets. Overall, crystalline technology accounts for over 80% of offers available on our exchange, as shown in Figs. 1, 2 and 3. About 20% of the offers – a figure that also accounts for the technology's share of global module production – are thin-film modules. As these figures are split across a number of different technologies and price levels, we will not report on their data at this point. According to various studies, the proportion held by these thin-film technologies will increase to about 30% by 2012 and, of course, will continue to form part of our quarterly market reports in future.

The cause for these low prices reflects an overall weakness in the spot market. Many investors are fazed by the uncertainty that still surrounds large markets such as Germany and Italy. At the same time, many buyers are continuing to bet that falling prices can remain stable, thereby avoiding the yields of PV systems despite decreasing feed-in tariffs. Suppliers and distributors with a sufficiently large capital base experience only limited effects from this uncertainty. Prices continue to decline slowly, and stores in European ports are well-equipped with goods from Asia.

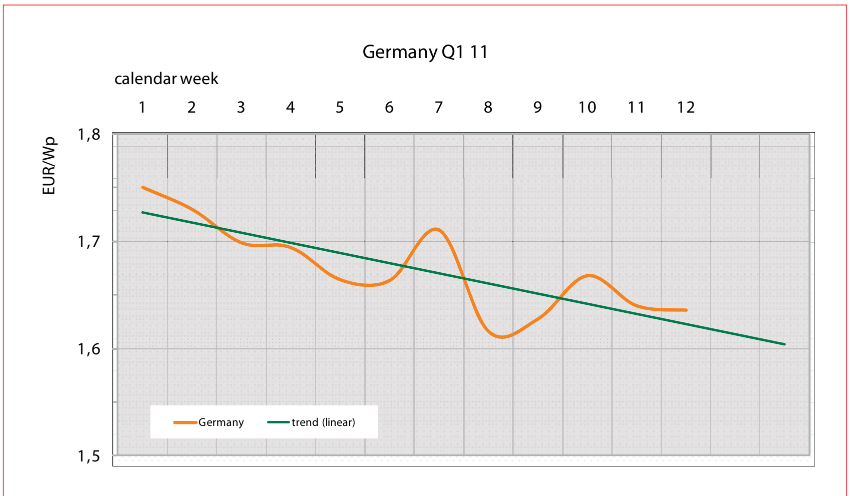

Figure 1. Development of module prices for modules produced by German manufacturers from January 2011 to beginning of April 2011.

However, this could be set for a change. Silicon prices on the spot market reached US$79/kg in March, the highest it has been since January 2009. Many cell producers whose prices remained unchanged are now suffering under tight profit margins, while those manufacturers that had the option of using the strength of the European currency have avoided much of the distress caused by the increase in commodity prices, which tend to be negotiated in USD.

One-third of module sales on the spot market for Q1 went to Italy. The country's Government's plans to amend the feed-in tariff led to a rush to complete and grid-connect PV plants by the end of May in order to avail of the higher remuneration. Italy will, together with Spain, Germany,

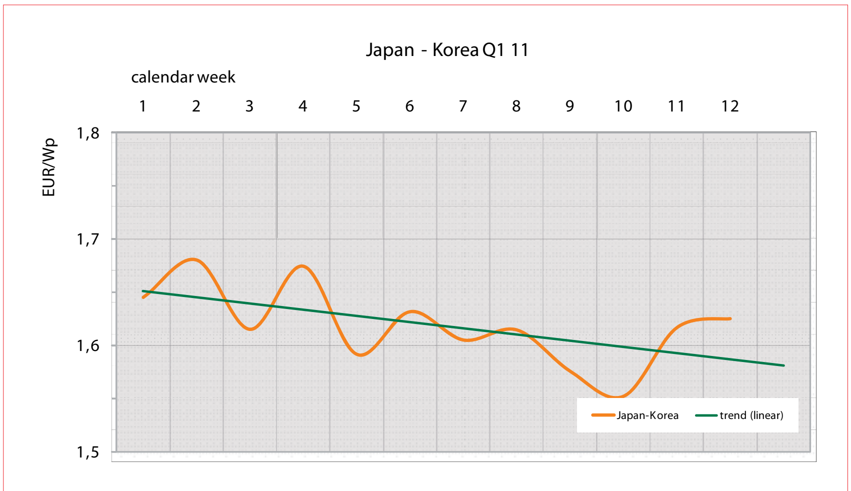

Figure 2. Development of module prices for modules produced by Japanese/Korean manufacturers from January 2011 to beginning of April 2011.

France and England, most likely see reductions in their respective feed-in tariffs. It is therefore not surprising that some experts anticipate a weak second half for 2011's market as a result of all of these changes. Global demand growth is expected in markets in the USA, Canada, China and India. Even Japan's market is on the up, with a new feed-in-tariff being introduced that will allow for an additional gigawatt to be connected to the grid. This is, of course, dependent on whether the frightening events of March will allow the Japanese government sufficient financial breathing room for the development of solar energy.

In Europe, Eastern European countries and Greece will again provide a revival of the market. Chinese module manufacturers in particular have their eye on the Eastern European markets and are more active now in Bulgaria, Croatia, Romania and Hungary than they have ever been.

The experts therefore remain optimistic in their predictions, projecting that the world market for 2011 will reach between 16 and 19GW of new installed power. Nevertheless, the percentage of strong markets such as Germany, Italy and the Czech Republic will dip in 2011. It is encouraging to note that more than 100MW of PV modules will be installed in at least 18 countries this year, says IMS Research. In 2009, this had spread to only eight nations. Thus, the expansion of the usage of global solar energy is distributed across more members than ever before.

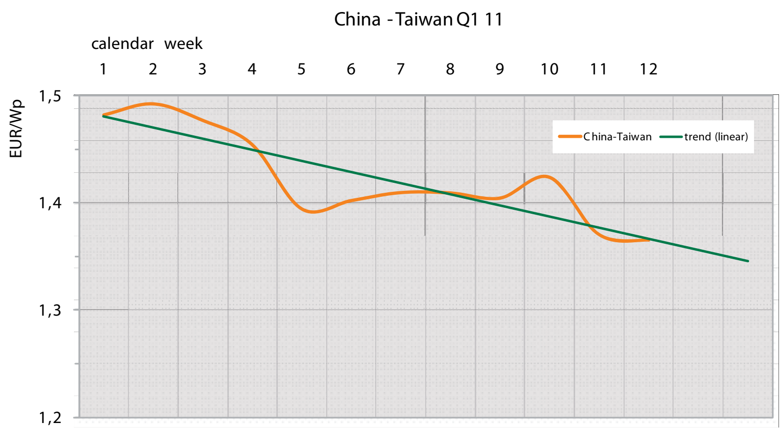

Figure 3. Development of module prices for modules produced by Chinese/ Taiwanese manufacturers from January 2011 to beginning of April 2011.

About the Authors

Founded in Berlin in 2004, **pvXchange GmbH** has established itself as the global market leader in the procurement of photovoltaic products for business customers. In 2010, the company procured solar modules with an output of around 180MW. With its international network and complementary services, pvXchange is constantly developing its position in the renewable energy market, a market which continues to grow on a global scale. Based in Europe, pvXchange also has a presence in Asia and the USA.

Enquiries

pvXchange GmbH
Tempelhofer Ufer 37
10963 Berlin
Germany

Tel: +49 (0) 30 236 31 36 0
Fax: +49 (0) 30 236 31 36 23
Email: info@pvxchange.de
Web: www.pvxchange.com
www.pvxchange-international.com

Power Generation

178

167

167

Total to buy SunPower as it makes major play into utility-scale solar business

SunPower's solar trackers installed at the Tolosa Winery in San Luis Obispo, California.

At an initial cost of approximately US$1.37 billion, French oil and gas company Total will purchase 60% of SunPower's outstanding Class A and B shares, taking a majority share in the US-based PV manufacturer and major project developer. The deal was said to have been approved by the boards of both companies. A further US$1 billion of finance will be made available to SunPower so that it can accelerate its project pipeline rollout, add manufacturing capacity, and further its R&D activities.

SunPower's board will be expanded to 11 members following the closing, with the current management team remaining to run operations. The agreement also includes conditions that mean Total will need to demonstrate its ability to purchase additional shares of SunPower in the future. However, Total will nominate a majority of directors to SunPower's board.

Total is not new to the PV market, as it has previously invested and nurtured activities in joint-venture affiliates Tenesol and Photovoltech and has small stake holdings in OPV developer Konarka and AE Polysilicon.

As part of the deal Total will offer to guarantee an amount up to US$1 billion for SunPower's repayment obligations with respect to letters of credit issued over the next five years for utility power plant and large commercial installation businesses.

According to SunPower, this credit support facility would enable the firm to substantially reduce the total costs LOCs and financing and lower its cost of capital and increasing its access to uncollateralized debt financing. Total had net income of US$13.6 billion in 2010.

US & Canada News Focus

BrightSource closes financing for 392MW Ivanpah Solar development

BrightSource Energy has closed financing for its record-breaking 392MW Ivanpah Solar Electric Generating System in California. The final round of funding for Ivanpah, which will be the world's largest solar project when it is completed in 2013, saw BrightSource secure US$1.6 billion in guaranteed loans from the Department of Energy (DOE) and a US$168-million equity investment from Google.

Ivanpah is made up of three separate solar thermal power plants and is situated on 3,500 acres of federal land managed by the US Department of the Interior's Bureau of Land Management (BLM). Around two-thirds of the power generated from the systems will be sold to Pacific Gas and Electric (PG&E), with Southern California Edison purchasing the other third. State and federal permits for the project were received in September and October 2010, respectively.

"The DOE's loan guarantee program is playing a vital role in realising our nation's clean energy and economic goals,"

Image: Ivanpah Power

Artist's impression of the Ivanpah Power system in California.

commented BrightSource's CFO, Jack Jenkins-Stark. "In partnership with the DOE, NRG, Bechtel and now Google, we're building at Ivanpah cost-effective, environmentally-friendly and reliable solar power plants. We're thrilled to work with two of America's leading utilities – PG&E and Southern California Edison – to provide their customers with clean, reliable and cost-effective solar power at a meaningful scale."

In October 2010, NRG Solar was unveiled as Ivanpah's lead investor, committing US$300 million towards the project. The date also coincided with BrightSource's engineering partner, Bechtel, starting work on the mammoth development, which will nearly double the amount of solar thermal electricity produced in the US.

Pegasus Energy petitions California ISO for interconnection to electric grid

Pegasus Energy Partners has submitted an application to California ISO for its 400MW Mountain House Solar Farm in Alameda County to be interconnected to the grid. The company anticipates submitting an application to the Alameda County Planning Department for a conditional use permit in the next few weeks. The Mountain House Solar Farm will be built across 2000 acres in the eastern area of Alameda County. Pegasus will develop, finance, own and operate the facility.

The company is looking to use the 1603 grant money that was approved as part of the American Recovery and Reinvestment act. Although the grant funds are set to expire by the end of this year, Pegasus is anticipating the approval of the fiscal year 2012 budget, where it is expected that the grant funds will be extended until January1, 2013.

Construction on the 400MW solar farm is expected to begin in the fourth quarter of 2012 and has a first phase completion date for some time in 2014.

CVEC selects American Capital Energy for 18MW solar project on Cape Cod and Martha's Vineyard

American Capital Energy (ACE) has won the Cape & Vineyard Electric Cooperatives (CVEC) bid to construct an 18.3MW solar project on Martha's Vineyard and Cape Cod. The solar project will be built across 10 proposed sites in seven of CVEC's member towns on the Cape and Vineyard, with one of the projects having a proposed installation site at the capped Harwich landfill. The 18.3MW solar installation should produce 22,552,200kWh of energy per year, equivalent to 26% of the Cape and Vineyard's municipal load and 1.1% of the total energy load for all customers on the islands.

As part of its agreement for selection to develop the solar projects, ACE will advertise for local installation and/or maintenance subcontractors to install the PV projects. The company is projecting that not only will the project create 500 full-time jobs during development, but will save CVEC member towns and counties US$1.4 million per year.

FRV starts building 30MW Webberville solar project

Fotowatio Renewable Ventures (FRV) has closed financing and started construction work on its 30MW Webberville project. Renewable Energy Systems Americas (RES Americas) is building the system, which is being fitted with Trina Solar's 270W crystalline modules and has a penciled-in completion date for the end of 2011.

Financial backing has come from Bayerische Landesbank, which has fully underwritten the construction debt for the project, and enabled RES Americas to forge ahead with construction. The site is located on Austin Energy-owned land in Travis County, approximately 15 miles east of Austin; Austin Energy has signed a 25-year power-purchase agreement to buy the electricity generated by the Webberville system.

SunPower receives conditional loan guarantee from DOE as it dedicates its 75MW plant in Milpitas

In future weeks, SunPower will almost certainly be marking April 12 as not only an eventful day, but a successful one as well. Not only did the company celebrate the opening of its Milpitas module manufacturing plant, but also announced that the US Department of Energy (DOE) has offered the company a conditional

Image: Americal Capital Energy

American Capital Energy's 3MW (DC) roof-mounted installation in York, Pennsylvania.

loan guarantee for its California Valley Solar Ranch power plant. US Energy Secretary Steven Chu and California Governor Edmund "Jerry" Brown joined company officials as it dedicated its 75MW solar panel manufacturing facility in Milpitas, California.

Built in cooperation with Flextronics, who is credited with bringing the plant into full production less than four months after the first panel was produced, the 75MW Milpitas manufacturing plant has created 100 new jobs. SunPower notes that its new manufacturing plant will allow the company to provide panels for solar installations in a more rapid, yet cost-effective way. Specifically, the Milpitas location will supply solar panels for SunPower's 250MW California Solar Valley Ranch (CVSR) in San Luis Obispo County.

The CVSR project received additional support today as well with an announcement by Secretary Chu advising that the US DOE offered the project a conditional commitment for a loan guarantee for up to US$1.187 billion. Construction on the project is anticipated to begin this summer once permitting and financing have been settled. Operations at the plant should begin by the end of this year with the balance coming on line in 2012 and 2013.

Although SunPower will design, build and initially operate and maintain the CVSR project, NRG Solar, a subsidiary of NRG Energy, will adopt all ownership and financing responsibilities, subject to certain conditions. Pacific Gas and Electric Company will plans to purchase all of the output energy from the project.

Fluor to build SunPower's 20MW Copper Crossing plant

SunPower has chosen Fluor to build its 20MW Copper Crossing photovoltaic plant in Pinal County, Arizona. The system, situated on 144 acres of formerly private agricultural land, will be owned and operated by Iberdrola Renewables and completed before the end of 2011.

SunPower's Oasis modular solar power block, which utilises the T0 Tracker and E19 solar panels, will power Copper Crossing and the electricity generated is to be sold to Salt River Project under a long-term power purchase agreement. Pinal County hopes the development will not only stimulate employment in the area, but also prove to be a revenue generator for schools and other public services.

San Diego Gas & Electric, Soitec to build 30MW portfolio

San Diego Gas & Electric (SDG&E) has signed contracts with subsidiaries of Soitec Solar Development to build three solar projects in San Diego County with a combined capacity of 30MW. All three systems will use Soitec Concentrix technology and are currently awaiting approval from the California Public Utilities Commission.

These contracts take SDG&E's portfolio of solar projects in the past 12 months to 520MW, which more than doubles the solar capacity of the County. Each of the new systems will be fitted with a ground-mounted dual-axis tracking CPV solar power system and Soitec modules, manufactured at the company's newly-built factory.

Avidan Management unveils US's largest solar rooftop system

Avidan Management has finished work on its 4.26MW rooftop solar system in Edison, New Jersey. The array, designed and installed by Solar Nation, generates 5

Image: Recharge

Avidan Management's Josh Avidan at the opening of the 4.26MW system in Edison, New Jersey.

million kWh of electricity a year, which will be used to help power the 656,255-square-foot office and storage facility on which the system is housed.

The 17-acre roof is populated by 17,745 SolarWorld panels, making it the largest roof array in the US, and its official unveiling was attended by local politicians and businessmen, including the head of Avidan Management, Avi Avidan.

Europe News Focus

Phoenix Solar plans 12MW solar park in southern France

Phoenix Solar has signed a deal to construct a 12MW turnkey solar park in Le Castellet, France for the joint venture formed between InfraClass Energie 5, a close-end fund of KGAL, and CRYO SARL. Set to be built over almost 62 acres in southern France, this solar project is Phoenix Solar's largest installation outside of Germany to date.

The solar installation will utilize nearly 150,000 First Solar modules and 35 Power One central inverters. Phoenix Solar will act as the EPC contractor, manage the planning, delivery and construction of the project, and assume maintenance and operation responsibilities once completed. Construction is underway at the site and has a scheduled completion date set for the end of August.

Electricity fed into the grid will be recompensed by EDF Energy based off the feed-in tariff still valid from 2009.

Google hands over US$5m for its first solar investment in Europe

Google has crossed over into Europe's renewable energy sector by investing US$5 million in an 18.7MW solar power plant near Berlin, Germany. The search giant will work with German private equity company Capital Stage, which will sell 49% of the recently acquired plant to Google. This is the company's first clean energy project investment this side of the pond.

Located in Brandenburg an der Havel, the plant covers 47 hectares (116 acres) of land and will provide solar energy to approximately 5,000 homes in the area.

Google is investing US$5 million in an 18.7MW solar power plant near Berlin, Germany.

The two companies have agreed to jointly operate the plant.

The transaction still requires the formal approval of the German competition authorities, and is subject to other customary closing conditions.

Although this is Google's first clean energy investment in Europe, the company previously backed renewable energy projects in the U.S. In total the Internet giant has invested approximately US$100 million in renewable energy projects in that region of the world.

Conergy installs Gran Canaria's largest rooftop solar system

Conergy has finished work on its 1.75MW rooftop PV system on the Spanish island of Gran Canaria. The system, situated on the roof of coffee roaster Emicela in Agüimes, took just two months to complete and will generate up to 2,600 MWh of electricity annually.

Image: Conergy

Conergy's 1.75MW system on the roof of Spanish coffee roaster Emicela.

This latest installation takes Conergy's solar portfolio on the Canary Islands past the 12MW mark, and with 7,600 Conergy Power Plus photovoltaic modules and 72 IPG series inverters it is the largest to date. Funding for the project was provided by Spanish banking conglomerate Bankia.

Conergy finish 2.2MW German solar park

Conergy has finished work on its new 2.2MW PV park in north Brandenburg, Germany. Once connected to the grid, the system, which is made up of 27,300 modules and spans 12 acres, will generate 2,134 MWh of electricity every year.

Despite this year's harsh winter, Conergy took just six weeks to complete the system, with project developers Helonius even resorting to using Bunsen burners to free mounting systems from the thick ice.

Enel to spend €1 billion on developing solar in Italy

Enel Green Power is planning to spend €6.4 billion (US$9.1 billion) on renewable power plants in Italy over the next four years. And a significant portion of this funding will be directed towards the construction of a new solar panel manufacturing facility in Catania, Sicily.

Around €1 billion has been put to one side to develop this panel factory and a portfolio of PV plants across the peninsula. Phase one of the Catania project will cost €300 million, with a possible second phase adding a further €500 million to this total.

Italy's state-controlled utility Enel SpA sold shares and listed Enel Green Power on the Milan Stock Exchange in November as part of an expansion plan to move into other European and the North American renewable market. Production is currently being ramped up in Italy, Spain, France, Greece, Turkey and Romania, with plans already afoot to establish Enel in North Africa and the Middle East after 2015.

Asia

ADB pledges US$150 million in credit guarantees to bolster solar power development in India

The Asian Development Bank (ADB) revealed plans to offer up to US$150 million in credit guarantees to local and foreign commercial banks to encourage the development of solar power as a renewable energy in India. The credit will cover 50% of the payment default risk on bank loans made to solar project developers with an aim to secure long-term funding for solar energy development in the country.

ADB's partial guarantees on loans of up to 15 years will back projects up to 25MW. The bank is also contemplating a separate direct finance program for larger solar power projects with the Indian private sector. Currently, ADB will additionally provide US$1.25 million for training on solar technology, risk issues and aiding participating banks in the technical due diligence for individual solar projects.

ADB's concessional technical assistance special fund will provide a grant of US$500,000, while the Asian Clean Energy Fund will supply a second grant of US$750,000. The latter Government of Japan-established grant is part of the ADB-administered Clean Energy Financing Partnership Facility.

Tata Power commissions 3MW solar power plant in India

India's largest private power utility firm, Tata Power, has commissioned a 3MW solar power plant in Mulshi. The project, which is one of the largest in the entire country and the first built in the province of Maharashtra, is spread over 12 acres and took nine months to complete.

The electricity generated by the system will be distributed in Mumbai in order to meet a Renewable Energy Purchase Obligation (RPO) as defined by Maharashtra Electricity Regulatory Commission (MERC). BP Solar provided the technology for the ground-breaking installation.

Areva Solar to build Southern Hemisphere's largest solar project

Areva Solar has won the right to install the Southern Hemisphere's largest solar power system in Queensland Australia. The 44MW solar thermal augmentation project will be installed at CS Energy's 750MW Kogan Creek coal power station and generate around 44,000 MWh of electricity per annum.

Building work to install Areva's Compact Linear Fresnel Reflector (CLFR) technology is scheduled to get underway in the next few months, with commercial operation planned for 2013. The total cost of the planned upgrade is estimated to be AU$104.7 million (US$109.9 million).

Kogan Creek will use Areva's CLFR technology to supplement the power station's coal-fired steam generation system, thus increasing its electrical output and fuel efficiency. The power station is already connected to Australia's electricity grid, which will enable the solar generated power to flow directly into the Queensland network.

Areva has also agreed to build and operate a manufacturing plant to support Kogan Creek. The factory will also help stimulate the Australian solar industry by supplying future projects in the region.

Conergy will construct 12.4MW solar park in Nakhon Pathom province, Thailand

Together with Annex Power, the Bangkok-based systems integrator, Conergy will build what will be its third solar power plant on Thai soil in the space of a year. The 12.4MW solar park in Nakhon Pathom province, which will cover an area of 268,500m2, follows on from the recently-completed 3MW Ayutthaya solar park, constructed for the investors Yanhee Solar and Ratchaburi Electricity, which have entered into a joint venture agreement to develop solar energy parks in Thailand.

The 12.4MW plant will be comprised of 56,000 Conergy PowerPlus Premium modules set on over 56km of Conergy SolarLinea mounting systems. Over 200 Conergy IPG 15T string and 25 IPG 300C central inverters will also be utilised to feed the 19,500MWh of annual energy production into the grid. This energy will be used to supply more than 7,700 Thai households with solar electricity.

Backing solar projects such as this, the Thai energy authority, the Department of Alternative Energy Development and Efficiency (DEDE), has revealed its intention to review the existing solar incentive scheme in the country, so that smaller residential systems can also benefit from the feed-in tariff. This path of action comes on the back of extremely volatile energy prices in the country which could, according to the authority, lead to an increase of 12-14% of the renewable energy production.

PLG Power launches 40MW solar plant

PLG Power Limited, the flagship energy and power division of PLG Group, launched India's biggest solar power generation plant of 40MW at Patan in Gujarat. This is one of the largest solar power projects in the country.

The PLG Group is also one of the leading manufacturers of crystalline PV modules in India with their manufacturing plant at Sinnar, Nasik. PLG has got the distinction of becoming the very first company to come up with 40MW of solar power generation at a stretch in India. It has the equity participation of 20MW with Zamil of Saudi Arabia and 20MW with Ashburg of Britain.

Speaking about the project, company chairman Punit Goyal said power generation from the project would be four phases of 10MW each. The first phase of 10MW is likely to be connected shortly for the power generation. And all four phases will be completed by the end of next financial year. PLG Power is one of the biggest EPC contractors for setting up grid connected solar power plants in the country.

Africa & Middle East

Belectric, Sun & Life to build 10MW PV carport system in Dhahran, Saudi Arabia

Belectric and Sun & Life are staking their claim in what they call the largest solar power plant in Saudi Arabia. The two companies are partnering on a 10MW PV carport system at Dhahran's North Park offices of Saudi Aramco. The large-scale power plant will cover all of the 4,500 parking spaces and feed into the public grid by the end of this year.

Image: Google Images

An artists impression of Belectric and Sun & Life's completed 10MW carport.

Solar Frontier will provide over 120,000 copper indium selenide (CIS) PV modules for the 10MW project. Belectric was granted the project by the Saudi Arabia based company Al Yamama, the project's principal. Furthermore, Sun & Life and Belectric plan to continue their partnership past the 10MW carport installation. Both companies intend to enter into a full-scale joint venture in EPC contracting for solar power plants and manufacturing of balance of system components in Saudi Arabia.

Saudi Arabia looking to invest in solar sector

Saudi Arabia is planning to embark on a renewable energy spending spree to help meet rising electricity demands and curb its dependence on crude oil. The Saudi government was set to unveil this new renewable-energy strategy at a conference in Riyadh on April 3.

Persian Gulf oil producers need to increase electricity output to sustain the region's 10% annual economic growth rate. However, countries in the region are also looking for new ways to generate power, thus helping them maximize income from oil exports.

Current electricity generating capacity stands at 45,000MW and this will need to rise to 120,000MW by 2030 if Saudi Arabia is to maintain its position as OPEC's leading oil supplier. To expand capacity and the electricity grid, the country will need to invest more than US$100 billion over the next 10 years, with a third of that going towards renewable and non-renewable energy power plants.

In February, Saudi Arabia reached an agreement with France to cooperate on developing nuclear energy and also announced that it would be looking to develop its solar, geothermal and wind energy sectors. Officials from the King Abdullah City for Atomic and Renewable Energy, the agency in charge of promoting alternative energy, are expected to announce guidelines and targets for solar at the Riyadh conference.

Frost & Sullivan expects Sub-Saharan Africa's off-grid PV sector to expand by 10% by 2015

Business research and consulting firm Frost and Sullivan has claimed that Sub-Saharan Africa's off-grid PV sector is set to expand by 10% between 2009 and 2015. The news is a boon to the continent's renewable energy sector, which is experiencing increasing governmental demand for small scale projects.

Due to the increased importance of energy diversification, the Sub-Saharan African renewable energy market as a whole is expected to triple in investment value between 2010 and 2015. And despite the slow pace of regulatory reform and the monopolies held by state utilities, countries such as South Africa, Kenya, Nigeria and Uganda are all seriously exploring the possibility of establishing solar power systems.

Energiebau Solarstromsysteme installs one of Africa's largest rooftop arrays in Nairobi

Energiebau Solarstromsysteme has installed one of Africa's largest solar rooftop systems on the headquarters of the United Nations Environment Programme (UNEP) in Nairobi, Kenya. The 515kW array took three months to construct and was connected to grid during the UN Global Ministerial Environment Forum on Monday; it will generate around 750,000 kWh of electricity annually.

Energiebau collaborated with Schott Solar, SMA Solar Technology and Kaneka on the project, which it claims is the first climate-neutral office building in Africa. Building work was carried out by local contractors and supervised by Energiebau.

SRC, Masdar Institute hosts first forum on photovoltaics in Abu Dhabi

Solar experts and university researchers gathered together in Abu Dhabi from March 27-28 to attend the city's first forum on photovoltaics. The event, presented by Semiconductor Research Corporation (SRC) and the Masdar Institute of Science and Technology, explored the route for development of cost-effective systems capable of achieving 25% energy conversion from solar resources in Abu Dhabi by the year 2020.

Attendees of the 'Forum on Solar-Electrical Energy Systems 2020' conference listened to presentations from 40 of the leading commercial and university researchers from North America, Europe, Asia, Japan and the United Arab Emirates. Topics ranged from new materials and nanostructures for PV, to industrial and commercial-scale PV systems and system integration challenges. Research directions needed for Abu Dhabi's solar future and potential smart grid were also discussed in detail.

The conference results are expected to drive future research initiatives for solar energy breakthroughs in Abu Dhabi that will be guided by the semiconductor and solar industries at the Masdar Institute and other education organizations.

Source: Energiebau / Mariantoinette Peru

Energiebau installed the largest rooftop solar installation in Africa for the United Nations Environment Programme (UNEP).

Concentrator photovoltaics ramps up, as project momentum accelerates and production cells enter age of 40% efficiency

By **Tom Cheyney**

There are still a lot of "ifs" when it comes to concentrator photovoltaics, but it's starting to look like the question of "when" the technology will start to gain serious market traction may be sooner than some think. With tens of megawatts of projects either recently finished, under construction, or in the last phases of project development — and hundreds more MWs in the longer-term pipeline — deployment of the high-efficiency systems may reach triple digits by the end of 2011 or beginning of 2012. On the technology front, as many as a half-dozen cell companies are bringing 40%-efficient cells to market this year, which will help to further reduce CPV's increasingly compelling levelized cost of energy.

When you talk about systems companies, none is bigger than the most experienced CPV player, Amonix — both in terms of its installed base of operational power plants and the size of its massive wall of megamodules on a pylon, the 7700 platform. During a presentation at the recent CPV-7 conference in Las Vegas, company R&D director Geoff Kinsey said that the beast (my term, not his), currently rated at 60KW with 27% efficiency, has been operating in the field above both its rating and its predicted performance, with no sign of degradation. Data from a Colorado site find the system hitting 70KW in the high DNI area.

Until recently, spectrally tuned multijunction CPV cells weren't on the menu, but that's changed significantly over the past few years, he noted. There are now multiple sources of high energy yield cells that are modelled to exceed the performance of currently deployed devices. Amonix is evaluating seven incumbent and newcomer vendors, with plans to integrate some of those cells into production in 2011.

The Seal Beach, CA-based company also expects to transition from 100mm (4-inch) to 150mm (6-inch) wafers this year. With a superior "packing fraction," the 2.25× larger substrate size should yield about a 2.5× increase in the number of cells per wafer and provide a substantial cost reduction, he explained.

The already robust PMMA Fresnel lens used by Amonix will be enhanced with better UV durability and lifetime, as well as higher optical efficiency. Recent tests conducted on some 10-year-old optics

Photo by Carlos Alejandro, courtesy of Amonix

Tracking the desert sun, a 2MW array of Amonix CPV systems generates clean electricity at the science and technology park at the University of Arizona (Tucson, AZ, USA).

pulled from the field showed the material's mean optical efficiency had dropped from 85% to 81%, when compared with a new lens of the same type — an annual degradation rate of 0.4%.

With the combination of higher performance cells, improved optics, optimized concentration levels and advanced thermal management, the next-gen modules will reach at least 32% efficiency sometime this year, according to Kinsey.

Multiple projects have just been completed, are being built, or will soon see shovels in action, including the recently energized 36 arrays making up the 2MW (AC) system on 12 acres of the Solar Zone at the University of Arizona's Science and Technology Park in Tucson. A time-lapse video (which can be found on YouTube) reveals the rapidity of the final part of the construction process, as towering cranes place a half-megawatt per day of 7700s to complete the installation.

Although he wouldn't comment on the specifics of projects under construction, CEO Brian Robertson told me that Amonix's factories are running flat out as the company ramps production to meet the demand pull. One of those sites he wouldn't discuss, the major 30MW field developed/constructed by Cogentrix Energy in Alamosa, CO, seems to be a major reason for the CPV manufacturing floor hustle and bustle.

While Amonix thinks big, Energy Innovations pursues a smaller-scale deployment approach with its dual-axis-tracked, 1200×-concentration single-module Sunflower systems. The Poway, CA-based firm has been relatively quiet of late and didn't make any presentations at CPV-7, but several members of its team were on hand at the conference, including CEO Joe Budano.

Up to almost three full work shifts at its factory, EI's first semiautomated line is fully built out and "cranking out modules," with a couple more automation production "cells" arriving soon, he said. The current 29%-efficient 270W units will be superseded by 300W models later this year; the higher-rated modules, which will be its first equipped with Spectrolab C3MJ+ cells, have been submitted for certification.

Although the company's supply chain is robust, some minor ripple effects from the Japanese earthquake/tsunami were seen, he revealed, with components like power FET devices (used in DC-DC converters) a bit tight and one robotics vendor relating that it was having trouble getting certain kinds of motors.

While "entertaining" possible 20, 40, and 60MW utility-scale installations in 2012 and beyond, he told me that the real sweet spots for his company reside within the distributed-commercial market — on warehouse and distribution center rooftops, ground-mount installations, and especially carports and truckports. If you had asked Budano two years ago what the company's primary strategy was, it would not have been carports. But he believes the segment has huge upside.

Among several projects under way, a 600kW site in Palm Desert is split 50:50 between ground-mount and carport systems. Compared to a flat-plate PV carport array which can't be tilted much beyond 5° because of wind load issues, he said the Sunflower produces 50% more energy, thanks to its higher efficiency and ability to track the sun throughout the day. Another positive aspect of the carport market that he pointed out is its relative simplicity compared to rooftops, which require more engineering and can present a host of difficulties, such as insufficient weight-bearing load factors and complex

News

roof architectures. Almost totally turnkey, a carport deal can be sold and an installation begun with a much shorter cycle time than a rooftop project.

The chief exec said the company will have 12MW installed (mostly groundmount and carport) in the US and a few overseas locales within the next year or so. Noting the tendency in the market to label Amonix, SolFocus, and Soitec (Concentrix) as the "big three" CPV systems companies, Budano thinks it's time to expand the list to four and include Energy Innovations, given its 10 years of experience and recent success pursuing its differentiated market strategy.

News

One thing all CPV systems firms have in common is the need for ever-increasing conversion efficiencies in the III-V multijunction cells at the heart of their power platforms. Even a slight increase in efficiency leads to a significant performance enhancement and reduction in the cost of overall energy production.

The company touting the top NREL-validated III-V multijunction solar cell conversion efficiency results — Solar Junction — kept a low profile at the CPV-7 conference, while just about every other cell developer and manufacturer made an appearance at the event. The newcomer's news that its "production-ready" 5.5 × 5.5mm spectrally adjustable cell hit a record-breaking 43.5% at >400 suns came on the heels of most of the other CPV cell players announcing that they were — or soon will be — at 40% efficiencies in manufacturing.

Although Solar Junction deserves kudos for cracking 43% and then some, there's a difference between what the start-up calls "production-ready" cells and other companies' cells that are actually in production and scaling. Until the new guys crank up a commercial manufacturing line (which they say will be done within a year) and get those kinds of eye-popping efficiencies consistently, at high yields and at relatively low costs, and then ship them in volume and see them perform reliably in the field, the NREL measurement lab results offer little more than bragging rights.

When it comes to the existing commercial CPV cell players, the conversation has to start with Spectrolab. The Boeing unit has more III-Vs embedded in deployed, under-sun concentrator systems than any other supplier. While Amonix, SolFocus, the newly rebranded Soitec Solar, Energy Innovations, and other systems companies may be working closely with the likes of Solar Junction, QuantaSol, Cyrium, JDS Uniphase, RFMD, and other new entrants, all of them count on Spectrolab cells for their current needs.

Russ Jones told me that the company released its 40%-efficient C4MJ cells into production in early March. Although there are not enough data available yet to analyze the efficiency distributions coming off the line, thousands of cells were qualified at 40%. The mainstreaming lattice-matched C3MJ+cell, which started production in October and has shipped since early 2011, has achieved average efficiencies of 39.2% across several hundred thousand units manufactured so far.

Since the C4MJ cells are the first employing an upright metamorphic device structure, he explained that a more extensive qualification program was needed — as in 2 million cell-hours on sun — in order to thoroughly check reliability and degradation on the widgets. As for those degradation rates, they've been found to be comparable to other cells made by the company. The business development director said that Spectrolab is taking orders for the C4MJs and has recently shipped the first batches to several customers. The new cells will likely start to show up in deployed CPV systems by the end of this year or the beginning of 2012.

Azur Space, the European incumbent III-V cell maker and veteran of the extraterrestrial and now terrestrial sectors, has also claimed membership in the "40%-class" club. Wolfgang Guter told CPV-7 attendees that the company has had its lattice-matched 3C40S (500×) triple-junction cells in production since late 2010. Engineering samples of its upright metamorphic (UMM), current-matched 3C42S (as in 42%) devices currently in development should be available by the end of the year with commercial cells on the market by 2013. The 3C40S cells feature a high-bandgap (1.9eV) top junction, with efficiencies of up to 41.2% seen in custom designs and the best wafers averaging about 40.3% at 500×.

Tunnel diodes are a key part of Azur's high-concentration design, as well as proprietary, customizable antireflective coatings that can be adapted to the reflectivity of the glass. (Note that the company sees broadband ARCs as a critical component of its next-gen UMM cells.) Stressing the narrow distribution of the maximum power current of the in-production devices as well as their customizable form factor (a recurring theme), Guter explained that they could be provided in diced wafers or in dense arrays,

Photo courtesy of Energy Innovations

At a 600kW project in Palm Springs, CA, USA, Energy Innovations is deploying both carport and field-mounted CPV systems.

in quantities from 50 to 3000 cells per wafer.

Azur is also part of what has become a cost-saving trend in the CPV cellmaking and systems community: transitioning from 100mm (4-inch) to 150mm (6-inch) germanium wafers within the next year or so. The first to make the plunge with the larger substrates may not be one of the incumbents, but a formidable newcomer — JDS Uniphase.

No stranger to volume manufacturing of high-tech components due to its experience in the telecom and photonics markets, JDSU has been carefully developing its CPV cell assets for about 2½ years, staying in stealth mode until September 2010. The company doesn't fab its own devices, but outsources production to its foundry partner in Taiwan. The company's Robert Duval told me that while shipments of 100mm wafers have begun, the focus has been on optimizing 150mm for volume production. JDSU is leveraging its previous tech experience to help fine-tune and tailor the process, with an emphasis on dialing in the post-epitaxial steps, such as lithography, as well as wafer automation and process control/yield management strategies.

The cells (which vary in size, but are trending smaller) made on the larger wafers will be qualified during the second quarter, he said, with shipments beginning in the following quarter. To fully scale to volume, a quarter or two would be needed, with no real constraint on the amount of capacity that could be brought to bear. The challenge, he pointed out, is to know where the market is going and calibrate production levels accordingly.

Duval's colleague Jan Werthen said that JDSU's cell performance roadmap puts production efficiencies at around 39% in the first half of 2011, climbing to 40% in the second half, with 1% absolute efficiency increases forecast for 2012 and 2013, respectively. These steady improvements will be accomplished through process optimization of ARCs and grid-lines, as well as innovations in epitaxial reactor design and epi growth techniques, which he described as the primary efficiency driver. All of this will be done on what he called the "6-inch-wafer, triple-junction [InGaP/Ga(In)As/Ge, top to bottom] workhorse," but by the middle of the decade, a fourth and eventually fifth junction will be necessary for the devices to achieve efficiencies into the mid 40s and beyond.

If the CPV cell market does start to blow up and hit 100MW this year (as Werthen and others believe) and then eventually jumps to 1GW in another few years (a transition that will truly test the manufacturing prowess of the industry), there will need to be a consistent, high-volume, high-quality supply of those 150mm substrates.

With the official October opening of Umicore's new germanium wafer facility in Quapaw, OK, the industry leader has added hundreds of megawatts of production capacity to the supply chain, according to the company's Frank Boghe. Most of the current capacity is running 150mm, with much of the 100mm still in qualification. The plant could be expanded from its current level of about 400,000 100mm wafer equivalents per year to 900,000, by using the existing building equipped with additional tools. (That larger amount is equal to about 750MW; gigawatt scale looms at a bit more than 1 million wafers.)

Some 70% of the wafers produced at the Oklahoma factory go for satellite projects, about 10% to CPV, and the remaining 20% to LED and other sectors. Boghe sees the concentrator PV sector as the source of future growth, with those market percentages adjusting accordingly. Umicore actually had the new facility up and running for sampling in May, with the first shipments trucked off in October. Four-inch wafers will start shipping in earnest over the next few months, as more customers get qualified.

The production flows on the two lines in Quapaw are similar to those found in more conventional silicon ingot/wafer factories. After converting the germanium oxide into Ge metal, the material is melted, grown, and pulled into ingots via the Czochralski method, resulting in a "zero EPD dislocation-free crystalline structure," according to Boghe. The ingots proceed to the wire-sawing station, where they are cut into thousands of ~175mm-thick wafers, which are laser-marked for tracking purposes as well as ground on the edge and surface areas. The substrates are cleaned before and after the sawing, and expedited to a Class 10,000 cleanroom for polishing to an "epi-ready" level. The wafers then enter a Class 100 cleanroom for a final epi-clean and inspection, with each slice getting eagle-eyed before being packaged and shipped.

Like any self-respecting wafer supplier in the semiconductor and PV sectors, Umicore closely collaborates with its customers to further optimize its substrates for the entire production flow, Boghe noted. Feedback on how the Ge wafers performed on the cellmakers' processes, including their possible impact on manufacturing yields and the like, will become even more important as those valuable slices of compound semiconducting material increase in size from 100mm to 150mm.

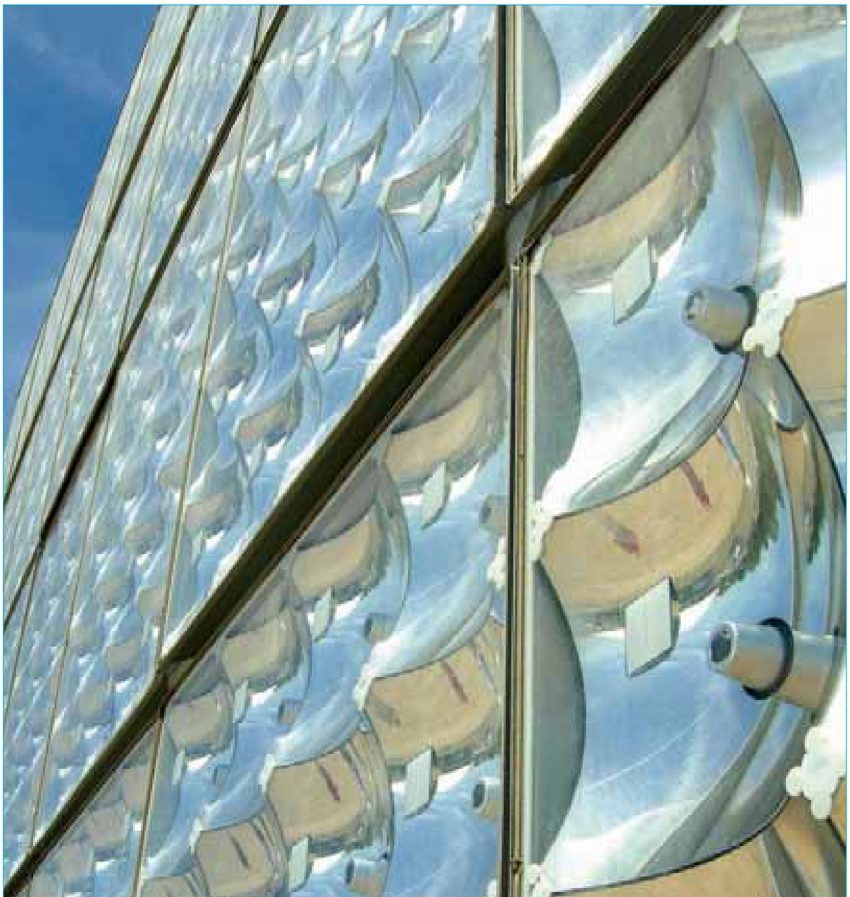

Photo by Tom Cheyney

Hundreds of Spectrolab's high-efficiency III-V solar cells are integrated into each SolFocus CPV array.

This article is a revised and updated version of a two-part blog that originally appeared on PV-Tech.org

Tom Cheyney is senior editor, North America, for *Photovoltaics International* journal and writes blogs and news for PV-Tech.org.

Product Reviews

Enecsys

Enecsys's 360W dual microinverter maintains individual MPPT

Product Outline: Enecsys has launched the Enecsys Duo microinverter, claimed to be the world's highest power density microinverter with dimensions of 262 × 160 × 35mm. Designated the SMI-D360W-72, it is designed to reduce system costs whilst supporting fully independent power point tracking of two connected photovoltaic modules.

Problem: Adopting microinverter architectures can result in dramatic reductions in output. Mismatching modules, shading caused by trees, chimneys or debris on the module's surface can all contribute to lower output.

Solution: The DC power generated by the two modules is converted into a single, grid-compliant AC output in the Enecsys Duo. System layout and planning is simplified and installation time and costs are reduced because each system needs only half the number of microinverters. Systems using the Enecsys Duo will have comparable capital costs to those using string inverters but, it is claimed, will realize 5% to 20% more energy. The degree of improvement in energy harvest depends on the installation configuration and the operating environment. Solar modules connected to the Enecsys Duo do not need to be matched or be located on the same plane.

Applications: Residential and small-scale industrial PV module installations.

Platform: The Enecsys Duo microinverter has 95% peak efficiency and 93% Euro efficiency, maintains full performance from -40°C to +85°C, and comes with a 20-year limited warranty. Reliability has been verified using HALT, HASS and accelerated life tests to IEC61215, the same methodology used to test solar PV modules.

Availability: Currently available (Europe).

AEG Power Solutions

AEG Power Solutions expands utility-scale solar power inverter portfolio

Product Outline: AEG Power Solutions has introduced a new solar power inverter for utility-scale applications. The Protect PV.500 expands the company's product range for the utility-scale market and has certified efficiency yields of 98.7% according to the European standard 50530. With an appropriate transformer, it can also be adapted to the medium-voltage grid (e.g. 10, 20 or 33kV), providing flexibility for a wider range of PV projects.

Problem: Utility-scale PV power plants require high-efficiency inverters to maximize operating yield while providing design flexibility to handle a wide variety of requirements. Features such as scalability and advanced remote monitoring functions have become key requirements.

Solution: Protect PV.500 is directly derived from the technology developed from AEG Power's Protect PV.250 inverter, which has certified efficiency yields of 98.7%. It is fully compliant with BDEW guidelines for energy-producing installations and thus contributes to overall grid stability. Maximum power point tracking (MPPT) is designed to meet the latest requirements for quick responses to dynamic weather conditions and reliable day/night detection (active/passive). Monitoring and power plant integration is based on Modbus Protocol and advanced CAN BUS communication as well as via optic fiber and ethernet between the containers.

Applications: Utility-scale PV power plants.

Platform: A key feature is the power stack with advanced-design measuring and control technology enabling DC input voltages of up to 1000V(DC). Available as part of AEG PS's turnkey container solution TKS-C 1000, which is equipped with two Protect PV.500 units.

Availability: Currently available.

Bentek Solar

Bentek Solar's MDSS offers reduced disconnect costs

Product Outline: Bentek Solar's Multiple Disconnect Safety System (MDSS), used for commercial and utility-scale PV power plant projects, has received UL 1741 listing and CSA 22.2 certification. The MDSSs are designed for large PV solar systems (250kW or greater), and are intended for installation next to the inverter. The MDSS provides multiple UL 600VDC load-break disconnects combined into one easily installed compact enclosure.

Problem: For most commercial and utility-scale installations, it is more economical to install one compact MDSS with up to eight integrated disconnects versus eight individual disconnects. The MDSS can provide significant benefits in labour, materials and time, resulting in up to a claimed 30% saving in total costs.

Solution: MDSSs are intended for installation next to the inverter and provides project developers with multiple UL 600 VDC or IEC 1000 VDC load-break disconnects. Bentek's offering provides reduced space requirements and claims lower material costs. The safety and protection for PV power systems is enhanced with the complete isolation of inverter fuses.

Applications: Commercial and utility-scale PV power plants.

Platform: Bentek Solar MDSSs offer a comprehensive selection of input, output and ampacity configurations to suit requirements. Product features include NEMA 3R, 4, or 4X; 600VDC load break disconnects; multiple 100A, 200A and 400A load-break disconnects in a single safety enclosure; three to eight integrated 600VDC disconnects per MDSS; protective covers on all live parts. UL1741 listed and CSA 22.2 certified.

Availability: Currently available.

EKO Instruments

EKO Instruments' solar radiation sensors enable CPV power plant optimization

Product Outline: EKO Instruments has introduced the new DNI pyrheliometer MS-56 with innovative compact design features and improved performance. The MS-56 DNI sensor fulfills the most stringent requirements of the CPV and meteorological market, particularly a very fast detector response for instantaneous and accurate direct normal incidence (DNI) measurements.

Problem: CPV power plants need to be monitored to optimize energy output to maximize ROI. Precise and accurate direct solar irradiance measurements enable plant owners and operators to better position tracking systems throughout the daily operating cycle.

Solution: The ISO First Class pyrheliometer MS-56 is a high-quality DNI solar radiation sensor suited for use as a reference instrument for precise and accurate direct solar irradiance measurements and routine operation on a solar tracker. The system uses a new ultrafast thermopile detector with 99% response time <1s and excellent thermal stability.

Applications: Solar irradiation measurement for routine operation on CPV solar trackers.

Platform: Each lightweight MS-56 sensor includes a passive temperature compensation module to minimize the common detector temperature dependency to less than 0.5% over a wide temperature range (-20°C to 50°C). The detector temperature can be accurately monitored with the built-in PT-100 RTD or YSI 44031 10kΩ NTC. Dew-deposition or condensation on the outside of the entrance optics is significantly reduced via a built-in low-power heater inside the sensor.

Availability: July 2011 onwards.

Hanwha SolarOne

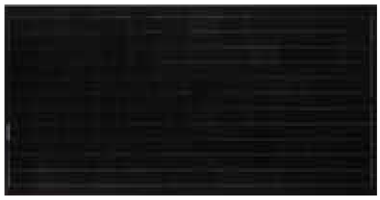

E-Star modules from Hanwha SolarOne deliver improved low-light irradiance

Product Outline: Available in sleek black or white design, Hanwha SolarOne's E-Star modules are designed to deliver enhanced aesthetics for residential and small commercial rooftop applications. High-efficiency cells coupled to lightweight modules (average 3kg lighter than conventional modules) are available in a variety of configurations with a 25-year limited warranty.

Problem: Small commercial and residential customers need quality solar modules from a reliable supplier that are lightweight and easy to use without the need for efficiency tradeoffs.

Solution: E-Star modules come with an average 2% increase in peak watts per square metre of surface area and are claimed to deliver higher power output compared to traditional PV modules. Attractive black or white aluminum frames allow them to complement many different design installation needs, while the glass surface provides durability proven to withstand significant impacts, including falling steel marbles that weigh over 1kg (2.2lbs). They are also field tested to support over 300kg (660lbs) of load per square metre (10.7 sq. feet).

Applications: Residential and small commercial rooftops.

Platform: E-Star modules feature improved low-light irradiance, and are certified to international ISO 9001 quality and ISO 14001 environmental standards. Available in 170, 175, 180, 185, 190 or 195W formats. Average cell efficiency: 16.5% with all electrical characteristics at standard test conditions (STC) of: irradiance 1000W/m^2, spectrum AM 1.5 and temperature of 25 ±2°C.

Availability: Currently available.

Kemper Solar

Kemper Solar's new tracker offers higher flexibility and greater choice of module selection

Product Outline: Kemper Solar is preparing to launch its new tracking system at Intersolar 2011. The KemTRACK two-axis tracking system has undergone a complete facelift and offers 70–120m^2 module area with improved control and increased stability. Automated robot welding and a reduction in the amount of material used in the fabrication are designed to further reduce costs and prices.

Problem: Cost-effective and efficient design of solar systems is increasingly important against the backdrop of falling subsidies, and the constant need to reduce BOS costs while also maximizing energy yield.

Solution: KemTRACK features a central support tube with built-elevation drive, and the new design now allows for flexible longitudinal and transverse mounting of modules. The lower height provides a significantly reduced shading range so that the tracking systems can be operated in more confined spaces or utilized to increase the number of systems deployed. Each tracking system is equipped with its own control unit so that the correct sun position can be determined and the optimum angle to the sun used, delivering up to 40% higher current efficiency compared to fixed systems. The integration of the elevation drive into the central support tube enables the tracker to complete the east and west pivot without the azimuthal direction changing.

Applications: Ground-mounted medium- to large-scale PV power plants.

Platform: The tracker uses a new Internet-based control system that was developed in cooperation with Siemens, which provides for the tracking of the tracker on an astronomical basis.

Availability: June 2011 onwards.

Product Reviews

Linuo Power

Linuo Power offers coloured modules for BIPV applications

Product Outline: Linuo Power Group has introduced c-Si modules with different cell colour characteristics that are designed to be attractive to the building integrated photovoltaic (BIPV) market. A special membrane plating technology is used to colour the cells while limiting the impact on cell/module conversion efficiency.

Problem: The introduction of coloured solar module could be an effective alternative to the shortcomings of monotonous design and single colour schemes seen with conventional mono- and multicrystalline solar modules.

Solution: Through the adoption of a special membrane plating technology, the Linuo solar cell not only ensures good efficiency, but also has strong colour formation, making it ideal for BIPV applications that aim to avoid conventional patterning formats. The tempered glass with high transmittance ensures the maximum efficiency from the c-Si cells, while the high-strength aluminium alloy frame ensures strong mechanical properties of the module. The module is encapsulated with high-performance material, which can prolong the service life of the module.

Applications: A wide range of BIPV applications from commercial to residential.

Platform: Linuo Power has certificates such as TÜV, UL, VDE and Golden Sun and conform to domestic and international standards such as IEC61125, IEC61730 and UL1703. Linuo Power offers a five-year product quality guarantee.

Availability: Currently available.

National Semiconductor

National Semiconductor offers new range of renewable energy grade ICs for smart system design integration

Product Outline: National Semiconductor has introduced 10 new SolarMagic integrated circuits (ICs), the first in a series developed to reduce cost, improve reliability and simplify design of PV systems. The new ICs are designed for a variety of PV electronic applications.

Problem: PV systems have historically been designed with limited electronics, mostly concentrated in the centralized DC/AC inverter.

Solution: The new SolarMagic ICs are the first developed to meet PV renewable energy-grade qualification requirements. Each IC is engineered specifically for rooftop environments that range from extreme cold to severe heat, and are designed to ensure long-term operation, meeting and exceeding the 25-year life expectancy of PV modules. For distributed PV power optimization applications providing maximum power point tracking (MPPT), National offers the SM72441 and SM72442 programmable MPPT controllers. Power processing circuitry in power optimizers, microinverters and charge controllers is possible with the SM72295 full-bridge and SM72482 dual 5A compound gate drivers, which can drive four discrete MOSFETS in a full-bridge configuration.

Applications: Microinverters, power optimizers, charge controllers and panel safety systems.

Platform: A full set of reference designs and application notes includes an evaluation board, bill of materials and schematic to aid the designer in developing a complete PV system.

Availability: Currently available.

Pictometry International

Pictometry's aerial imagery solutions available online for solar contractors

Product Outline: Pictometry International has developed Pictometry Online, a web-based technology offering a vast library of 3D-like, high-resolution aerial images. The solution is designed to enable solar contractors to quickly, easily and accurately calculate solar exposure, panel placement, sizing, roof pitch and square footage – information that is essential for positioning panels for maximum sun exposure and energy output.

Problem: Determining whether or not a home or commercial building is suitable for mounting solar panels can be a daunting task. Steep, multi-storey and chopped-up roofs increase the complexity involved in determining panel placement. Factors such as tilt and direction of a roof, identifying obstacles that could make installation difficult or cause shade problems, or excessive cost can be huge deterrents to retrofitting rooftops with solar panels.

Solution: Pictometry can assist in calculating accurate roof measurements. Unlike satellite or aerial images which provides orthogonal (straight down) views, Pictometry specializes in oblique (an approximate 40° angle) image capture. It can capture and process images of each targeted geographic area from 12 to 20 different views. As a result, buildings, properties and areas are identifiable and recognizable in a 3D life-like format.

Applications: PV projects and installations from residential to utility-scale.

Platform: Pictometry International specializes in aerial oblique image capture and software solutions for professionals in government agencies and commercial industries.

Availability: Currently available.

Schneider Electric

Schneider Electric's 1000VDC disconnect switch designed for harsh environments

Product Outline: Schneider Electric has launched the Square D 1000 VDC disconnect switch, the first enclosed heavy-duty 1000 VDC solar disconnect on the market. The easy-to-install switch functions as a local disconnect for strings of PV panels, and is designed for an extended life expectancy in harsh environments.

Problem: Commercial and utility-scale PV power plants are increasingly using higher voltages in order to improve overall plant efficiency. Systems up to 1,000V are becoming more popular. However, contrary to AC which has two zero crossings per cycle (16.6ms), DC current is more difficult to interrupt. When a DC circuit is in the open position, an arc is generated between the switch contacts, which must be broken quickly and in accordance with safety procedures.

Solution: Suitable for both grounded and ungrounded PV systems, the Square D 1000 VDC disconnect switch offers a preconfigured solar solution and familiar enclosed safety switch design, with no additional components required. The extended life expectancy exceeds IEC 60947-3 mechanical endurance requirements by a factor of 18 and IEC 60947-1 electrical endurance requirements by a factor of 10.

Applications: Commercial and utility-scale PV power plants.

Platform: The NEMA Type 3 and IP63 enclosure is resistant to windblown dirt and dust and exceeds NEMA type 3R. It operates within a temperature range of -37°C to 50°C, using a white enclosure that can reduce solar gain by up to 35% over standard grey enclosures.

Availability: Currently available through Schneider Electric distribution channels.

Schott Solar

Double-glass modules from Schott Solar offer high resistance to environmental influences

Product Outline: Schott Solar has introduced a new multicrystalline module manufactured using double-glass technology. Schott's Poly 185 uses glass on both the front and rear sides. This new, long-life module is said to be more resistant to environmental influences and particularly robust against stormy conditions and snow, which enables the company to offer a 30-year linear performance guarantee.

Problem: Schott Solar has developed a patented production process which dispenses with the need to apply high pressure or use vacuum processes that can damage the cells and affect the module's quality and long-term stability. Unlike conventional glass foil modules, contaminants do not affect Schott's module's active cell layer.

Solution: The Schott Poly 185 is based on the Schott Poly 290, which came out on top in an independent PV+ test conducted by TÜV Rheinland and Solarpraxis with a rating of 'very good (-). The glass protects the module from condensation, vapour, gases such as ammonia or methane, many acids and bases, as well as fats, oils and solvents, as there is no route for ingress into the module's active cell layer.

Applications: Rooftops and harsh environments.

Platform: The module's 48-cell layout makes maximum use of even small roof spaces with output classes of 175/180/185Wp and a weight of 24kg. The carrying capacity per module, as confirmed by IEC certification and by TÜV, is 5,400Pa, corresponding to snow load zone 3, wind load zone 4, and wind speed of up to 200km/h, with a safety factor of 3. Glass thickness: 3.2mm (front side), 3.0mm (rear side).

Availability: Currently available.

Transphorm

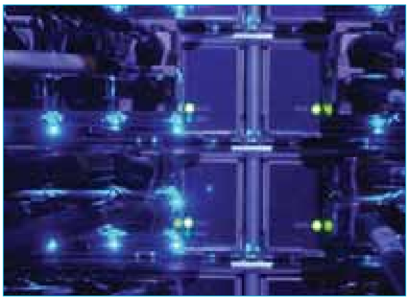

Transphorm's gallium nitride diode DC-DC boost converter claims 99% efficiency

Product Outline: Transphorm has launched its new power diode based on patented, high-performance EZ GaNTM (gallium nitride) technology. The power converters are designed with 600V transistors and low-loss power diodes, which makes for a fast and efficient conversion technology.

Problem: Energy loss that occurs during power conversion is equivalent to the daily output of 318 coal plants, and can cost in the region of billions per year. Transphorm claims to be the first company to provide a viable solution to inefficient power conversion by commercializing a high-voltage normally-off GaN solution.

Solution: Power conversion works via rapidly switching circuits, which enable the transformation of electricity from one form to another. Transphorm's efficiency breakthrough comes in the form of a GaN-based platform, which switches at far higher frequencies than traditional components. The diodes come in industry-standard packages and are designed for optimum high-frequency switching, lowest loss and highest efficiency.

Applications: Commercial PV power plants.

Platform: By using a proprietary EZ-GaNTM platform, Transphorm's technology design uses fewer components, minimizes snubbers and filters, simplifies module packaging, and enables high-frequency design by reducing transients.

Availability: Currently available.

PV inverter industry – boom to bust?

Tom Haddon, IMS Research, Wellingborough, UK

ABSTRACT

Exceptional demand characterized the PV industry in 2010. Uncertainty regarding incentive schemes in a number of key markets drove global installations, and inverter shipments grew by over 160% as investors and developers rushed to complete projects, fearing that incentives would be reduced or removed altogether. IMS Research estimates that inverter shipments exceeded 20GW in 2010 and sales of small three-phase inverters, rated between 10-20kW, grew by around 200% in 2010. Inverters rated at over 500kW are estimated to have grown at a similar rate, but continue to represent a smaller share of revenues.

Expanding capacity in 2010

Many inverter suppliers announced major capacity expansions and total industry capacity reached over 35GW in 2010 – an increase of 125% on the previous year. In spite of this massive capacity expansion, factory utilization still increased significantly in 2010 to around 66%, hitting close to 85% in Q3'10. In 2010 however, the market was greatly affected by both extremely high demand and low production issues caused by a severe shortage of many key components. Inverter delivery times extended dramatically, and a wait of 30 weeks became the norm throughout much of 2010. Inverter suppliers could not keep up with demand – a sure sign that the industry was struggling to adapt to rapid demand swings.

Current situation

By Q4'10, slowing installations in several core markets – most notably Germany – cooled the demand for PV inverters and eased the component shortage. The former was due to rate cuts in Germany and government intervention in other markets such as France and the Czech Republic. Market conditions had reversed and the industry was faced with oversupply as distributors and installers had overestimated demand in the final part of the year. Order cancellations were also common.

Inventory levels built up throughout the supply chain with string and multi-string inverters the most affected. IMS Research estimates end-of-year inventory was almost 3.8GW, with Germany and France the main markets affected.

Weak demand for inverters in Q1'11 further compounded the problem as the inventory served much of this and shipments fell by over 45% from Q4'10. Although the first three months of a year are traditionally weaker in terms of demand, weather conditions also delayed installations and FiT cuts were enforced January 1st, so this year has seen a bigger slowdown than previous years. Uncertainty over the Italian government's support for PV and the sheer amount of demand pulled forward into 2010 contributed to this situation.

Future outlook

IMS Research estimates that demand will increase considerably in Q2'11 and a recent survey of inverter suppliers suggests that inventory levels will return to normal in the same timeframe. However, although installations are forecast to grow in 2011 by about 14%, inverter shipments are forecast to decrease by about 7% due to the high levels of inventory in the supply chain carried over from 2010. These market dynamics have caused inverter suppliers to delay many of the capacity expansions that were planned for 2011 as capacity utilization is forecast to dip to under 30% in Q1'11, failing to reach the levels seen in 2010. The build-up of inventory, even within suppliers' warehouses, means that delivery times have dramatically shortened to around one or two weeks. With the demand softening compared to 2010, the pressure on inverter pricing will most likely increase. It is estimated that prices will fall by around 10–15%, as weakened demand puts the balance of power back with the customer.

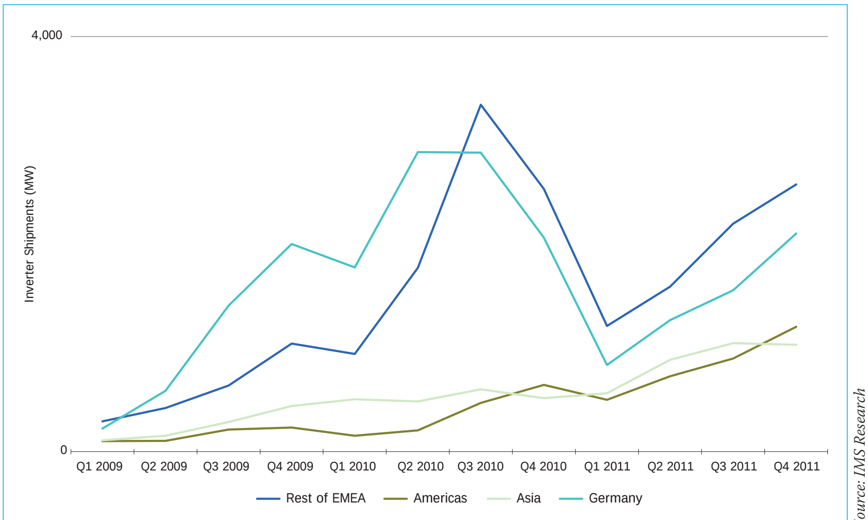

Figure 1. Quarterly PV inverter market forecasts by major region.

Opportunities for microinverters

With 2011 preventing markedly different conditions in 2011 for suppliers' operations, the need for product differentiation becomes all the more important. With the previous measure of inverter efficiency becoming ever narrower across the industry, suppliers are finding new ways to separate their products from the competition. Claims of lowering installation costs, increasing reliability, in-depth servicing packages and new product features are all appearing on the market. Of all the new products entering the market, microinverters are garnering the most attention with Enphase Energy currently leading the way. With module level DC/AC conversion these units claim to increase efficiency and safety and lower installation time and cost. Success has been achieved in the US residential market but has thus far been limited to the US. Traction in the European market is an objective for the various emerging microinverter suppliers, although the UK-based supplier Enecsys is hoping to break the European barrier first. Installers with vast experience of using string inverters will take some persuading to switch to this new technology and IMS Research forecasts that in MW terms, microinverters will capture less than 5% of the market by 2014, but with an inherently higher price per watt, the revenue share will be slightly larger.

European demand faltering

In the medium term it is forecast that Europe will account for less global demand than it does currently – which is estimated to have been over 80% in 2010. Emerging markets located in the Asia region (China, India, Australia), South America (Brazil, Mexico) and Africa (South Africa) are forecast to grow faster than the more mature European markets and capture their share of the market. Installations being planned here are almost exclusively MW-scale ground-mount power plants and therefore the suppliers of large central inverters are targeting the markets heavily. Satcon has already opened up manufacturing facilities in China using a partnership with GCL and it is thought that many other suppliers will follow suit. Turnkey inverter solutions are reported to be most in demand in these emerging markets. These are fully prefabricated inverter sub-stations, typically 1MW in size or bigger, which are delivered with all the components needed for grid connection, promising simpler installation and servicing. These units are forecast to account for almost 30% of the market by 2014.

It is clear that the competitive conditions of 2010 have changed considerably and the PV inverter industry may not ever see another year like it, which saw shipments increase by over 160%. Suppliers are now faced with a situation where driving down costs will be paramount in order to make systems commercially viable in markets where FiT rates are far lower. Module prices will also have a dramatic effect: if a price collapse happens in this sector, then PV may experience another year of strong growth.

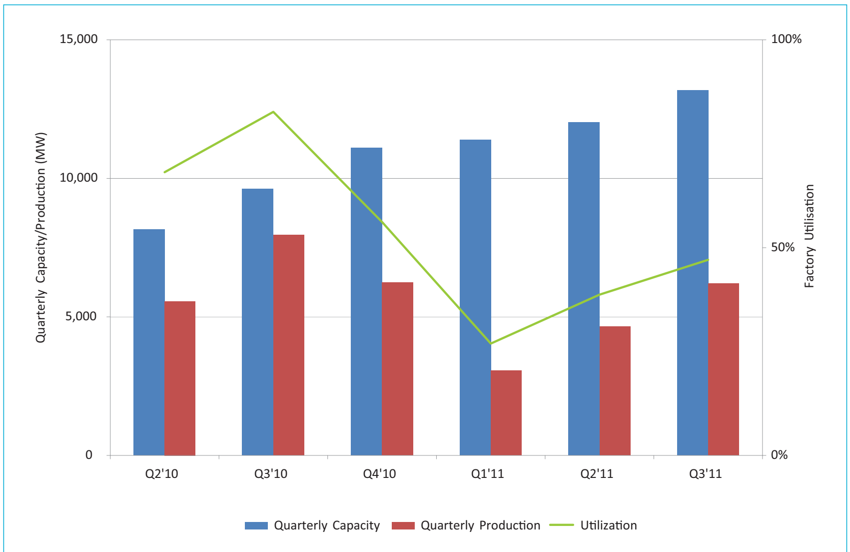

Source: IMS Research

Figure 2. Quarterly capacity, production and utilization rates of inverter facilities by quarter (MW).

Despite the gloomy short-term outlook for the PV inverter market, IMS Research forecasts that the market will grow to be worth almost US$8 billion by the year 2014. The key driver will be that PV becomes economically competitive with traditional electricity generation as the price of inverters and other system components fall.

About the Author

Tom Haddon is a research analyst with IMS Research's PV group with a background in economics and business. He is responsible for IMS Research's PV inverter market intelligence reports, authoring several annual and quarterly studies.

Enquiries

IMS Research
3-5 Huxley Close,
Wellingborough, NN8 6AB
Tel: +44 1933 402255
Email: tom.haddon@imsresearch.com

Market Watch

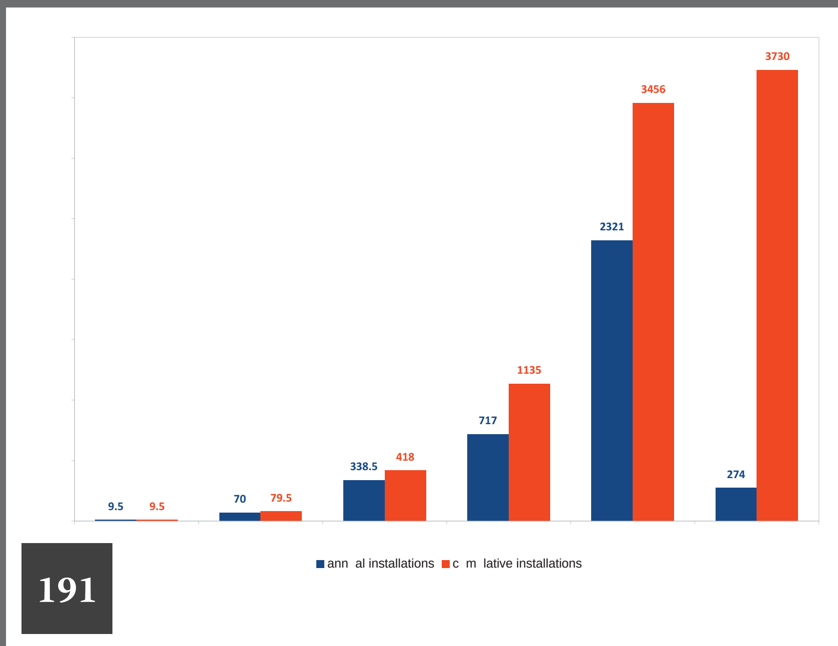

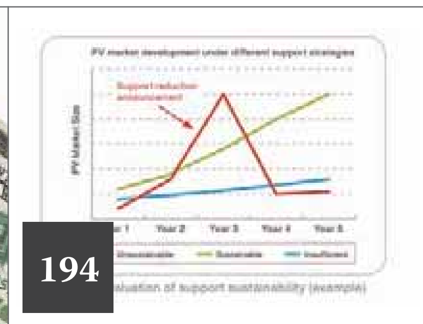

News

Applied Materials to acquire Varian Semiconductor for US$4.9 billion

Applied Materials will acquire Varian Semiconductor Equipment Associates for approximately US$4.9 billion.

Ion implant market leader Varian Semiconductor Equipment Associates will be acquired by Applied Materials for approximately US$4.9 billion. The deal is said to enhance Applied's product offerings for transistor formation for front-end semiconductor processing as IC process complexity, transistor scaling and 3-D design implementation require complete and integrated product and process offerings. The deal also offers Applied new market opportunities in solar, display and light emitting diodes, where Varian has made significant investments in recent years to broaden implant technology market opportunities. Varian recently reported second-quarter 2011 revenue of US$330 million.

Applied said it would fund the transaction with a combination of existing cash balances and debt. This includes a US$2 billion, one-year senior bridge loan facility with plans in process to arrange for a better longer-term debt financing structure. Applied also has an undrawn revolving credit facility in place worth US$1 billion. A new four-year, US$1.5 billion revolving credit facility is also being used to finance the deal, which has been approved by the boards.

However, this is not Applied's first foray into ion implant technology, having closed down its ion implant business unit in 2007. The closure meant that Applied acknowledged that its competitive position against market leader Varian was not sustainable. Varian went on to dominate the semiconductor implanter space with approximately 80% market share. However, Varian has also made a move to bring implant technology to the PV space with the potential to boost cell efficiencies by 2%.

According to Applied, Varian will operate as a business unit within its Silicon Systems Group and continue to be based in Gloucester, Massachusetts.

Market Trends News Focus

US VC investments in solar firms strong in first quarter, according to Ernst & Young report

Solar investments were hot in the first quarter, even if overall PV market demand cooled considerably. According to the latest quarter report on US venture capital (VC) investment in cleantech companies from Ernst & Young, solar-based companies received US$362.7 million in new investments in the first quarter of 2011, up 162% compared to the same period a year ago. This accounted for 39% of the total dollars raised for the quarter, which is compiled from data provided by Dow Jones VentureSource. In total, VC investments totalled US$1.14 billion in the first quarter of 2011.

Specifically, MiaSolé generated the largest deal of the quarter, raising US$106 million in a later-stage round of financing, 24% of total dollars in Q1 2011. Alta Devices, a Northern California company that focuses on improving the production economics of high-efficiency solar PV applications, had the fourth-largest deal of the quarter with US$72 million third-round financing.

According to the Ernst & Young report, corporate investments in solar were also in play with Innovalight and Taiwan-based Motech's partnership to develop solar cells using silicon ink. Citigroup and SolarCity also set up a US$40 million fund for solar power projects.

Q1 solar investment totals US$641 million, according to Cleantech

Global research firm Cleantech has revealed that global investment in green technology for Q1 2011 totalled US$2.57 billion, with the solar sector accounting for US$641 million. Investment came from 159 companies in North America, Europe, China and India, and was up 13% on the figure of US$2.28 billion from the same period last year.

Cleantech's CEO Sheeraz Haji finds the latest figures on global investment in green technology "encouraging".

In addition to being responsible for one quarter of the total investment figure, the 26 separate rounds of funding secured by solar made it the most popular sector in terms of the total number of deals. Among the leading investment recipients were BrightSource Energy (US$201 million), MiaSolé (US$106 million), Alta Devices (US$72 million) and SoloPower (US$13.5 million).

"In the first few months of the new year there have been a rash of large later-stage deals which have propelled 1Q11 to the second highest quarter ever for cleantech VC investment," Cleantech's CEO Sheeraz Haji said. "It's encouraging to see some big private equity firms entering the space and continued strength with M&As."

Solarbuzz sees challenging PV module market in 2011 stemming from effects of European incentives

Coming off the strong year that was 2010 in the global solar photovoltaic world, Solarbuzz's Quarterly report has countered that 2011 may present a rockier road. The research company is estimating that Germany's first-quarter 2011 end-market demand for solar PV has been performing at less than 50% of what it was in the first quarter of 2010 and maintains that even though module manufacturers worldwide have been reducing prices, the market has yet to feel a positive effect.

Solarbuzz contends that 2011's first quarter has seen module manufacturers trying to grow their sales channels and take on a more diverse set of distributers and brokers in the hope of producing higher production volumes and achieving better factory gate prices. According to the quarterly report, these actions have led to unsustainable levels in downstream inventories in both Europe and the US.

"2011 will be a challenging year for the industry as it manages a slowdown in the market," said Craig Stevens, President of Solarbuzz. "Europe will not be the growth engine it has been in recent years, and manufacturers will need to access new markets or be exposed to the risk of rising inventories or production cuts during a period of falling prices."

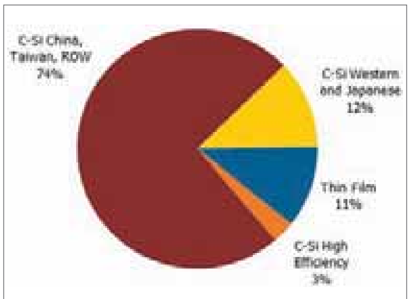

Solarbuzz.

Image: Solarbuzz Quarterly

However, despite the rather dull results that Solarbuzz has found in this year's first quarter, it notes that global demand in 2011's second quarter is still predicted to reach 7.4GW, which would show a 77% year-over-year growth. The growth will be a direct result of the feed-in tariff (FiT) cuts that are scheduled to occur by the middle of this year in the top five European markets.

Financial & Business News Focus

Microinverter firm Enecsys attracts US$41 million in new funding round

In what is claimed to be the largest private equity investment in the European cleantech sector so far this year, microinverter firm Enecsys has attracted US$41 million in a new Series B funding round to support further growth.

"The resources from this financing will be used to execute our growth strategy by accelerating our product development and cost reduction plan and expanding our global presence in sales, marketing, customer service and manufacturing to serve every major market," commented Henrik Raunkjaer, Enecsys's CEO.

Climate Change Capital Private Equity led the latest round with an investment of £11 million (US$18 million). The remaining funding of £14 million (US$23 million) was secured from the existing Enecsys investors, Wellington Partners, NES Partners (formerly known as Bankinvest New Energy Solutions) and Good Energies, who together previously invested £8.5 million (US$14.3 million) in Enecsys in a Series A financing in 2009.

Enecsys's solar microinverter.

Image: Enecsys

Deutsche Bank names solar PV market analyst Vishal Shah as managing director

Deutsche Bank has selected Vishal Shah as its managing director for its US-based alternative energy and semiconductor capital equipment divisions. One of the leading solar market analysts, Shah joins Deutsche Bank from his former role at Barclays Capital. He previously worked as a senior vice president with Lehman Brothers where he managed the research coverage of the solar and semiconductor capital equipment divisions. Additionally, Shah served as a research analyst at Morgan Stanley and in his early career worked with Needham & Co.

Vishal Shah has left Barclays Capital to join Deutsche Bank as managing director for its US-based alternative energy and semiconductor capital equipment divisions.

Image: Enecsys

Evergreen Solar in call for cash as sales slump

Citing a slowdown in module sales and pricing pressure in the first quarter of 2011, Evergreen Solar has declared that its near-term liquidity has been negatively impacted, which could lead the company to find new sources of cash sooner than expected. The struggling String Ribbon module producer said shipments were only 18MW in the first quarter, down significantly from 47MW in the fourth quarter of 2010.

"As a result of our low year to date sales volume and potentially slower sales for the remainder of this year as the industry balances inventory levels, along with significantly increased pricing pressure, the cash that we had previously expected to realize through the reduction in accounts receivable and inventory from our recently closed Devens facility will be less than expected and will take longer than expected to realize," noted Michael El-Hillow, President and Chief Executive Officer. "Therefore, our near-term liquidity has been negatively impacted and may require us to secure additional sources of cash sooner than expected."

The company continued to sell modules at a loss with average selling prices of US$1.86 per watt, down from US$1.90 per watt in the previous quarter. Cash and cash equivalents stood at only US$33 million as of April 26.

Evergreen Solar is also in the process of completely changing its business model towards becoming a solar wafer producer using its String Ribbon technology - as it offers the potential for lower cost (less silicon usage) and high-quality wafers compared to conventional multicrystalline production methods.

BrightSource Energy makes move on an IPO in the US

Solar thermal power tower developer BrightSource Energy has confirmed recent rumours that it would file for public listing in the US. The IPO is to generate up to US$250 million as part of its capital requirements to build out its 392MW Ivanpah Solar Electric Generating System in California's Mojave Desert.

BrightSource Energy has already been successful in attracting investments in the project, including US$168 million from Google, US$300 million from NRG Energy and a US$1.6 billion loan guaranteed by the US Department of Energy's Loan Programs Office.

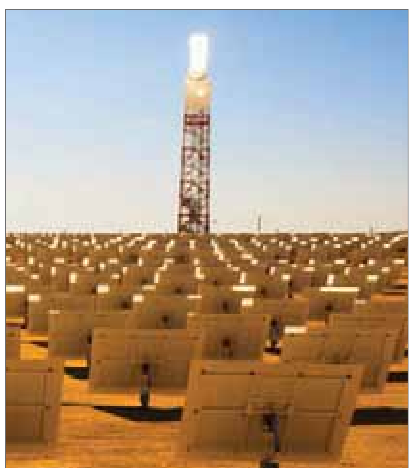

BrightSource Energy-built solar thermal power tower.

Image: BrightSource Energy

The number of shares to be issued and the offering price have not been determined, according to an S-1 filing. Goldman, Sachs & Co., Citigroup Global Markets, Inc. and Deutsche Bank Securities, Inc. are acting as lead underwriters. Investors in BrightSource include VantagePoint Venture Partners, Draper Fisher Jurvetson, Alstom, CalSTRS, Chevron Technology Ventures and BP Technology Ventures and Keating Capital.

US Bancorp commits to partnership with SunRun for US$200 million purchase of solar equipment

SunRun has been on the receiving end of US Bancorp's latest renewable energy tax equity commitment. The two companies formed a partnership, which will support the acquisition of US$200 million in residential solar systems. The companies assert that this is US Bancorp's largest tax equity fund to date and SunRun's fifth and largest commitment from US Bancorp.

The transaction is supported by the 1603 Treasury Grant Program, which allows renewable energy projects to use a cash grant of equal value to the Investment Tax Credit.

"It's critical for US Bancorp to have an existing portfolio of proven renewable energy investments as we expand our financing in the space, and SunRun is a core part of that base," said Darren Van't Hof, director of renewable energy investments for US Bancorp. "With strong management and a solid business model, SunRun exemplifies the partners we look for to help facilitate the growth of the renewable energy industry."

ADB pledges US$150 million in credit guarantees to bolster solar power development in India

The Asian Development Bank (ADB) has revealed plans to offer up to US$150 million in credit guarantees to local and foreign commercial banks to encourage the development of solar power as a renewable energy in India. The credit will cover 50% of the payment default risk on bank loans made to solar project developers with an aim to secure long-term funding for solar energy development in the country.

ADB's partial guarantees on loans of up to 15 years will back projects up to 25MW. The bank is also contemplating a separate direct finance program for larger solar power projects with the Indian private sector. Currently, ADB will additionally provide US$1.25 million for training on solar technology, risk issues and aiding participating banks in the technical due diligence for individual solar projects.

ADB's concessional technical assistance special fund will provide a grant of

The Asian Development Bank is offering up to US$150 million in credit guarantees to encourage the development of solar power as a renewable energy in India.

US$500,000, while the Asian Clean Energy Fund will supply a second grant of US$750,000. The latter Government of Japan-established grant is part of the ADB-administered Clean Energy Financing Partnership Facility.

Quarterly revenues down at First Solar; high end of 2011 sales guidance at US$3.8 billion

First Solar saw its net sales revenues decline in the second quarter, citing as reasons the allocation of modules to its systems projects in order to meet project contractual deadlines, seven fewer production days during the period, and the full-quarter impact of the pricing changes started in December. The thin-film PV module manufacturer and EPC/project developer's Q1 revenues reached US$567 million, which was a decrease of US$42.5 million from the fourth quarter of 2010 and just about even with Q1 2010's US$568 million, because of lower ASPs. Conversion efficiencies and production line run rates both increased, although manufacturing costs per watt were flat.

Quarter-over-quarter net income was also down, primarily driven by lower net sales and gross margin. Year-over-year, the net income decrease was primarily driven by reduced average selling prices and higher expenses, partially offset by increased module production and lower module cost per watt, the company said.

The company updated its 2011 guidance as follows: net sales of US$3.7–3.8 billion; operating income of US$900–970 million; earnings per fully diluted share of US$9.25–9.75; US$50–60 million of manufacturing start-up expenses and US$10–15 million of factory ramp costs; total capital spending of US$1.0–1.1 billion; and operating cash flow of US$0.8–1.0 billion.

The company produced 407MW of modules during the first quarter, while conversion efficiencies ticked up from Q4, moving from 11.6% to 11.7%. Manufacturing costs were flat, remaining at 75 cents per watt.

On the project side, the company has increased its guidance of North America installations for this year from 400MW to 450MW (DC), a number that could rise to as much as 600MW.

A pleasant surprise for First Solar is what it sees as the significant growth in a relatively new market – India. The company believes it has a 100MW-plus module supply pipeline potential in the South Asian country in 2011, up from what it saw as around 10MW a few quarters ago.

Lincoln Renewable Energy and Macquarie close US$41 million deal on 10MW Oak Solar project

Lincoln Renewable Energy (LRE) has finalized the sale and project finance deal with Macquarie Energy worth US$41 million. The agreement sees Macquarie Energy enter a long-term purchase agreement for power and renewable energy credits from LRE's New Jersey-based 10MW Oak Solar PV project. LRE will remain the long-term owner of the facility, while

Image: First Solar

First Solar's manufacturing plant in Perrysburg, Ohio, USA.

News

Macquarie Energy provides construction finance and term debt for Oak Solar.

The 10MW project should begin construction in June and reach completion by December. LRE and the Ryan Company, a subsidiary of Quanta Services, have signed an agreement to provide engineering, procurement and construction services for the project with Quanta managing the operation and maintenance of Oak Solar upon completion.

EDF to acquire EDF Energies Nouvelles

French utility EDF will acquire the outstanding 50% share in EDF Energies Nouvelles after the renewable energy firm accepted an offer of €40 per outstanding share. This represents a premium of 10.4% on the share closing price on April 7, 2011 and a 23.8% premium compared to the daily volume-weighted average over the last six months. The deal will require state approval.

EDF Energies Nouvelles had revenue of over €1.57 billion in 2010. The deal is being financed by cash and the remaining half tendered in a share exchange offer. The acquisition will allow for greater collaboration on a wide range of renewable energy projects between the companies. EDF Energies Nouvelles installed 267.1MWp of solar projects in 2010.

Pâris Mouratoglou, a major shareholder in the company with a holding of 25.09%, will continue as chairman of EDF Energies Nouvelles. David Corchia will also continue to lead the company after the acquisition.

MEMC's SunEdison project pipeline stands at 1870MW


Image: SunEdison

SunEdison's 70MW plant in Rovigo, Italy.

SunEdison's PV project pipeline has risen sharply since the fourth quarter of 2010, an increase of 32% or 454MW, and now stands at 1,870MW, making the MEMC subsidiary a major player in the PV project developer market. SunEdison sales for the first quarter were US$158.1 million, compared to net sales of US$307.6 million in the 2010 fourth quarter. However, seasonal factors and the sale of large projects in the previous quarter exaggerated the fall in sales. In comparison, SunEdison sales in the first quarter of 2010 had been US$60.7 million.

"In the current environment, where the market situation in Italy is unresolved, for example, market diversification is key," noted Ahmad Chatila, CEO of MEMC, during a conference call to discuss financial results. "While SunEdison's pipeline growth was impressive during the quarter, so was the diversity in project size and geography. We have a pipeline that encompasses projects from less than 1 megawatt to greater than 10 megawatts, and we have transitions from North America-centric organizations to building a balanced pipeline in multiple regions around the world, from China to India and the rest of Asia, to Europe, Canada and United States. This diversity reduces risks and offers more stability to this business."

Chatila also noted that MEMC expects SunEdison's PV installations to more than double this year, with the US remaining the largest market. However, greater geographic diversity, especially in Asia, is set to enable more installations during the winter months as the climate does not suffer from snow or icy conditions.

SunEdison connected 40MW in 2009 and 167MW in 2010. Total first-quarter interconnections were 20.3MW, including 12.1MW of direct sales and sale-leaseback projects and 8.2MW of debt-financed projects.

Germany

Germany's cabinet will cut solar power subsidies by up to 15% in July 2011; however, if the market slows and projected market growth for the entirety of 2011 is less than 3.5GWp, the first feed-in tariff adjustment will not come into play until the beginning of 2012, as previously planned. Furthermore, the new mechanism allows for a FiT increase should installations not reach 2.5GW.

Meanwhile, the figures for 2010 are in, and are 2GW less than analysts expected. The disappointing numbers are a consequence of the two feed-in tariff cuts already implemented by the Government during the past 12 months. The official figure published by the German Federal Network Agency saw 242,893 systems, totalling 7.25GW, installed in 2010 – considerably less than the expected total of 9.5GW; installations for December were 1.17MW.

Spain

CNE, Spain's energy sector regulator, has suspended feed-in tariff subsidies for 350 installations after it emerged they were providing fraudulent electricity production figures.

Out of Spain's 55,000 registered PV systems, as many as 9,000 may be guilty of making false electricity generation claims, according to the country's solar association, APPA. To date, only 350 have had their subsidies actually cut, although with 7,200 suspected plants still to be investigated, more may follow.

The Spanish Government has also proposed that a cap is placed on the number of hours of subsidized generation that solar plants can sell to the grid, reducing this limit from 1,753 hours down to 1,250 processing hours.

Additionally, systems mounted on single-axis trackers will now only be funded for the first 1,644 hours; systems with double-axis trackers will see payments for the first 1,707 hours only. This will apply to all PV plants connected to the grid by September 2008. As a form of reimbursement, PV plants will receive the feed-in tariff payments for three more years – an extension from the original 25 years to 28.

France

The French Government has confirmed reports that it is to introduce a 500MW annual cap on PV installations. The decision was reached in February at a meeting between the French Prime Minister, François Fillon, the Minister for Ecology and Sustainable Development, Nathalie Koscciusko-Morizet and the Minister for Budget, François Baroin. This came into force on March 10, 2011.

With completed and planned projects for 2010 already totalling 3,400MW, the French Government believes the annual limit of 500MW to be fair, although it has left itself room to manoeuvre; the ceiling could be increased to 800MW if a certain proposed projects are not realized.

UK

The UK Government has proposed significant cut to subsidies for large-scale solar installations as part of its fast-track review of the feed-in tariff (FiT) scheme. Systems with a capacity between 50kW and 5MW will be affected by the reductions, with the largest seeing their subsidies cut by as much as 70%.

In February, the Government launched the review, citing fears that larger projects (>50kW) were taking a disproportionate share of available subsidies. With the UK solar industry still in its infancy, the announcement was a major setback and the cuts are even more severe than initially expected. The industry had until May 6 to respond to the proposals. Any changes agreed will only affect new recipients of FiT subsidies and, subject to the outcome of this consultation and Parliamentary scrutiny, will come into force on August 1.

Italy

After months of uncertainty, the Italian government has finally passed its new renewable energy bill, Conto Energia IV. The bill comes into force on June 1 and will shape Italy's solar policy until 2016.

The first stage of the decree, which runs until December, will see feed-in tariff rates reduced by around 4% per month – with cuts of 4-11% in June followed by 2-5% cuts every month for the remainder of the year. Large-scale installations are also to be capped at 1.2GW during this transitional period, with this number rising to 1.49GW in 2012.

In 2012, there will be further subsidy cuts, ranging between 23-44%, while from 2013 until 2016 a system of graded reductions will be carried out.

Italian PV market development

Valerio Natalizia, GIFI (the Italian PV Industry Association), Milan, Italy

ABSTRACT

The Italian PV market is poised to become the leading market worldwide. However the recent GSE estimates have revealed unexpected volumes installed in 2010. This may lead to an adjustment of the feed-in tariff (FiT) level in the course of this year. GIFI (the Italian PV industry association) is preparing the field for a proposal to make the market development more sustainable, long-lasting and to upgrade the 2020 target.

Italian PV market in 2010

In 2009 Italy became the second market worldwide for annual installed capacity. 2010 saw Italy become the second market for cumulative installed capacity, surpassing Spain. In fact, last year the peninsula saw between 5.5 and 6GWp of new installations: a huge increase in volume, which was partly unexpected.

We all knew that the last year of the second Conto Energia was anticipated to be very strong in terms of installations. On top of that, in August 2010, a measure called the Salva Alcoa was approved by Parliament without any explicit request from the industry. This measure has allowed all PV systems installed by the 31st of December 2010 to benefit from the 2010 FiT if they are connected to the grid by the 30th of June 2011.

GSE has received around 59,000 applications for the Salva Alcoa measure worth 4GWp. Some of them have already been found to be incomplete applications (i.e. missing documents and/or data). In any case, GSE estimates that the applications that can be considered valid amount to about 3.5GWp. Ultimately, it is still unclear whether or not those 3.5GWp will all be connected to the grid. In fact, from the beginning of January 2011, only 0.65GWp (out of 3.5GWp valid

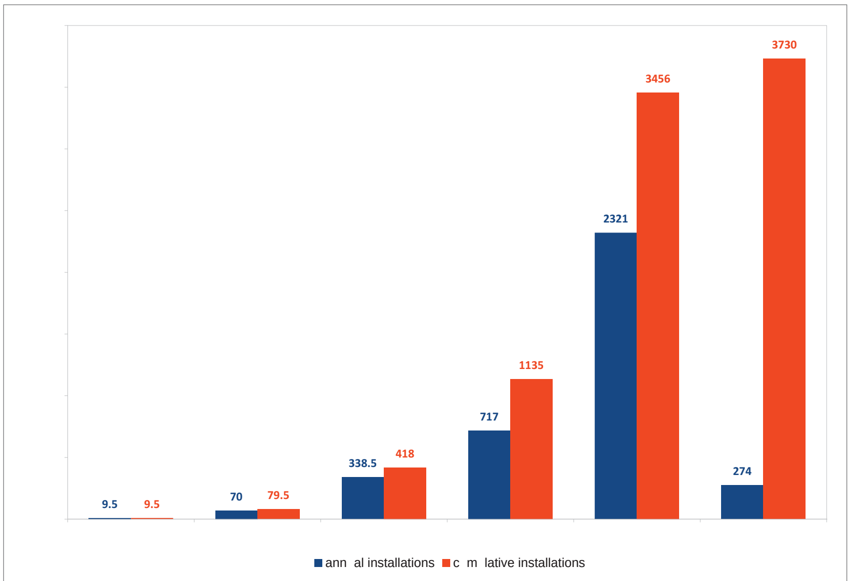

Figure 1. Annual versus cumulative installations from 2006 to 2011.

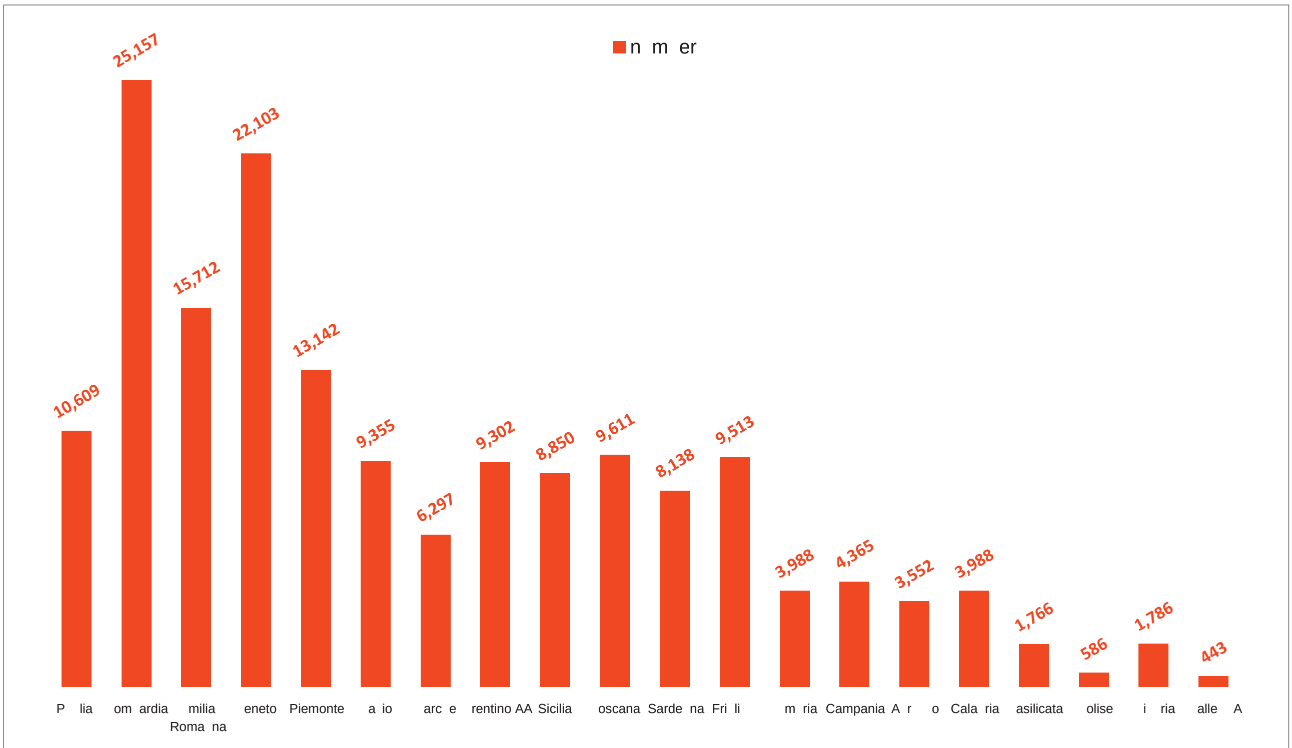

Figure 2. Regional uptake of the Salva Alcoa incentive scheme.

applications) were connected to the grid.

These figures are still estimates; final figures, considering the time gap between the connection to the grid and the FiT award, will be available, most likely, after the summer 2011 break.

In the meantime, it is important to take a look at how the market has developed so far in terms of types of installations, market segments and regional distribution.

While the number of ground-mounted solar PV systems is still a small percentage (7%) of the total amount, their power installed share is fast becoming significant (46%). Thanks to the generosity of the FiT, in 2010, this market segment has risen at an impressive rate.

At the regional level, the top five regions that represent nearly 50% of the cumulative power installed in Italy, are: Puglia, Lombardia, Emilia Romagna, Veneto and Piemonte.

> "Puglia has been one of the first regions to adopt clearer licensing procedures for the authorization to build PV systems."

It is worth mentioning that Puglia is the only southern region amongst the top five, most likely a direct result of the fact that Puglia has been one of the first regions to adopt clearer licensing procedures for the authorization to build PV systems. Also, Puglia hosts the largest PV systems: the average size is 70kWp, while in the Lombardia region (the second in the list for installed capacity) the average size goes down to 16kWp.

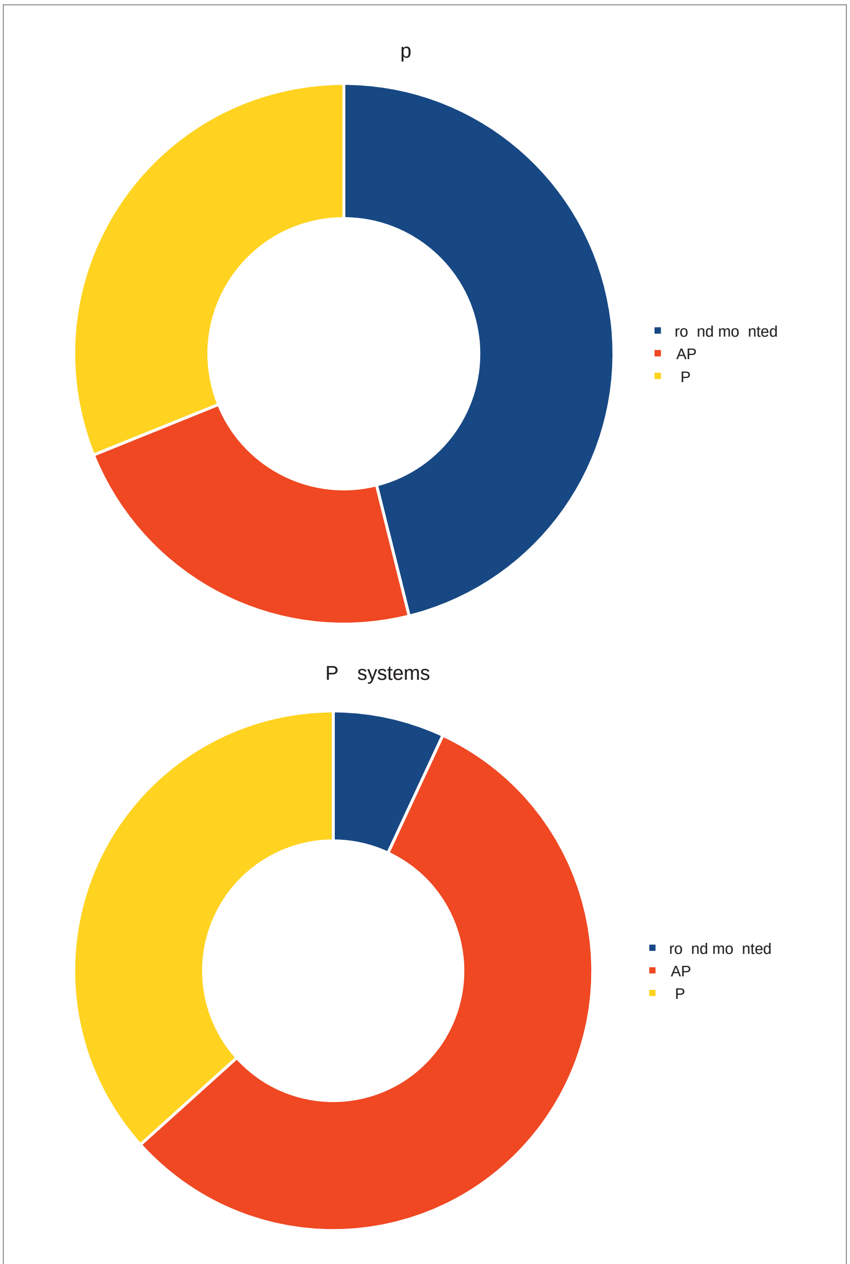

Figure 3. Types of installation by (top) total power output and (bottom) number of systems.

The third Conto Energia came into force, but...

The third Conto Energia was approved in August 2010 and came into effect from January 1st 2011. The new 'solar bill' has a rather different structure when compared with the second Conto Energia. First of all, it has lower levels of FiT and different power classes (from three to six). A decrease in three steps of the tariff during 2011 is needed in order to have a 15–20 % decrease by the end of 2011.

Unfortunately the third Conto Energia is already obsolete. On March 3rd 2011, the Italian Council of Ministers approved the so-called Renewable Legislation: the legal framework to allow the development of renewable energy in Italy. The PV relevant contents of Renewable Legislation can be summarized as follows:

- limitations for PV system size in agricultural land;
- when the 2020 target (8GWp) for PV has reached, the FiT will expire. Looking at the volumes in 2010 we can assume that 8GWp can be reached by the end of 2011; and
- all systems connected to the grid by May 31st 2011 will still be able to be granted with the FiT of the third Conto Energia. All PV systems connected to the grid from June 1st 2011 onwards will be granted with a different FiT which will be defined and published by April 30th 2011.

The approval of this legislation has been largely unexpected by all PV stakeholders. Since late November 2010, when the first draft was disclosed by the Italian Council of Ministers, there have been a number of meetings, negotiations and parliamentary hearings amongst all PV sector stakeholders in order to find a common position for the development of renewable energy in Italy.

The final document, however, is going in a different direction and in the PV industry we immediately experienced drawbacks and criticism. As a direct consequence the Italian PV sector has halted:

- €8 billion of orders are now blocked;
- €20 billion of contracts are now on standby; and
- 10,000 workers are at risk of being made redundant.

On top of that, many investors, national and foreign, have redirected their funding towards different markets and many companies have suspended the recruitment processes planned for 2011, thus jeopardizing the development of the whole PV industry.

Towards the fourth Conto Energia

What has caused this radical change in the Government's approach to renewable energy? The main reason behind it is the fact that the impact of renewable energy (mainly wind and photovoltaic) in the energy bill is considered by many industry players to be too high. What has emerged from the recent happenings is the need for a better control of the costs related to incentivizing solar electricity.

> "What has caused this radical change in the Government's approach to renewable energy?"

We at GIFI (the Italian PV industry association) have always considered the FiT as the most appropriate legislative tool to achieve full competitiveness within the sector. The FiT needs to be decreased according to the cost of the PV systems. The administrative burden linked to the licensing procedures has a rather high impact on the final cost (up to 20% in some cases) of the PV system. Therefore, while we are ready to negotiate lower FiT as of June 2011, we expect the Government to make an effort to help us to reduce the bureaucratic burden and to promote clear and fast licensing and connection to the grid procedure.

On the topic of grid systems, a strong support for the development of the distributed generation comes from the development of the smart grid. In Italy we have around 20 million smart meters already installed and thus we are in a privileged position to overcome the bottleneck of an inadequate energy transmission and distribution infrastructure.

Negotiations with the relevant institutions, Government representatives and a member of the Italian Parliament are already underway and (at the time of writing this article) and the first draft of the fourth Conto Energia is about to be disclosed by the Minister of the Economic Development, Mr Romani. The draft will be the result of many meetings amongst stakeholders and we are confident this time there will not be any surprises.

What is our position? We aim to regulate transition from the third to the fourth Conto Energia. As the fourth Conto Energia will start in 2012 with an annual decrease of the FiT, we need to make sure that from June to December 2011 the decrease of the FiT is gradual enough to allow all PV systems and investments already planned to be safeguarded. In regulating this transition it is important to avoid any legislative measure that may potentially harm the sustainable growth of the installations.

- six power classes (1kWp to 3kWp; 3kWp to 20kWp; 20kWp to 200kWp; 200kWp to 1000kWp; 1000kWp to 5000kWp; and over 5000kWp);

- different tariff for PV systems built on buildings and ground-mounted systems;

- feed-in premium for:
  - the removal of asbestos roofing;
  - the energy efficiency intervention to buildings;

- PV systems ground-mounted in abandoned and contaminated land;
  - promotion of the self consumption of solar electricity;

- finally we have a strong position against any form of caps: this will make the installations slow down significantly (as in Spain a couple of years ago) and lead to market instability. These are all consequences we want to avoid.

About the Author

Valerio Natalizia is president of GIFI (the Italian PV Industry Association). Since 2003 he has been involved in the production of modules, distribution systems, photovoltaic inverter production and participates in international working groups, conferences, workshops and forums with an extensive knowledge of the Italian and European PV market. In 2005 Valerio was made director general of SMA Italy, the Italian subsidiary of the world's largest inverter, SMA Solar Technology AG.

Enquiries

ANIE - Gruppo Imprese Fotovoltaiche Italiane (GIFI)
viale Lancetti, 43 – 20158 Milan, Italy
Tel: +39 02 3264 228
Email: comunicazione@gifi-fv.it

Editor's note: data contained in this paper was compiled during the period of uncertainty surrounding the Italian FiT status. We now know that the tariff format has been revised as of May 6th, but it was not possible to update this paper to reflect the amendment prior to going to press.

Policy recommendations for European photovoltaic markets

Marie Latour, European Photovoltaic Industry Association (EPIA), Brussels, Belgium

ABSTRACT
The behaviour of PV markets over the last decade in Europe has taught us that not only it is necessary to optimally design support schemes, but that priority access to the grid for renewable energy sources and the reduction of administrative barriers are the key market drivers for sustainable development and essential for the markets to sustainably develop in the long term. This paper provides an overview of Europe's PV market performance and delivers policy recommendations by means of EPIA's PV Observatory model.

Introduction

The monitoring of support schemes and the consequent development of markets throughout Europe has, until now, led to the conclusion that for a market to develop in the long term three essential conditions need to be met, otherwise the attempt will fail. These are:

1. The support scheme in place needs to be sustainable in the long term.

2. The administrative authorization process needs to be streamlined.

3. The grid-connection process needs to be efficient.

Many of the lessons that have already been learnt come from Germany which has the longest and most successful experience so far. Furthermore, the Spanish case in 2008 and the Czech Republics more recent experience have shown that had these countries been given the chance to benefit from a larger experience in more advanced markets, the situation could be vastly different today. Other markets are opening or reviewing their support in Europe, but on a global scale, EPIA believes that to sustainably develop in the long-term, these markets could learn a lot from the experience of their predecessors. The details of these recommendations are as follows.

Implementing sustainable support mechanisms

Experience has shown that the most effective support schemes so far for developing a PV market has been via feed-in tariffs (FiT) or similar mechanisms. These should be well designed and adjusted to a level which allows a market development. Feed-in tariff laws introduce the obligation for utilities to conclude purchase agreements for the solar electricity generated by PV systems. The cost of solar electricity purchased is passed on through the electricity bill and therefore does not negatively affect government finances. In markets where FiTs were introduced as reliable and predictable market mechanisms, they have proven their ability to develop a sustainable PV industry that in return has progressively reduced costs towards competitiveness. In order to be sustainable, it is critical that FiTs are guaranteed for a significant period of time (at least 20 years), without any possibility of their being retroactively reduced.

Feed-in premium (FiP) is a new mechanism that may prove to be a viable alternative to FiTs. Under the FiP, utilities pay a premium on top of the price of electricity while the invoice of the consumer is reduced by the amount of PV electricity produced. If PV electricity exceeds consumption, the difference should be eligible for a FiT.

However, the FiP concept is new and is yet to be proved. It should be carefully considered and worked out in more detail before it is tested on the market. With the growing penetration of PV in many countries, support policies can be fine-tuned in order to drive the development of a specific market segment where this is relevant. Direct consumption premiums, additional incentives for building-integrated PV (BIPV), compensation for regional irradiation variations, orientation premiums such as east or west-oriented PV systems, as well as storage premiums are all examples of possible additional provisions.

Encouraging development of a sustainable market

Sustainable market growth allows the industry to develop and creates added value for society and the economy as a whole. A critical aspect of sustainable development is ensuring adequate levels of profitability that in turn ensures the availability of capital for investments while avoiding speculative markets. Consequently, investments in PV projects need to be on a par with other investments of equivalent risk levels. Fig. 1 illustrates market developments under different support strategies. The green line represents sustainable market growth; the red line shows a rapid and uncontrolled market peak, followed by a collapse due to sudden policy adjustment; while the blue line illustrates a stagnating market due to an incentive deemed insufficient.

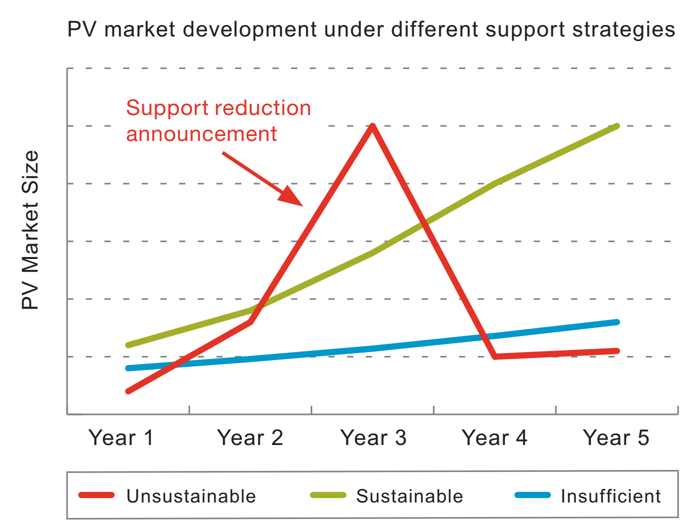

Figure 1. Evaluation of support sustainability (example).

	Insufficient support	Sustainable support	Unsustainable support
Private investor	<6%	6-10%	>10%
Business investor	<8%	8-12%	>12%

Table 1. Internal rate of return levels.

Assessing the profitability through IRR calculations

All available support scheme components (including FiT, tax rebates and investment subsidies) must be taken into account when calculating the internal rate of return (IRR) of a PV investment. Its sustainability must be assessed by considering all local factors that impact the relative profitability of a PV investment. Table 1 presents an estimate of average sustainable IRR levels in a standard European country. Those percentages need to be adapted depending on local market conditions.

Guaranteeing gradual market development

An uncontrolled market evolution tends to create 'stop-and-go' policies that risk undermining stakeholders' confidence and investor appetite for PV. In that respect, there is need for a flexible market mechanism that is able to take more rapid cost digressions in the market into account and to adapt support schemes in order to ensure a sustainable growth path. The *market corridor* (as introduced in Germany for example) regulates the FiT based on market development over the preceding period (i.e. quarter, semester or year). This allows FiTs to be adapted as to maintain growth within predefined boundaries. The FiT level is decreased on a regular basis in relation to the cumulated market level over a period passing below or above a set of predefined thresholds (quarterly or semi-annual revisions). The review periods should typically be set once a year to keep the administrative burden manageable for governments and to remain compatible with the visibility needed for investment cycles.

Developing a national roadmap to PV competitiveness

With the ongoing decrease in installed PV system costs and the increase in conventional electricity prices, the use of financial incentives will be progressively phased out as competitiveness is reached. A realistic roadmap to grid parity should be defined for every country along with concepts for market mechanisms that treat all electricity sources equally.

Ensuring electricity costs for consumers

As the cost of renewable energy sources such as PV is very transparent to the consumer through the FiT component on the electricity bill, the same transparency should exist for the cost of electricity from other conventional sources. These typically benefit from significant government support schemes that are not always reflected in the electricity price but are financed through other public means; in particular taxes paid by the same consumers but not accounted for on their electricity bill. On average, estimates suggest that conventional sources of electricity generation benefit from seven times as much support as renewable energy sources. In addition the lack of transparent carbon costs indirectly supports non-renewable energies.

The increased mix of energy from renewable sources such as PV has raised a greater awareness among consumers about the need to increase the efficiency of their electricity consumption. While the FiT has a visible impact on the electricity bill, it is at least partially compensated by the decrease in electricity demand. In addition, marginal cost of electricity produced from PV systems after the expiration of the FiT period is close to zero, therefore electricity prices will benefit in the long term.

Most importantly, and in view of continued reduction of FiTs over time, the PV industry is committed to significantly reducing the cost of PV systems to make it an affordable, mainstream source of power.

Streamlining administrative procedures

Although many countries have implemented support policies favourable to PV, when it comes to realising PV projects the bureaucratic issues and highly complex procedures and requirements (such as notification, registration or permits) tend to significantly hold back installation processes. As a result, the cost of projects is kept artificially high, hampering PV market development or requiring unnecessarily high levels of FiTs to compensate.

In order to assess the situation in a given country and facilitate comparisons with identified best practices EPIA – as partner of the PV LEGAL project – has been involved in the collection of information on administrative frameworks by national PV associations and system developers. The main recommendations drawn from this analysis are detailed in the following section.

Assess the administrative process

In order to identify the major obstacles to the success of the legal-administrative process, a series of key characteristics need to be assessed thoroughly:

- **Transparency:** the process must be clear and understandable; the information necessary to complete each step must be available, complete and exhaustive.
- **Linearity:** when multiple institutions must be contacted, it is essential that each institution's approval does not depend on the decision of the following one.
- **Simplicity:** the number of institutions required in the process must be justifiable and reduced to a minimum; redundancies must be avoided.
- **Proportionality:** the procedure must be proportionate and well-suited to the specific features of each market segment.
- **Cost effectiveness:** the total cost of the administrative process should not represent a consistent share of the entire cost of the project.
- **Reasonable duration:** the time necessary to complete the whole process must not exceed a few weeks, particularly in the case of small and medium rooftop installations.

In this respect, the PV LEGAL database represents an important source of

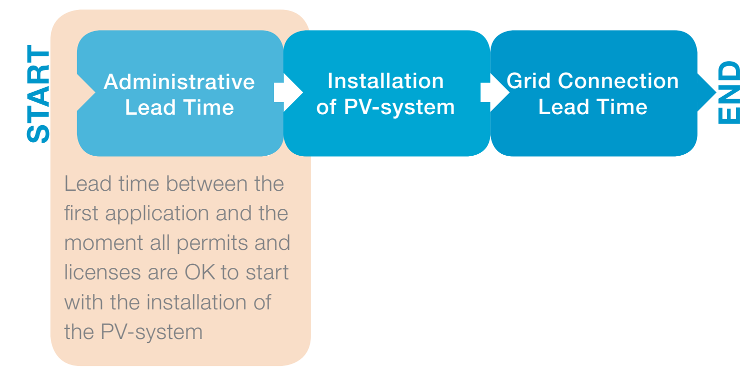

Figure 2. Administrative lead time.

information on the legal-administrative procedures required in 12 European countries. The database illustrates the administrative procedures and also quantifies the impact of administrative barriers in terms of time and cost [1].

Establish a 'one-stop-shop' process

Long administrative delays, combined with the need to contact multiple agencies or government bodies, increases the lead time as well as the global cost of the project. The implementation of a simplified process is required, with one single step to be completed by the project developer. All authorizations, certifications and licensing applications must be assessed and delivered through this 'one-stop-shop' concept.

Reduce administrative lead times to reasonable periods

The reduction of lead times must be a priority, especially for small-scale systems. Any delay in the authorization process can result in loss of profitability for the investor; reduce returns and consequently, the attractiveness of the project. In the absence of action from the administrative body in charge of a project within a reasonable time limit, approval should be given automatically. In the case of a small system, this should be limited to a couple of weeks. For large systems, the approval process should remain proportionate and transparent. The lead time should not exceed a couple of months for large systems.

Accompany the administrative simplification by an adjustment of the support mechanisms

Once the administrative process has been simplified, the combination of support mechanisms should be adapted to take into account the cost reduction related to such simplification.

Ensure a fast and reliable monitoring system

The ability to control the market requires the constant monitoring of PV installations. Long delays prevent regulators from understanding the evolution and to take appropriate action in due time. An online registration system for installers, combined with the appropriate IT infrastructure, should guarantee an almost real-time access to the installation data.

The PV LEGAL project aims at identifying legal-administrative barriers in EU markets and providing recommendations for their removal.

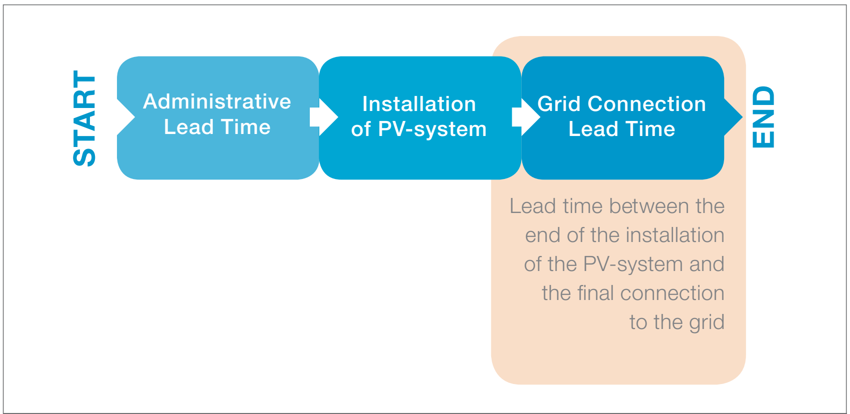

Figure 3. Grid-connection lead time.

Guaranteeing efficient grid connection processes

The grid-connection process is often the most severe roadblock in completing a PV project. It is able delay the project and dramatically increases its overall cost; the confidence of the investor lies in the guarantee that the electricity produced will be sold and transported. The PV LEGAL project has also draw up some recommendations to ensure an efficient grid connection process is in place.

Assess the grid connection process

In order to identify the major points of blockage in the grid connection process, the following elements need to be analyzed:

- **Transparency:** transparency of the connection process is essential for developers to ensure they will be able to connect to the grid at an already existing connection point and at a clear and predictable cost (connection fees).
- **Information:** comprehensive and necessary information must be available for new connection requests.
- **Appropriateness:** the installation of small decentralized systems should simply require a notification to the Distribution System Operator (DSO).
- **Lead time:** reasonable time to connection must be guaranteed and respected by either the DSO or the Transport System Operator (TSO).
- **Cost sharing:** connection costs must be properly shared between the PV system operator and the DSO/TSO. This can be combined with network usage fees in order to provide both parties with incentives to make an efficient use of the electrical grid.

The PV LEGAL database represents an important source of information on the grid connection procedures required in 12 European countries.

Reduce grid connection lead times to a few weeks

The reduction of lead times must become a priority, especially for small-scale systems. Any delay in the authorization process may result in a loss of profitability for the investor and reduce return, thereby reducing the attractiveness of the project. Electricians (preferably certified) must be able to connect small-scale systems to the grid by only a notifying the distribution system operator.

Ensure priority access to the grid

Once the connection permit has been granted, the transport and the distribution of the electricity produced by PV systems must remain guaranteed during the entire lifetime of the installation. The obligation for utilities to buy PV electricity must be guaranteed. This must remain valid at a predefined price (FiT) until the end of the grant period. After this period, the market price must apply automatically.

Issue grid-connection permits to reliable project developers

Policy announcements can be followed by a flood of grid connection requests, to the extent that virtually all existing capacity could be exhausted. To avoid such a situation and counteract speculation, permits ought only be issued to reliable investors. The validity of permits must be limited in time and large project developers may be asked for bank guarantees to ensure they live up to their commitment.

Ensure the financing of network operators

The benefits that PV bring to electricity networks, especially at the distribution level come at a cost. The development of PV and its smooth integration to electricity networks must be accompanied by necessary investments. Ensuring funding for DSOs or TSOs may be necessary to secure maintenance and the upgrading of the electricity grid.

Conclusion: observing market dynamics to ensure rapid PV evolution

In the context of the fast evolution of the European PV market in recent years, the need to permanently monitor market dynamics has led to the creation of the Photovoltaic Observatory. The Photovoltaic Observatory identifies recommended conditions for market development and best practices for the sustainable development of PV by basing its analysis on examining existing policies of several key countries. The Photovoltaic Observatory also focuses on relevant regulatory issues, financial incentives, administrative barriers and grid connection procedures.

The Photovoltaic Observatory aims to:

- Identify best practices among existing support policies in Europe;
- Promote market transparency and PV deployment in the energy sector across Europe; and
- Advise national decision makers on the successful implementation of their support policies.

The methodology of the PV Observatory is based on the systematic study of regulatory frameworks in European countries and their impact on market development.

In this respect, the administrative barrier analysis refers partly to the PV LEGAL project while financial schemes are analyzed using, among other indicators, the Internal Rate of Return (IRR) methodology. The system price evolution is also assessed on a regular basis.

References

[1] PV LEGAL [available online at: http://www.pvlegal.eu]

About the Author

Marie Latour is national policy advisor at EPIA. Within EPIA's policy department she takes care of coordinating the activities with national European policy stakeholders and makes sure the position of EPIA are conveyed at a national level. She deals with national policy developments, supports national associations and manages the participation of EPIA in the PV LEGAL project. Latour led the communication activities of EPIA until 2008. She holds a Master's degree in European Management from the Bordeaux Ecole de Management and Madrid Cámara Oficial de Comercio. She also holds a Master's in European Affairs from the Institut Catholique de Paris.

Enquiries:
European Photovoltaic Industry Association (EPIA)
Renewable Energy House
63-67 Rue d'Arlon
1040 Brussels, Belgium

Tel: +32 2 400 10 13
Email: m.latour@epia.org
Web: www.epia.org/pvobservatory

Photovoltaics – entering new dimensions

Matthias Fawer, Sarasin Sustainable Investment, Basel, Switzerland

ABSTRACT
Over the past two years the solar industry has shown itself to be incredibly resilient to general economic crisis. Supported by cost-cutting and efficiency improvements, the PV industry managed to achieve a growth rate of 120%, or 16.2GW, of newly installed capacity in 2010. Although individual companies are feeling the strong price and margin pressure and intensifying competition, the large, international and vertically-integrated companies are surviving. At least eight new PV markets with a potential annual capacity of 500MW are expected to be added over the next two years. The PV industry will therefore acquire the stability and political autonomy it needs to be able to grow unimpeded and to enter new dimensions. There might also be further tailwind for the PV industry from the catastrophic nuclear crisis in Japan.

PV industry holding up well

PV companies have had to contend with difficult economic conditions over the past two years: the wake of the global financial crisis, mounting overcapacity, intensifying competition and reductions in feed-in tariffs. Last year the turnover of the global PV industry reached almost €40 billion. Total installed solar energy capacity worldwide has now passed the 35GW mark, which is enough to supply 12 million households with clean electricity.

Constant price and margin pressure affects all companies

Falling prices have put pressure on companies' margins, but not to the same extent for all cell and module manufacturers. The reasons for this development are found in the rapid increase in the number of providers and the associated expansion of production capacities. Competitive pressure has also intensified due to the market entry of Asian (especially Chinese) companies that benefit from specific cost advantages compared to their European counterparts. The overall effect of this has been that companies have had to reduce their prices more rapidly than their production costs in order to expand their market share.

With the sudden change of a market supported by generous subsidies in 2008, to more stunted growth in 2009, almost every company has been forced to improve its cost structure. This has allowed some PV companies to increase their margins again in 2010. Margins of well over 20% seen in the boom years are virtually inconceivable now. In the longer term, however, we think margins between 10 and 15% are perfectly realistic. They should be attainable for both Western and Asian producers; compatible with the normal development of a mature industry with competitive mass production.

Feed-in tariffs: what are the current parameters, and how much longer will they apply?

At present, seldom a week passes without a government somewhere announcing fresh cuts to feed-in tariffs. The aim is to cut back tariffs and prices to a reasonable level so as to prevent excessive returns. No politician wants to see an overheated solar energy market develop in his own country and be forced to defend rising electricity prices. Because of this, attractive remuneration is rapidly being adjusted to the relevant system prices. At the moment there is a vicious circle of intensifying cutbacks in individual countries.

With so much criticism about costs, the many positive aspects of solar energy seem to have been forgotten about. For example, this growing industry provides a lot of jobs, wages and tax revenues at the communal level. Solar energy, along with other forms of renewable energy, also cuts the price of publicly traded energy due to the so-called 'merit order' effect. Since most energy from renewable sources is fed into the grid, large quantities of wind and solar power reduce demand for conventional electricity. The most expensive conventional electricity offerings can no longer be sold on the exchange, so the price drops. In 2010 many governments made adjustments to the national PV subsidy programs and in some cases implemented them. Some have also announced further cuts for 2011. This affects important markets such as the Czech Republic, Germany, France, Italy and Spain. The decisive question for industry is how this affects the appeal of these markets.

Country attractiveness index

Our annual global forecast for the photovoltaic (PV) market is derived from the systematic and comparative assessment of the most important countries' potential in a country attractiveness index (CAI). This assessment has been developed in close collaboration with the Clean Tech Department of Rabobank's *Food and Agribusiness Research and Advisory (FAR)* in the Netherlands. The CAI for 2011 shows which countries are most likely to attract PV projects. The evaluation is based on the following four criteria:

- **Financial attractiveness:** We use the internal rate of return (IRR) on a standard 1MW free-standing PV system project and a small 4kW roof-mounted PV system as an indicator for a market's financial attractiveness. Our calculations are based partly on the feed-in tariffs, local electricity tariffs and natural incidence of sunlight and are rated on a scale of one to 10. In order that the financial attractiveness can be compared over time and countries, the PV system costs (BOS, installation) are set at €2400/kW. It is assumed the company provides all its own financing.

- **Market maturity**: This criterion assesses to what extent the infrastructure and companies are available for the installation of PV systems. The scores are rated from one to five. The largest PV market receives the highest score (five), while the smallest PV market receives the lowest (one).

- **Growth potential:** Here we assess certain legal upper limits or caps stipulated for feed-in tariffs or overriding political goals that have been set for photovoltaics, as these determine the capacity potential that can be exploited in the long term. Countries with no annual cap and with ambitious long-term targets score five points. The lowest cap, combined with the absence of any politically motivated targets on photovoltaics, produces a score of one.

- **Effective administrative processes:** Here, the administrative and regulatory hurdles within a country are assessed. To this end the latest information from the PV LEGAL project supported by

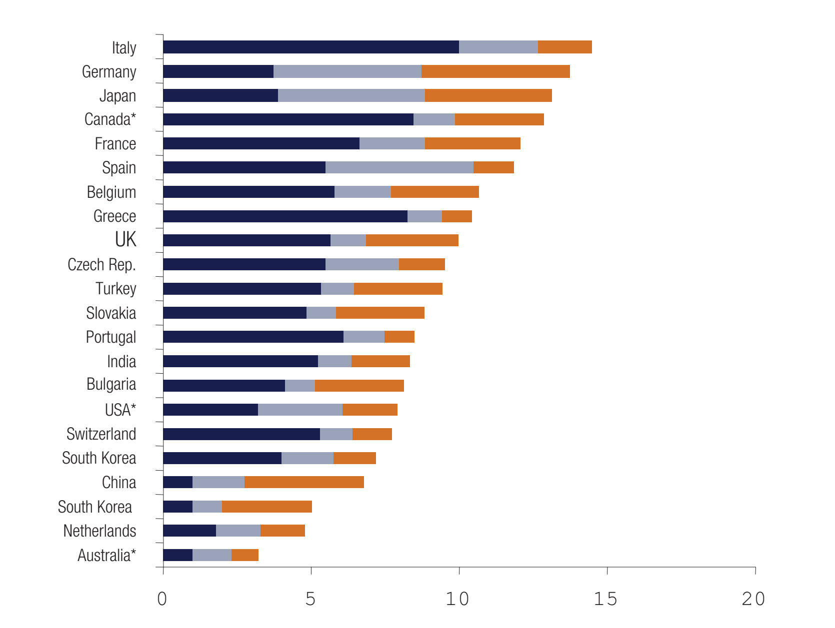

Figure 1. Country attractiveness scores for rooftop PV systems in 2011.

Source: Rabobank and Bank Sarasin, Nov. 2010

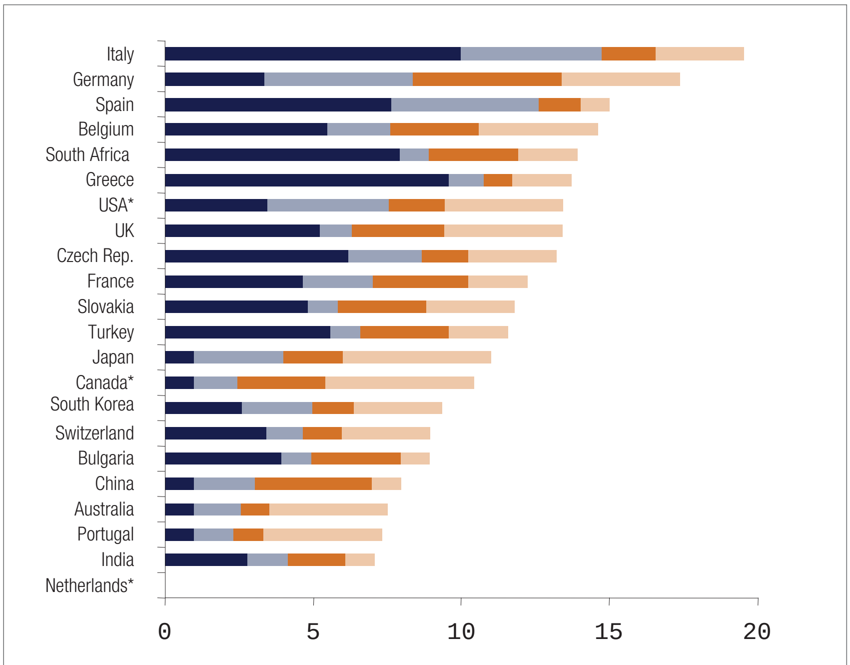

Figure 2. Country attractiveness scores for large-scale PV systems in 2011.

Source: Rabobank and Bank Sarasin, Nov. 2010

the European Photovoltaic Industry Association (EPIA) has been incorporated (see www.pvlegal.eu); in practice, the average length of time required for implementing a project varies between 12 and 24 months. A short time span scores five points; a long period of time scores one point. This criterion reflects a certain medium-term perspective. One new aspect is an assessment of the general stability or effectiveness of the state authorities, with reference to the Worldwide Governance Indicators (WGI). This criterion is not taken into account for small rooftop systems, as it is very hard to assess accurately with such a small size, and the necessary permits are relatively easy to obtain.

By employing the broader scale of one to 10 when assessing the financial attractiveness, a higher weighting is deliberately given to the financial aspect rather than the other criteria (rated on a scale of one to five) in order to reflect the comparative importance of this criterion.

New countries powering the PV industry forward

By introducing feed-in tariffs, Germany showed the way forward and played a pivotal role in making the enormous growth of the global PV industry possible. In the past, the German market has proven to be very elastic on the price front, making it the most important motor of the global PV industry even in difficult times. Other dynamic markets are now needed to provide effective support for Germany's PV market. It is definitely in the entire industry's interests to break into new geographical territory. By 2012, at least eight new markets will drive the industry's expansion, with newly installed PV capacity exceeding 500MW p.a. These include France, Italy, Spain, the US, Canada, China, India and Japan. They will provide a diversified regional platform for stable growth in future. Figs. 1 and 2 show the most 'attractive' countries for rooftop PV systems and large-scale PV systems.

Further cutbacks, stiffer competition, and huge market potential

For the coming year and beyond, the industry has prepared itself for further cutbacks in subsidies for solar power. There will be a significant reduction in tariffs in Italy, Germany and also in the Czech Republic. The politicians responsible fear, amongst other things, a rise in energy prices and instability in their power distribution grids. This will intensify competition among module manufacturers across Europe.

PV market forecasts up to 2015

Taking into account the attractiveness rating for each country, we anticipate the market trends shown in Fig. 3 for the period to 2015. Globally, our forecast for the period 2010 to 2015 produces annual average growth of 25%. This results in newly installed PV capacity of 16.2GW for 2010, 18.3GW for 2011 and 22.3GW for 2012. The growth rates for the individual countries and years vary enormously, however. Following 120% growth in 2010, we anticipate global growth of just 12% in 2011, rising to 22% in 2012.

In Europe, the strongest growth countries for the period to 2015 are primarily France (CAGR 2010 to 2015 of 41%), Portugal (39%), Greece (34%) and Spain (30%). The USA will grow by on average 62% per year over the same period, and will also gain massively in importance in terms of volume (an additional 11.3GW in 2015). Other important growth markets are China (CAGR 2010 to 2015 of 69%), India (62%), Japan (24%), the rest of Asia (30%) and other countries (59%).

205GW of newly installed PV capacity in 2020

An important trend which we mentioned last year can now be confirmed as fact. Several markets will achieve an annual volume of over 500MW of newly installed PV capacity this year or over the coming two years. This is a decisive factor, because it will

	Newly installed PV capacity (MW)							CAGR*
	2009	2010	2011	2012	2013	2014	2015	10-15
Germany	3,845	7,400	6,500	5,500	4,500	4,635	4,681	-9%
Italy	723	2,300	3,450	3,795	3,985	4,264	4,903	16%
Spain	60	367	535	660	900	1,110	1,375	30%
Greece	36	159	225	326	440	529	645	34%
France	250	700	1,120	1,680	2,352	3,011	3,838	41%
Portugal	34	45	70	105	144	182	232	39%
Czech Rep.	411	1,400	230	120	140	176	225	-31%
Belgium	292	361	120	130	135	170	217	-10%
Switzerland	26	30	60	70	80	90	100	27%
Rest of Europe	43	300	600	1,170	2,223	4,113	7,403	90%
Europe	**5,720**	**13,053**	**12,910**	**13,556**	**14,900**	**18,269**	**23,619**	**13%**
USA	**473**	**1,000**	**2,000**	**3,600**	**5,760**	**8,352**	**11,275**	**62%**
China	165	377	778	1,458	2,500	3,685	5,159	69%
India	30	80	152	274	443	629	887	62%
Japan	483	800	1,040	1,300	1,599	1,951	2,360	24%
South Korea	84	130	160	204	256	319	394	25%
Rest of Asia	186	300	420	546	699	888	1,118	30%
Asia	**948**	**1,687**	**2,550**	**3,782**	**5,497**	**7,472**	**9,919**	**43%**
Rest of the World	261	500	800	1,360	2,244	3,590	5,027	59%
Total newly installed	**7,402**	**16,240**	**18,260**	**22,297**	**28,401**	**37,683**	**49,840**	**25%**
Annual growth rate	24%	119%	12%	22%	27%	33%	32%	

*Source: Bank Sarasin, Apr. 2011; *CAGR: compound annual growth rate*

Figure 3. Sarasin PV market forecast to 2015.

mean that the PV industry is less susceptible to changes to the general operating conditions in individual key markets. A globally based PV industry of this kind will therefore grow in a more stable manner. We anticipate average annual growth of 29% for the period 2010 to 2020, which will produce newly installed PV capacity of 205GW in 2020. The tendency will be for sunny, non-European markets to grow more rapidly in the period to 2020, as they still have a great deal of catching up to do in terms of solar power generation. Over the past two years the solar industry has demonstrated that it can survive and continue to grow even in a challenging economic and political environment. We are convinced that costs can also be reduced by an average of 10% per year over the coming years, and that our scenario can therefore be realised in practice. Scepticism resulting from the nuclear crisis in Japan in March may lead to the establishment of close to 220GW of additional PV installations by 2020.

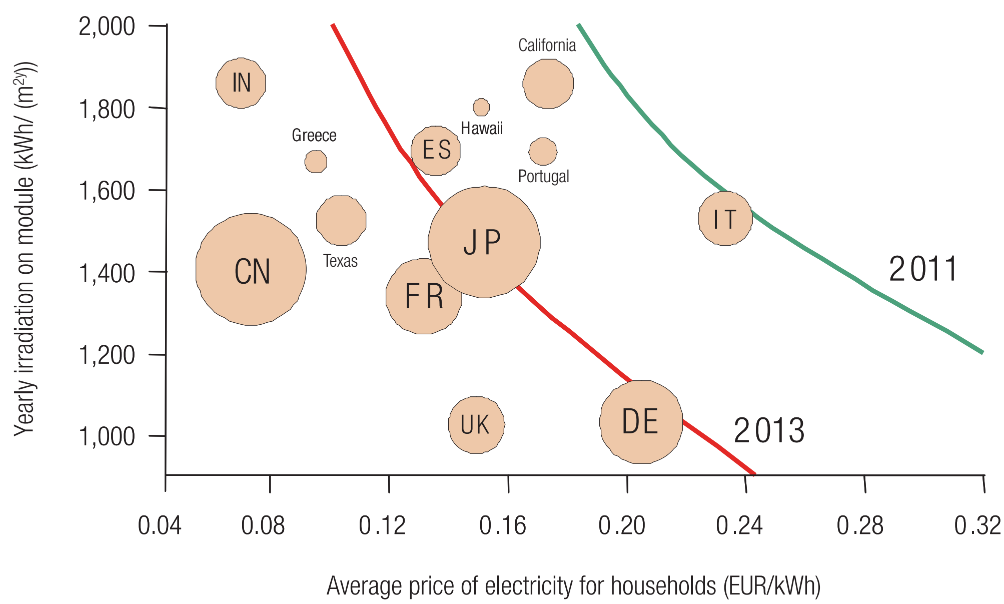

Source: EPIA, REC, Bank Sarasin, Nov. 2010

Figure 4. Trend toward grid parity for private customers.

Grid parity arriving sooner than expected

The solar industry has already achieved incredible feats. Since 2006, prices for solar electricity have fallen by 40% and, over the coming years, it will converge with the price level of retail consumer electricity tariffs. The key goal at present is to ensure an efficient and sustainable broadening of the photovoltaic market and to secure both the investments already made and those still required by this forward-looking industry. It will only take a few more years before the solar industry can survive without subsidy programmes in many key markets. Even in Germany, the electricity produced by solar panels on one's own roof will match the price charged for electricity by conventional energy suppliers or regional public utilities from 2013 onwards. This will mark an important milestone on the road to commercial competitiveness.

For this reason, the industry is currently developing a roadmap towards further successful development of the photovoltaic market, and in the course of this process will demonstrate ways in which this commercial competitiveness may be achieved in a speedy manner. In addition, the solar industry is making efforts to underline its positive economic and commercial achievements, and is increasingly bringing hard facts and figures to bear to counter one-sided arguments centred on cost.

Grid parity will be an important driver for demand in future. Compared with feed-in tariffs, which are being continually reduced and forcing house owners and investors into rash decisions, where grid parity applies, the returns become better the longer one waits. A market with grid parity will therefore tend to see more gradual progress, and will not create a 'gold-digger' mentality as is the case in subsidized markets.

In sunny regions of the world such as Italy, California, Hawaii and Spain, we expect this household grid parity to be achieved as early as 2011/2012 (Fig. 4). In Japan, which was the highest electricity prices, PV systems on the roof of a private home will soon become the norm, simply because it makes economic sense. From 2013 onwards, solar electricity will be as cost-effective as conventional grid power even in the countries of central Europe.

Environmental and social standards becoming increasingly important

From the start, Bank Sarasin has always tried to assess PV companies according to extensive sustainability criteria. For Sarasin it was never simply enough that the companies produced products for 'green electricity'. To begin with, it was very difficult to get hold of the necessary information. However, there are now a few PV companies which undertake comprehensive corporate social responsibility (CSR) reporting, for example, SolarWorld AG. In order to raise the transparency and depth of the information provided by other solar energy companies, Bank Sarasin supports the Sustainable Solar Initiative from Henderson Global Investors. With invested assets of US$1,500 billion, this initiative has huge investor power behind it, enabling it to exert sufficient pressure on the companies concerned.

About the Author

Dr. Matthias Fawer is the director of Bank Sarasin & Co. Ltd and joined as a sustainability analyst in 2000. He is responsible for the renewable energies, oil, gas and utilities sectors. Since 2004 he has been the main author of Bank Sarasin's annual solar energy study. Matthias has a Ph.D. degree in biotechnology from the Swiss Federal Institute of Technology (ETH) in Zurich, from which he went on to work for the Ecology department of the Swiss Federal Materials Testing and Research Institute (EMPA) in St. Gallen, where he was senior expert in environmental impact projects on behalf of Swiss and European industry associations.

Enquiries

Bank Sarasin & Co. Ltd
Elisabethenstrasse 62
4002 Basel
Switzerland
Tel: +41 (0)61 277 73 03
Email: matthias.fawer@sarasin.ch

Advertisers & Web Index

ADVERTISER	WEB ADDRESS	PAGE NO.
26th EU PVSEC	www.photovoltaic-conference.com	137
3M Renewable Energy	www.3m.com/solar	153
3S Modultec	www.3-s.ch	163
ACI Ecotec	www.aci-ecotec.com	41
Air Products and Chemicals, Inc.	www.airproducts.com/sunsource2	55
ASYS Solar	www.asys-solar.com	83
BASF	www.basf.com	69
BTU International	www.btu.com	101
CH2M Hill	www.ch2mhill/solar	19
Coveme Spa	www.coveme.com	151
CM Navigo	www.criticalmanufacturing.com	17
Crane Nonwovens	www.cranenonwovens.com	165
DEK Solar	www.deksolar.com	75
Despatch Industries	www.despatch.com	107
develop Mechanics MV	www.develop.be	99
EKO Instruments Co., Ltd	www.eko.co.jp	167
Elkem Solar	www.elkem.com/solar	45
EPIA	www.eupvplatform.org	53
Festo	www.festo.com	27
GBR Schmid	www.schmid-group.com	73, 143
Grenzebach Maschinenbau GmbH	www.grenzebach.com	115
GT Solar, Inc.	www.gtsolar.com	IFC
Hanwha SolarOne	www.hanwha-solarone.com	6, 7
Horiba	www.horiba.com/scientific	125
Hyundai	www.hyundaisolar.com	11
IEEE	www.ieee-pvs.org	39
Indium	www.indium.com/solar	37
Innolas Systems	www.innolas-systems.com	97
Intersolar Europe	www.intersolar.de	85
Intersolar North America	www.intersolar.us	177
J.A. Woollam Co., Inc.	www.jawoollam.com	129
Kipp + Zonen B.V.	www.kippzonen.com	171
Komax Solar	www.komaxsolar.com	145
Kommerling Chemisch Fabrik GmbH	www.adcocorp.com	147
Kuka Systems GmbH	www.kuka-systems.com	9
Linde Group	www.linde.com/electronics	33
Linuo Power	www.linuopower.com	141
Lisec	www.lisec.com	157
M+W Group GmbH	www.mwgroup.net	13
Madico	www.madico.com	149
Manz Automation AG	www.manz-automation.com	OBC
Meyer Burger AG	www.meyerburger.ch	51
Otto Chemie	www.otto-chemie.de	161
Pasan	www.pasan.ch	159
Q-Cells	www.q-cells.com	25
REC Silicon ASA	www.recgroup.com/silane	3
Rena Solar GmbH	www.rena.com	63
Renusol	www.renusol.com	169
Roth & Rau	www.roth-rau.de	61, 67, 105
Schott	www.schottsolar.com/solar-yield	175
SNEC PV Power Expo	www.snec.org.cn	47
Sony Chemical & Information Device Corporation	www.sonycid.jp	155
Spire Corporation	www.spirecorp.com	23
Sputtering Components	www.sputteringcomponents.com	117
Testbourne Ltd.	www.testbourne.com	131
Umicore SA Thin Film Products	www.thinfilmproducts.umicore.com	135
Vacon	www.vacon.com	183

To advertise within Photovoltaics International, please contact the sales department: Tel +44(0)20 7871 0123

Photovoltaics International

DON'T MISS: **Fast-track PV facility construction** | **LCOE and grid integration issues** | **ALD in PV manufacturing**

I would like to purchase a subscription.

Price: ☐ 1 x Issue **$59.00 USD** (includes international delivery)
☐ 4 x Issue **$199.00 USD** (includes international delivery) Please start my subscription with edition ....

Method of payment: ☐ Credit Card ☐ Bank Transfer

Name: ....
Job Title: .... Job Function: ....
Company: .... Div/Dept: ....
Street Address: ....
City: .... Post Code/Zip: ....
Country: ....
Telephone Number: .... Web URL: ....
E-mail: ....
For the purposes of our circulation audit, please indicate the last digit of your birth year (YYYY): ....

Company Activity (tick where appropriate):

☐ PV Manufacturer (inc. Thin Film & Module) ☐ Materials Supplier ☐ Equipment Supplier

If you ticked any of the above three options, please indicate the company technology type by ticking one or more of the boxes below:

☐ Si Cell ☐ Thin Film ☐ Module ☐ Concentrator ☐ Emerging ☐ Polysilicon ☐ Ingot/Wafer

☐ University ☐ Energy Utility Supplier ☐ Government Agency
☐ R&D Facility ☐ Financial Community ☐ Other (please specify ....)

In order to continually improve Photovoltaics International we require your feedback. We would be very grateful if you would answer the following questions:

(Q) Which section(s) of the publication are of interest to you? (please tick)

☐ Fab + Facilities ☐ Materials ☐ Cell Processing ☐ Thin Film
☐ PV Modules ☐ Power Generation ☐ Market Watch

(Q) What technical subjects do you wish to see in future editions?..........

....

Signature:.......... Date ....

Payment Details:

Fax on +44 (0) 20 7871 0101 or email info@pv-tech.org:

Type of credit card: ☐ VISA ☐ MasterCard ☐ American Express

Card Number: ....
Expiry Date: ....
3 Digit CVV Code (back of card): ....
Cardholder's name: ....

Post: Make cheques payable to **"Solar Media Ltd."**
Photovoltaics International, Trans-World House,
100 City Road, London EC1Y 2BP, UK
Online: PayPal - visit **www.pv-tech.org/shop**

To request an invoice please call on 020 7871 0148
or **email:** subscriptions@pv-tech.org

Bank Transfer Details:

Account Name:	Solar Media Ltd.
Account Number:	80686832
Sort Code:	20-39-53
Swift Code:	BARC GB 22
IBAN Number:	GB 42 BARC 203953 80 68 68 32
Bank:	Barclays Bank Plc, 10 Hart Street, Henley-on-Thames, Oxon, RG9 2AX.

All invoices are calculated in Pounds Sterling.

Any payments made in US$ must be made according to the appropriate exchange rate at the time of payment.

TBEA SunOasis has ambitious 'dreams beyond China'

Despite the Suntechs, Yinglis, LDKs, and other few-dozen names familiar to most solar industry folks, a plethora of second-tier/emerging firms do business in the People's Republic that most non-China hands have never heard of.

The big question is, which of these heretofore "unknown" Chinese companies have a shot at taking their enterprises global? One possible contestant is TBEA Xinjiang SunOasis. During SNEC 2011, the company's senior marketing manager, Hou Yangang, talked about the company and its ambitious gigawatt-scale expansion plans.

The parent of TBEA SunOasis is Tebian Electric Apparatus, or TBEA, a mostly privately held, 20 billion RMB (nearly US$3.1 billion) firm, which already has an international reputation in the transformer industry as one of the top three players, along with Siemens and ABB. Although not the main bread-winner in the corporation, Hou told me that the PV unit did account for a not-insignificant 1.8 billion RMB (US$277 million) during the most recent fiscal year.

Image courtesy of TBEA SunOasis.

While not totally vertical, the company does focus on several key parts of the PV value chain: wafering, module assembly, controllers/inverters, and system integration/installation. The parent also owns a sister company, TBEA Polysilicon, in which it has invested nearly two billion RMB and which produces about 120mt of poly per month at its Xinjiang factory, according to Hou.

Current ingot/wafering production capabilities (which feature Meyer Burger and GT Solar equipment and include mono- and multicrystalline substrates) sit at about 180MW of annual manufacturing capacity with another 170MW being built out this year, and a total of 500MW expected to come online by the end of 2012, he said. By 2015, TBEA SunOasis plans to have 1GW of wafermaking capacity available.

Cellmakers buying the Xinjiang-based company's 125mm and 156mm wafers include Motech, China Sunergy, and JA Solar, which then sell back the finished cells to TBEA SunOasis for its moduling operations.

The company has made somewhat of an international name for itself in the module arena, since it is the majority partner with BP Solar in a manufacturing joint venture, which has a 250MW nameplate capacity facility in Xi'an. Hou said TBEA SunOasis wants to expand its module capacity to at least 500MW in the next few years, but is likely to do so under its own brand. "BP Solar is quite slow in making a decision," he explained, noting that the energy multinational has had some other things (like big oil spills) on its mind of late.

The company has been doing R&D and a little bit of business in off- and on-grid inverters since its inception in 2000, but now the segment is gathering momentum and has become a major focus. Land in Xi'an has been acquired for a new inverter production facility, with plans for increasing capacity from the current 70-80MW level to 1GW by 2015, Hou said, and the company recently won an 80MW order. The parent company's transformer expertise serves it well in the PV power electronics area, and its UL/TUV-certified 500Kw grid-tied inverters have all the efficiency, MPPT, monitoring, reliability, and other bells and whistles of the competitors' equipment.

Those inverters also will play an increasing role in the company's already successful systems integration and project business. Hou informed me that TBEA SunOasis was the first PV integrator in China (and remains one of the top three, along with Suntech and GCL) and already has deployed more than 3,000 solar power systems, totaling about 150MW of installed capacity (much of that done in the past year).

The project list includes what is said to be the largest off-grid system in Asia, a 500Kw power plant in rural Xinjiang province; the largest rooftop BIPV array in China, a 6.6MW installation on top of the Shanghai Hongqiao high-speed railroad terminal; and a trio of 10MW systems tied to the grid in Yunnan, Ningxia, and Qinghai provinces.

Hundreds of TBEA SunOasis systems have brought off-grid solar power to remote areas of China – many telecom relay and water-pumping stations rely on PV systems built by TBEA, for example – as well as in neighboring countries such as Pakistan and Kazakhstan. The company is bidding on 280MW of new Chinese projects and has won 40MW of EPC work so far, according to Hou.

He emphasized that while TBEA SunOasis wants to reach 500MW of installed generating capacity inside its home country by 2015, the company "definitely wants to become more international, and expand our leadership…We have dreams beyond China." Those plans include the possible opening of subsidiary companies in Germany, Italy, the United States, India, Japan, South Korea, and Australia.

As with any Chinese corporation with expansionist aims, it doesn't hurt – and in fact remains pretty much essential – to have connections among the top echelons of the Communist Party. In a series of slides within the TBEA SunOasis presentation provided by Hou, six members of the standing committee of the Politburo – including the top two leaders, Hu Jintao (secretary-general, president) and Wen Jiabao (premier) – are shown visiting its facilities along with company chairman Zhang Xin at various times over the past few years.

The ruling elite's keen interest in the company, along with its proven domestic track record, bodes well for its international aspirations.

(Thanks to Cathy Li for the translations during the interview. This column is a revised version of a blog that originally appeared on PV-Tech.org.)

Tom Cheyney is North American editor for the *Photovoltaics International* journal and writes blogs and news for PV-tech.org.